THE ROLE OF NERVE GROWTH FACTOR IN EPIDERMAL WOUND REPAIR IN A HUMAN SKIN *EX VIVO* MODEL

A thesis submitted to the University of Manchester for the degree of

Doctor of Philosophy

in the Faculty of Biology, Medicine and Health

2019

Nur Azida Mohd Nasir

Centre for Dermatology Research,

School of Biological Sciences,

Faculty of Biology, Medicine and Health

The University of Manchester

Contents

Word count: 45280

List of figures

List of tables

List of Abbreviations

µL	Microlitre
µm	Micrometre
ANOVA	Analysis of variance
AUC	Area under curve
BDNF	Brain derived neurotrophin factor
CMFDA	5-chloromethylfluorescence diacetates
CMTPX	4-({[4-(chloromethyl)phenyl]carbonyl}amino)-2-(1,2,2,4,8,10,10,11-octamethyl-10,11-dihydro-2H-pyrano[3,2-g:5,6-g']diquinolin-1-ium-6-yl)benzoate
CO_2	Carbon dioxide
DAPI	4',6-diamidino-2-phenylindole
DDW	Double distilled water
dH_2O	Distilled water
DMEM	Dulbecco Dulbecco's Modified Eagle's Medium
ECM	Extracellular matrix
EDTA	Ethylenediaminetetraacetic acid
ELISA	Enzyme linked immunosorbent assay
FBS	Fetal Bovine Serum
H&E	Haematoxylin and Eosin
HRP	Horse-reddish peroxide
IHC	Immunohistochemistry
IMS	Industrial methylated spirit
JNK	c-Jun N-terminal kinase
mM	Milimolar
mm	Millimetre
MMP	Matrixmetalloproteinase
mRNA	messenger RNA
NF-kB	Nuclear factor-kB
NGF	Nerve growth factor
NNA	NGF Neutralising antibody
NS	Normal skin
NT	Neurotrophin
NT-3	Neurotrophin 3
NT-4	Neurotrophin 4
NTR	Neurotrophin receptor
p75NTR	pan-75 neurotrophin receptor
PBS	Phosphate buffered saline
RNA	Ribonucleic acid
SD	Standard deviation
SEM	Standard error of the mean
SP	Substance P

TBS	Tris buffer saline
TNT	Tris-NaCl-Tween$_{20}$
TrkA	Tyrosine kinase receptor A
TrkB	Tyrosine kinase receptor B
TrkC	Tyrosine kinase receptor C
TSA	Tyramide signal amplification
UK	United Kingdom
USA	United States of America
WE	William's E medium

ABSTRACT

Introduction: One of the main aims of ongoing wound healing research is to identify improved methods for accelerating epidermal repair and/or wound closure. Previously, the impact of nerve growth factor (NGF) on human skin wound healing has been tested in various assays, however the results were inconclusive. Therefore, instead of using *in vitro* cell culture assays or animals this study opted to assess the effects of NGF in experimentally wounded, organ cultured human skin, since this *ex vivo* assay mimics clinical wound healing conditions under preclinical conditions more closely than cell culture or 3D skin "equivalent" assays

Aims: My main aim was to study epidermal repair in human skin wounds *ex vivo* in the presence or absence of NGF, NGF-neutralising antibody or the neurotrophin receptor antagonist, K252a. In addition, I aimed to examine the protein expression of endogenous NGF and its cognate receptors; TrkA and p75NTR in healthy human skin and over the course of healing *ex vivo*, and understand how this might be affected by NGF treatment.

Methods: Utilising human skin excised during routine surgery, a partial-thickness 2 mm wound was created within a 6 mm full-thickness skin biopsy (punch-in-a-punch design) and cultured at the air liquid interphase in serum-free Williams E (WE) media for up to six days. Wound healing was assessed by quantitative histomorphometry and *en face* planimetry. In order to assess epidermal repair by planimetry (longitudinally), organ cultured skin was co-treated with 5-chloromethylfluorescein diacetate (CMFDA) daily and images were taken under a fluorescence upright microscope. The wound bed was treated with the assigned treatments (NGF, K252a and NGF neutralising antibody) on a daily basis. Tissue was processed for immunohistochemistry and immunofluorescence microscopy with antibodies against the proliferative marker Ki-67, or against NGF, TrkA, p75NTR, CD68 (macrophage marker) and CD1a (Langerhans cell marker). Quantification of endogenous NGF in human skin organ culture was performed using enzyme-linked immunosorbent assay (ELISA).

Results: Wound healing could be quantified *ex vivo* via CMFDA fluorescence, which yielded rapid and robust results when compared to histological assessment. CMFDA also successfully traced cells during epidermal repair and indicates that epithelial migration in human skin wounds occurs via a collective migration mechanism. NGF treatment had no beneficial effect on the re-epithelialisation of acute human wounds *ex vivo* under the current assay conditions. There was little fluctuation in NGF protein expression and of its cognate receptors in wounded human skin in organ culture, suggesting that human skin *ex vivo* already contains abundant of NGF and its receptors. This was confirmed by ELISA.

This study also localised and quantified for the first time the changes of endogenous NGF and its cognate receptor in wounds and confirmed that NGF expression was independently expressed even in denervated human skin *ex vivo*. However, inhibiting TrkA-mediated signalling with K252a or neutralising endogenous NGF with a specific antibody, revealed significantly impaired epidermal repair.

Conclusion: This study confirms that the chosen design for studying experimentally wounded human skin *ex vivo* is well-suited to interrogate candidate wound healing-promoting agents. Moreover, this thesis project introduces and accurate, yet simple, fluorescent dye-based new method for rapidly assessing human epidermal repair *ex vitro*. The study also provides evidence that endogenous NGF and TrkA-mediated signalling are required for normal epidermal repair, even in the absence of functional skin innervation, at least under *ex vivo* conditions. However, the addition of excess exogenous NGF does not accelerate epidermal repair under the examined assay conditions. This raises the possibility that topical NGF administration may promote human skin wound healing only under conditions of relative NGF deficiency. The current thesis project, therefore, suggest to test healing impaired human skin (e.g. leg ulcers) in the future for insufficient NGF skin content, in which case NGF therapy might beneficial.

Declaration

I declare that no portion of the work referred to in the thesis has been submitted in support of an application for another degree or qualification of this or any other university or other institute of learning

Copyright statement

i. The author of this thesis (including any appendices and/or schedules to this thesis) owns certain copyright or related rights in it (the "Copyright") and she has given The University of Manchester certain rights to use such Copyright, including for administrative purposes.

ii. Copies of this thesis, either in full or in extracts and whether in hard or electronic copy, may be made only in accordance with the Copyright, Designs and Patents Act 1988 (as amended) and regulations issued under it or, where appropriate, in accordance Presentation of Theses Policy You are required to submit your thesis electronically Page 11 of 25 with licensing agreements which the University has from time to time. This page must form part of any such copies made.

iii. The ownership of certain Copyright, patents, designs, trademarks and other intellectual property (the "Intellectual Property") and any reproductions of copyright works in the thesis, for example graphs and tables ("Reproductions"), which may be described in this thesis, may not be owned by the author and may be owned by third parties. Such Intellectual Property and Reproductions cannot and must not be made available for use without the prior written permission of the owner(s) of the relevant Intellectual Property and/or Reproductions.

iv. Further information on the conditions under which disclosure, publication and commercialisation of this thesis, the Copyright and any Intellectual Property and/or Reproductions described in it may take place is available in the University IP Policy (seehttp://documents.manchester.ac.uk/DocuInfo.aspx?DocID=24420), in any relevant Thesis restriction declarations deposited in the University Library, The University Library's regulations (see http://www.library.manchester.ac.uk/about/regulations/) and in The University's policy on Presentation of Theses

Journal publication arising from this study

Nasir, N. A., Paus, R. and Ansell, D. M. (2019), Fluorescent cell tracer dye permits real-time assessment of re-epithelialization in a serum-free *ex vivo* human skin wound assay. Wound Rep and Reg, 27: 126-133. doi:10.1111/wrr.12688

Manuscript in preparation

Exploring the role of NGF in human skin re-epithelialisation *ex vivo*

Nasir NA[1,2], Ansell DM[1,5], Tomic-Canic M[6], Jozic, I[6] & Paus R[1,3,4,6]✱

[1]Centre for Dermatology Research, School of Biological Sciences, The University of Manchester, MAHSC and NIHR Manchester Biomedical Research Centre, M13 9PT Manchester, United Kingdom.
[2]School of Medical Sciences, Universiti Sains Malaysia, Health Campus, Kubang Kerian 16500 Kelantan, Malaysia.
[3]NIHR Manchester Biomedical Research Centre, Manchester, UK.
[4]Manchester Academic Health Sciences Centre
[5]Division of Cell Matrix Biology and Regenerative Medicine, The University of Manchester, UK
[6]Department. of Dermatology & Cutaneous Surgery, University of Miami Miller School of Medicine, Miami, FL, U.S.A.

To be submitted to Arch Dermatol Res

Published abstracts

Nasir N.A, Paus R and Ansell D.M. Real-time planimetry assessment of re-epithelialization in wounded human skin organ culture (2018), British Society for Investigative Dermatology Annual Meeting 2018 26–28 March 2018 Blizard Institute, Barts and The London School of Medicine and Dentistry. Br J Dermatol, 178: e397-e435. doi:10.1111/bjd.16590

Ansell D.M, Nasir N.A. and R. Paus. A novel approach to assessing wound healing in human skin organ cultures (2017), British Society for Investigative Dermatology Annual Meeting 2017, Hilton Deansgate Hotel, Manchester, 3–5 April 2017. Br J Dermatol, 176: e40-e81. doi:10.1111/bjd.15392

ACKNOWLEDGEMENTS

First and for all I would like to thank my dedicated supervisors Professor Ralf Paus and Dr David Ansell for their guidance, support and encouragement over my study period.

My deepest appreciation and thanks to all dear friends who always support me with my work or emotionally especially Eleanor Smart, Carina Nicu and Bethany Barnes for their assistance with proof reading, and entire office and the rest of the Paus Lab not to forget the guidance and support I received from experienced scientists, Dr Jonathan Hardman, Dr Talveen Purba Singh and Dr Christopher Platt. Mr Derek Pye and Mrs Stella Pearson, I would like to give you my heartfelt thanks for helping me in making my laboratory work run smoothly and for teaching me the relevant lab skills.

Also, I would like to send my gratitude to the skin donors, surgeons and hospitals for all their cooperation and to Manchester Skin Biobank, without whom this study would not have been possible.

I gratefully acknowledge Dr Steven Marsden and staff at the Bioimaging facilities for technical support, Mr Peter Walker and staff at the Histology Core Facilities Centre for providing access to equipment, and Dr Jack Wilkinson, Centre for Biostatistics for assistance and guidance with statistical analysis.

To my sponsors, the Universiti Sains Malaysia and Ministry of Higher Education of Malaysia, I am most grateful and thank them for this post-graduate study opportunity.

Finally, I would like to thank my family especially my father Mohd Nasir B. Ismail and mother Azizah Bt Bakar, for your endless love and prayers in my life. Last but not least, my gratitude goes out to my Malaysian friends who are always there for me whenever I need you.

PREFACE

I received my Bachelor of Science (BSc.) majoring in Biohealth Science from the University of Malaya, Malaysia in 2003. My final project for undergraduate thesis was on Forensic Entomology: *Chrysomya ruffifacies* and *Chrysomya megacephala* life cycle in entomology: Forensic skill to identify the post–mortem interval in Malaysia. However, upon graduation I worked as research assistant in the Optometry Department, Universiti Kebangsaan Malaysia. In 2005 I started a new job as a Research Officer at the Tun Hussein Onn National Eye Hospital and I was involved in clinical trials and a person in-charged for research secretariat. In 2008, I decided to pursue my Master's degree and was conferred with Master of Science (MSc.) in Reconstructive Science in 2012. During my MSc. I worked on the project: Microbiology and angiogenesis properties of burn wound healing. Upon graduation I was hired as a Research Officer at my department, Reconstructive Science Unit, School of Medical Sciences Universiti Sains Malaysia. During this employment I worked for the prospective multicentre clinical studies on the use of chitosan derivatives as wound dressings. My job descriptions were to manage daily activities in the research center, patient screening and recruitment (randomization handling), data management and analysis, manuscript preparation as well as presenting our findings at national and international conferences. I won the best oral presentation (in Clinical Science) at the International Conference on Medical & Health Science, Malaysia (2013), presenting one of the Chitosan study and this was recently got published (Halim *et al.*, 2018). In order to pursue my ambition as an academician and researcher I decided to continue my education to PhD. I was fully funded by the Ministry of Higher Education, Malaysia and Universiti Sains Malaysia under Academic Staff Training Scheme scholarship. Here at the University of Manchester I also work as Graduate Teaching Assistant. Part of the research conducted during my PhD and contained within this thesis was recently published in Wound Repair and Regeneration (Nasir *et al.*, 2019). Soon at the end of March 2019 I will present my study at The Wound Meeting 2019 Seoul. I was also invited as a speaker for the 3rd International Burn and Wound Conference in Conjunction with the Malaysian Society of Plastic Reconstructive Surgery & Malaysian Society of Burn Injuries (26-28th April 2019).

CHAPTER 1

INTRODUCTION

1.1 The structure of human skin

Skin is the largest organ of the body and provides the primary protection to the underlying tissue and internal organs (internal physiological environment) from the external non-physiological environment (Byrd *et al.*, 2018, McGrath and Uitto, 2010, Murphrey and Zito, 2018), with the ability for self-maintenance and self-repair except for appendages (Agache *et al.*, 2017, Braun and Prowse, 2006). Anatomically, skin can be divided into three layers (Yagi and Yonei, 2018): epidermis, dermis and hypodermis and is accessorized with skin appendages (Figure 1.1). In general, skin is built from varieties of cells such as keratinocytes, fibroblasts, adipocytes, melanocytes, Merkel cells, Langerhans cells, macrophages and mast cells; the skin's connective tissue, is complemented by, extracellular matrix (ECM) molecules such as collagen and by numerous growth factors; the skin is also densely innervated and highly perfused (Martin, 1997, Agache *et al.*, 2017, Menon *et al.*, 2012, Ng and Lau, 2015, Eming *et al.*, 2014, Yagi and Yonei, 2018).

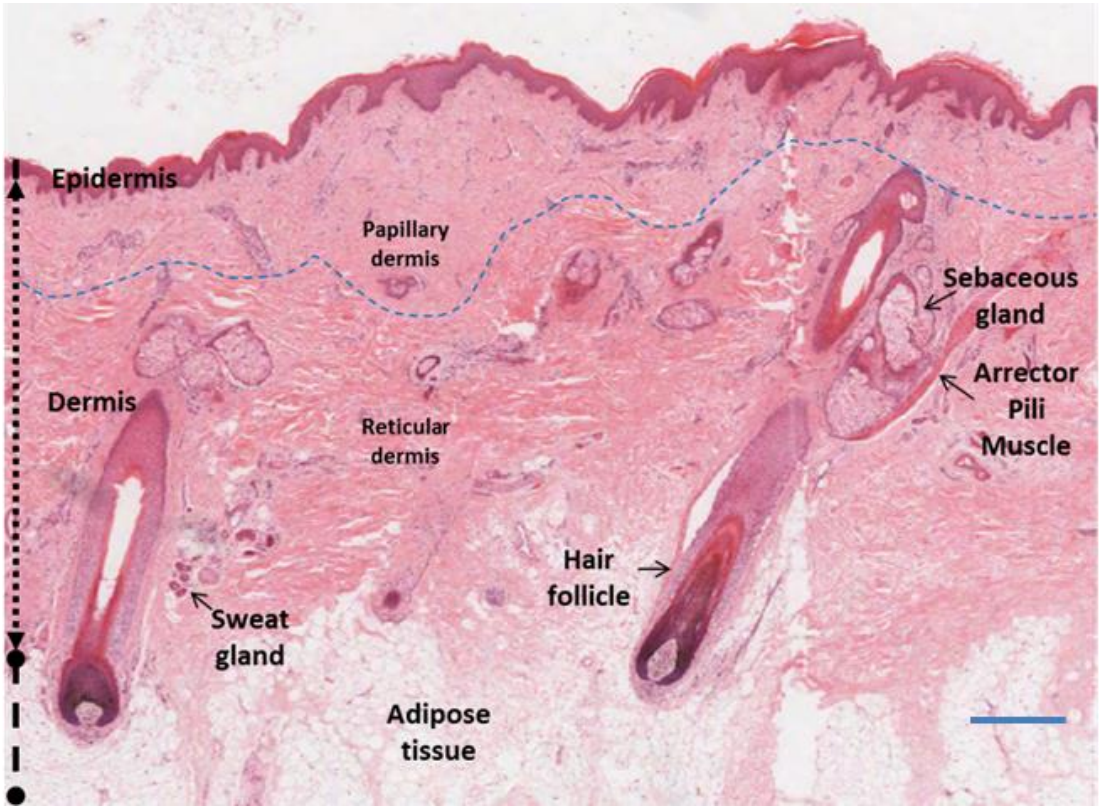

***Figure 1.1**: Anatomy of human scalp skin. Human scalp skin consists of epidermal layer, dermis and subcutaneous layer. Skin also contains skin appendages like hair follicles, sebaceous glands and sweat glands. Bar – 500 µm. Histology [H&E] and image generated by Nur Azida Mohd Nasir.*

1.1.1 Epidermal layer

The epidermal layer consists of 95% of stratified epithelium that can be subdivided from inside to outside into stratum basale (also known as the stratum germinativum or basal layer), stratum spinosum, stratum granulosum (granular layer), stratum lucidum (a clear layer that can be observed on thickened skin) and stratum corneum (horny layer) (Yagi and Yonei, 2018) (Figure 1.2).

Stratum basale is the deepest layer of epidermis composed of a single layer of columnar cells that contains stem cells which proliferate and produce new cells (Yagi and Yonei, 2018). The cells at the basal layer divide at a high rate and differentiate, migrating upward to form the stratum spinosum. The stratum basale is crucially required for re-epithelialisation during wound repair. Other cells that reside in the basal layer are melanocytes, Langerhans cells and Merkel cells (Yagi and Yonei, 2018).

The stratum spinosum is so-called due to the shape of cells following shrinkage of the microfilaments (prickle cell) (Yousef and Sharma, 2018) and intercellular junctions rich in desmosomes (McGrath and Uitto, 2010) and also produced lamellar granules (Wertz, 2018). The complex process of keratinization starts at this layer. The cells in this layer migrate superficially, becoming the granulosum layer, and contain keratohyalin granules to bind intermediate keratin filaments together. While the stratum basal provides lividity to the skin, the stratum corneum is formed by corneocytes (flattened and elongated) which are non-living cells derived from terminally-differentiated basal cells which migrate (from basal →spinosum → granulosum) superficially until they reach the outermost surface of the skin (Murphrey and Zito, 2018).

Formerly cell layers from the stratum granulosum, these corneocytes are contained within cross-linked keratin filaments and surrounded by a cornified enveloped and an outer lipid coating (derived from sebaceous gland secretion and epidermal lipids) (Ludovici *et al.*, 2018). Even though this layer contains dead cells, the stratum corneum acts as a primary barrier to protect the human body from the external environment (Elias, 2012, Menon *et al.*, 2012, Ng and Lau, 2015, Archer, 2010, Murphrey and Zito, 2018, Danzberger *et al.*, 2018).

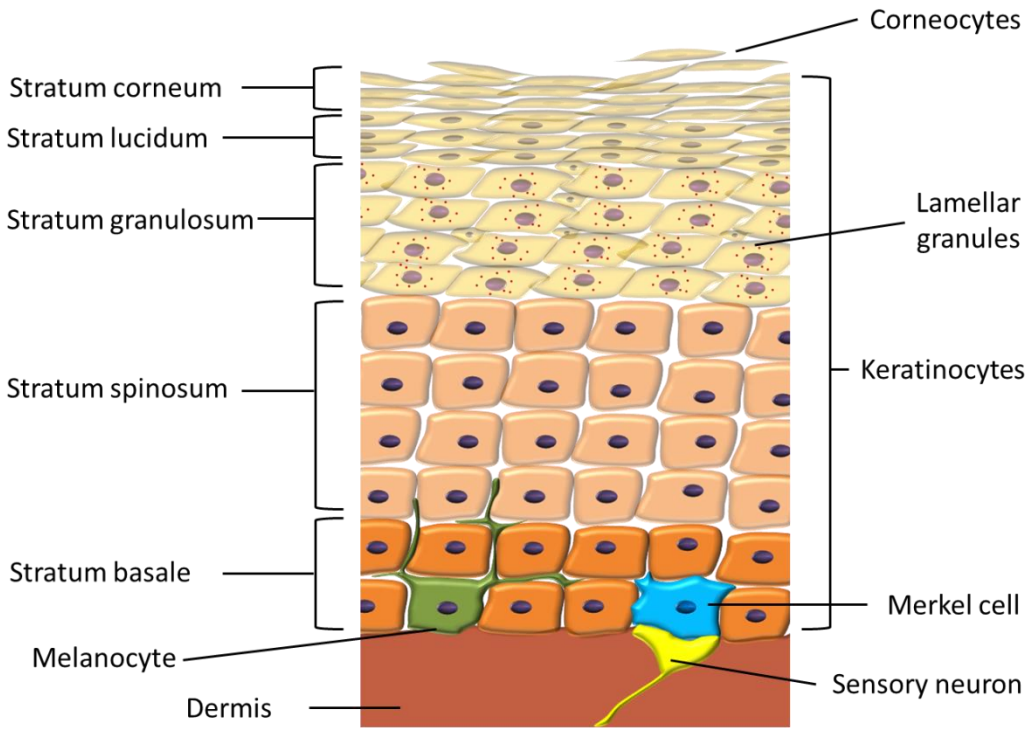

***Figure 1.2: Human skin epidermal layers**. The epidermis of thick skin has five layers named stratum basale, stratum spinosum, stratum granulosum, stratum lucidum and stratum corneum. Cartoon prepared by **Nur Azida Mohd Nasir**.*

1.1.2 Dermal layer

The main components that build up the dermis are fibroblasts, myofibroblasts, collagen, other ECM molecules, skin appendages such as hair follicles, sweat glands, sebaceous glands, sensory nerves and vasculature that extend from the hypodermis layer to the dermo-epidermal junction to nourish the epidermis and also act as waste removal (Yousef and Sharma, 2018, Thulabandu *et al.*, 2018) (Figure 1.1). The dermis can be sub-divided into papillary dermis and reticular dermis. The papillary dermis has thinner and looser collagen arrangement compared to the reticular dermis and is attached to the basal epidermal layer by papillae that interdigitate at the dermo-epidermal junction (Ng and Lau, 2015, Yousef and Sharma, 2018). The reticular layer is rich in vasculature and nerve networking also containing elastin fibres to provide elasticity to the skin. The collagen fibres not only provide structure but also tensile strength.

1.1.3 Subcutaneous layer

The subcutaneous layer also called the hypodermis is comprised of adipocytes (Figure 1.1). This is the deepest layer of the skin and important for body thermoregulation; it also cushions the underlying integuments as well as the internal organs. Within this layer reside hair follicles, nerves and the vasculature system to nourish the dermis and epidermis (McGrath and Uitto, 2010, McGibbon, 2010, Yousef and Sharma, 2018).

1.2 Wound repair

A wound can be described as a disruption of skin protection (Martin, 1997, Sen and Roy, 2013). This protection can be breached in various ways including thermal injury

(Rafla and Tredget, 2011), surgical incision or excision, infections, chemicals, immunological reactions, radiation, abrasions or lacerations. The disruption will allow the skin's normal floral and microorganisms from outside to invade the exposed tissue (Roth and James, 1989, Tüzün *et al.*, 2015). Hence, an immediate mechanism is needed to protect the affected area and to counter the invasion of the microorganism to prevent infection. In 1919, wound healing was defined as a composite process involving many activities and interaction with definite quantitative factors (Loeb, 1919). Later, the definition of wound healing was re-fined as the well-orchestrated and overlapping stages of haemostasis, inflammation, proliferation and migration, and remodelling (Figure 1.3) (Sen and Roy, 2013, Martin, 1997, Rieger *et al.*, 2015, Janis *et al.*, 2010, Eming *et al.*, 2014, Morton and Phillips, 2016, Wang *et al.*, 2018, Singh *et al.*, 2017).

1.2.1 Type of wounds

Generally, there are two major wound types which are acute (Stunova and Vistejnova, 2018) and chronic wounds (Dreifke *et al.*, 2015, Qing, 2017). The term acute refers to normal skin disruption accidentally or intentionally such as traumatic lesions (abrasion or laceration), burn wounds, or surgical wounds. Depending on injury size and depth, this type of wound could heal within a week or over several months with optimal treatment provided in a timely manner (Mirastschijski *et al.*, 2013, Martin and Nunan, 2015). An abrasion is a superficial wound when one loses nothing other than their epidermis. It can be caused by sun burn or grazes and healed within 3-5 days (Odland and Ross, 1968), while lacerations are more severe than abrasions due to tears in the soft tissue or the wound extending into the papillary dermis layers due to a blunt trauma or burns (partial-thickness burn). This wound can

be painful since it exposes the Meissner corpuscle which responds to pressure and touch (Heimbach *et al.*, 1992, Johnson and Richard, 2003). This type of affected tissue is also called a superficial partial-thickness wound. If the injury extends into the reticular dermis, this wound can be classified as a deep partial-thickness wound.

In contrast, wounds are classified as full-thickness when the penetration extends to the subcutaneous tissue. Here, the dermis and adipose tissue will be exposed. This type of wounds may close by primary intention (if the wound is clean, well vascularised and the tissue margins are approximately precise), by suture or by delayed wound closure after preparation of the wound bed (if the wound needs debridement, or the bone, ligament or tendon has been exposed) with split-skin grafting or full-thickness skin grafting (Salcido, 2017, Mirastschijski *et al.*, 2013, Nawaz and Bentley, 2011).

Generally, a wound is classified as chronic when it fails to heal after 4 weeks with less than 20-40% reduction of wound area after optimal therapy, or within 3 months or longer (Mirastschijski *et al.*, 2013, Sen and Roy, 2013). The three major categories of chronic wounds are venous and arterial ulcers, diabetic ulcers and pressure ulcers (Nunan *et al.*, 2014, Morton and Phillips, 2016). The epidermal keratinocytes become hyperproliferative and non-migratory across the wound bed due to chronic inflammation, cellular senescence, infection and worse by formation of biofilm due to unresolved infection (Eming *et al.*, 2014, Morton and Phillips, 2016, Martin and Nunan, 2015).

1.3 Phases of wound repair

1.3.1 Haemostasis and inflammation phase

Haemostasis (Figure 1.3-1.4) is the primary action (immediately after injury and lasting a few hours) to stabilize the blood fluidity during injury involving the blood vessels (Sen and Roy, 2013, Delavary *et al.*, 2011). During this stage, the injured blood vessels vasoconstrict to seal the injured vessels and thromboplastic product is produced from the exposed sub-endothelial cells, forming a haemostatic plug (clot)(Mirastschijski *et al.*, 2013, Wallace and Bhimji, 2018, Martin, 1997). Haemostasis is accomplished once the clot formed of platelet and fibrin fibres is stable. The clot then serves as growth factor, cytokine and chemokine reservoirs (Wallace and Bhimji, 2018, Sen and Roy, 2013). Chemoattractants released by de-granulating platelet-fibrin complexes (PDGF,IGF-1, EGF, TGF-β) are very potent for the recruitment and activation of inflammatory cells as well as fibroblasts, endothelial cells and vasoconstrictors at the wound site (Sen and Roy, 2013, Mirastschijski *et al.*, 2013, Colman *et al.*, 2006, Janis *et al.*, 2010).

During the inflammatory phase (Figure 1.3-1.4), the vasodilated blood vessels become more permeable causing erythema (rubour), heat (colour), swelling (tumour) and pain (dolour). These phenomena are due to the secretion of prostaglandin (PG 12, PG A, PG D and PG E) and bradykinin C3a and C5a (from the coagulation and complement cascades)(Delavary *et al.*, 2011). The increment of vascular permeability will further attract neutrophils and monocytes, and stimulate mast cells to produce histamine and leukotrienes. On the other hand, the appearance of endothelial cells will break cell-to-cell contact, thus increasing infiltration of inflammatory cells and

leakage of plasma protein to the wound site (Mirastschijski *et al.*, 2013, Sen and Roy, 2013, Gonzalez *et al.*, 2016).

Taking advantage of vasodilated blood vessels, neutrophils released through the vessel wall by diapedesis (Filippi, 2016) are the first white cells to arrive within 24-48 hours (Singh *et al.*, 2017). TNF-α, IL1-β and IL-6 mediators are released and stimulate VEGF and IL-8. Neutrophils are scavengers for cellular debris, bacteria and other foreign bodies. After 2-3 days, neutrophils are primed by macrophages to phagocytose necrotic tissue, bacteria and cellular debris (Singh *et al.*, 2017). The shift is necessary as prolonging the action of neutrophils may delay wound healing (Dovi *et al.*, 2003). Monocytes known as macrophages outside the blood vessels secrete multiple growth factors to attract and stimulate local endothelial cells, fibroblasts and keratinocytes to begin wound repair (Mirastschijski *et al.*, 2013, Sen and Roy, 2013, Delavary *et al.*, 2011). Depletion of macrophages will cause poor debridement (removal of dead tissue), delayed fibroblast proliferation and inadequate angiogenesis (Lucas *et al.*, 2010). Interestingly, Jameson *et al* found that γδ T cells (a major component of the T cell repertoire) play a role in detecting stress or damage within keratinocytes. Upon detecting antigens from nearby damaged keratinocytes, γδ T cells produce factors such as FGF7 and FGF 10 to help keratinocyte proliferation (Jameson *et al.*, 2002).

1.3.2 Proliferative phase

The proliferative phase of repair (Figure 1.3-1.4) is a continuation from the inflammatory phase. Macrophages activate fibroblasts to release growth factors from the local extracellular matrix (ECM) migrating to the wound via a deposited

fibrin-fibronectin matrix (Martin, 1997, Stunova and Vistejnova, 2018). In clean non-infected wounds, fibroblasts become the dominant cells within 3-5 days so as to synthesize and secrete the ECM (Singh *et al.*, 2017, Thulabandu *et al.*, 2018). The initial wound matrix is primarily composed of fibrin and glycosaminoglycan (GAG) and hyaluronic acid (Singer and Clark, 1999, Olczyk *et al.*, 2014). The GAG scaffold holds the collagen type I and III previously deposited by fibroblasts. At this stage, the wound bed contains a dense capillary network clinically known as neo-angiogenesis giving the granulation tissue a pink, soft and granular appearance (Mirastschijski *et al.*, 2013, Gonzalez *et al.*, 2016, Janis *et al.*, 2010).

At the same time contraction pulls the surrounding skin toward the open wound, thus decreasing wound size and amount of scarring. The main players to pull the surrounding skin toward the wound for contraction are the myofibroblasts (Chitturi *et al.*, 2015, Gabbiani *et al.*, 1971). Clinically, contraction will disturb the mobility and function of affected organs as the tissue becomes shortened or distorted (Mirastschijski *et al.*, 2013).

Wound repair would not be completed without re-epithelialisation. This process starts within 24 hours after injury (Mirastschijski *et al.*, 2013, Balañá *et al.*, 2015). The basal epidermal layer of the skin contains a pool of progenitor cells that contribute to epidermal haemostasis. These progenitors are self-renewing and differentiate into keratinocytes that migrate to the skin surface, guided by glycoproteins (tenascin & fibronectin). This process will continue until the newly-generated cells (wound tongue) come in contact with other wound tongue (Balañá *et al.*, 2015, Martin, 1997). Another major influence in epithelial migration are matrix metalloproteinases

(MMP). MMPs modify the wound matrix to dissolve the basal epidermal keratinocyte hemidesmosomes thus allowing epidermal migration through the wound matrix (Caley *et al.*, 2015).

1.3.3 Remodelling phase

In general, after three weeks of acute injury, the stronger vascular scar tissue (inactive fibroblasts, dense collagen, fragments of elastic tissue and ECM components) replaces the temporary granulation tissue (Mirastschijski *et al.*, 2013, Robson *et al.*, 2001, Reinke and Sorg, 2012). The tensile strength is reduced 20-30% compared to the normal strength (Morton and Phillips, 2016). At this stage, collagen deposition and degradation is determined by fibroblasts, neutrophils and macrophages mainly by the production and activity of metalloproteinases (MMP1, MMP2, MMP3 and MMP9) (Sen and Roy, 2013, Janis *et al.*, 2010), and regulated by tissue inhibitor of metalloproteinase (TIMP) (Caley *et al.*, 2015). The scar produced at the end of this stage has no epidermal appendages, and a different collagen pattern densely packed at the wound site. This remodelling phase (Figure 1.3-1.4) may last a few months or longer than a year until the scar has matured (Canady *et al.*, 2013).

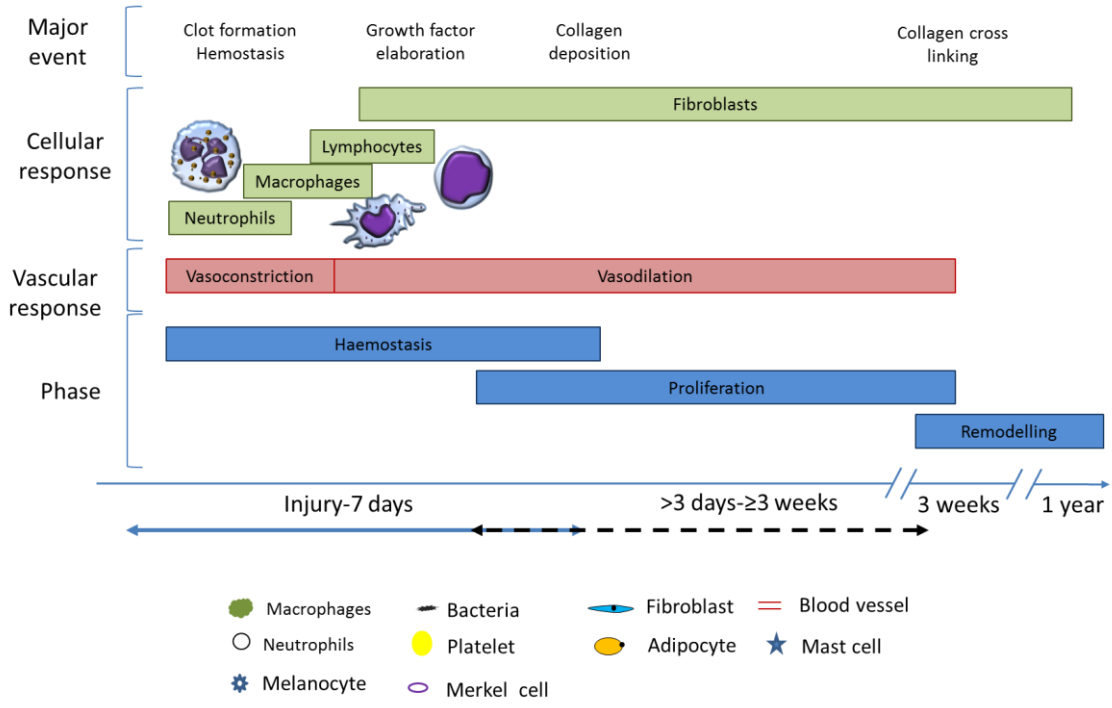

Figure 1.3: Diagrammatical representation of a wound healing timeline. *Normal wound healing occurs in timely manner with overlapping phase of haemostasis and inflammatory, proliferation and remodelling. These phase of wound healing trigger differences vascular and cellular responses that will create major events in healing process. Diagram modified from (Mirastschijski et al 2013).*

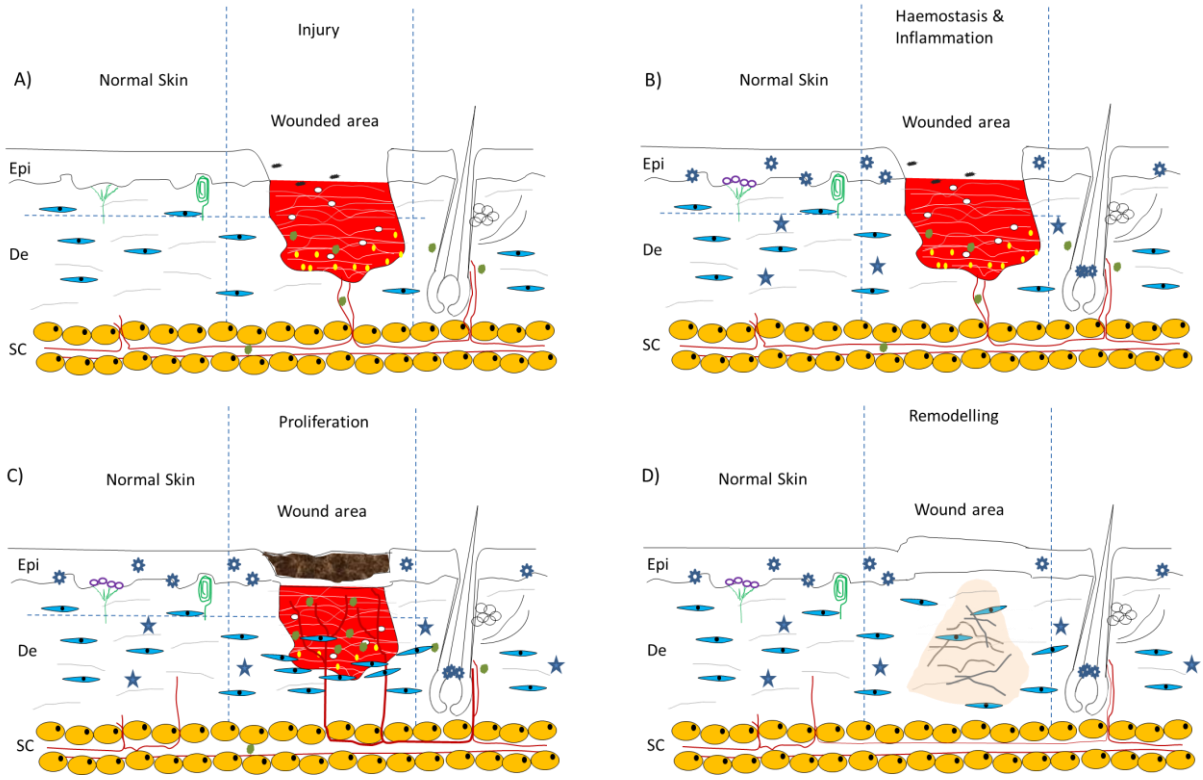

Figure 1.4: Diagrammatical of wound healing phases*. Wound healing occurs through co-ordinated phases. Following wounding to the skin (A), a Haemostasis and inflammatory phase starts within seconds after an injury occurs (B), and is followed by the proliferation phase and re-epithelialisation to close the wound (C). Wound closure is completed by the remodelling phase (D). Epi-epidermis, De-dermis, SC-sub-cutaneous (drawn by author* ***Nur Azida Mohd Nasir****).*

1.4 Experimental models of wound healing

Before a treatment can be translationally used on patients, researchers have to carry out various experiments at the laboratory phase to gain a better understanding of the basic wound healing mechanism. Presented here are the experimental models of wound healing used in laboratory: *in vitro*, *ex vivo* and *in vivo* using animal or human cells or/and skin. Some researchers will start their experiment using *in vitro* models which may consist of a simple and inexpensive assay, yet reliable and reproducible such as a scratch assay (Liang *et al.*, 2007, Chen *et al.*, 2014, Ueck *et al.*, 2017, Schenck

et al., 2017). The assay is performed on monolayer cells in culture using the tip of pipette (or sharp edge) to remove a strip of cells, thus leaving a gap (Liang *et al.*, 2007). Cells from the gap edges cells migrate towards the gap centre thus mimicking epidermal migration seen in the *in vivo* and *ex vivo* models. The scratch wound closure can be assessed either by the percentage of wound closure or number of cells migrating into the gap/wound (Liang *et al.*, 2007, Schenck *et al.*, 2017).

Given the limited physiological and clinical relevance of the scratch assay, researchers have complemented it by establishing the skin equivalent and gel contraction assays. The skin equivalent (also known as reconstituted skin cultures) normally consists of a few layers of epidermal keratinocytes with dermal substitutes but a lacking inflammatory cells, nerves and blood vessels (Egles *et al.*, 2010, Safferling *et al.*, 2013, Herman and Leung, 2009, Yildirimer *et al.*, 2017). The skin equivalent model used for wound healing study displays epithelial migration across the wound bed which results in wound closure (Safferling *et al.*, 2013, Egles *et al.*, 2010). In contrast, the gel contraction assay is done by culturing cells inside collagen and the assessment is carried out by the percentage of gel contraction or surface area (Elgharably *et al.*, 2013, Hashimoto *et al.*, 2018, Ngo *et al.*, 2006).

In vitro models by monolayer or bilayer of cells (same or different cells) allow direct quantitative investigation on specific cells in wound healing but the *in vitro* model incorporated with dermal substitute enhances the results, generating more information (Ud-Din and Bayat, 2017).

Other options exist in terms of wound healing models. The *ex vivo* skin organ culture model offers more advantages compared to the *in vitro* assays mentioned above. This

model can be created from animal (Meier *et al.*, 2013, Ueck *et al.*, 2017) or human skin (Kratz, 1998, Mendoza-Garcia *et al.*, 2015, Xie *et al.*, 2010, Xu *et al.*, 2012). Human skin *ex vivo* organ culture offers more advantages in terms of the whole skin structure, containing various cells including mast cells, inflammatory cells, Langerhans cells, Merkel cells and others (Kratz, 1998, Egles *et al.*, 2010).

In the past 20 years, wounded human skin organ culture has become an invaluable tool to understand basic mechanisms of human wounds in translational pre-clinical studies (Kratz, 1998, Stojadinovic and Tomic-Canic, 2013, Xu *et al.*, 2012, Meier *et al.*, 2013, Mendoza-Garcia *et al.*, 2015, Tomic-Canic *et al.*, 2007). Kratz shows that *ex vivo* skin models can be used to study different wound types including burn wounds (Kratz, 1998), while Ueck et al., and Meier et al., suggest that *ex vivo* pig (Ueck *et al.*, 2017), frog and human (Meier *et al.*, 2013) skin can be used for drug screening and develop porcine *ex vivo* hyperglycaemic wound healing model (Ueck *et al.*, 2017). The *ex vivo* models evaluate more than just one cells type but also the surrounding cells and tissue following the application of test agents or experimentally induced changes in growth/culture conditions (Ud-Din and Bayat, 2017). Furthermore, the skin substitute and *ex vivo* human skin assay can reduce the use of animals in experiments (Stephens *et al.*, 2013, Andrade *et al.*, 2015, Ansell *et al.*, 2012).

Animal study is still the best option to carry out *in vivo* wound healing experiments despite the well-known controversies surrounding animal work in order to at least approximate the very complex, clinically relevant human wound healing conditions *in vivo* (Dunn *et al.*, 2013, Ansell *et al.*, 2014, Moreira *et al.*, 2015, Wong *et al.*, 2011, Dovi *et al.*, 2003, Grada *et al.*, 2018).

However, animal models also have important limitations. Firstly, even animal skin, like pig skin that provides the greatest level of morphological similarity to human skin, still shows major differences in anatomy, physiology, microbiology and drug responses. The pig is also expensive to manage requiring surgically and anaesthesiologically skilled researchers (Seaton *et al.*, 2015). While mice are easier and cheaper to manage the skin structure i.e. the existence of the *panniculus carnosus* muscle is quite different from that of humans (Driskell *et al.*, 2014, Nicu *et al.*, 2018), therefore results obtained from mouse experiments routinely require confirmation in the human system before the results generated with them can be accepted as clinically relevant reach a translational status (Grada *et al.*, 2018, Gerber *et al.*, 2014).

1.5 Wound healing assessment

Systematic and standardised wound assessment is vital to monitor the healing process. Through the assessment it can indicate if the wound is healing or progressing towards a chronic wound status so that appropriate countermeasures can be prepared. Wound assessment can also be used indirectly to monitor the efficacy of therapies used as a treatment so that the time required for healing can be predicted (Meaume and Humbert, 2017, Gethin, 2006).

In a clinical setting, initial assessment is done on the skin surrounding the wound site, appearance of erythema, rubour, colour or dolour because these can all be indicators of wound infection (Kramer *et al.*, 2018, Frantz, 2005). Further inspection will be on the wound exudates (quantity and quality). Patients are also asked if they experience any pain and itchiness at the wound site. Appearance of the wound area itself is

important whether it is filled with healthy tissue or necrotic tissue (Jones, 2018, Frantz, 2005).

In term of wound closure assessment, the standard assessment for wound closure or re-epithelialisation in clinical trials (including *in vivo* models) is normally assessed using a transparent grid film (acetate tracing) where it is placed on the wound surface and the wound edge is traced. This is then followed by counting the grid box to know the changes in wound area, or by photographs with a ruler on the wound surface to calculate the wound dimension based on length and width (Plassmann, 1995, Gethin and Cowman, 2006, Chang *et al.*, 2011, Samad *et al.*, 2002, Meaume and Humbert, 2017, Zhang *et al.*, 2018). Continuing from this assessment, punch biopsy (might be obtained in clinical trials) and wound excision (in animal study) can be assessed by histology.

The assessment using grid paper is similar with planimetric techniques, however the use of this grid paper is believed to interrupt or damage the new epithelial layer (Gethin and Cowman, 2006) and it is impossible to recognise a thin layer of new epithelial layer by naked eye.

In contrast, histology assessment is widely accepted as a gold standard to assess wound re-epithelialisation. It can be done by measuring a single-plane tissue section (centre of the wound)(Ueck *et al.*, 2017) or by measuring multiple sections within the same wound, (Safferling *et al.*, 2013) or by measuring the whole wound tissue section from the same wound (Wang *et al.*, 2016). Assessment by one or multiple tissue sections will only provide relative wound closure. The histological assessment on wound closure/re-epithelialisation is normally conducted by measuring the distance

between wound edges or measuring the distance of new epithelial tongue migration on a one-plane tissue section (Gupta and Kumar, 2015). Since the result only comes from one plane of the tissue section, it is highly unlikely that it is an accurate method to measure the whole wound closure. Researchers know that wounding occurs in different shapes and at distinct depths, and healing also does not happen in a uniform pattern even within the same wound (Figure 1.5) and (Glinos *et al.*, 2017). Based on Figure 1.5 it is impossible to point out where exactly the wound centre lies, or from which side the section should be made.

Therefore, it is better to measure the wound closure or re-epithelialisation in planimetry and some more in real time manner to obtain accurate results. In a recent study by (Glinos *et al.*, 2017), the use of optical coherence tomography adds a new flavour to wound healing assessment in laboratory. The findings are very useful since they can measure and asses the wound re-epithelialisation *planimetry* longitudinally in a real-time manner. However, the apparatus used is very expensive. Several other different studies on *ex vivo* and organotypic or skin equivalent models reported the use of UV auto-fluorescence (Wang *et al.*, 2016), Magnetic Resonance Imaging (Lone *et al.*, 2015), infra-red and Raman spectroscopy (Pielesz *et al.*, 2017), and fringe projection for revealing wound topography (Ferraq *et al.*, 2007).

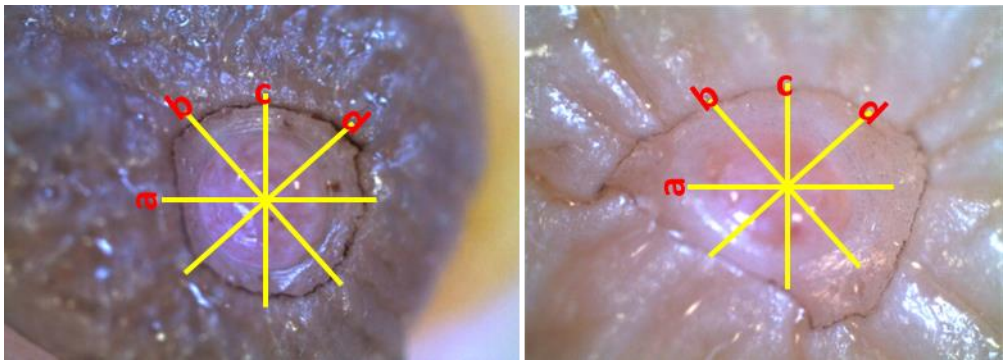

Figure 1.5: Representative images of wound closure in the ex-vivo model. *The new epithelised tissue can be seen using dissecting microscope but healing at the centre of the wound cannot be determined precisely. These images also show the irregularity of wound shape and hence one has to decide at which plane one would want to section the explant (Images by Nur Azida Mohd Nasir).*

1.6 Neurotrophins and their receptors in human skin

Neurotrophins (NT) are structurally- and functionally-related proteins promoting either neuronal or non-neuronal cell survival, differentiation or cell death (Levi-Montalcini and Angeletti, 1968, Levi-Montalcini *et al.*, 1954, Levi-Montalcini, 1987). NTs exist as either/both matured and pro-neurotrophins. Matured NTs comprise of noncovalent associated dimers of ~13500 Da protomers (Bothwell and Shooter, 1977) made of two pairs of antiparallel β-strands (as their backbone) which create an elongated shape and are stabilised by three disulphide bonds (Figure 1.6)(McDonald and Chao, 1995).

Nerve growth factor (NGF) was among the first growth factors discovered by the Levi-Montalcini study (Levi-Montalcini, 1987), whereas BDNF was found while experimenting on target-derived trophic factors that were needed for developmental

survival of neural crest-derived and placode-derived peripheral sensory neurons (Barde *et al.*, 1982). The other NT family members discovered later are NT-3 and NT-4. Neurotrophins mediate their action via tropomyosin-related kinase family and pan-75NTR neurotrophin receptor (p75NTR) (Huang and Reichardt, 2003). NGF most specifically binds to the high affinity receptor known as TrkA (~140 kDa (p140))(Kaplan *et al.*, 1991) and the low affinity receptor, p75-NTR (~75 kDa) (Raychaudhuri *et al.*, 2004, Pincelli *et al.*, 1994b, Johnson *et al.*, 1986, Chao and Hempstead, 1995) that also binds to other neurotrophins (Pincelli *et al.*, 1994a, Micera *et al.*, 2007, Chao and Hempstead, 1995). In contrast, NT-3 binds to TrkC while BDNF and NT-4 both bind to TrkB (Bothwell, 1995, Chao and Hempstead, 1995).

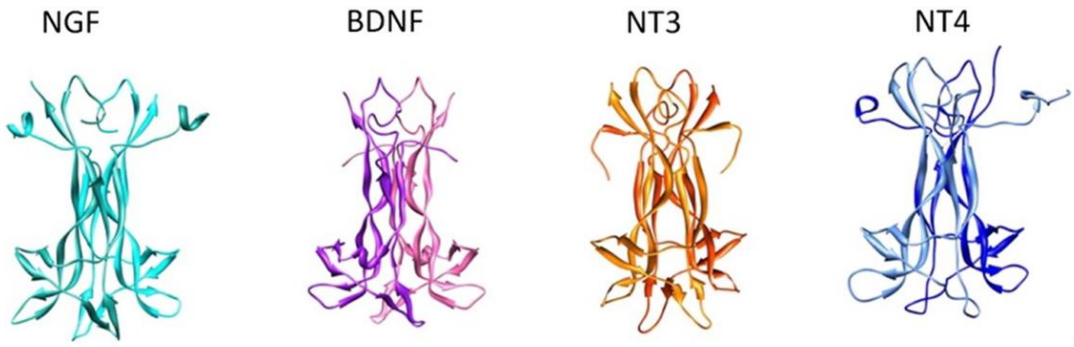

Figure 1.6: X-ray crystal structures of the neurotrophins. *The X-ray crystal structures of the neurotrophins. NGF (cyan), the BDNF (purple), NT3 (orange) and NT4 (blue). Image adapted from (Allen et al., 2013).*

1.6.1 Nerve growth factor

NGF has mainly been studied in neuronal development (Levi-Montalcini and Angeletti, 1968, Levi-Montalcini *et al.*, 1954), although this conventional belief about NGF has changed in recent years. The NGF molecule consists of three subunits of alpha, beta and gamma (α_2, β, γ_2: molecular weight 130kD)(Wiesmann and de Vos, 2001)(Figure 1.7) , however only the beta subunit (2.5S)(26.5 kDa) harbours biological activity (Levi-Montalcini, 1987, Sofroniew *et al.*, 2001).

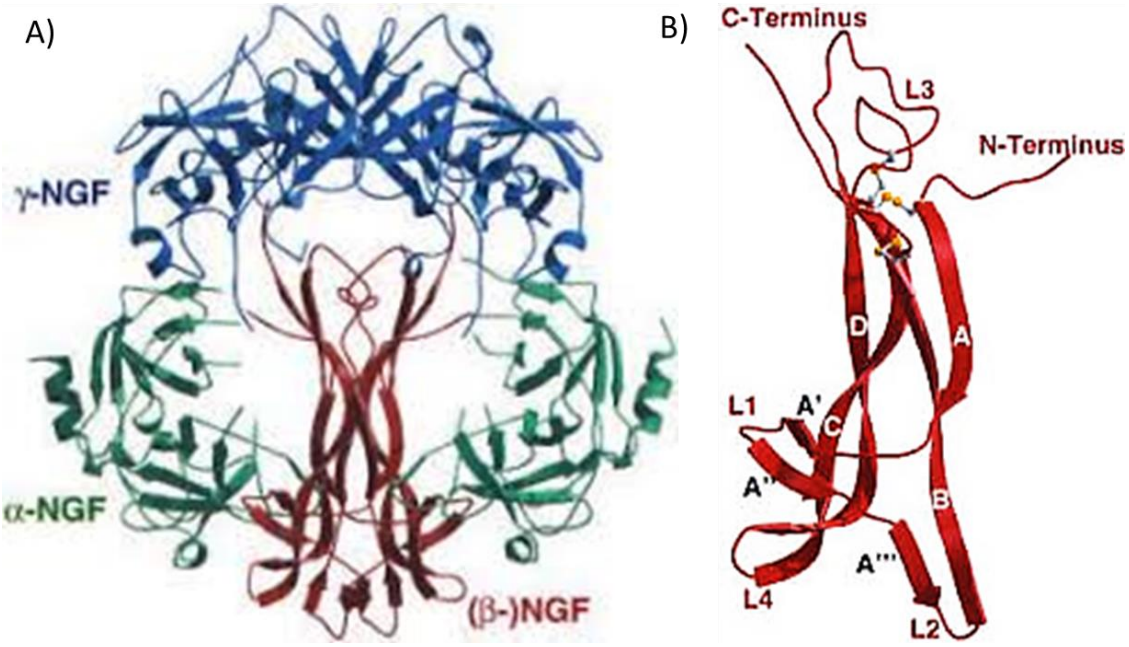

Figure 1.7: Structures of NGF and its high molecular weight and monomeric forms. *Ribbon diagram showing the structure of the 7S NGF complex (A). The dimer of β-NGF is depicted in red, two copies of α-NGF are shown in green, and two copies of γ-NGF in blue. Ribbon diagram depicting the structure of the NGF monomer (B). The secondary structure elements are labelled and depicted according to (McDonald et al., 1991). The termini as well the loop regions, L1-L4 are labelled in red, and the cysteine-knot motif near the top of the molecule are shown in gray and yellow ball-and-stick rendering (B). Images adapted from (Wiesmann and de Vos, 2001).*

In addition to its importance in neuronal system development, NGF also acts as a growth factor in non-neuronal cells across various tissues including skin (Sivilia *et al.*, 2008, Truzzi *et al.*, 2011, Botchkarev *et al.*, 2006) by promoting tissue morphogenesis, regulating proliferation and HAS direct involvement in tissue repair (Botchkarev *et al.*, 2004, Sariola, 2001, Paus *et al.*, 1994, Hirose *et al.*, 2016) as well as in immunology (Otten *et al.*, 1994). Many other studies have reported that inflammatory cells are capable of synthesising and releasing NGF (Leon *et al.*, 1994, Barouch *et al.*, 2000, Solomon *et al.*, 1998, Braun *et al.*, 1998, Raychaudhuri and Raychaudhuri, 2004, Sivilia *et al.*, 2008, Hasan *et al.*, 2006, Skaper, 2017).

NGF can be secreted by and/or detected by most cells in the skin (Pincelli *et al.*, 1994a, Murase *et al.*, 1992) because the skin itself is a well-known neurotrophic organ (Albers and Davis, 2007) since NGF acts through autocrine and paracrine loops (Di Marco *et al.*, 1993, Yaar *et al.*, 1991) as well as the neuroendocrine immune system (Sivilia *et al.*, 2008). NGF also has effects upon hair follicle morphogenesis (Botchkareva *et al.*, 1999, Botchkareva *et al.*, 2000) and a study by Adly and colleagues reported that NGF was expressed in the human epidermal scalp and hair follicle. Additionally, they also showed that NGF and TrkA was highly expressed in the anagen hair follicle (central region of the anagen hair follicle), sebaceous and sweat glands, but found at low levels in catagen or telogen phases. A recent study by (Blais *et al.*, 2013) shows that NT-3 and GDNF are expressed solely in epidermal cells, while NGF and BDNF were expressed in both epidermis and dermis.

Several studies showed the effect of NGF to enhance and accelerate wound healing in animals (Sivilia *et al.*, 2008, Lawman *et al.*, 1985, Kawamoto and Matsuda, 2004,

Chen *et al.*, 2014, Pincelli and Yaar, 1997, Cellini *et al.*, 2006, Li *et al.*, 1980, Costa *et al.*, 2002, Shi *et al.*, 2003, Blanco-Mezquita *et al.*, 2013, Chiaretti *et al.*, 2002) (Table 1), in human studies (Lambiase *et al.*, 1998, Landi *et al.*, 2003, Tuveri *et al.*, 2000, Generini *et al.*, 2004, Cellini *et al.*, 2006, Bernabei *et al.*, 1999, Bonini *et al.*, 2000) (Table 2) and *in vitro* studies (Chen *et al.*, 2014, Blanco-Mezquita *et al.*, 2013, Paus *et al.*, 1994, Schenck *et al.*, 2017)(Table 3).

A study conducted by Cellini *et al*. showed that NGF plays an active role in tissue remodelling and repair. It not only hastens wound repair of surgery to the cornea but recovers its surface sensitivity as well. It was reported that NGF was increased as well as TrkA. The NGF influence epithelial and keratinocytes proliferation, fibroblast migration and endothelial tropism to the wound area and reduce cellular apoptosis by inhibiting mitochondrial cytochrome C release hence accelerate healing (Cellini *et al.*, 2006).

Later, Sivilia *et al*., reported that NGF and p75 was increased during the inflammation (on day 21) after complete Freud's adjuvant (CFA) injection in rats then the expression decreased until it rose again on the 88th day. On the 21st day, the expression of NGF was higher followed by protein expression in cells in the dermis as well as in the epidermis cytoplasm of single cells or small cell clusters whereas, high expression on the 88th day is related to sensory neuropathy (Sivilia *et al.*, 2008).

The effect of NGF (topical application) on mouse and rat cutaneous wounds has been studied (Matsuda *et al.*, 1998, Chen *et al.*, 2014), and showed that NGF accelerates cutaneous wound healing. The Matsuda study also showed that NGF accelerates wound healing under both normal and diabetic conditions, whereas Chen et al.,

showed that NGF accelerates healing by promoting fibroblast migration to the wound site. This migration was stimulated by signalling pathways such as PI3K/Akt, JNK, and ERK. However, there is no study on neurotrophins and their receptors during human wound healing.

NGF was also reported to upregulate substance P (Skoff and Adler, 2006) and calcitonin gene-related peptide in neurons and mature sensory neurons (Lindsay and Harmar, 1989) and is highly increased in nerves in the inflammatory area (Pincelli and Yaar, 1997, Shi *et al.*, 2013). The release of these neuropeptides during inflammation can induce mast cells to secrete histamine as well as dilate the blood vessels which cause tissue oedema (Theoharides *et al.*, 2012). This may indicate that NGF is involved in the inflammatory stage of wound healing as well. The study by (Burbach *et al.*, 2001) shows that treatment with substance P and neurokinin A promotes increased NGF expression in human and murine keratinocyte cultures. The study conducted by (Galkowska *et al.*, 2006) suggested that the insignificant differentiation in expression of SP, CGRP, fibroblasts and leukocytes in ulcer tissue causes reduction in recruitment of immune cells and consequently impairs the formation of granulation tissue.

1.6.2 Brain derived neurotrophin factor

The brain-derived neurotrophic factor (BDNF) was discovered by (Barde *et al.*, 1982) whilst they were searching for NGF target-derived trophic factor. Even though BDNF is widely expressed in mammalian tissues, there are very few studies on BDNF and human skin. BDNF has mostly been studied for its role in promoting nerve healing (Lopatina *et al.*, 2011) and touch, dome study as well as its effect upon hair follicle

innervation (Albers *et al.*, 1996). A study by Botchkareva et al. (2000) identified that BDNF was prominently expressed in keratinocytes of the hair plug and in the basal epidermal keratinocytes during hair follicle morphogenesis and within the hair follicle itself (Botchkareva *et al.*, 2000). BDNFs are expressed in the developing skin, influence the development and survival of specific types of sensory afferent by activating the TrkB receptor. A mouse study where BDNF was overexpressed in the developing skin exhibited increased hair follicle innervation, Meissner corpuscle size and Merkel cell number (LeMaster *et al.*, 1999). Another study on BDNF carried out by (Rössing *et al.*, 2011) shows that serum BDNF concentrations and protein expression (IHC) were significantly elevated in patients with chronic urticaria compared to normal skin.

1.6.3 Neurotrophin 3

After the discovery of NGF and BDNF, researchers noticed that some conserved regions of NGF and BDNF transcripts can be used to create new primers that allow joint amplification; both NGF and BDNF sequences were amplified by polymerase chain reaction and thus, an additional neurotrophin member was discovered called neurotrophin 3 (NT-3) (Hohn *et al.*, 1990, Jones and Reichardt, 1990). NT-3 works specifically through its high-affinity receptor TrkC but sometimes it can interact via TrkA and B at a low affinity (Teng and Hempstead, 2004). NT-3 is highly expressed in ovaries, and is widespread in all human tissues (Ip *et al.*, 1992).

1.6.4 Neurotrophin 4

The youngest member of the neurotrophin family (Hallbook *et al.*, 1991, Berkemeier *et al.*, 1991), Neurotrophin-4 (NT-4; also called NT-4/5 or NT-5) shares the same high

affinity receptor with BDNF which is TrkB (Klein *et al.*, 1992). Studies on the distribution of NT-4 in human tissue showed that highest levels can be found in prostate, while lower levels can be found in thymus, placenta, skeletal muscle and testis, with no presence in brain tissue (Ip *et al.*, 1992). A murine study showed that overexpression of NT-4 can increase sensory innervation to dermal papillas of the foot pad, hair follicles and Meissner corpuscles (LeMaster *et al.*, 1999).

1.6.5 Neurotrophin Receptors

The tropomyosin-related tyrosine kinase (Trk) is a neurotrophin receptor discovered from a colon-derived oncogene (Kaplan *et al.*, 1991, Martin-Zanca *et al.*, 1986). This receptor is involved in many aspects of cell development, survival, differentiation and migration in neuronal (Deinhardt and Chao, 2014) or non-neuronal tissues (Kermani and Hempstead, 2007). Trks are activated by ligand-induced formation of non-covalently associated receptor dimers (Jing *et al.*, 1992) and bind neurotrophins with high affinity and specificity. The NGF/TrkA complex is formed when the ratio is 2:2, TrkA/NGF/p75NTR, 1:2:1, NGF/p75NTR, 2:1 and finally, p75NTR can form a homodimer without the ligand (Figure 1.8)(He and Garcia, 2004).

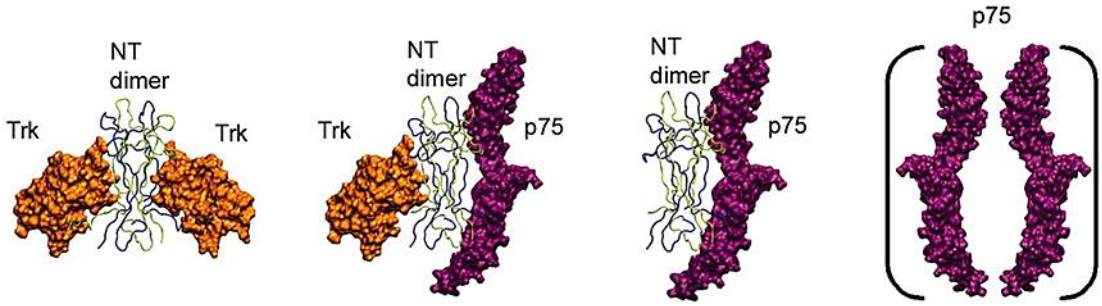

Figure 1.8: The neurotrophin-receptor complexes*. Diagram of various neurotrophin, p75, and Trk receptor complexes, including potential model of p75–Trk–neurotrophin trimolecular complex. NGF is depicted as tubes, and the receptors are depicted as surfaces. From high to low TrkA/p75 ratio, the complex could choose to be 2:2 NGF/TrkA, 1:2:1 TrkA/NGF/p75, 2:1 NGF/p75, and finally an unliganded p75 dimer. Modified from (He and Garcia, 2004).*

There are three Trk neurotrophin receptors: TrkA, TrkB and TrkC. The function between neurotrophins-receptors are carried out through major signalling cascades i.e. the mitogen-activated protein kinase (MAPK), phospholipase Cγ (PLC PLCγ), extracellular signal-regulated kinase (ERK) and phosphatidylinositol 3-kinase (PI3K) pathways (Beattie *et al.*, 2000, Paoletti *et al.*, 2009, Chetty, 2019).

In contrast, p75NTR regulates three other signalling pathways: NF-κB, Jun kinase pathways (JNK) and Rho (Meakin and Shooter, 1992, Mohamed and El-Remessy, 2015, Allen *et al.*, 2013). These signalling pathways are involved in transcription, translation and trafficking of proteins (Bothwell, 1995, Yoshii and Constantine-Paton, 2010, Segal, 2003).

1.6.5.1 Tyrosine kinase receptor type A

The tyrosine kinase receptor A (TrkA) also known as neurotrophin receptor kinase (NTRK1) is a high affinity receptor for NGF (Segal, 2003). This type I transmembrane protein was discovered by merging tropomyosin into tyrosine kinase domain in

colon cancer-derived oncogene (Martin-Zanca *et al.*, 1986).The organisation of TrkA structure consists of an extracellular (N-terminus) and intracellular domain (C-terminus). The extracellular domain is important for ligand binding consisting of immunoglobulin-like domain and two cysteine-rich domains that flank a leucine-rich motif (Wiesmann *et al.*, 1999, Jullien *et al.*, 2002).

Several signalling cascades can be activated when NGF binds to TrkA (Figure 1.8); The mitogen-activated protein kinase (MAPK), phospholipase Cγ (PLC PLCγ), extracellular signal-regulated kinase (ERK) and phosphatidylinositol 3-kinase (PI3K) pathways (Beattie *et al.*, 2000, Paoletti *et al.*, 2009, Chetty, 2019, Allen *et al.*, 2013).

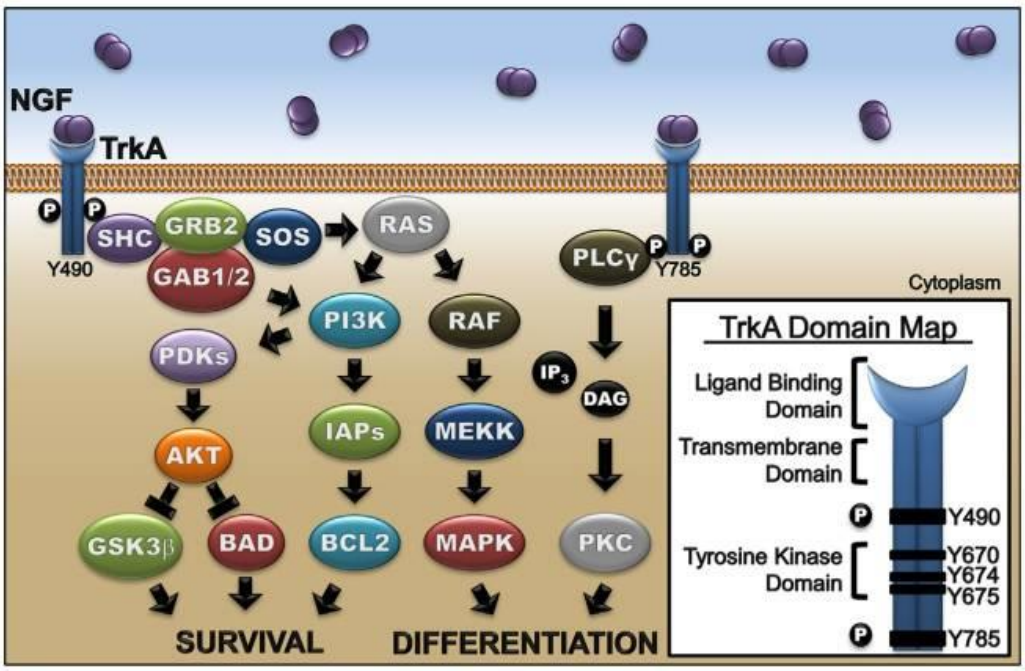

Figure 1.9: NGF/TrkA signal transduction pathways in survival and differentiation of neurons. *TrkA (blue bars) signaling is best characterized for activation of MAPK, PI3K and PLC γ pathways mediated mainly by the phosphorylation (black spheres) of two tyrosine residues in the cytoplasmic domain, Tyr490 (Y490) and Tyr785 (Y785). NGF dimers (purple spheres) bind to the extracellular ligand-binding domain of two TrkA monomers promoting homodimerization, activation of the tyrosine kinase domain in the activation loop, and trans-phosphorylation of Y490 and Y785. Phosphorylation of these residues recruits pro-differentiation and pro-survival adaptor and signaling molecules and activates the SHC-Ras-MAPK, PI3K-AKT, and PLCγ-PKC signaling pathways. Figure adapted from (Marlin and Li, 2015).*

In normal skin, TrkA mRNAs are highly expressed in basal epidermal cells, and dispersed throughout the granular and spinosum layer of epidermis (Terenghi *et al.*, 1997, Pincelli *et al.*, 1997), hair follicles, skeletal muscles and sweat glands (Shibayama and Koizumi, 1996). In contrast, in glabrous skin TrkA protein expression is primarily located in the stratum basale and throughout the epidermis, sweat glands, blood vessel walls (muscular layer), Schwann and perineurial cells and periaxonic cell (Meissner's and Pacini's corpuscles), nerve bundles and sensory corpuscles (Bronzetti *et al.*, 1995). In scalp skin, TrkA protein is well-known to be expressed in the epidermis and hair follicle (Adly *et al.*, 2006). Study by (Micera *et al.*, 2001) showed that TrkA protein expression is detected in lung tissue as well as skin.

In diabetic skin, the expression of TrkA mRNAs is higher throughout the epidermis compared to normal skin (Terenghi *et al.*, 1997). This result suggests that the upregulation of TrkA occurs as a result of a decreased activity in autocrine neurotrophins.

1.6.5.2 Tyrosine kinase receptor type B

The tyrosine kinase receptor type B (TrkB) or neurotrophin receptor kinase 2 (NTRK2) is a high-affinity receptor for BDNF and NT-4 (Klein *et al.*, 1992, Segal, 2003). TrkB is a key factor for neural differentiation and cell survival (Allen *et al.*, 1999). In the skin TrkB is present in the basal and upper (granular) layers of the epidermis (Shibayama and Koizumi, 1996). It was also shown to be expressed in diseased skin such as chronic urticarial as well as normal skin (Rössing *et al.*, 2011). During hair follicle morphogenesis, TrkB is expressed in keratinocytes of the hair plug and epidermis

(hair morphogenesis stage 1-2), in the developing ORS (hair morphogenesis stage 5-6), strictly in the distal ORS, dermal papilla fibroblasts and hair matrix (hair morphogenesis stage 7-8) (Botchkareva *et al.*, 2000). Peters *et al*., suggests that TrkB –mediated signalling promotes the switch between anagen and catagen via TGFβ2 (Peters *et al.*, 2005).

1.6.5.3 Tyrosine kinase receptor type C

The tyrosine kinase receptor type C (TrkC) or neurotrophic receptor tyrosine kinase 3 (NTRK3) is a high-affinity receptor for NT-3 (Segal, 2003). In neurons, TrkC receptors are expressed by larger-size neurons compared to TrkA which is expressed in small-sized unmyelinated neurons (Moqrich *et al.*, 2004). In the skin TrkC is present in the basal and upper (granular) layers of the epidermis (Terenghi *et al.*, 1997, Shibayama and Koizumi, 1996) and skeletal muscle (Shibayama and Koizumi, 1996). Terenghi et al., also demonstrated that TrkC mRNA is expressed at higher levels within diabetic skin. During hair follicle morphogenesis, TrkC and NT-3 are expressed by follicular keratinocytes and the dermal papilla (Botchkarev *et al.*, 1998). Further investigation by Botchkarev et al. (2000) supports the involvement of TrkC in hair follicle maintenance since TrkC is co-expressed with p75NTR and gradually disappears during the transition from anagen to catagen (Botchkarev *et al.*, 2000).

1.6.5.4 p-75 neurotrophin receptor (p75NTR)

P75-NTR is a low-affinity receptor that binds to all neurotrophins with low affinity and specificity but p75NTR is also the high affinity receptor for proNGF. The p75NTR was identified from tumour necrosis receptor superfamily long before Trks were discovered (Johnson *et al.*, 1986). p75NTR is built up from four cysteine-rich motifs,

a single transmembrane domain and cytoplasmic domain including 'death' domain which is a specific feature for TN receptor superfamily members (He and Garcia, 2004). As per its family name (TN), NGF/p75NTR is mostly known to activate the apoptosis signalling cascade (cell death programming) but this receptor is also able to regulate and increase the affinity of Trk receptors for individual neurotrophins (Bothwell, 1995, Chao and Hempstead, 1995, Bibel *et al.*, 1999, Zaccaro *et al.*, 2001, Chao, 1994, Negrini *et al.*, 2013). The ligand-receptor NGF/p75NTR can activate 2 major signalling cascades: nuclear factor-κB (NF-κB) and c-Jun kinase (JNK) (Figure 1.10), which can subsequently activate either gene transcription or programmed cell death through their different signalling branches (Meakin and Shooter, 1992, Mohamed and El-Remessy, 2015).

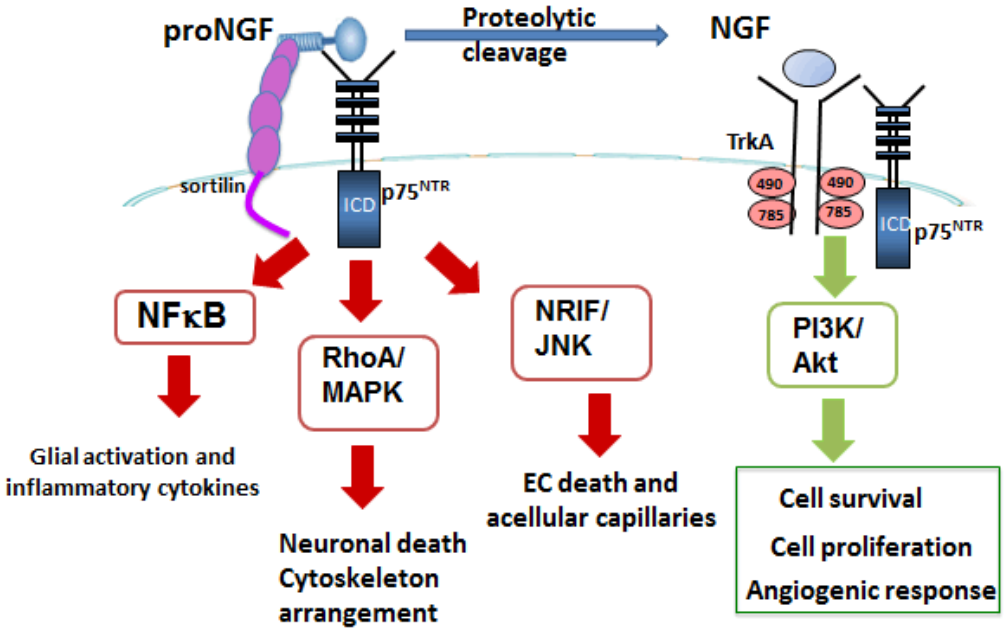

Figure 1.10: Schematic representation of the multiple pathways of proNGF/NGF and NGF/Trka/p75NTR signaling pathways. *Mature NGF binds to tyrosine kinase TrkA receptor in combination with p75NTR causing autophosphorylation of TrkA receptor and activation of P13K/Akt pathway leading to cell proliferation, cell survival and angiogenic response. ProNGF preferentially binds to p75NTR, in combination with its co-receptor sortilin, to activate multiple pathways depending on the interaction of the intracellular domain (ICD) and a given adaptor protein. Interaction of p75NTR ICD with NFkB results in activation of proinflammatory cytokine production. Interaction of ICD with RhoA/MAPK pathway resulting in neuronal death, cytoskeleton arrangement and BRB breakdown. Interaction of the ICD with the neurotrophin interacting factor (NRIF) will activate c-Jun kinase (JNK) resulting in endothelial cell (EC) apoptosis and formation of acellular capillaries, surrogate marker of ischemia. Adapted from (Mohamed and El-Remessy, 2015).*

Interestingly, p75NTR is the first growth factor receptor expressed by fibroblasts in the murine hair bulb before it differentiates into dermal papilla cells (Botchkareva *et al.*, 1999). It has also been shown that p75-NTR plays a negative role in hair morphogenesis. Adly and colleagues found p75-NTR expression to reside within human epidermis scalp skin as well as hair follicles (Adly *et al.*, 2010). Contrastingly, in human glabrous skin p75NTR protein is localised primarily in the stratum basal and sweat glands, Schwann and perineurial cells and periaxonic cell (Meissner's and Pacini's corpuscles), nerve bundles and sensory corpuscles (Bronzetti *et al.*, 1995). A study by Botchkarev et al. (2006) showed that p75-NTR is expressed in mouse and human skin (Botchkarev *et al.*, 2006) and p75NTR signalling is critically important for apoptosis as well as in modulating catagen phase (Botchkarev *et al.*, 2000).

1.7 The role of neurotrophins and its receptors on wound healing

Wound healing is a research topic of worldwide interest. A multitude of studies have been carried out to find the best wound treatments i.e. drugs, dressing or gene therapy and wound management strategies (Enoch *et al.*, 2006, Yamaguchi and Yoshikawa, 2001, Halim *et al.*, 2018, Ansell *et al.*, 2014, Gethin, 2006, Loeb, 1919, Martin, 1997). Among those studied treatments for wound healing there is nerve growth factor (NGF). It has been underestimated or ignored as a potential key factor in wound healing (Eming *et al.*, 2014, Gurtner and Chapman, 2016, Harn *et al.*, 2017, Moore *et al.*, 2018), despite the substantial evidence for NGF being beneficial for promoting wound healing in humans (Tuveri *et al.*, 2000, Bernabei *et al.*, 1999) and animals (Muangman *et al.*, 2004). For example, Matsuda et al., showed that NGF provides beneficial effects for wound healing in diabetic impaired and normal mice

while Muangman et al., reported that only diabetic mice may benefit from NGF treatment to achieve faster wound healing.

Previously, *in vitro* (scratch assay) and *ex vivo* studies (Table 1.1) have shown that NGF treatment accelerates migration as well as promoting cell proliferation. A recent study carried out by Schenck et al., demonstrates that recombinant human NGF (rhNGF) accelerates wound healing by promoting human oral mucosal proliferation and migration (Schenck *et al.*, 2017). The same effect of NGF treatment was reported on telomerase-immortalised human corneal epithelial cells (HCLE) (Blanco-Mezquita *et al.*, 2013). Meanwhile, dermal fibroblasts in a culture scratch assay showed that NGF induces cell migration but not proliferation (Chen *et al.*, 2014), whereas an *ex vivo* study on mouse skin also showed that NGF treatment stimulated epidermal proliferation (Paus *et al.*, 1994). However, the effective dose of NGF used in various scratch assays was highly varied (between 50 – 250 ng/mL) and the differential effects reported may be dependent on cell types and densities.

The efficacy of NGF in accelerating wound healing was also demonstrated in animal studies (Table 1.2). The effect of NGF was further explored in animal studies not just in normal healing, but also in impaired healing experienced by diabetic subjects. The study conducted by (Chen *et al.*, 2014) demonstrates that topical treatment of 10-20 µg of NGF applied daily accelerate cutaneous wound healing in rats. They also showed that NGF promotes migration of epidermal keratinocytes (re-epithelialisation) resulting in thicker granulation tissue as well as an increase in collagen content. Another study on rats also showed that wounds treated with NGF incorporated in collagen gel healed faster than the control group (Nithya *et al.*, 2003).

The effectiveness on NGF was also tested in hens' corneal wound healing as a result of laser ablation; encouragingly, NGF treatment accelerates corneal epithelium migration and enhances proliferation faster compared to control groups (Blanco-Mezquita *et al.*, 2013).

There are a few studies that investigate the effect of NGF upon wound healing in mice (Li *et al.*, 1980, Matsuda *et al.*, 1998, Muangman *et al.*, 2004, Shi *et al.*, 2003). Matsuda et al., and Muangman et al., both studied the roles of NGF in impaired wound healing in diabetic mice. Their findings showed the beneficial effects of NGF in treating diabetic wound healing. In addition, Muangman et al., also found that NGF treatment did not benefit normal wound healing in mice. NGF has also been proven to stimulate beneficial healing in combined injuries in mice. Irradiated and wounded mice that were treated with NGF either topically or administered intraperitoneally displayed significantly accelerated wound healing and enhanced survival (Shi *et al.*, 2003).

In the early 1980s, one group has reported the beneficial effect of high molecular weight (HMW) NGF in sialodenectomised wounded mice which showed accelerated wound healing (Li *et al.*, 1980). A different experiment also showed that dose-dependent NGF administration induces and accelerates cellular events that are associated with wound healing. They suggested that this might be due to the chemotactic effect of NGF upon inflammatory cells (Lawman *et al.*, 1985). The effects of NGF spawn across different species; for instance, NGF has been reported to improve lameness in goats, a condition that is associated with cutaneous ulcers, abscesses and granulomas. Therefore, topical application of NGF to the ulcers not

only promoted ulcer healing but also improved quality behaviour of these goats (Costa *et al.*, 2002).

Tables 1.1 and 1.2 show the various uses NGF *in vitro* and in some mammals to treat wound healing. However, it remains unclear whether and to which extent NGF treatment affects epidermal repair in wounded human skin.

Limited clinical evidence suggests that local administration of NGF accelerates the repair of corneal ulcers and promotes the recovery of corneal surface sensitivity (Cellini *et al.*, 2006, Aloe *et al.*, 2008, Lambiase *et al.*, 2007, Lambiase *et al.*, 1998).

Previously published evidence in support of NGF as a promoter of human skin wound healing is based on small case report series or was sub-optimally controlled (Table 1.3). Moreover, these studies exclusively assessed the overall healing outcome, not specifically epidermal repair, and did not examine how the expression of NGF and its receptors changes during normal and pathological human skin wound healing as a consequence.

Case reports on the use of NGF have mainly focus on treating diabetic ulcers or chronic wounds (Bernabei *et al.*, 1999, Generini *et al.*, 2004, Landi *et al.*, 2003, Tuveri *et al.*, 2000). Their reports demonstrated that NGF accelerates wound healing but in a case report by Generini et al., the healed wound can relapse after treatment and NGF is not beneficial to treat wounds found in systemic sclerosis patients This might suggest that the action of NGF is selective and not suitable for use in all wounding scenarios. One randomised double-blinded placebo control trial showed that NGF significantly reduced the ulcer area in a pressure ulcer. However, this study was insufficiently controlled with basic salt solution as placebo and the patients' in the

trial were elderly, conditions that might favour the action of NGF compared to a younger cohort.

In a single human case study, NGF promoted skin re-vascularisation in a child with crush syndrome (Chiaretti *et al.*, 2002), in line with NGF's recognised effects of promoting vascular endothelial growth factor and neo-vascularisation in rodents (Calza *et al.*, 2001).

1.8 Impact of wound care on patient's lifestyles and economics

Research on wound healing remains important because delayed wound healing has a great impact on patients' health and lifestyles, while economically it is a strain on healthcare providers (Olsson *et al.*, 2019). In the UK it is estimated that £5.3 billion is spent by the NHS on wound care annually (Guest *et al.*, 2015, Phillips *et al.*, 2016, Guest *et al.*, 2017), which is in the context of an entire NHS budget of around £120 billion (https://fullfact.org/health/spending-english-nhs/). Meanwhile, the United States, spends more than US$25 billion annually on wound treatment (Sen *et al.*, 2009, Nussbaum *et al.*, 2018, Frykberg and Banks, 2015). The huge financial burden on patients and health systems might be reduced if one can find better treatments to hasten wound healing. Chronic wounds normally take many months to heal (Frykberg and Banks, 2015, Nunan *et al.*, 2014), so these in particular will result in significant ongoing costs such as regular dressing changes. For patients with chronic wounds there is a significant impact on their overall health and lifestyle (Goldberg and Beitz, 2010). For example, the non-healing wound might interfere with sleep due to the itchiness, pain and reduce mobility (Goldberg and Beitz, 2010, Gould *et al.*, 2015, Smith *et al.*, 2015). Moreover, the immobility and odour from a chronic wound

may lead to social isolation, which may impact on their mental wellbeing (https://www.england.nhs.uk/rightcare/wp-content/uploads/sites/40/2017/01/nhs-rightcare-bettys-story-narrative-full.pdf). Patients might also need to take medical leave, presenting a cost to their employer (InformedHealth.org[Internet], Update 2018 Jun 14).

Therefore, further basic science research is urgently required to understand what causes wounds to develop into chronic ulcers, and to uncover mechanisms that will promote repair. This will enable the development of better treatments that can improve quality of the patient's life and reduce the economic burden (Gould *et al.*, 2015).

Table 1.1: NGF treatment on wound healing in *in vitro* and *ex vivo* studies

Type of cells	Source of NGF	Treatment	Outcome	Refs.
Human oral mucosa keratinocyte	rhNGF-β	50 ng/mL	Healed-induced proliferation and migration	(Schenck *et al.*, 2017)
Human fibroblast	Unknown	100 ng/mL	Healed -Induced migration	(Chen *et al.*, 2014)
Telomerase-immortalized HCLE	Murine	250 ng/mL	Healed – induced migration and promotes proliferation	(Blanco-Mezquita *et al.*, 2013)
Mouse skin organ culture	Mouse	10 -200 ng/mL	Stimulated epidermal keratinocytes proliferation	(Paus *et al.*, 1994)

Table 1.2: NGF treatment on wound healing in animal studies

Species	Form of NGF	Wound Treatment	Normalised wound dose*	Length of treatment	Outcome	Refs.
Rats	Unknown (Likely produced recombinantly)	10, 20 or 40 µg/ dosed daily topically to dorsal skin	0.025-0.1 µg/mm^2	10 days	Accelerated healing with all doses though 10 and 20 µg/mL doses showed more pronounced effect	(Chen *et al.*, 2014)
Hens	Murine NGF	0.08 µg/wound, dosed 5 times daily for 5 days as drops. Study used a model of laser ablation injury to eye	1.41 x10^{-5} µg/mm^2	7 days	Accelerated re-epithelialisation and enhance proliferation	(Blanco-Mezquita *et al.*, 2013)
Mice	Murine	1, or 10 µg/dosed daily topically to dorsal skin wounds.	0.035-0.354µg/mm^2	30 days	Accelerated re-epithelialisation with high and low NGF doses in diabetic mice. No difference in non-diabetic mice.	(Muangman *et al.*, 2004)
Mice	Human placenta	50 µg/0.2 mL normal saline/ dosed daily intraperitoneal		5 days (Intraperitoneal)	Accelerated wound closure in wound healing and survival in irradiated mice	(Shi *et al.*, 2003)
Mice	Human placenta	250 µg/mL normal saline / dosed daily to dorsal skin		5 days (topical)	Accelerated wound closure in wound healing and survival in irradiated mice	(Shi *et al.*, 2003)
Rats	Murine	1 µg/1.2 mg collagen/cm2		10 days	Treatment group healed 1 week earlier than control group	(Nithya *et al.*, 2003)

Mice	Murine 2.5S NGF	1 µg dosed daily to dorsal skin wounds	0.051 µg/mm^2	3 days	Accelerated wound closure in both diabetic and non-diabetic animals.	(Matsuda *et al.*, 1998)
Goats	Mouse	1 µg/100 mL		3 weeks	Healed	(Costa *et al.*, 2002)
Mice	Murine HMW NGF	0.1 mL of 150 nM NGF injected into air sacs (chemotaxis model)	N/A as no skin wounds	3 days	Chemoattract to inflammatory cells	(Lawman *et al.*, 1985)
Mice	Murine HMW and 2.5S NGF	50 µL of 110µg/mL HMW NGF or 27 µg/mL 2.5S NGF. Dosed 12 hourly to dorsal skin wounds in sialoadenectomised mice.	0.11 µg/mm^2 HWW NGF or 0.027 µg/mm^2 2.5S NGF. Equivalent molar ratios were used	3 days	Accelerated wound contraction with HMW NGF but not 2.5S NGF	(Li *et al.*, 1980)

*normalised wound dose

Table 1.3: NGF treatment on wound healing in human studies

Types of wound	Source of NGF	Treatment	Days of treatment	Study type	Outcome	Refs.
Surgical wound on cornea	Murine	10 µg per eye, 4 times daily for 3 weeks	3 weeks	Clinical trial	Healed	(Cellini *et al.*, 2006)
Diabetic foot ulcer	Murine	2.5 µg/50µL/25mm^3	4 weeks	Case report (n=3)	Healed but relapse within 5-15 weeks after starting the treatment	(Generini *et al.*, 2004)
Pressure ulcer	Murine 2.5S NGF	50 µg/mL	6 weeks	*Randomised, double-blind, placebo control trial (n=36)	Reduction of ulcer area	(Landi *et al.*, 2003)
Crush syndrome	Murine	10 µg/mL	8 hourly/7 days	Case report (n=1)	Improve ischaemic skin revascularisation	(Chiaretti *et al.*, 2002)
Vasculitis ulcer	Murine	50 µg/day	8 weeks	Case report (n=8)	Ulcers healed in rheumatoid arthritis patients but failure to heal in systemic sclerosis patients	(Tuveri *et al.*, 2000)
Pressure Ulcer	Murine	200 µg/mL	15 days	Case report (n=1)	Reduced ulcer size	(Bernabei *et al.*, 1999)
Human corneal ulcer	Murine	200 µg/mL	34 – 56 days	Case report (n=12)	Healed the ulcers	(Lambiase *et al.*, 1998)

*Insufficiently controlled since NGF was compare with balanced salt solution only, number of patients and patients' age.

1.9 Hypothesis

As NGF and its cognate receptors are highly expressed in epidermal keratinocytes, and function to maintain skin homeostasis during inflammation (Sivilia *et al.*, 2008), the working hypothesis for this project is that NGF signalling is important for human wound re-epithelialisation to progress efficiently. Therefore, it is predicted that re-epithelialisation will be impaired when NGF signalling does not occur, while it may be accelerated when NGF signalling is enhanced.

Moreover, many different skin cell types (i.e. dermal, epidermal and immune) can produce and utilise NGF to regulate their activities (Botchkarev *et al.*, 2006; Pincelli *et al.*, 1994; Pincelli and Yaar, 1997), therefore the hypothesis is that NGF will act pleiotropically to affect many aspects of wound repair in addition to re-epithelialisation.

It is not fully understood why clinical trials in treating human wounds with NGF treatment did not yield consistent positive results even though this was achieved in *in vitro* and in animal studies (Chen *et al.*, 2014, Li *et al.*, 1980, Matsuda *et al.*, 1998, Muangman *et al.*, 2004, Paus *et al.*, 1994). There are several potential reasons for this including intrinsic differences between animals and humans, or that the preclinical models being used do not properly reflect the situation in chronic wounds. However, NGF signalling has never been examined in human wounds (acute or impaired), so it is not yet known if NGF signalling is altered in chronic wounds, or if there is high variability in levels of NGF in chronic wounds between patients.

The working hypothesis is that a proportion of chronic wounds are impaired by a lack of NGF signalling. If true, NGF may provide an effective treatment for some patients, namely those where NGF expression is impaired.

1.10 Aims of the study

Previous research using NGF as a wound treatment did not yield consistent results when used in humans, despite showing a strong positive effect in animals (Table 1.2). The last clinical trial on wound healing using NGF was conducted some 15 years ago (Generini *et al.*, 2004), with the topic of NGF in wound healing receiving little attention of late, with only one recent study by Schenck *et al.*, (2017) in human oral mucosa keratinocytes wound healing (*in vitro*). Therefore, the overarching aim of the project is to revisit the topic of NGF in repair, to determine if this once promising therapeutic candidate might yet prove beneficial for chronic wounds.

It would be unethical to manipulate patients to examine the as yet unclear effects of NGF and collect skin samples before and after treatment. Therefore, the 1st aim is to understand whether human skin wounded ex-*vivo*, could provide a model system to examine NGF effects and NGF-related test agents (though NGF has previously been tested in mouse skin organ culture (Paus *et al.*, 1994), its effects on human skin repair *ex vivo* remains to be examined in detail), and to determine the best way to analyse the data. If true, this model could be used and manipulated for NGF-related drug testing more generally.

The second aim is to characterise the normal protein expression pattern of NGF and its cognate receptors during human skin repair *ex-vivo* (this expression pattern is so far unknown in any human wound setting).

Previously *in vitro* and animal studies showed very promising data that NGF might accelerate repair, though this has not been corroborated in robust clinical trials. Thirdly, as its main aim, this study therefore also investigates the effect of manipulating NGF signalling on human epidermal repair *ex vivo*, either by adding excess exogenous NGF or blocking endogenous NGF/TrkA-mediated signalling.

Lastly, this PhD project also aims to assess whether adding exogenous NGF alters the intracutaneous protein expression level of the endogenous ligand itself and the protein expression of its cognate receptors.

1.10 Experimental design flow chart

Refer to flow chart

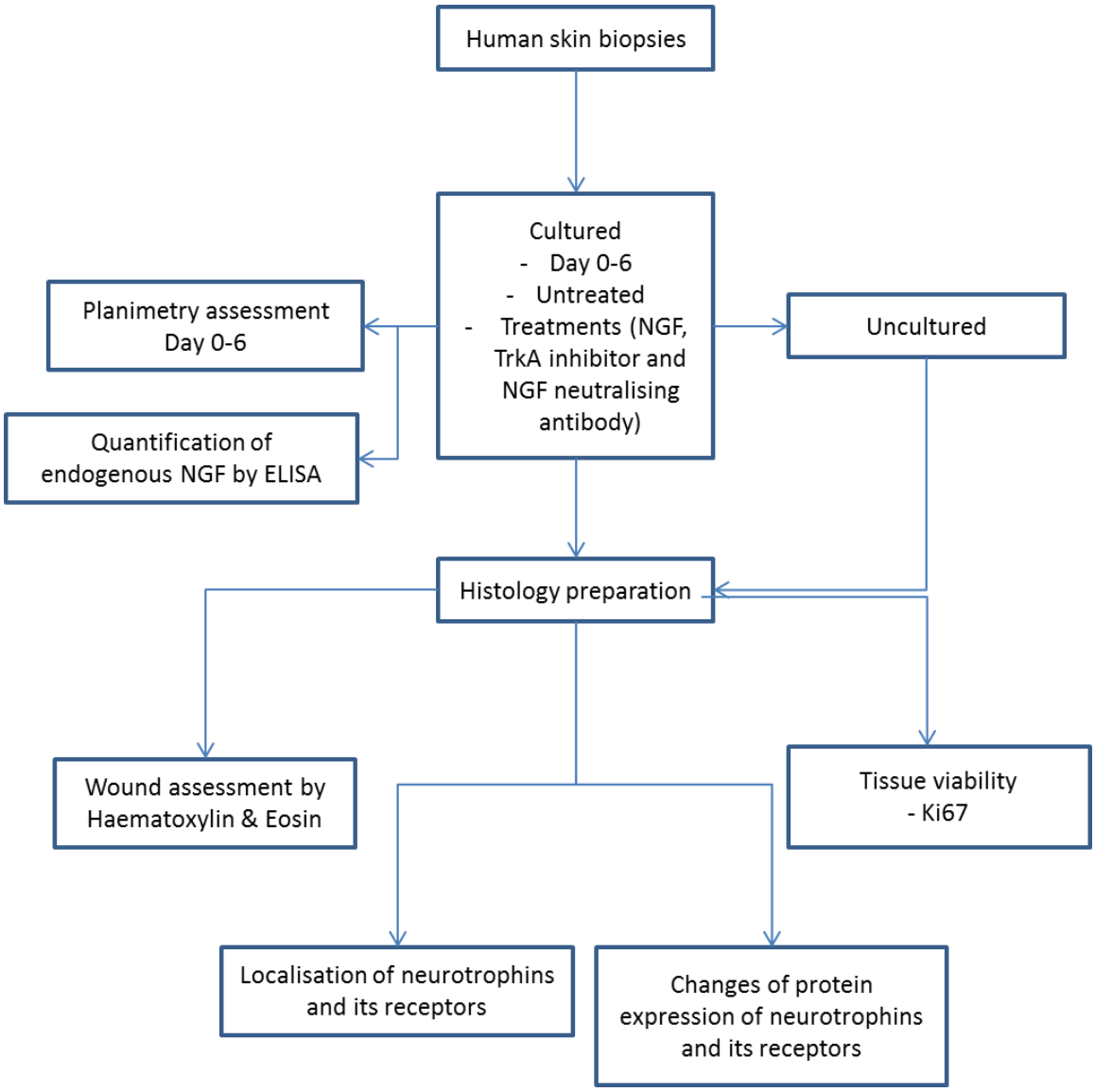
Human skin biopsies
Cultured
- Day 0-6
- Untreated
- Treatments (NGF, TrkA inhibitor and NGF neutralising antibody)
Planimetry assessment Day 0-6
Quantification of endogenous NGF by ELISA
Uncultured
Histology preparation
Wound assessment by Haematoxylin & Eosin
Tissue viability - Ki67
Localisation of neurotrophins and its receptors
Changes of protein expression of neurotrophins and its receptors

CHAPTER 2

MATERIAL AND METHODS

2.1 Human skin ethics

All human tissue was obtained through the Manchester Skin Health Biobank (NHS REC 14/NW/0185), from consented patients undergoing elective abdominoplasty surgery (Table xx: List of donors). This study has been reviewed and approved by the Manchester Skin Health Biobank steering committee. All paraffin embedded tissue was stored in the Paus Lab (Room 2.202) at the Stopford Building, University of Manchester in accordance with the Human Tissue Act legislation. Abdominal skin harvested from surgery was kept in transport media and transferred to the lab within 12-24 hours of tissue harvest and dissected in William's E medium.

Table 2.1: List of donors

MSHB No.	Donor no.	Date received	Date collection	Sex	Age/ Ethnicity/hospital	Skin type	Co-morbidity (if any)	Culture condition or treatment	Analysed/used for figure:
0724	1	19/11/15	18/11/15	Female	46/Caucasian/ Bradford	Abdominal		DMEM vs WE	Fig 3.1
0729	2	20/11/15	19/11/15	Female	46/Caucasian/ Bradford	Abdominal		WE w/wo serum	Fig 3.2-3.3
0751	3	03/02/16	02/02/16	Male	51/Caucasian/ Bradford	Abdominal		NGF	Fig 3.6 / Fig 3.21 / Fig 3.31 / Fig 3.33 / Fig 3.34 / Fig 3.37 / Fig 3.39
0807	4	06/05/16	06/05/16	Female	25/ Caucasian/ Bradford	Abdominal		Untreated	Fig 3.4-3.5
0887	5	13/09/16	12/09/16	Female	39 /Caucasian/Bradford	Abdominal		Untreated/NGF	Fig 3.7 / Fig 3.9 / Fig 3.10
0901	6	22/05/17	22/05/17	Female	Unknown/ Unknown/ MRI	Abdominal	Morbidly obese, Type 2 diabetes	NGF	Not analysed
0941	7	17/01/17	17/1/17	Female	36 /Caucasian/Bradford	Abdominal		NGF	Fig 3.12-3.14/Fig 3.18 / Fig 3.20-3.21 / Fig 3.31 / Fig 3.33-3.34 / Fig 3.37 / 3.39
0945	8	24/01/17		Female	38 /Caucasian/ Bradford	Abdominal		NGF	Fig. 3.12—3.20

0947	9	26/01/17	26/01/17	Female	43 /Caucasian//Bradford	Abdominal		NGF	Fig 3.12-3.2
0983	10	15/05/17	15/05/17	Female	Unknown/ Unknown/ MRI	Abdominal	Morbidly obese	K252a	Fig 3.20
0990	11	22/05/17	22/05/17	Female	55/ Unknown/ Bradford	Abdominal		NGF/NNA	Fig 3.27
1040	12	10/10/17	09/10/17	Female	43/ Unknown/ Bradford	Abdominal		K252a	Fig 3.10 / Fig 3.15-3.18 / Fig 3.20-3.21 / Fig 3.23-3.26
1069	13	13/12/17	12/12/17	Female	36/ Caucasian/ Bradford	Abdominal		K252a	Fig 3.20 / Fig 3.24
1088	14	08/02/18	07/02/18	Female	38 /Caucasian/Bradford	Abdominal		K252a	Fig 3.8 / Fig 3.15-3.21 / Fig 3.23—3.26 / Fig 3.34 / Fig 3.37 / Fig 3.39
1097	15	13/2/18	12/02/18	Female	Unknown/ Unknown/ MRI	Abdominal		K252a/NNA	Fig 3.15-3.20 / Fig 3.24 / Fig 3.27
1113	16	19/04/18	18/04/18	Female	47/ Caucasian/Bradford	Abdominal		Untreated-ELISA	Fig 3.28
0624		28/04/15	28/04/15		Unknown/ Unknown/Crown Clinic	Scalp			+ve control for immune staining
0629		05/05/15	05/05/15	Female	62/ Asian/Crown Clinic	Scalp			+ve control for immunostaining

2.2 Human skin organ culture

2.2.1 Wounded human skin explant preparation

Once skin arrived in the lab, the adipose tissue was excised and trimmed. Then, full skin thickness skin explants were made with a 6 mm punch biopsy (Steifel, UK) after a 2 mm partial thickness wound was created in the centre of the explant (Figure 2.1A). Skin explants were placed in 6 well culture dishes on top of sterile pads (Millipore, Merck, UK) in culture media (Life technologies, UK) (Figure 2.1B). Any explants with inconsistent of size (<2 mm>) or depth (which was identified by the appearance of adipose tissue inside the wound (Figure 2.1C) of wound were excluded prior to culture on day 0 or if found later (i.e. day 1). The skin explants were cultured at an air-liquid interface in the desired culture media in an incubator at 37°C with 5% CO_2. Part of the media inside each culture dish was removed and replaced with 1 mL fresh media every day. Only 1 mL of fresh media was added because absorbent pads already contained about 1 mL media. Samples were collected on day 1, 2, 3 and 6. Some explants were collected on day 0 as a control/normal skin sample.

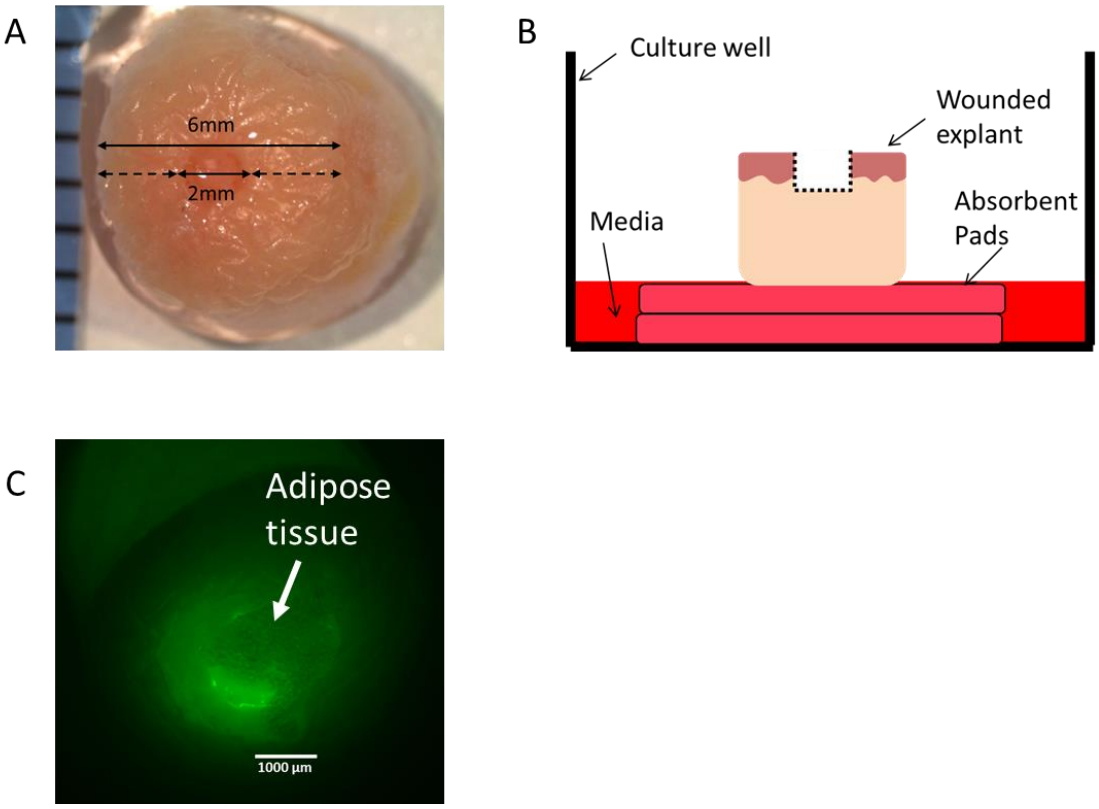

Figure 2.1: Wounded human skin organ culture and culture assay*. Six millimetres biopsy with 2 mm partial thickness wound in the centre (A). The skin was cultured in air-liquid interphase as shown in (B). Representative image of human skin explant with full-thickness wound at the centre (indicated by adipose tissue filling) (C).*

2.2.2 Culture Media

In an evaluation experiment, two different culture media were used. One media comprised William's E (WE) (Life technologies, UK) supplemented with 1% of Penicillin/Streptomycin (Life technologies, UK), 2 mM of L-glutamine (Life technologies, UK), 10 µg/mL of insulin (Sigma-Aldrich, USA), 10 ng/mL of Hydrocortisone (Sigma-Aldrich, UK). The other media was Dulbecco's Modified Eagle's Medium (DMEM) supplemented with 1% of Penicillin/Streptomycin (Life technologies, UK), 2 mM of L-glutamine (Life technologies, UK), 10 µg/mL of insulin (Sigma-Aldrich, USA), 10 ng/mL of Hydrocortisone (Sigma-Aldrich, UK).

For the rest of the experiment William's E media was used exclusively. To evaluate the utility of the *ex vivo* assay system, some groups were cultured in WE media supplemented with 10 % of Foetal Bovine Serum (FBS) (Life technologies, UK) to act as a known healing promoter (Nasir *et al.*, 2019, Pastar *et al.*, 2014b, Etxebarria *et al.*, 2017). For all test treatments and their respective vehicle controls, William's E media was used without serum in the culture system.

2.3 Intravital fluorescent dye tracers

2.3.1 Application of dye tracers and imaging

Throughout this study, 4 µL of 25µM 5-chloromethylfluorescein diacetate (CMFDA) (ThermoFisher Scientific, UK) was added to the wound surface for 30 minutes prior to imaging. Explants were then washed with PBS, and imaged using a Leica M205 FA upright Stereomicroscope using a [5x / 0.50 pLANapo LWD] objective at the equivalent of [64x] magnification. Images were captured using a [DFC 565FX (Leica)] camera through LAS AF v3.1.0.8587 software (Leica). Specific band pass filter set for GFP was used. (Leica, Germany).

During this experiment, some unlabelled cells were present on day 0, so for the next experiment some wounds were co-treated with the membrane impermeable nuclear dye propidium iodide (PI) to identify any cells with damage plasma membranes. One microgram per millilitre of PI was co-treated with 4 µL of CMFDA added to the wound surface for 30 minutes and washed with PBS prior to imaging as described above.

Also, in order to test whether CMFDA dye is not labelling specific cells or regions another dye CMTPX (4-({[4-(chloromethyl)phenyl]carbonyl}amino)-2-(1,2,2,4,8,10,10,11-octamethyl-10,11-dihydro-2H-pyrano[3,2-g:5,6-g']diquinolin-1-ium-6-yl)benzoate) was added to the wound bed. A combination of CMFDA and CMTPX was used to trace cell migration at different timepoints. The CMFDA and CMTPX were added to the wound bed and collected at the designated day (Table 2.1).

Table 2.2: Treatment of wound bed in wounded human skin *ex vivo* with CMFDA and/or CMTPX

Experiments	Day 0	Day 1	Day 2	Day 3	Collection day
CMFDA/ CMTPX	**+/-**	**-/+**			Day 1
CMFDA/ CMTPX	**+/-**	**-/+**	**-/-**	**-/-**	Day 3
CMFDA	**+**				Day 0
CMFDA	**+**	**+**			Day 1
CMFDA	**+**	**+**	**+**		Day 2
CMFDA	**+**	**+**	**+**	**+**	Day 3

(+)-cell tracer was added to wound, (-)-not added. Green represent CMFDA and red represent CMTPX.

2.3.1 Analysis of intravital fluorescent dye tracer

The wound closure experiment using CMFDA was conducted daily. Fluorescent images were assessed using Image J (Fiji) for the area of the initial wound at day 0 (IW_0). On subsequent days (where day is denoted by n) the area of initial wound (IW_n), and the area of open wound remaining (OW_n) was measured (see Figure 2.2). Epithelial wound closure was calculated from measurements of area of initial wound and the open wound remaining and expressed either as the % of wound closure on each day, or on the area of healing achieved on each day in mm^2.

$$\text{Percentage closure} = 100 - (OW_n / IW_0 \times 100)$$

$$\text{Area healed} = IW_0 - OW_n.$$

Tissue contraction was also calculated by assessing changes to the initial wound defect over the wound healing period.

$$\text{Tissue contraction} = 100 - (IW_n / IW_0 \times 100).$$

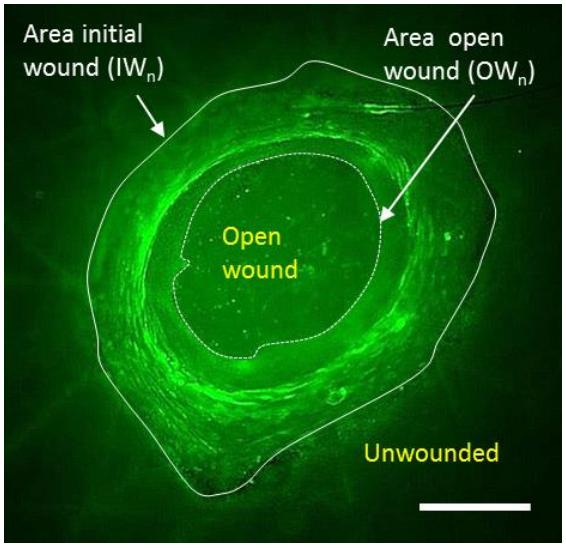

Figure 2.2: Measuring en face wound closure with CMFDA. *CMFDA images show a distinctive border line which represents initial wound (uninterrupted white line) and open wound (white dotted line) which were used to assess wound closure as percentage or area of healing. Bar = 500mm.*

In addition, the neo-epidermis was further assessed by measuring the area of the dim band of epidermal tissue towards the migrating front and the remaining brighter area (Figure 2.3). The bright area represents stratified healing (SW_n) and the dim area represents unstratified epidermis (UW_n). The bright area was calculated from measurements of the area of initial wound (IW_n) and the front of stratified healing (SW_n) and expressed as area of bright area achieved on each day in μm^2.

$$\text{Bright area, } \mu m^2 = IW_n - SW_n$$

The dim area was calculated from the front of stratified healing (SW_n) and front of unstratified epidermal (UW_n).

$$\text{Dim area, } \mu m^2 = SW_n - UW_n$$

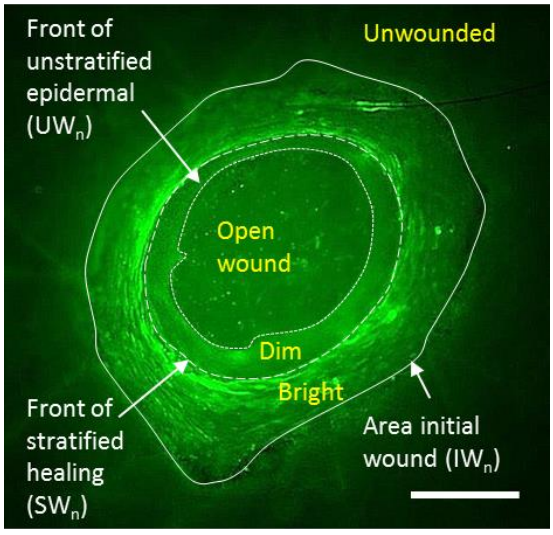

Figure 2.3: CMFDA imaging en face highlights different wound regions. *CMFDA images show distinctive features which provided additional information to be assessed. Regions of dimly fluorescent (i.e. newly laid unstratified epidermis) and bright areas of epidermis can be delineated (white dashed line). The area of the initial wound (uninterupted white line), the area of newly laid unstratified epidermis (white dotted line). Bar = 500mm.*

Virtual histology was performed by measuring the whole length or width (Yellow line) of wound at four angles as shown in figure 2.4. This whole length or width was subtracted by unhealed length (red dash line) which was also measured at the same angle. The mean of these readings was used to calculate the percentage of wound closure.

Percentage of wound closure = (whole length –unhealed area)/whole length x 100.

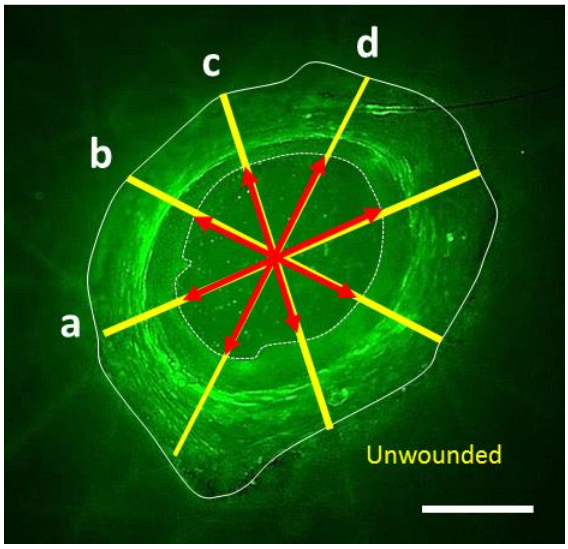

Figure 2.4. Measuring "virtual histology". *The Virtual histology was assessed by measuring the whole of wound length (Yellow line) and subtracting the unhealed portion (red dash line). Percentage of wound closure = (whole length –unhealed length)/whole length x 100. Mean of four readings taken from each explants at 4 angles as shown. CMFDA images shows a distinctive border line that represents initial wound (uninterrupted white line) and open wound (white dotted line), which were used to assess wound closure as percentage or area of healing. Bar = 500mm.*

Tissue from 5 individual donors was used, with 3-4 explants per donor used for each treatment. The mean value of the 3-4 replicate explants per donor used for analysis (i.e. assessed as n=5 replicate experiments from separate donors).

2.4 Culture treatment

Wounded human skin organ culture (WHSO) was cultured and treated once daily for 6 days with the respective treatment. Each experiment consisted of normal skin (unwounded), untreated group (negative control), treatment, vehicle (s). Each condition and timepoint had 3 – 4 per time point (n=3 or 4 explants). Normal tissue biopsies were collected on day 0 for comparison.

2.4.1 Nerve growth factor

Wound bed (2 mm wound) at the centre of human skin *ex vivo* was topically treated with 10 µL of 25 µg/mL (0.08 µg/mm^2) of nerve growth factor 2.5S from murine submaxillary gland (Sigma-Aldrich, USA) (NGF). The treatment was made once daily effective similar dose been used by Generini *et al.*, case report, the aliquot 0.5 mg of NGF in 10 ml of saline solution was dropped on the lesion approximately 50 µL/25mm^3 equivalents to 2.5 µg of NGF or 0.1 µg/mm^3. Moreover, in the diabetic mice study by (Chen *et al.*, 2014), wounds treated with 10 and 20 µg/mL accelerated speed of wound closure while at 40 µg/mL saw no significant difference to the saline group.

2.4.2 TrkA inhibitor

To investigate the effect of blocking the NGF signalling pathway, K252a (Alomone, Israel) was used to block TrkA. K252a is known to be a potent inhibitor of protein kinase A, C and G. One milligram of K252a was diluted with 534.76 µL of DMSO as a stock solution of 2 mM. For this experiment only 2 µM of K252a was used by diluting 1 µL of stock solution in 1 mL of culture media. Then 10 µL of K252a was topically applied on the *ex vivo* wound surface organ culture. Vehicle for this group was 0.001% DMSO in culture media.

2.4.3 NGF neutralising antibody

To investigate the effect of endogenous NGF and exogenous NGF treatment, *ex vivo* wound bed was treated with NGF neutralising antibody (NNA). NNA has to be applied at the same relative dose as NGF treatment or in exces to neutralise NGF. NNA is a isotype if IgG1 with molecular weight of about 150 kDa, while molecular weight for 2.5s NGF is around 30 kDa (26.5 kDa to be exact). Therefore, 5 µg of NNA was needed to 1 µg of NGF. In order to block 25 µg/mL (0.08 µg/mm^2) of NGF, ≥300 µg/mL (≥0.4 µg/mm^2) of NNA was needed. NNA stock solution was prepared by diluting 0.25 mg of NNA with 125 µL with double distilled water (DDW). 5 µL of NNA stock was then topically administered to the wound surface 3.18 µg/mm^2.

2.5 Protein Extraction

The skin explants from day 0 (normal human skin biopsies) and cultured explants from day 1 until day 6 were frozeN down by placing in A cryovial and immersing in liquid nitrogen, and kept in -80 °C until required. The explants were weighed and minced before being homogenised using a handheld homogeniser (Ultra Turax, Germany) on ice. Protein extraction was done using A total protein extraction kit (Merck, UK). 50 X Protease inhibitor cocktail (PI) solutions (from the kit) were diluted to 1X in TM buffer (from the kit) on ice. The 1X PI was then added to the minced tissue at 2.5 mL per gram of tissue and put on ice for 5 minutes. Tissue was homogenised for 20 seconds and then put on ice for 15 seconds before being homogenised for a second time and cooled down on ice for another 20 seconds. This step was repeated if tissue was not well homogenised. Homogenised tissue was then placed on a rocker at 4 °C for 20 minutes and centrifuged at 11 000 *rpm* @ 4 °C for 20 minutes. The supernatant was then collected.

2.6 ELISA

NGF levels in the extracts were measured via sandwich ELISA (NGF ELISA kit, Cat #OKEH00186, Aviva System Biology, San Diego, USA) with minimum detection level of 15.60 pg/mL of NGF as per manufacturer's instructions. Total protein levels of the samples were measured by the density of colour reaction read at 450 nm.

2.7 Tissue processing

All samples collected were fixed in 4% of formalin overnight and transferred into 70% of industrial methylated spirit (IMS)(Fisher Scientific, UK) for another 24 hours. Samples were then put into a Miles Tissue –Tek VIP 3000 processor (Miles, CA) or sent to the Histological core facility at the University of Manchester, before being embedded with paraffin wax. Table 2.2 shows general steps, solvents used with respective temperature and time required for tissue processing.

Table 2.3: General tissue processing conditions

Step	Solvents	Temperature (°C)	Time
1	70 % IMS	35	60
2	70 % IMS	35	60
3	90 % IMS	35	60
4	100 % IMS	35	90
5	100 % IMS	35	90
6	100 % IMS	35	90
7	50 % IMS: 50 % Xylene	35	30
8	Xylene	35	30
9	Xylene	35	30
10	Xylene	50	60
11	Wax	60	30
12	Wax	60	30
13	Wax	60	30
14	Wax	60	60

2.8 Histology

5 µm sections of paraffin embedded tissue were made with a microtome (Leica, Milton Keynes, UK), and used for all histology and immunohistology. All incubations were conducted at room temperature unless stated otherwise. Prior to staining, sections were dewaxed by two immersions in Xylene for 5 minutes each, followed by rehydration through graded alcohols for 2 minutes each in 100% IMS, 90% IMS, 70% IMS, then 50% IMS and then transferred to tap water. A number of different reagents were prepared and used for histological and immunohistological staining (section 2.8 and 2.9) and are documented in table 2.3.

Table 2.4: Preparation of solutions for immunohistology

Solution	Preparation
PBS	1 x Phosphate buffer saline was made with 200 ml of 10x stock solution (Fisher Scientific, UK), and 1800 ml of dH_2O
TBS	1 x Tris buffer saline was made with 200 ml of 10x stock solution (Sigma-Aldrich, UK), and 1800 ml of dH_2O
TBS-T	1x Tris buffer saline with 0.5% of Tween 20 was generated by adding 10ml of Tween 20 (Sigma) to 1xTBS buffer
TNT (pH 7.5)	Tris-NaCl-Tween buffer was made with 8.77 g of 0.15M NaCl (Fisher Chemical, UK) and 15.76 g of 0.1M Tris-HCl was weighed out on a fine balance. 1000 ml of dH_2O was added and pH adjusted to 7.5, before the adition 0.05% of Tween 20
TNB	Tris-NaCl buffer with blocking reagent was made by supplementing 0.5% (1g=1%) of blocking reagent into required TNT buffer
Citrate buffer (pH 6)	Citrate buffer was made with 5.88 g of Sodium citrate in 2000 ml of dH_2O and pH adjusted to 6, before added 0.05% Tween 20
Tris-EDTA	Tris-EDTA was made with 1.21 g of 10mM Tris Base, 0.37 g of 1mM EDTA in 1000 ml dH_2O and pH adjusted to 9 and 0.5 ml of Tween 20 was added.
TritonX	0.5 % or 1% of Triton was made by adding the required percentage of stock solution of Triton X-100 (Fison, UK) in the 1 x buffer.
H_2O_2	0.3% of hydrogen peroxide (Sigma Life Science, Germany) was made by adding 700 µL of 30% hydrogen peroxide in 70 ml of buffer
Periodic acid	1% solution of periodic acid was prepared by adding 0.5g Periodic acid to 100 mL dH_20

2.8.1 Haematoxylin and eosin staining

Slides were washed in running tap water for 1 minute and incubated with Mayer's Haematoxylin (Sigma-Aldrich, USA) for 7 minutes before being washed in running tap water for 2 minutes. Slides were then immersed in 0.2% of acid water for 20 seconds and washed for another 1 minute. Slides were incubated with 37mM ammonia (Thermo Scientific, USA) for 2 minutes followed by Eosin (Leica,UK) for 3 minutes. After that slides were dehydrated by placing into 70% IMS for 20 seconds, 100% IMS for 15 seconds and 50:50 Xylene:IMS consecutively before immersion in Xylene twice for 1 minute each and mounted using Depex (Serva Electrophoresis, Heidelberg, Germany).

2.8.2 Periodic acid Schiff staining

Slides were dewaxed and rehydrated with xylene and graded alcohols (as described above) and washed with distilled water for 5 minutes. Then slides were incubated in 1% periodic acid for 15 minutes at room temperature. Slides were washed for 1-2 minutes in dH_20 prior incubated with Schiff's reagent for 30 minutes. Then slides were washed thoroughly in dH_20 for 3 x 5 minutes and with running tap water for 5 minutes and once again rinsed with dH_20. Followed by incubation with Meyer's Haematoxylin for 30 seconds and dehydrated by placing into 70% IMS for 20 seconds, 100% IMS for 15 seconds and 50:50 Xylene:IMS consecutively before immersion in Xylene for 10 minutes. Slides were then ready for mounting using Depex.

2.9 Immunohistochemistry and immunofluoresence

In order to develop a number of optimised antibody based staining protocols, several factors such as antigen retrieval buffer, washing buffer and signal amplification were adapted as required.

Antigen retrieval of rehydrated slides was performed either with sodium citrate buffer pH 6 or Tris-EDTA pH 9. Slides were microwaved for 10 minutes at medium/low power, followed by a further 5 minutes at low power. Tris buffered saline (TBS) was used for subsequent washes in the staining protocol when using Tris-EDTA. While phosphate buffered saline (PBS) was used for washes when sodium citrate buffer retrieval was used.

The antigen retrieval with sodium citrate was done after cell permeabilisation with 0.5% Triton X (Fison, UK) for 10 minutes and followed by 0.3% hydrogen peroxide for 10 minutes to quench peroxide enzymes within the tissue. The individual detailed protocols for each antibody stain are documented in Table 2.4.

To ensure non-specific binding generated by the fluorescence conjugated secondary antibody, all immunofluorescent staining was conducted in parallel with negative controls that were incubated with blocking agent in PBS instead of primary antibody. Data from this study was compared to results on human skin found within The Human Protein Atlas (http://www.proteinatlas.org/) and the published literature. If there was no existing comparison data in which the result could be corroborated, positive controls tissues were used as appropriate, to confirm an expected staining pattern was observed.

2.9.1 Chromogenic staining protocol for Ki-67, CD68 and Cytokeratin 6

Slides were dewaxed and rehydrated with xylene and graded alcohol (as above) and washed with distilled water for 5 minutes. Antigen retrieval was performed with Tris-EDTA (for TrkA and CD1a) or sodium citrate (for Ki-67 and p75NTR) and then slides were cooled down for 30 minutes. Slides were washed for 3 x 5 minutes for each wash (implied hereafter) with respective washing buffer followed by 10 minutes tissue solubilisation with 0.5% of Triton X-100 in washing buffer and washed (Ki-67 omitted this step). Tissue sections were encircled with a hydrophobic pen and incubated with 10% normal goat serum in washing buffer for 30 minutes, followed by incubation with respective primary antibodies diluted in 2% NGS overnight at 4°C.

After overnight incubation, slides were washed and incubated with 1 drop of ImmPress reagent anti-primary antibodies IgG for 30 minutes and subsequently washed again. Slides were incubated with ImmPact Novared peroxidase substrate for 2-15 minutes until the required colour developed. Slides were rinsed in distilled water to stop the reaction and counter stained with haematoxylin for 7 minutes. Slides were then dehydrated through grades alcohols and Xylene (2 mins each of 50% IMS, 70% IMS, 90%IMS, 100%IMS, 1:1 mix of 100% IMS and Xylene, Xylene) and mounted with Depex medium. For cytokeratin 6, inhibition of endogenous peroxidase activity step was skipped before antigen retrieval but tissue was solubilized with 0.5% of Triton X-100 in washing buffer and washed for 3 x 5 minutes with washing buffer after antigen retrieval before proceeding with blocking step.

2.9.2 Immunofluorescence staining protocol for TrkA, Ki-67, CD1a and p75NTR

Slides were dewaxed and rehydrated with xylene and graded alcohol (as above) and washed with distilled water for 5 minutes. Antigen retrieval was performed with Tris-

EDTA (for TrkA and CD1a) and sodium citrate (for Ki-67 and p75NTR) and then slides were cooled down for 30 minutes. Slides were washed for 3 x 5 minutes for each wash (implied hereafter) with respective washing buffer followed by 10 minutes tissue solubilisation with 0.5% of Triton X-100 in washing buffer and washed (Ki-67 void this step). Tissue sections were encircled with hydrophobic pen and incubated with 10% normal goat serum in washing buffer for 30 minutes, followed by incubation with respective primary antibodies diluted in 2% NGS overnight at 4°C. After overnight incubation, slides were washed and incubated with secondary antibody for 45 minutes and subsequently washed again. Slides were incubated in 4', 6-diamidino-2-phenylindole (DAPI) for 2 minutes and washed before mounting in fluoromount mounting medium. While for p75NTR tissue was solubilised in 0.5% of Triton X-100 in washing buffer for 10 minutes. Slides were washed 3 x 5 minutes (implied after this) and blocked with 0.3% H_2O_2 in washing buffer and washed prior to antigen retrieval.

2.9.3 Immunofluorescence using the Tyramide Signal Amplification protocol for NGF

Slides were deparaffinised and rehydrated through xylene and graded alcohol. After washing with distilled water for 5 minutes, antigen retrieval was performed by 10 mM Tris-EDTA pH 9.0 in a microwave for 10 minutes at medium/low power and 5 minutes low power setting and cooled down for 30 minutes. Slides were washed 3 times (5 minutes each) with TNT buffer (pH 7.5) and blocked with 3% H_20_2 in TNT for 15 minutes at room temperature then washed for 3 times (5 minutes each) with TNT buffer. Sections were circled with a hydrophobic pen (PAP pen) and pre-treated with Avidin and Biotin (Vector, blocking kit-SP2001) for 15 minutes at room temperature

respectively and washed 3 times (5 minutes each) with TNT buffer in between each of the pre-treatments. Slides were washed 3 times (5 minutes each) with TNT buffer before blocking with 10% normal goat serum in TNT for 20 minutes at room temperature and then drained by tapping off the serum. Slides were incubated with primary antibody rabbit anti-human NGF beta antibody (1:100) (Abcam, ab6199) diluted in 0.3% Triton X100 in TNT and 2% normal goat serum for overnight at 4°C. After overnight incubation, slides were washed and incubated with goat anti-rabbit biotinylated secondary antibody diluted (1:100) (Vector, BA 1000) in TNT and 2% normal rabbit serum (in humidifier chamber) for 45 minutes at room temperature and subsequently washed again before being incubated with Streptavidin-conjugated HRP (1:100) (Perkim Elmer TSA kit, NEL741001KT) for 30 minutes at room temperature. Slides were washed and then incubated with amplification reagent TSA Cy5 (1:50 in amplification diluent in TSA) (NEL7450011KT). Slides were washed and counterstained with DAPI for 1 minute and finally washed before mounting in fluoromount mounting medium.

2.9.4 Immunofluorescence dual staining protocol for TrkA and CD1a

Slides were dewaxed and rehydrated with xylene and graded alcohol (as above) and washed with distilled water for 5 minutes. Followed by antigen retrieval with Tris-EDTA and cooled down for 30 minutes. Slides were washed for 3 x 5 minutes for each wash (implied hereafter) with respective washing buffer followed by 10 minutes tissue solubilisation with 0.5% of Triton X-100 and washed. Tissue sections were encircled with a hydrophobic pen and incubated with 10% normal goat serum for 30 minutes, followed by incubation with respective primary antibodies cocktail diluted in antibody diluent overnight at 4°C. After overnight incubation, slides were washed

and incubated with secondary antibody cocktails in antibody diluent for 45 minutes and subsequently washed again. Slides were incubated in DAPI for 2 minutes and washed before mounting in fluoromount mounting medium.

Table 2.5: List of antibodies used in this study

Antibodies	Species/vendor	Primary antibody dilution	Secondary antibody/(dilution)	Antigen retrieval buffer	Washing buffer	Note
NGF (ab6199)	Rabbit/ Abcam	1:100	Goat anti-rabbit biotinylated (1:100)	Tris-EDTA pH 9.0	Tris-NaCl-Tween (TNT)	Tyramide signal amplification kit (PerkinElmer)
TrkA [EP1058Y] (ab76291)	Rabbit/ Abcam	1:200	Goat anti-rabbit (AF 594 - 1:200)	Tris-EDTA pH 9.0	Tris buffer saline (TBS)	
P75NTR [EP1039Y] (ab52987)	Rabbit/ Abcam	1:200	Goat anti-rabbit (AF 594 - 1:200)	Sodium citrate pH 6.0	Tris buffer saline with 0.5% Tween 20 (TBS-T)	
Ki-67 [SP6](Ab16667)	Rabbit/ Abcam	1:20	Goat anti-rabbit (AF 594 - 1:200)	Sodium citrate pH 6.0	Phosphate buffer saline (PBS)	
CD1a [C1A/711]	Mouse/Abcam	1:100	Goat anti-mouse (AF 594 – 1:200)	Tris-EDTA pH 9.0	Tris buffer saline (TBS)	
Ki-67 [SP6](Ab16667)	Rabbit/ Abcam	1:100	Impress HRP IgG rabbit (MP-7401, Vector Lab, UK)	Sodium citrate pH 6.0	Phosphate buffer saline (PBS)	IHC-ImmPACT NovaRED Peroxidase (HRP) Substrate (SK-4805, Vector, Lab, UK)
CD68 (Clone PG-M1)	Mouse/Dako	1:50	Impress HRP IgG mouse (raised in horse) (MP-7402, Vector Lab, UK)	Sodium citrate pH 6.0	Phosphate buffer saline (PBS)	IHC-ImmPACT NovaRED Peroxidase (HRP) Substrate (SK-4805, Vector, Lab, UK)
Cytokeratin 6 [Ks6.KA12](ab18586)	Mouse/Abcam	1:50	Impress HRP IgG mouse (raised in horse) (MP-7402, Vector Lab, UK)	Sodium citrate pH 6.0		IHC-ImmPACT NovaRED Peroxidase (HRP) Substrate (SK-4805, Vector, Lab, UK)

2.10 Image capture

Haematoxylin and eosin and chromogenic staining were visualized and photographed with a slide scanner, Scanscope (Aperio, Germany). The Keyence Biozero-8000 microscope (Keyence Corporation, Japan) was used to visualise immunofluorescence staining. Some images were also acquired on a 3D-Histech Pannoramic-250 microscope slide-scanner using a [*20x/ 0.30 Plan Achromat*] objective (Zeiss) and the [*DAPI and FITC*] filter sets. Snapshots of the slide-scans were taken using the Case Viewer software (3D-Histech) at Bioimaging core facilities, University of Manchester. During imaging, the exposure from negative control sections was used as a baseline. All images were taken at an exposure below or equal to the baseline

2.11 Image analysis

A minimum of one but usually 2 - 4 tissue sections from each wounded human skin organ explant were examined for each antibody or staining. For the protein expression of NGF, TrkA, p75NTR and the percentage of Ki-67 immunofluorescence staining three regions were identified for assessment; neo-epidermis (also applied for measuring neo-epidermal length and area), peri-wound and unwounded as described in Figure 2.5A. While for measuring length and area of neo-epidermal (at the wound bed or tissue edges) in H&E and assessment for CD68 in chromogenic, assessment was made as described in Figure 2.5B.

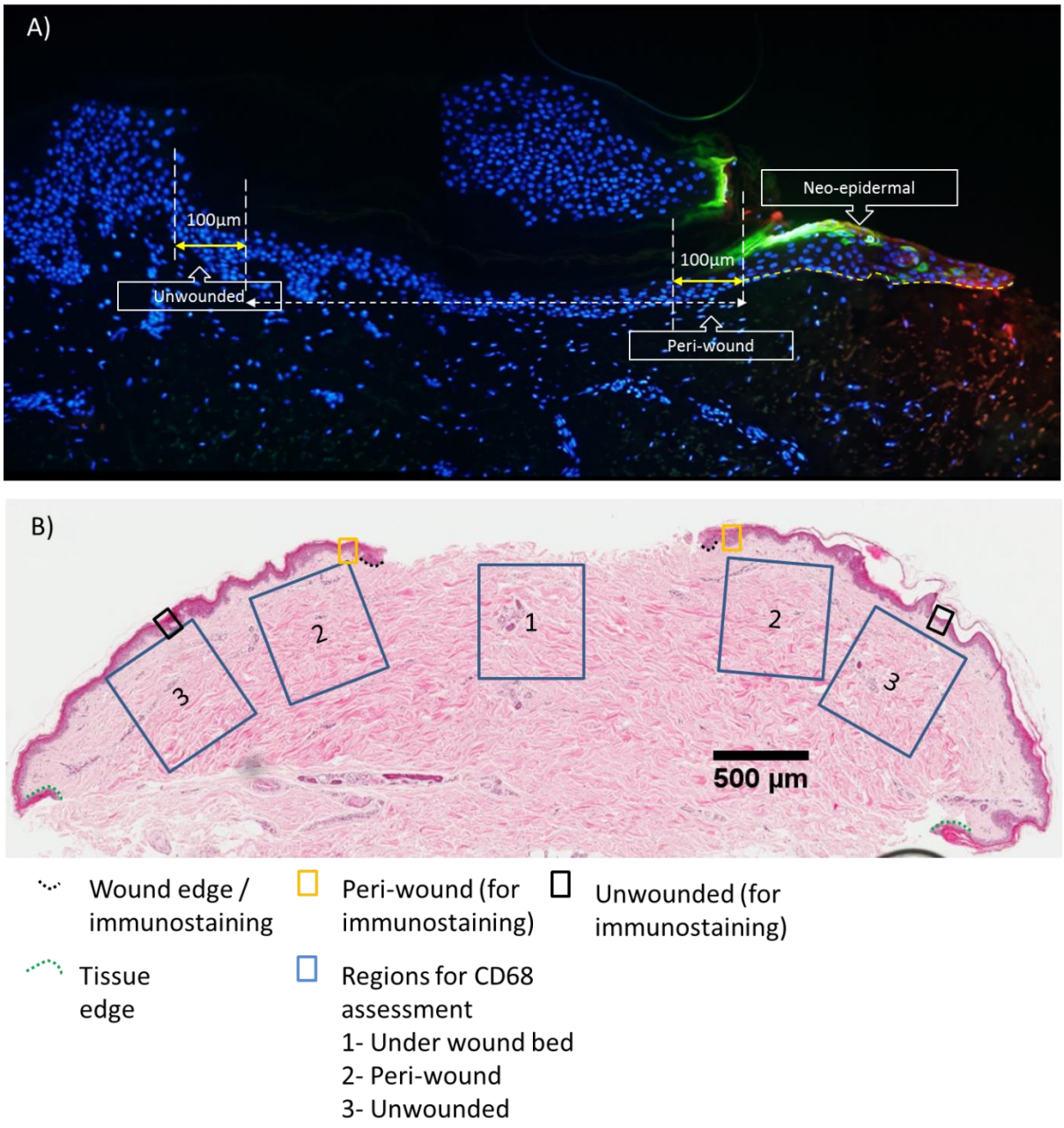

Figure 2.5: Defined regions used for immunohistology assessment of epidermal repair ex vivo*. Selection of regions for protein expression of NGF, TrkA, p75NTR and Ki-67 analysis (A). Neo-epidermis marked the new epithelised tissue. Peri-wound represented the tissue at wound edge and unwounded referred to 800-1000 µm from wound edge. Selection of regions for assessment in chromogenic or other staining staining (B).*

2.13 Statistical analysis

All statistical analyses were performed using GraphPad Prism (v 7.0.4), San Diego, USA. All data presented include standard error mean (SEM) or standard deviation (SD).

A paired t test was used to assess the compatibility of organ culture in different culture media.

A two-way analysis of variance (ANOVA) with repeated measures was used to analyse percentage wound closure, area healed and contraction between groups, over the 6 days in culture. This analysis allowed for a statistical evaluation of differences in healing due to timepoint, or treatment group. In addition, the interaction between the two processes determined whether the evolution of healing response over time differed between treatment groups. Each analysis makes the assumption that data was normally distributed.

Different statistical analysis was also used to analyse the percentage wound closure, area healed as described (Matthews *et al.*, 1990). This approach calculates wound closure by area under curve (AUC) and summary measure for all samples (n=8) including one with missing data. The missing data occurred due to a technical problem with the fluorescence upright microscope on a certain assessment day therefore no data was obtained.

While in immunohistomorphometry analyses, one way ANOVA was applied to all assessments. Further details on statistical analyses are described within figure legends.

RESULTS

Part of the data appearing in chapter 3 has been published in Wound Repair and Regeneration. Publication paper can be found in appendix 1

3.1 NOVEL APPROACH IN CHARACTERISING WOUND REPAIR IN HUMAN PARTIAL THICKNESS WOUND ASSAY

As outlined in chapter 1, the use of human skin organ culture was my favoured approach since it provides – despite the absence of functional skin nerves and normally perfused skin vasculature - the real/complete human skin structure including all cellular constituents of the epidermis and tissue resident inflammatory cells and collagen, and hopefully provides a more realistic environment to the *in vivo* situation than other lab-based assays available (Xu *et al.*, 2012, Glinos *et al.*, 2017, Mendoza-Garcia *et al.*, 2015, Stojadinovic and Tomic-Canic, 2013, Sarkany *et al.*, 1965).

First of all this study needed to optimise the assay conditions of human skin explants with partial thickness wounds *ex vivo*, which later could be used to evaluate NGF. To be specific, this study wanted to understand skin organ culture viability over time in totally defined serum-free media (Lu *et al.*, 2007, Meier *et al.*, 2013) by assessing the histology of the skin as well as of proliferative capacity via Ki-67 immunofluorescence. Fluorescent cell tracer dyes CMFDA (green dye) and CMTPX (red dye) have previously been used to follow epidermal cell migration in skin equivalents, and so this project wanted to apply this approach in order to better understand the re-epithelialisation process in human skin. In addition, this study wanted to define the parameters that I would use to measure repair, and confirm that these could detect alterations to healing.

3.1.1 Assessing the viability of wounded human skin organ cultures

In a pilot experiment from one donor, wounded human skin organ was cultured in two selected media; DMEM and WE. This preliminary experiment revealed no differences in length or area of wound tongue (Figure 3.1). Extending this experiment, tissue viability of wounds cultured in these media was measured by the percentage of Ki-67 positive cells, which was slightly higher in the neo-epidermal and peri-wound regions from wounded human skin explants cultured in WE.

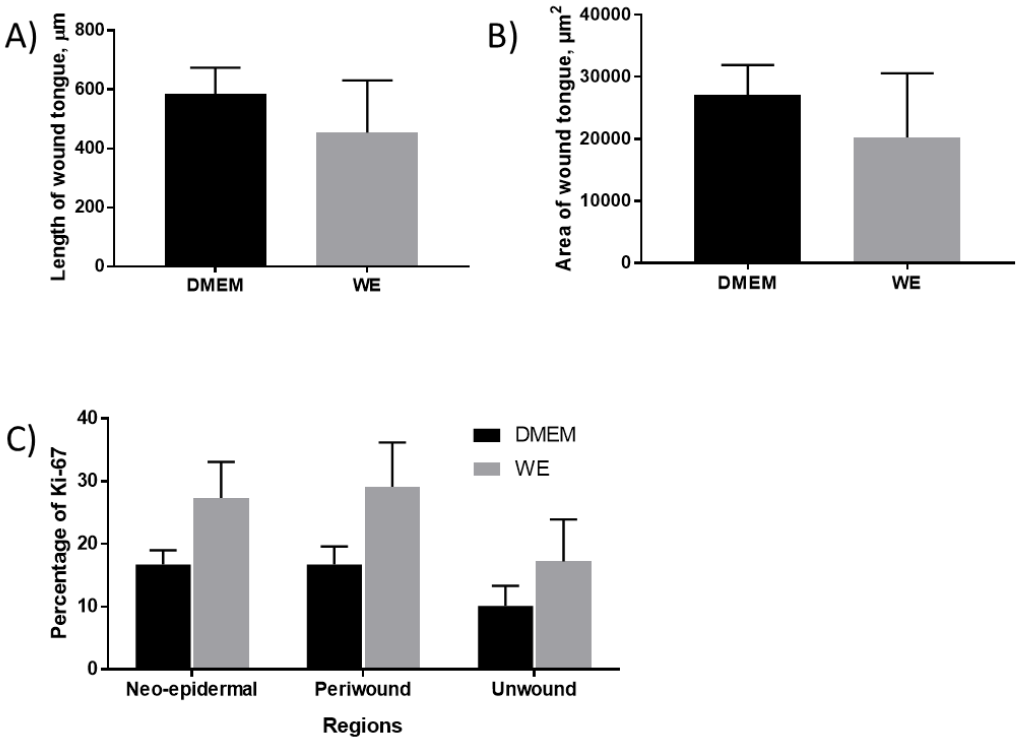

***Figure 3.1: Assessment of wounded skin organ culture in DMEM and WE media**. Wound re-epithelialisation tongue in Dulbecco's Modified Eagles Medium (DMEM) and Williams E medium (WE) on day 3. Wound tongue was measured by length (A) and area (B). Wounds organ cultured in WE display a higher percentage of Ki-67 positive cells in neo-epidermal and peri-wound regions, however no statistical analysis was performed since this pilot data was from one donor (n=1) with 4-5 explants per condition.*

Since there is no difference in the length or area of the new epithelial tongue (neo-epidermis) in organ-culture with DMEM or WE, and since the data on the percentage of Ki-67 positive cells favoured the use of WE as medium, all subsequent assays were performed with WE media.

In the next experiment the effect of serum in organ-culture wound human skin in WE media was investigated. There is no significant effect of serum on the area or length of wound tongue (Figure 3.2) for this pilot experiment (n=1). This result was obtained from measuring histological section therefore it might not as accurate as result obtained from planimetry result.

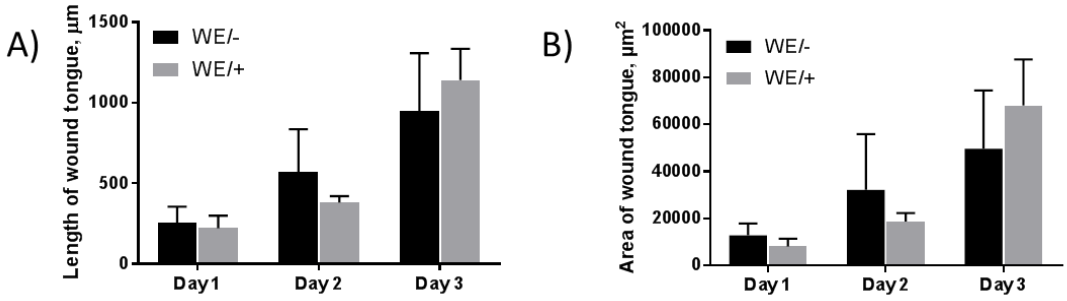

Figure 3.2: Effect of serum in wounded human skin organ culture. *Wounded human skin organ, cultured in WE with or without serum (10% Foetal Bovine Serum). Using histology the wound tongue was measured by length (A) and area (B). This experiment showed no difference between media with serum (WE/+) or without serum (WE/-) in the length or area of wound tongue. Graphs show mean from one donor (n=1) (Refer to Table 2.1) with 2-5 explants/day. On day 2, only 2 explants for the WE/- group.*

Additional data from the same pilot study (Figure 3.2) on proliferative cells (Ki-67 positive cells) showed there is no significant changes in the percentage of proliferative cells in organ culture with or without serum compare between regions across timepoints, except in the peri-wound region from wounded human skin *ex vivo* cultured in serum-free media showed significant difference on day 3 compared to the one cultured in serum media (*p* 0.0107) (Figure 3.3). This result might shows that the donor perhaps not responding or alternatively there could be a compensatory mechanism as the no serum ones needed to proliferate more as they were not healing so well.

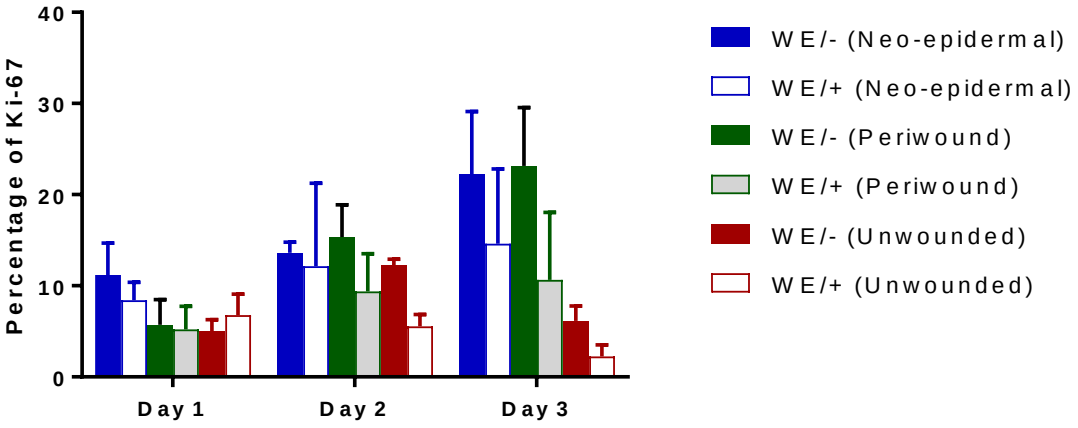

Figure 3.3: Effect of serum on proliferative cells in wounded human skin organ culture. *Quantification of Ki-67 positive cells showed no difference between regions and culture media except, Ki-67 positive cells in peri-wound region cultured without serum, which was slightly higher on day 3. Graph from n=1 donor (Refer to Table 2.1) with 2-5 explants/day. On day 2, only 2 explants for the WE/- group.*

In the next experiment, wound culture time was prolonged until day 14 (Figure 3.4). The results show that organ cultures survived in defined serum-free media optimum up to 7 days. During the experiment I observed (by naked eye and under a dissecting microscope) the tissue looked 'healthy', which was determined by the surrounding skin colour. This imprecise and subjective qualitative assessment was followed up by histology, which observed that the epidermal layer was thicker on day 1 and 3, but then became thinner onwards as observed on day 7 and 14 (Figure 3.4-Panel B).

Sections stained with Periodic Acid Schiff (PAS) showed that on days 1, 3 and 7 the basement membrane was intact, but no intact basement membrane was observed histochemically on day 14 (Figure 3.4 – Panel B & C). Panel C also shows the changes in epidermal cells arrangement from day 1, 3, 7 and 14. On day 1 the epidermal cells can be seen in tightly close arrangement with their neighbouring keratinocytes. By day 3 one can observe slightly bigger spaces between cells. This could be due to cell shrinkage. By day 7 some cells started to appear like pyknosis (nuclear shrinkage) and karyolisis (nuclear fading) (Rowden *et al.*, 1975). From these findings 6 days was chosen as the longest culture period for the next experiments.

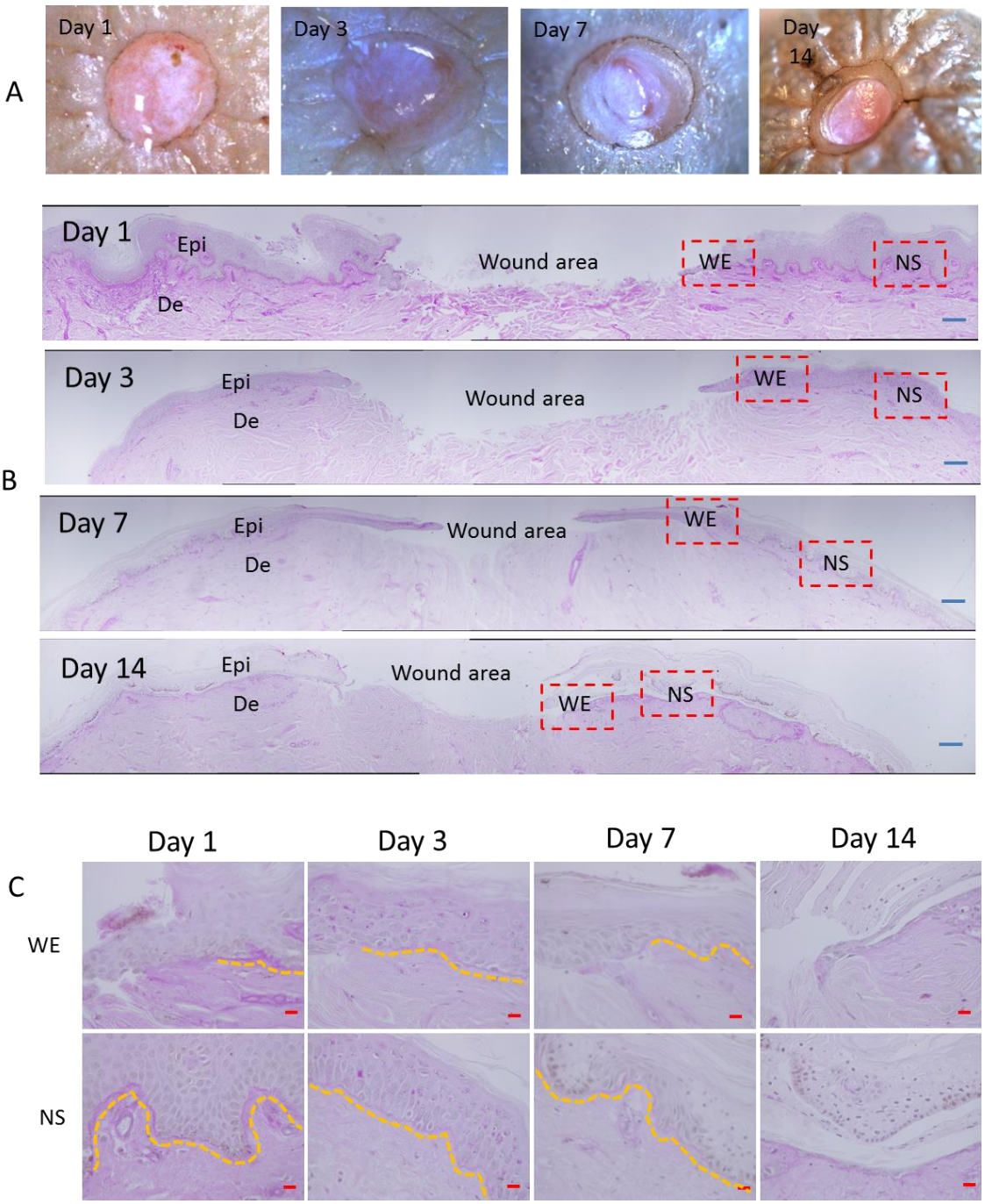

Figure 3.4: Tissue condition across the time points. *Panel A shows representative images of wounded human skin organ culture across time point (Day 1, 3, 7 &14). Panel B shows representative image of tissue section from respective explants with Periodic Acid Schiff (PAS) staining. Panel C shows magnified image of basement membrane at wound edge (WE) and normal skin (NS) area from the respective explants. Red dash box represent magnified area of (WE) and (NS) and yellow dash wiggly line showed intact basement membrane between epidermis and dermis. Blue bar=100 µm, red bar=50 µm*

In some explants a skin “blister” phenotype (epidemiolysis) was observed around the wound edge of organ culture from day 5 onwards (Figure 3.5). This might be because of fluid collection under the new epithelial tissue or this also might be because of the infection but this has been rule out since there was no indicator of contamination/infection of the culture media (no cloudiness). Further investigation showed that tissue viability was preserved optimum until day 7. However this condition does not occur frequently, but is included in this report to show that this phenomenon can occur under these organ culture condition.

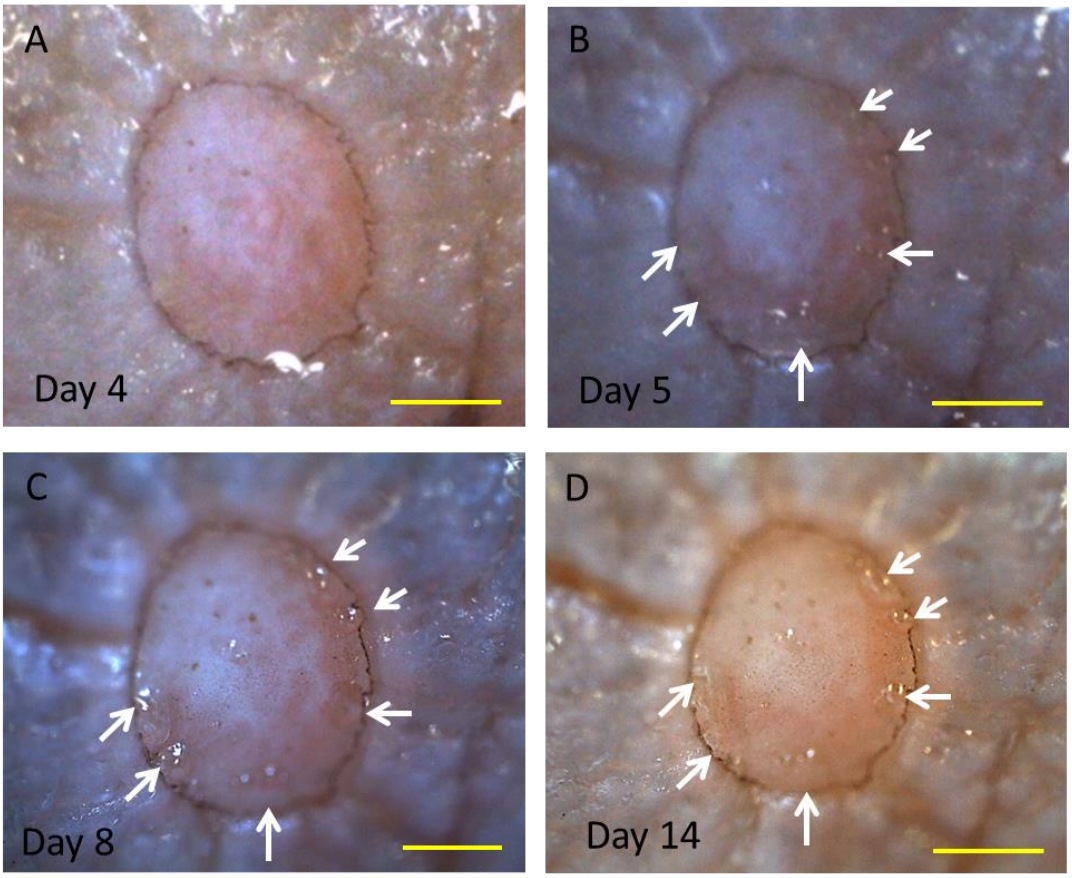

Figure 3.5: “Blister” phenotype in wounded human skin organ culture*. Representative images of wounded human skin organ culture with “blisters” phenotype along wound edge across time point (A-D). White arrows identify the blister phenotype. Bar=1 mm.*

The perseverance of tissue viability was confirmed by Ki-67 positive cells distribution in organ culture from day 0 – 6 (Figure 3.6). It shows that the Ki-67 positive cells sparsely distribute on day 1 like in normal skin, by day 2 and 3 more Ki-67 positive cells can be seen at the wound edge and new-epithelised tissue respectively. This report correlates well with the previous report by (Leydon *et al.*, 2014).

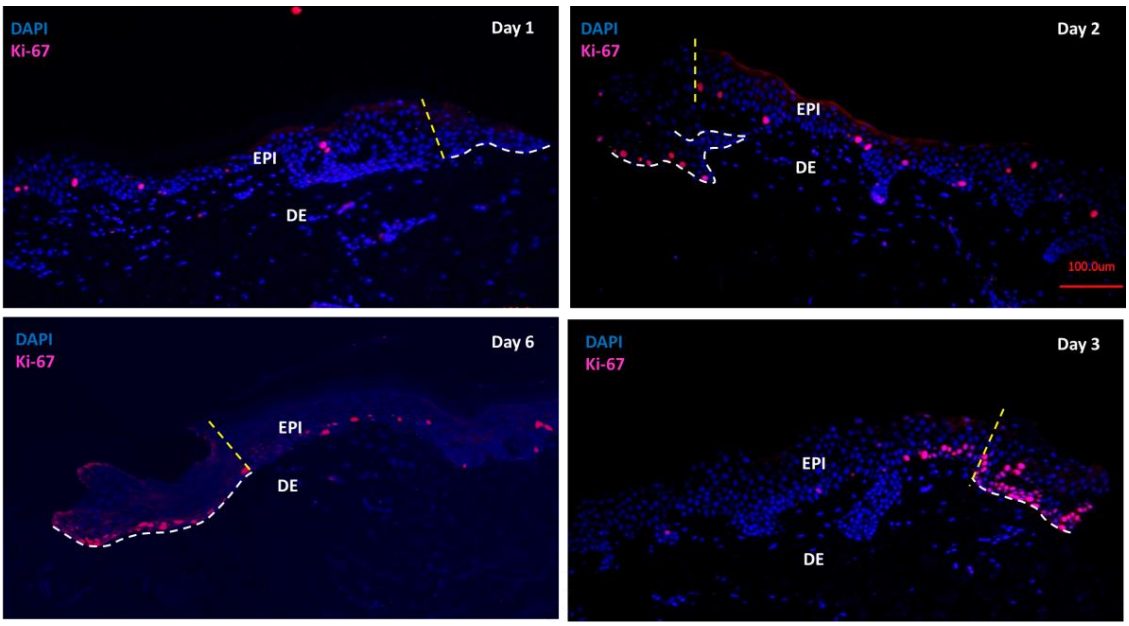

Figure 3.6: Proliferative cell distribution across the timepoints*. Images show representative images of proliferative cells stained with Ki-67 distribution in wounded human skin organ culture at different timepoints (white arrow showed toward wound area and yellow arrow showed tissue edge) from wounded human skin organ cultured in WE/-serum across time points.The Ki-67 +ve cells were scattered in epidermis at day 1, at day 2 Ki-67 can be seen to line up at wound edges, while many more Ki-67 +ve cells were accumulated at peri-wound and neo-epidermal regions by day 3 and were decreasing by day 6.*

3.1.2 Fluorescent cell tracers aid in wound re-epithelialisation assessments

The Ki-67 immunofluorescence in this study showed high levels of cell proliferation in the basal epidermis following injury, extending away from the wound. To further explore cell behaviour the vital fluorescent cell tracer, CMFDA was then employed. This dye should get taken up by viable cells and be retained, which gets passed to daughter cells and remain visible for several rounds of cell division (Lu and Rollman, 2004, Safferling *et al.*, 2013). This dye might allow one to examine localisation within *ex vivo* wound *in situ* by histology since the dye will be remain in the skin even after fixation.

Wounds treated with CMFDA on day 0 and collected immediately show that epithelial cells at the wound edge were labelled (Figure 3.7i). In addition, day 0 labelled cells trace to the suprabasal portion of the emerging epithelial tongue on day 1 and day 3, with the basal neo-epidermal cells entirely unlabelled (Figure 3.7ii-iii).

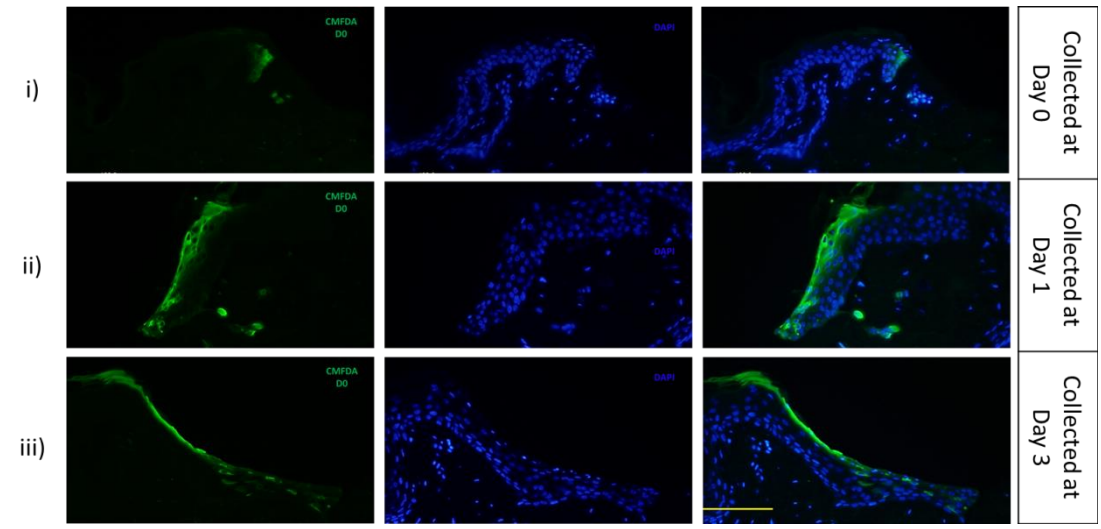

Figure 3.7: CMFDA was retained in wounded human skin organ tissue and marks viable cells at the wound edge*. Human ex vivo wounds were cultured in the presence of the fluorescent cell tracker dyes. Green CMFDA dye treatment at time of injury (D0) shows localisation to the immediate injury site (i). When organ culture was treated with green dye on day 0 and collected on day 1 or day 3 (ii-iii) it shows the migration of the cells labelled on day 0 and unlabelled cells at the neo-epidermal front as well as basal cells. Bar =100 µm.*

Some unlabelled cells were found at the wound edge on day 0, so in the next experiment some wounds were co-treated with the membrane impermeable nuclear dye Propidium Iodide (PI) to identify any cells with damage plasma membranes. This revealed some PI +ve nuclei directly at the injury site, which do not express CMFDA. Some treated wounds were then cultured until day 1, and no PI +ve nuclei were remaining within the wound epidermis (Figure 3.8).

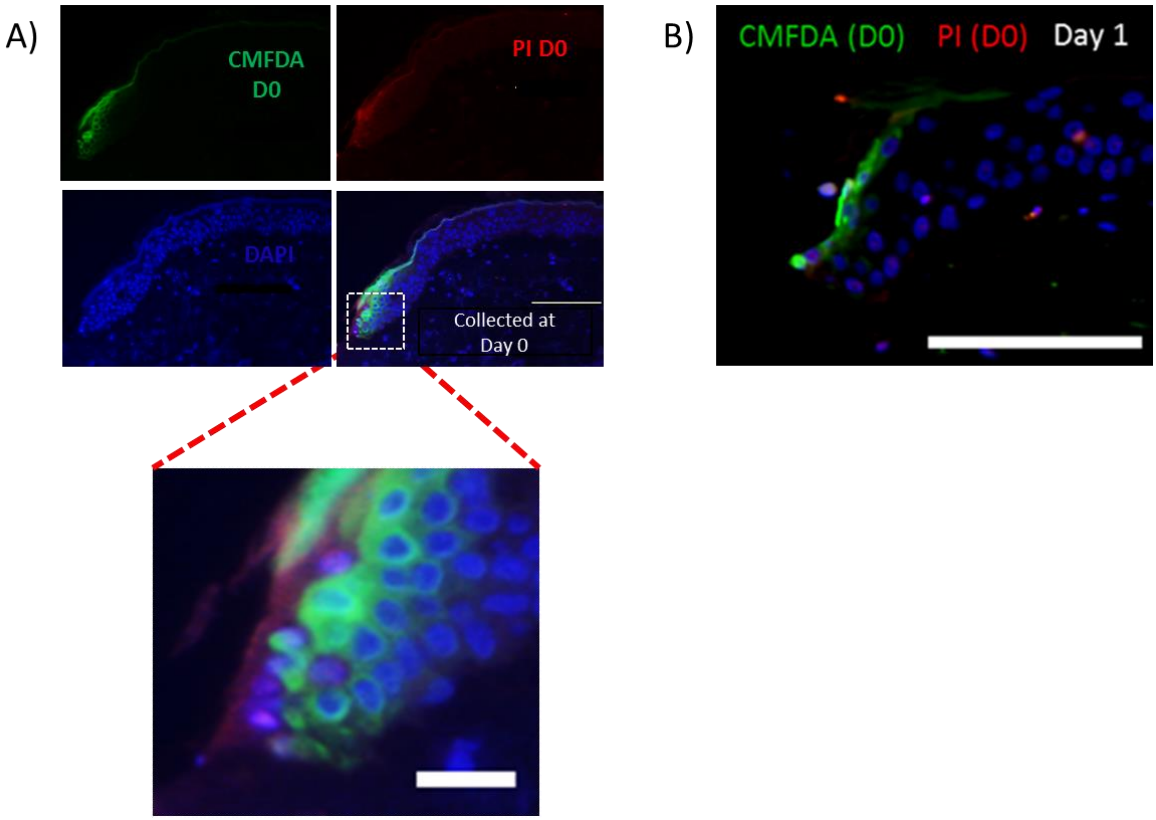

Figure 3.8: Co-treatment with Propidium Iodide revealed cell damage at the wound edge on Day 0. *Human ex vivo wounds were cultured in the presence of CMFDA and Propidium Iodide (PI)(A). Co-treatment at time of injury (D0) identifies live (CMFDA; green) and dead (PI; red) cells around the injury site (A: see inset), and these wounds traced to day 1 indicate PI labelled cells are no longer present (B). Bar =100µm, 20µm (inset image).*

By using multiple dyes at the same time in this experiment, it shows that CMFDA and CMTPX dyes do not label specific cells or regions. These multiple dyes allowed one to label cells at the wound surface or any viable cells that been exposed to the dye (Safferling *et al.*, 2013). It could label the same cells that had been labelled on the previous day or it might label totally different cells, or new unlabelled cells might emerge after the first labelling. In this experiment, wounds treated with CMFDA on day 0 and CMTPX on day 1 revealed cells at the tip of the epidermal front on day 1 were predominantly labelled by CMTPX. Moreover, at the wound edges, CMTPX was strictly labelled to the outermost surface of the new epidermis. When the same treatment with CMFDA (day 0) and CMTPX (day 1) and tissue were collected on day 3, it shows that bands of green and red staining within the neo-epidermis extending to the wound edge with red dye label reaching closer to the neo-epidermal front (Figure 3.9).These data showed strong agreement with an "extending shield mechanism" for epithelial repair as reported in skin equivalent wounds (Safferling *et al.*, 2013). However, the tip of the neo-epidermis at day 3 was highly variable and contained a mixture of unlabelled, CMFDA positive cells, CMTPX positive cells and also a few double positive cells (Figure 3.9). This region was heterogeneously labelled and sometime one can also observed some basal cells have been labelled (Figure 3.9). This could be because the dye seeps underneath the forming wound tongue therefore it can stain the basal cells (like mentioned above, the dye will label any expose viable cells). This experiment concluded that CMFDA or CMTPX dyes stained any expose viable cells and does not stain specific cells.

From here onward, this study opted to use CMFDA only in my experiments. The organ culture was treated with CMFDA every day until harvesting day because the

fluorescence tends to fade in 72 hours (Figure 3.10). Treating daily labelled the entire length of the neo-epidermis.

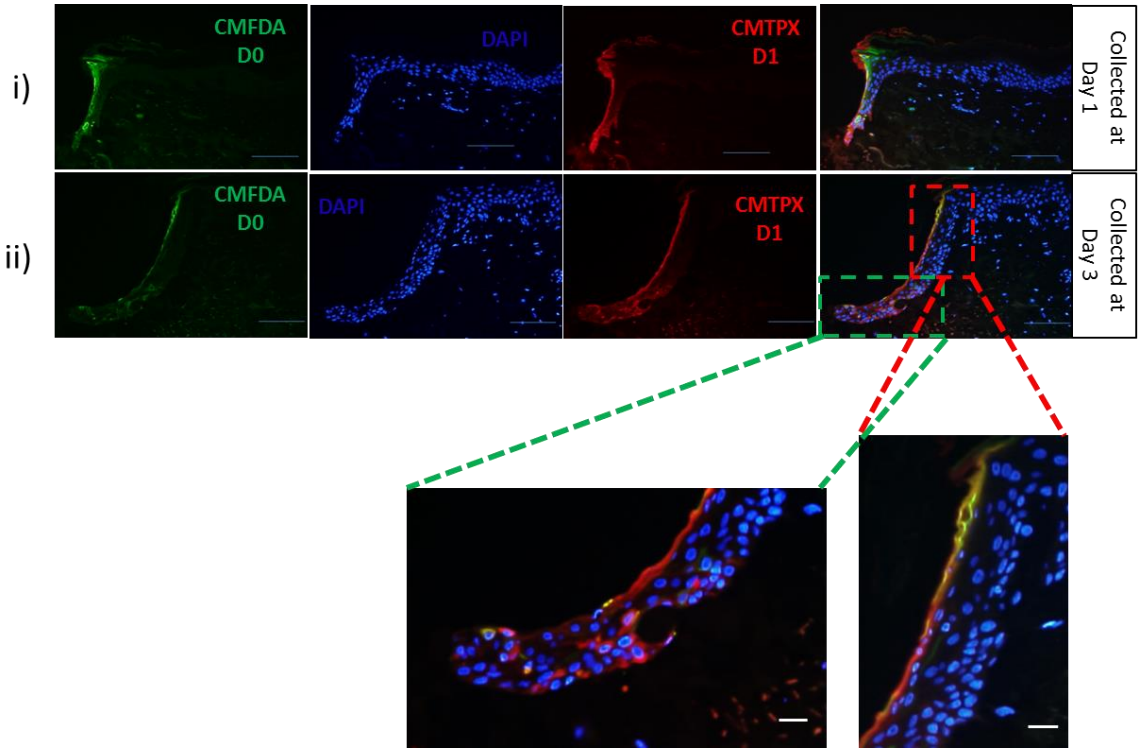

Figure 3.9: Epithelial repair of wounded human skin ex vivo progresses via an extending shield mechanism*. Human ex vivo wounds were cultured in the presence of the fluorescent cell tracker dyes and CMTPX. Green CMFDA dye treatment at time of injury (D0-Day 0) shows localisation to the immediate injury site (i and ii). Treatment on day 1 (D1-Day 1) with red CMTPX reveals previously unlabelled cells at the epidermal tip (i). Wounds left till day 3 shows a mixture of red, green and unlabelled cells at the neo-epidermal front (ii-see insets).Some cells at basal layer might be label due to the dye penetrating underneath the wound tongue on day 1. (D). Bar =100um, 50um (all inset images).*

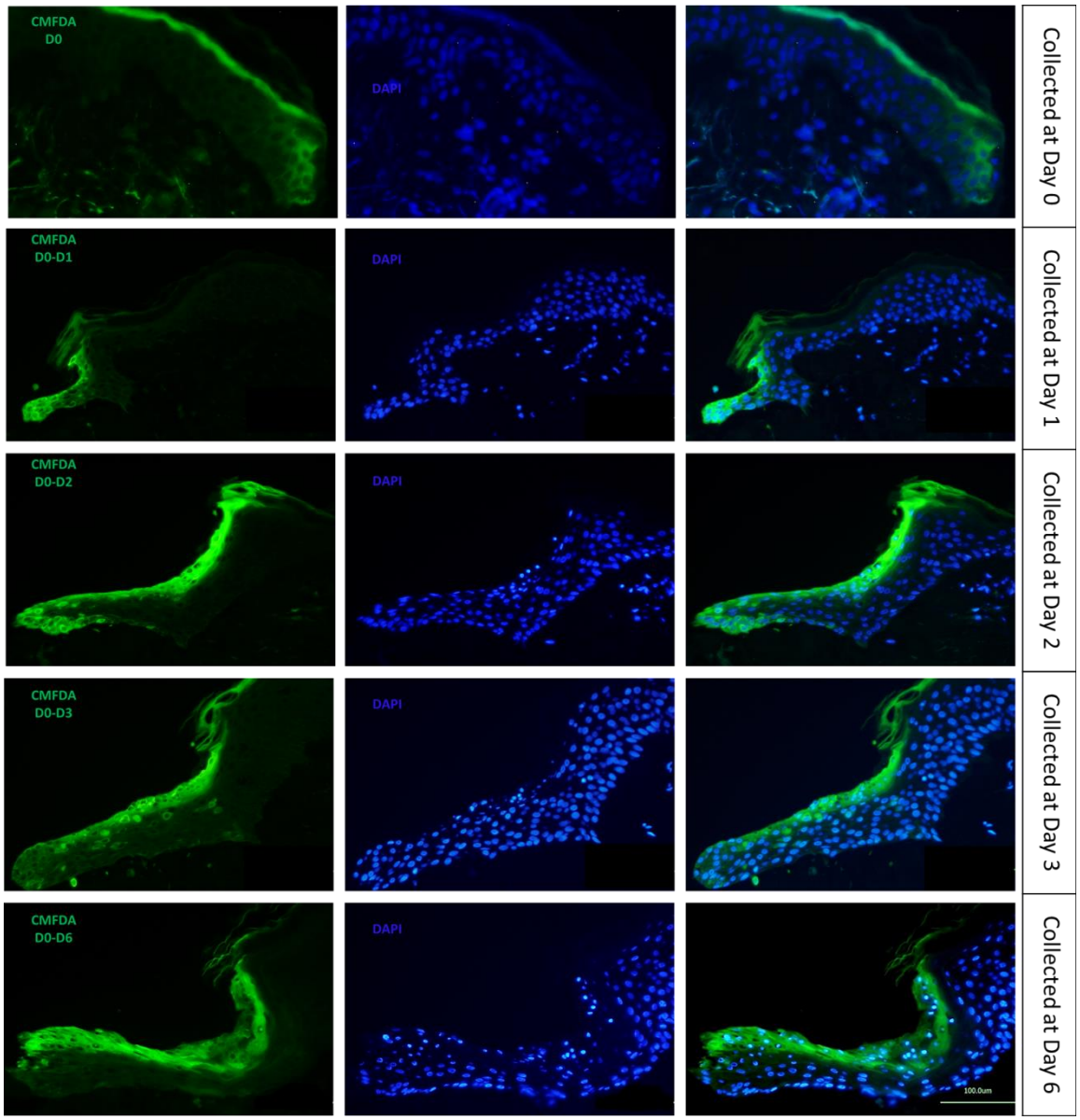

Figure 3.10: Daily treatment with CMFDA*. The CMFDA labelled the entire length of neo-epidermis of human ex vivo wounds. The dye needed to be added daily to maintain its intensity. Bar =100um.*

3.1.3 Fluorescent cell tracer dye enables daily wound assessment

From here onwards, CMFDA was then used to visualise the labelled wounded tissue in culture by an upright fluorescent microscope. This technique differentiates the neo-epidermis from areas of open wound and the surrounding wounded tissue without the need for histology (Figure 3.11A) and from the inset of Figure 3.11A one can visualise the centripetal migration that cannot be seen when using brightfield microscope or without dye. The newly laid epidermis of these wounds in culture is not obvious using conventional bright field microscope (Figure 3.11). However, the most vital point is this fluorescent cell trace dye allows one to measure the wound closure in a longitudinal manner. One can used this combination of technique with intravital dye and fluorescent microscope to yield robust and rapid result in wound closure assessment.

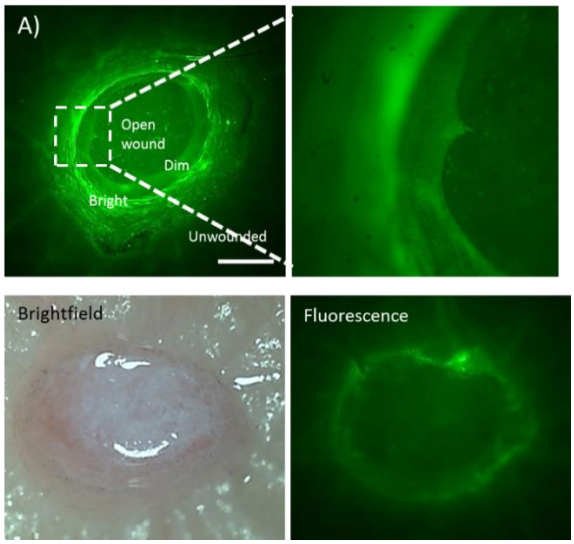

Figure 3.11: Application of CMFDA in wounded human skin ex vivo culture allows visualisation of centripetal forces. *This assay can be visualised in en face images using an upright fluorescent microscope (A). The fluorescence imaging revealed areas of centripetal migration in the wound while this feature might be missed when using brightfield microscope (see inset). Using brightfield microscopy the outer wound edge is visible, though other features of wounds are not obvious, while moisture within the wound adds glare that interferes with imaging (b). Bar- 500 µm (A).*

Three donors were used for an initial experiment comparing planimetric and histological assessment. The fluorescent cell tracer allowed for wound closure within individual wounds to be monitored on a daily basis over 6 days. For this experiment standard serum-free explants (untreated) were compared to those cultured in the presence of 10% Fetal Bovine serum (FBS), to determine whether significantly accelerated repair could be correctly detected in this model (Pastar *et al.*, 2014a).

Figure 3.12 showed daily assessment of wound healing with fluorescent cell tracer, where a clear (yet no significant) trend towards increased closure with FBS emerged from day 3 onwards. While with histology, organ cultures have to be sacrificed on the designated day and the result obtained represented an average of snapshot photo of tissue sections from those tissue explants harvested on the designated day (Figure 3.12C). Histology showed a slight trend towards increased healing with FBS on day 3, but no change at the other timepoints. The results show that no significant differences were observed between untreated and FBS group when measured by either planimetry or histology (Figure 3.12). This could be because of the small number of samples used (n=3 donors).

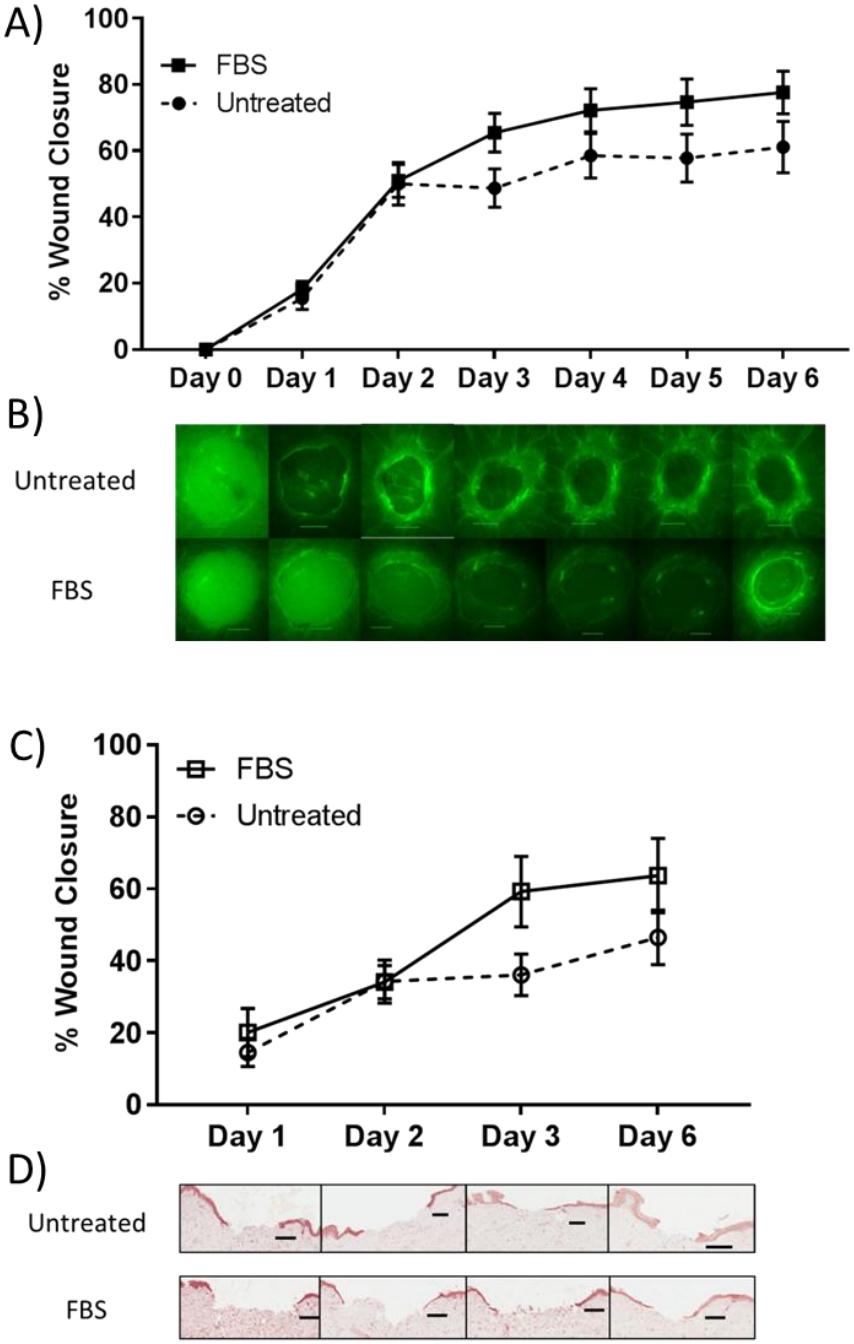

Figure 3.12: Planimetry versus histology assessment*. Planimetry live imaging with green cell tracker can profile epithelial wound closure on the same explant over time. Graph showed there are no significant difference in wound closure between untreated and FBS group across timepoints (A). Representative images of wound with green cell tracker assessed by planimetry (B). Graph showed wound healing assessment by histology (C) and representative images of wounds by histology (D). No significant difference in wound closure between untreated and FBS group across timepoints. Both graphs showed mean data from 3 donors (n=3), each with 4 replicate explants per condition. All wounds from donor 8 in the FBS group were fully healed on day 5 onwards. Error displayed as SEM. Bar = 500µm (for planimetry image), Bar = 300µm (for histology image).*

The effectiveness of planimetry and histology assessments was determined by the signal to noise ratio (mean divided by standard deviation) (Ansell *et al.*, 2014). Signal (S) is the mean difference between treatment and control group and Noise (N) is the standard deviation for the control group .The signal to noise (S/N) ratio analysis (Figure 3.13C) revealed that in this experiment there was a high signal to noise for both planimetry and histology in wound closure assessment (S/N<2), suggesting that under these conditions neither would be likely to yield significant data.

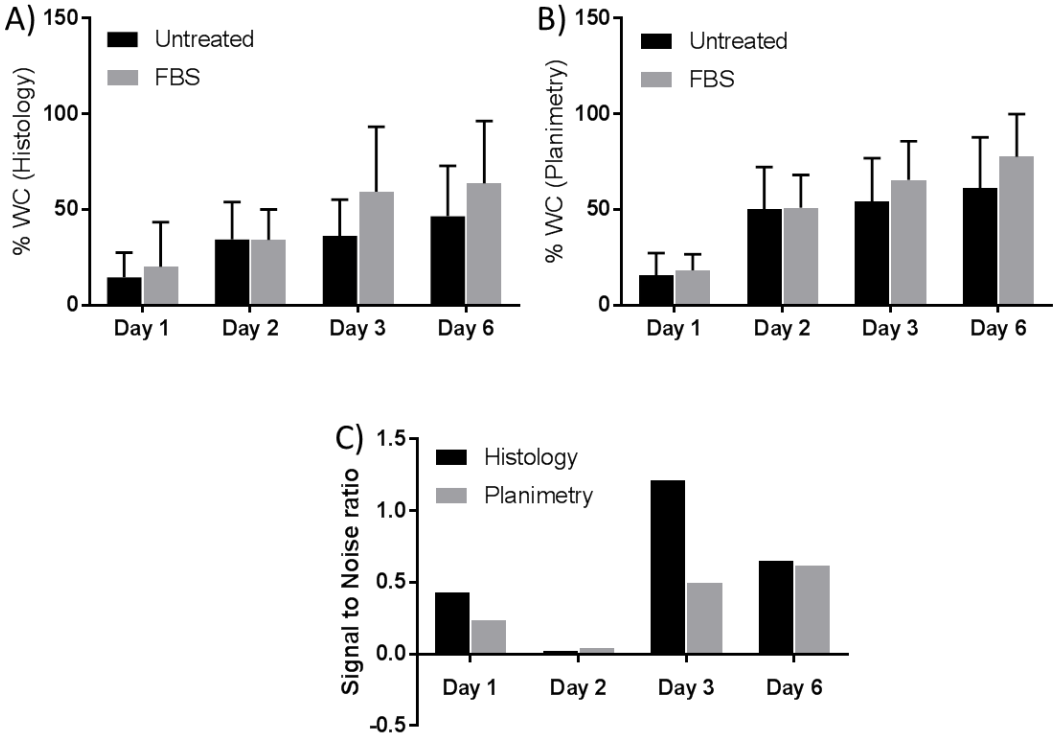

Figure 3.13: Histological assessment shows lower variability compared to planimetry. *Wound closure of organ culture treated with FBS and untreated was assessed by histology (A) and planimetry (B). The histology assessment on wound closure showed that healing occurs across the timepoints but no significant difference was detected between groups. Same result was obtained when wound closure was analysed by planimetry. No significant difference was observed between treatment groups but across timepoints. Data was analysed by one way ANOVA. The signal to noise ratio (S/N) was then used to analyse the variability between histology and planimetry assessments (C). However, S/N are expressed lower (<2) for both assessments; histology and planimetry . Graphs show mean +/- SD (n=11-12 explants) from 3 donors.*

The correlation between planimetry and histology measurements also was analysed using linear regression. Figure 3.14 shows that the measures were highly correlated to each other. Additionally, I also compared between virtual histology and histology which shows a weaker correlation and also planimetry versus virtual histology was highly correlated. Virtual histology was done as shown in figure 2.4. The readings are means from four measurements taken on the same wound measured for planimetry on the same day.

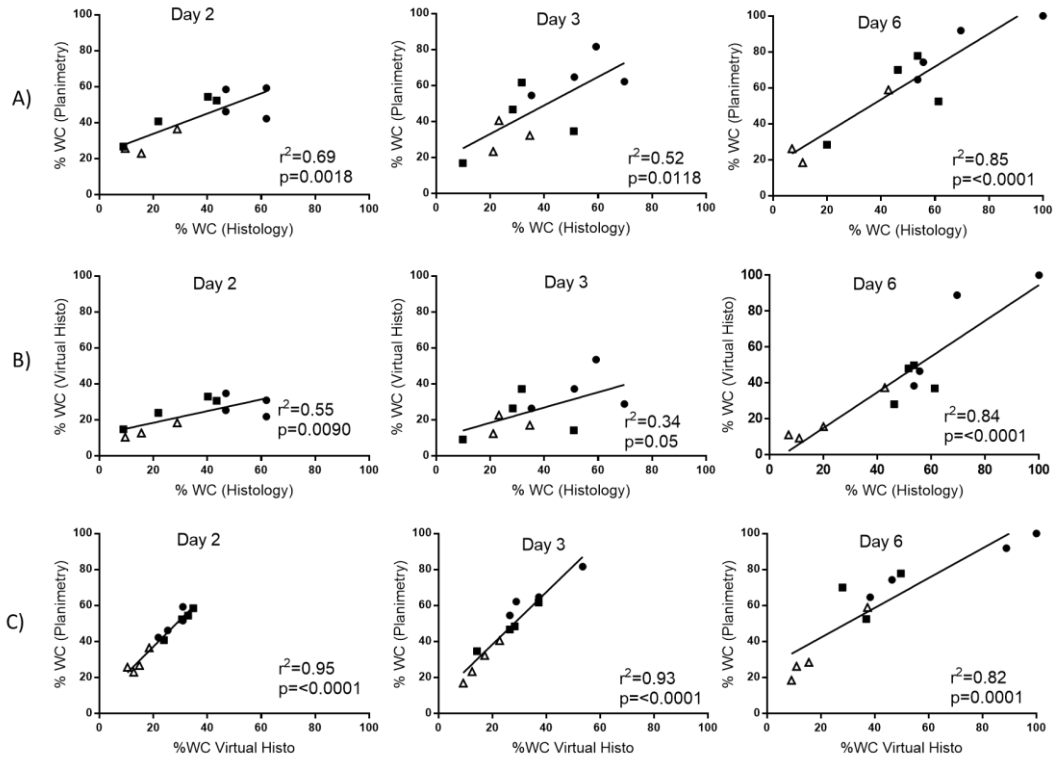

Figure 3.14: High correlation exists between planimetry and histology assessments*. Linear regression reveals correlation between assessments by planimetry and histology (p=0.0018, p=0.0118 and p=<0.0001) on day 2, 3 and 6 respectively (A). Linear regression between virtual histology and histology also showed significant (p=0.0090, p=0.05 and p=<0.0001) on day 2, 3 and 6 respectively (B) and assessment by planimetry and virtual histology revealed the highest correlation (p=<0.0001, p=<0.0001, p=0.0001) on day 2, 3 and 6 respectively(C). Data from 3 donors (n=3), each with 3-4 replicate explants per condition. Error displayed as SEM. ●- Donor 7, ■-Donor 8 and △-Donor 9 (Refer to Table 2.1).*

At this point of experimentation it became clear that the sample size was insufficient. The previous analysis was supplemented so that 5 donors were examined via planimetry.

With this expanded data set results reveal that using green cell tracker and planimetry assessment not just show that the epithelial healing can be monitored longitudinally, but also confirmed that with additional n numbers a clear divergence in the evolution of repair with the addition of FBS (i.e. the interaction between time and treatment factors), when the % epithelial closure (Figure 3.15B), or the area of healed epidermis (Figure 3.9C) was evaluated. These two measures gave similar data. Measuring the explants each day also revealed that some wound contraction occurs over time (Figure 3.15D). However, this only account for around 20% of total healing observed, indicating that re-epithelialisation provides the major healing mechanism. The level of contraction between control and FBS treated wounds was unchanged (Figure 3.15D). Also, the rate of healing between individual donors is variable; for example the mean re-epithelialisation in control wounds fluctuated between 13.45% and 58.87% at day 2, and 27.81% and 72.22% at day 4. However, a response to FBS was reproducible and acceleration in the rate of re-epithelialisation of between 31.48% and 76.67 at day 2 and 38.29% and 96.39% at day 4 was observed.

In addition, quantification of the % re-epithelialisation using a paired t-test showed a significantly accelerated healing at both day 2 and day 4, confirming the reliability of the model (Figure 3.15E).

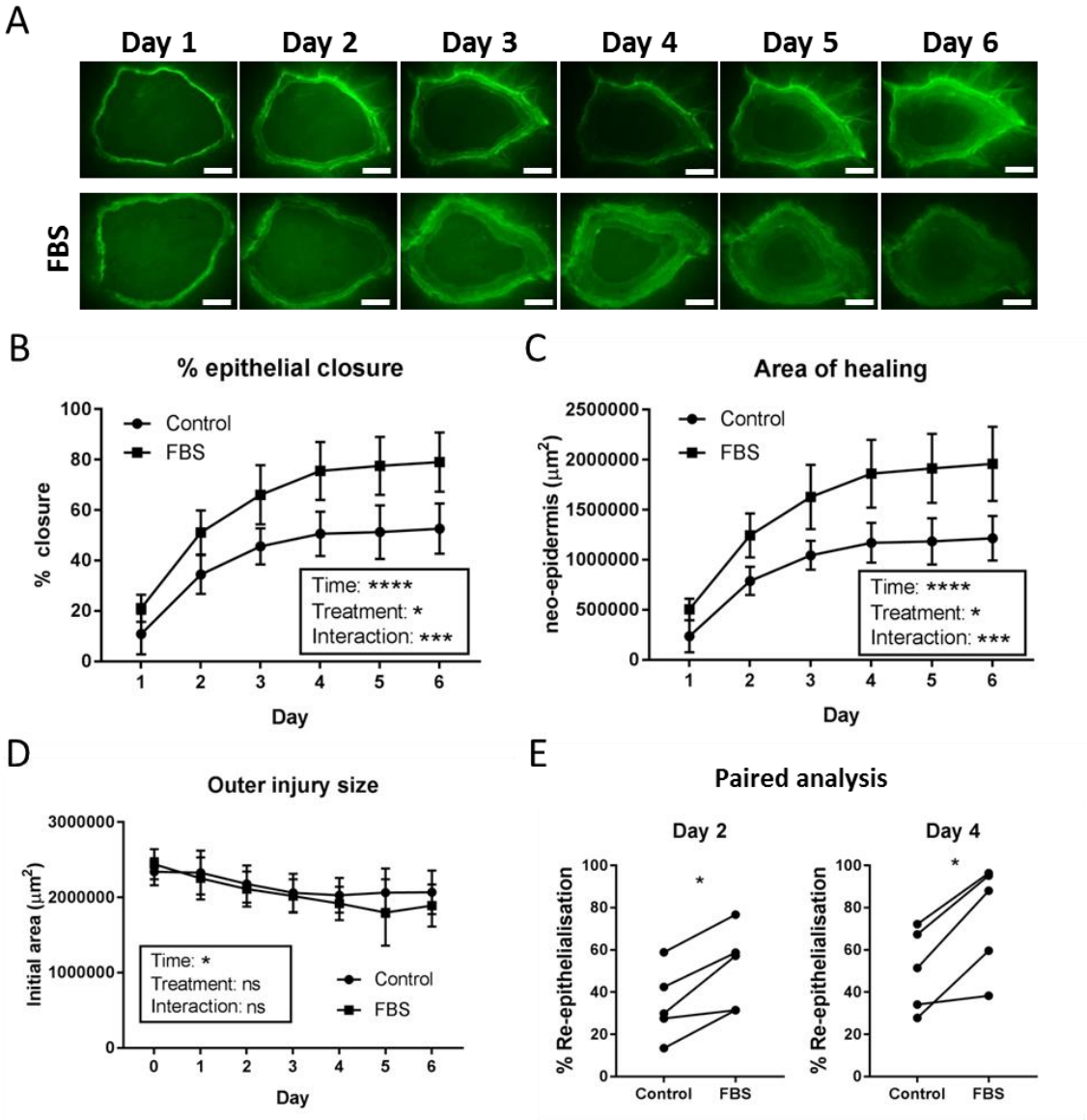

Figure 3.15: Daily en face fluorescent images longitudinally assesses epithelial healing. *Human ex vivo wounds were cultured with daily treatments of the green fluorescent cell tracker dye CMFDA, with 10% Fetal Bovine Serum (FBS) compared to standard media control arm. Daily en face imaging tracks epithelial formation over time (A). Quantification revealed a significant acceleration between FBS and control in the % epithelial closure (B), and the area of neo-epidermis (C). Slight contraction was observed of the wounds in culture, although there was no difference between FBS or control wounds (D). Paired analysis demonstrates the variability in healing between donors, but that the FBS response is reproducible (E). Data in B-D analysed using 2 way ANOVA with repeated measures, while E used a paired t test. Graphs show mean +/- SEM in B-D and in E the mean of each individual donor (n=5 donors). * P<0.05, *** P<0.001, **** P<0.0001. Bar = 500um.*

Within the daily imaging images, distinct areas of epidermal healing was identified with a band of dim expression towards the epidermal front, with brighter areas nearer to the margin (Figure 3.16A). As the CMFDA dye accumulates over time and based on observations with CMFDA and CMTPX dual labelling (Figure 3.4), one hypothesis drawn was that these dim cells likely reflected newly laid tissue that were not labelled until a late timepoint. These areas might define cornified and non-cornified regions of the healing epidermis, as described to occur in human *ex vivo* wounds (Lu and Rollman, 2004). To further explore this, histology of serial sections to compare H&E morphology to the CMFDA intensity was conducted, and this revealed that the bright area showed cells with a granular appearance also stratum corneum can often be identified within the neo-epidermis within the CMFDA bright cell population (Figure 3.16B).

Quantification of these dim and bright regions in my serum-free and 10% FBS treated explants, showed a trend towards immature epidermis being laid down more quickly with FBS, although this did not reach statistical significance (Figure 3.10D). On the other hand, while the increase in extent of more stratified epidermis over time is highly significant, we find no change between treatments.

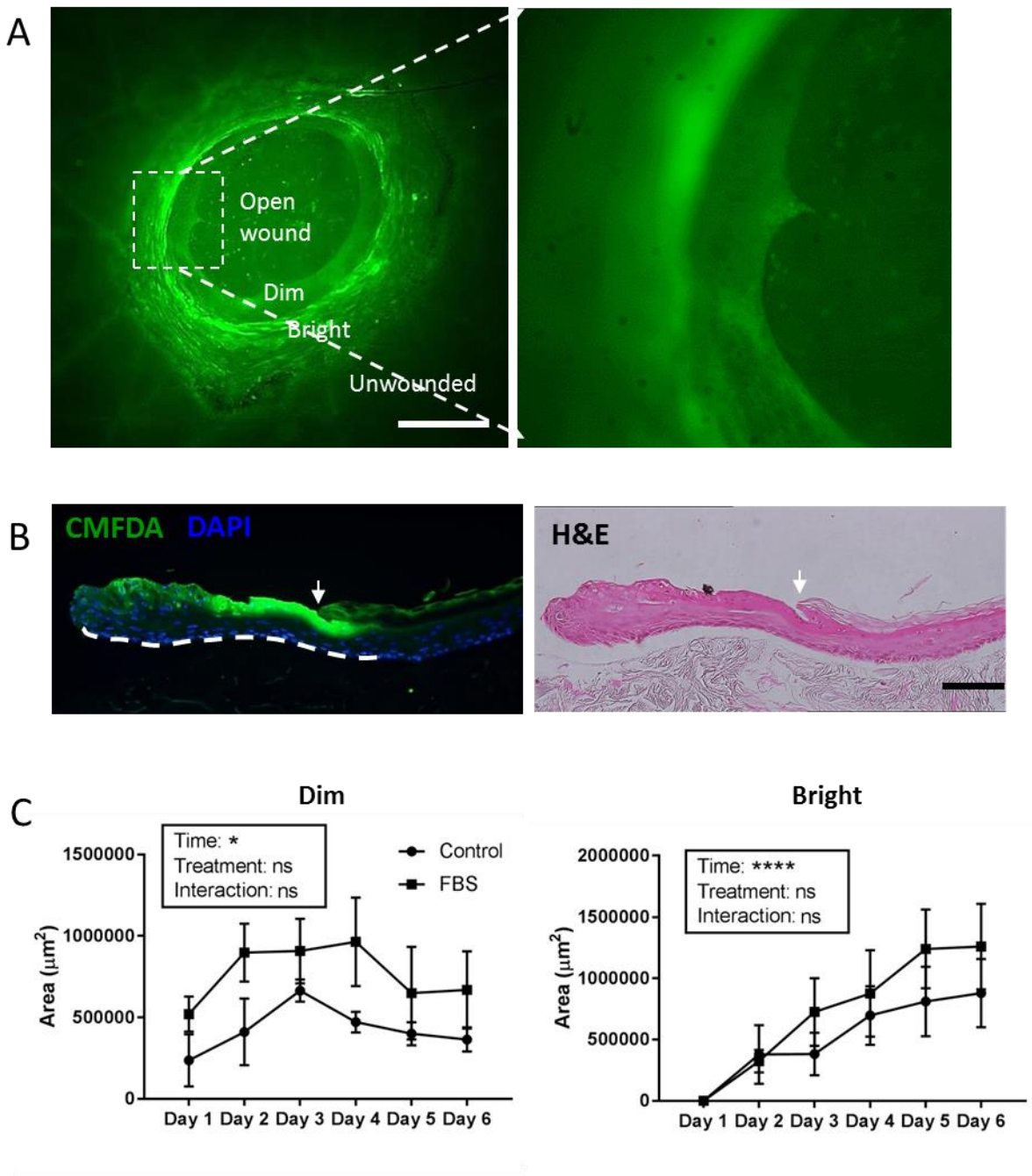

Figure 3.16: CMFDA en face imaging can distinguish between healing and non-healing area*. Daily en face imaging shows regions of dim and bright CMFDA intensity (A). Histology identifies mature stratified neo-epidermis at the edge of the band of bright epidermis (white arrow) (B). Quantification revealed a trend towards increased area of dim epidermis in the presence of serum (C). The area of bright epidermis was unchanged (D). Graphs D show mean with error expressed as SEM, data analysed using two way ANOVA with repeated measures. Bar = 500mm (A) and 100mm (B-C). * P<0.05, **** P<0.0001*

In summary, this chapter discovered that some serum free media conditions i.e. WE-serum free, can culture wounded human skin explants for up 6 day with no/minimal loss of viability. Most importantly, this chapter highlighted that fluorescent dyes can labelled cells at the wound edge and suggests the wound heal occurred by the shield mechanism. The fluorescent dye used also established a new way to examine *ex vivo* wounds planimetry longitudinally and the planimetry assessment has a high correlation to histological measures. This method shows that it can detected changes to healing with a known healing promoter i.e. FBS.

3.2 INVESTIGATING THE MANIPULATION OF NGF SIGNALLING DURING SKIN WOUND REPAIR

This main chapter of the thesis focuses on topical treatment of the wound bed *ex vivo* that should stimulate or inhibit NGF signalling, in order to establish whether this pathway influences epidermal repair in the *ex vivo* skin repair model. Therefore the first aim of this chapter was to examine application of NGF exogenously to wounds, as this has been used in some clinical trials (see table 1.3). The effect of NGF on epidermal repair and proliferation was investigated.

Next, a known inhibitor for tyrosine kinase receptor A, K252a (natural alkaloid) was used to treated the wound and investigate its effect on epidermal repair (Byrd *et al.*, 2018, McGrath and Uitto, 2010). For this study, the inhibitor for p75NTR has not been tested since it was proven before that blocking this receptor does not influence the epidermal cells migration *in vitro* (Pincelli and Yaar, 1997).

In addition, NGF neutralising antibody was also used to block NGF-TrkA signalling by neutralising the endogenous NGF in organ culture and investigate its effect in epidermal repair.

3.2.1 Exogenous NGF does not accelerate epidermal repair in acute wounded human skin *ex vivo*

The rationale that exogenous NGF was topically applied to the wound bed in skin organ culture is that topical NGF is the preferred mode of application in human skin since subcutaneous or intravenous injection can produce severe adverse effect such as pruritus, myalgia and hyperalgesia (Murphrey and Zito, 2018, Agache *et al.*, 2017). The NGF could be added into culture media if one wants to mimic the systemic

administration. The wound re-epithelialisation was mainly assessed primarily by planimetry, as my data shown in Chapter 3 section 3.1 demonstrated this was capable of capturing multiple data points for each wound. However, my data also was supplemented with histology assessment at day 1, 2, 3 and 6 for three donors (Figure 3.12).

Direct application of NGF (25 µg/mL murine 2.5S NGF) to the wound bed imitated the clinically most relevant mode of application in an ulcer management setting. This is the dose that had been used in Generini *et al.*, (2004) and is cost effective for this study – details in chapter 2 section 2.4.1. Due to insufficient availability of human skin samples a dose-response could not be established, therefore this study had to choose a dose that has already been used in a clinical trial to be tested in this model.

Total wound closure as measured by intravital planimetry over 6 days using cell tracker dyes (Figure 3.17A), showed no statistically significant effect of the tested dose of NGF experimentally wounded human skin under serum-free conditions *ex vivo* when measured by the percentage of wound closure (Figure 3.17B). While analyses by area of wound closure showed that NGF group significantly delayed wound closure on day 1, 4-6 (Figure 3.17C). Neo-epidermis was also measured histomorphometry by the length and area of epidermal migration (Figure 3.17D and E) also yielded same result as measured by the percentage of reepithelialisation (planimetry).

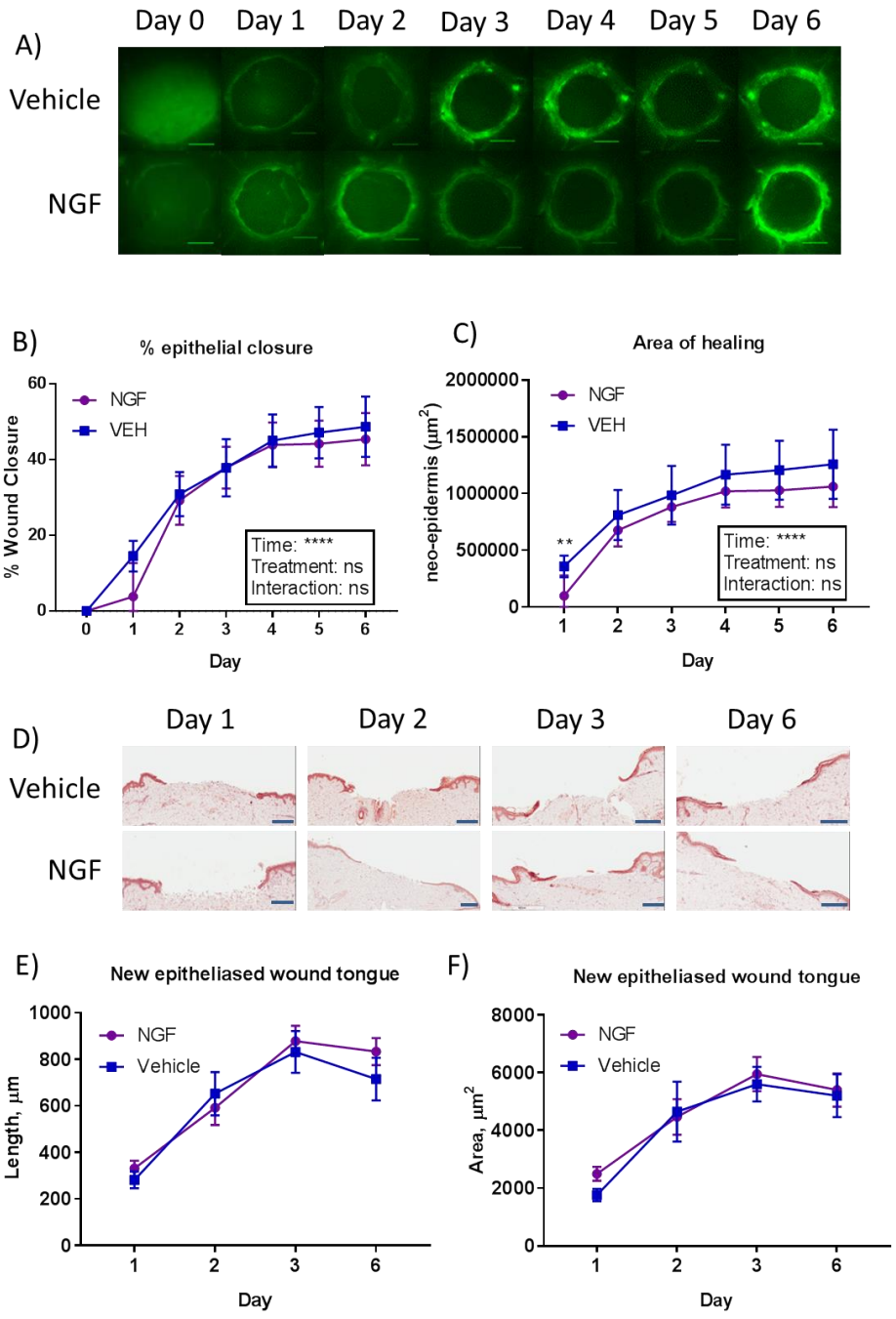

Figure 3.17: Assessment of NGF effect on skin wound healing by planimetry and histology. *Representative images showing the effect of treatments on wound closure by planimetry (A). Bar=500 µm. Data analysed by the percentage of wound closure showed no significant different between groups of treatment (B) but data analysed by the area of neo-epidermis showed vehicle group (1% BSA in PBS) has more neo-epidermis on days 1 (C). Data in A-C was analysed from 5 donors (3-4 explants in each donor)). **-p<0.001, *-p<0.0001. Representative images of epithelial wound closure Day 1, 2, 3, 6 (D) (Bar=300µm) by quantitative immunohistomorphometry of keratin 6+. Newly formed wound epithelium was measured by length (E) and area (F) (n=3) revealing no significant effect of NGF compared to vehicle group. A section in the centre of each wounded explant shown in Fig. 4.D = Fig 4A (day 6).*

Previously, repeated measure ANOVA was used to determine the effect between groups of treatment across the timepoints (Figure 3.15 and 3.17). However, according to (Matthews et al., 1990) there are a few flaws in presenting such data with lines joining the means at each time point as presented in the (Figure 3.15 and 3.17) and placing an indicator of significance by each time point to summarise the results of the separate significance test (if any). As mentioned by (Yagi and Yonei, 2018), by referring to (Martin, 1997) the curve joining the means might obscure the variation of the individual curve shapes.

Therefore this chapter also presents the individual curve for every explant in every condition across the time points by the percentage of unclosed wound (Figure 3.18) and by the area of wound closure (Figure 3.19). Generally the wound are closing or the size was reducing but at variable rates. You can observe this variation (marked by blue dashed circle) in donors 3, 4, 5 and 6. This variation can happen within the same explant, or different explants at different time point and different treatment group. For example explant 10 in NGF group (Figure 3.19) showed a higher peak on day 1 compared to other explants in the group.

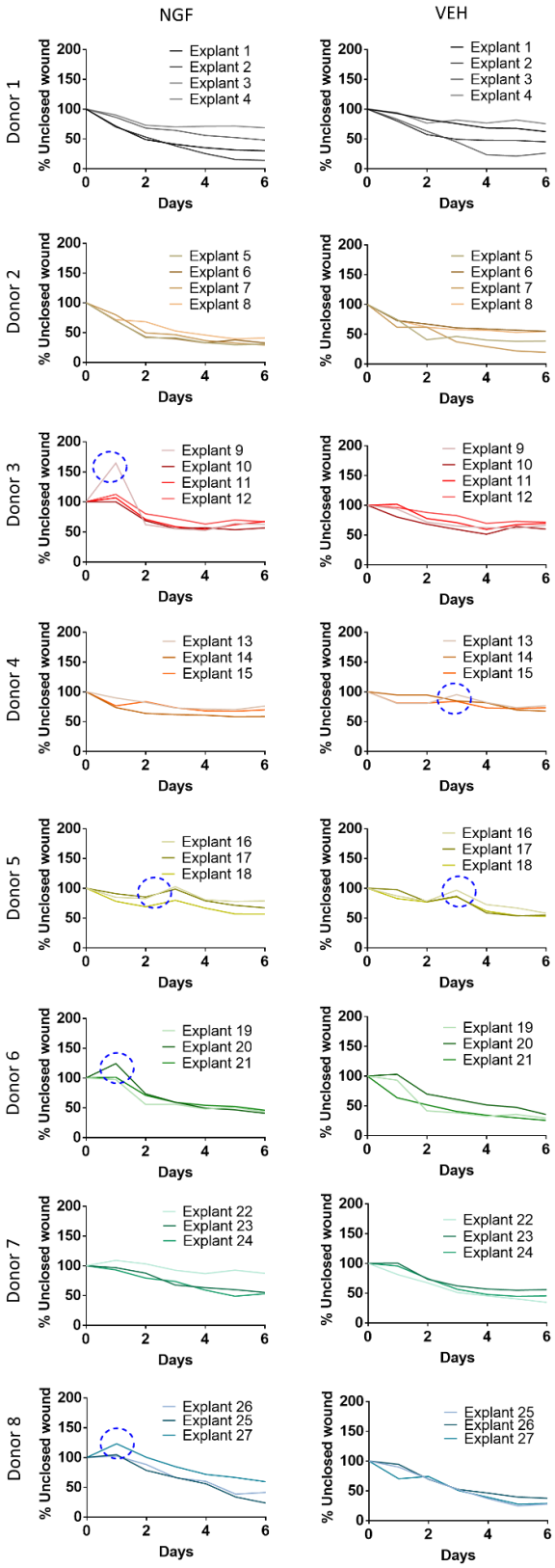

Figure 3.18: *Individual plots of percentage wound closure against time in two groups of treatment with 8 donors (3-4 explants/treatment). Blue dash circle mark the variation that occur during wound assessment within the explant itself at different timepoints.*

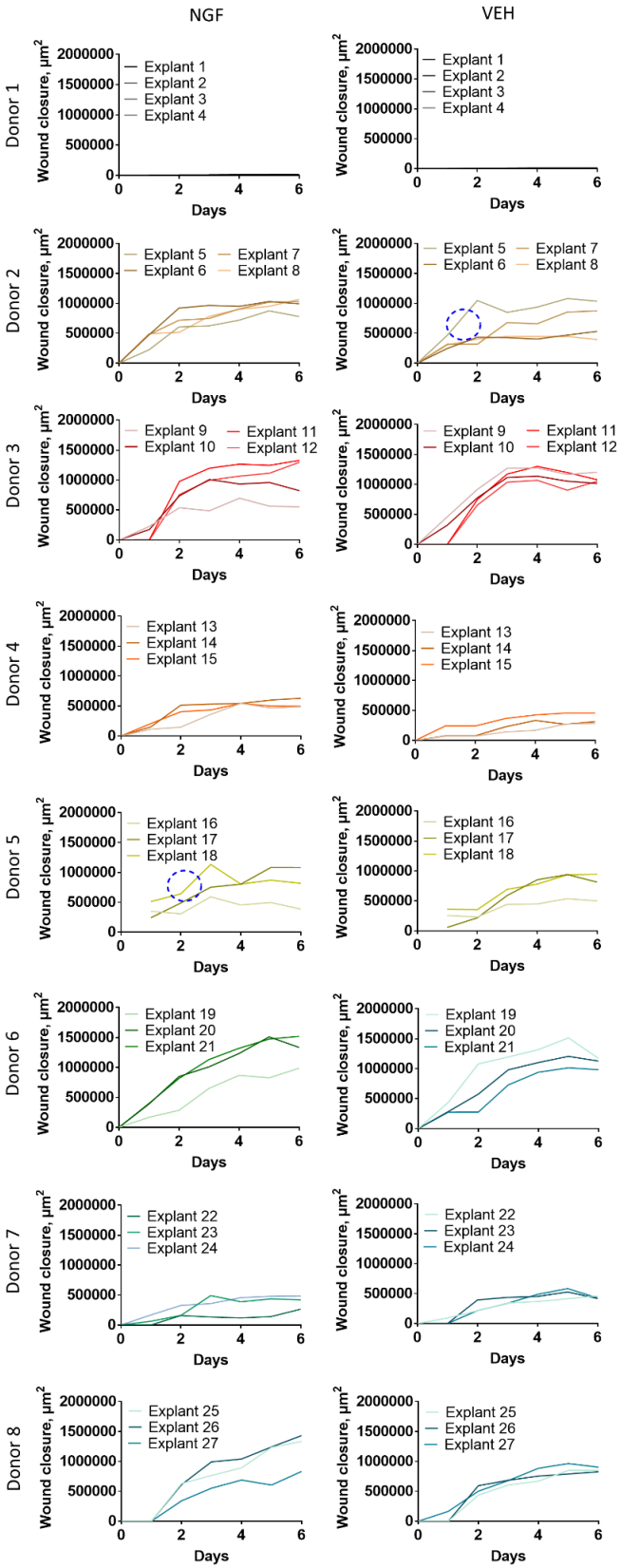

Figure 3.19: *Individual plots of area of wound closure against time in two groups of treatment with 7 donors (3-4 explants/treatment). Blue dash circle mark the variation that occur during wound assessment within the explant itself at different timepoint.*

From the individual curves (Figures 3.18 and 3.19) the effect of topical NGF and its vehicle was re- analysed as a summary measures of overall healing, by transforming the data into an area under curve (Figure 3.20). Again, no significant difference was found between NGF treatment and vehicle in the percentage of wound closure (*p* 0.4001) and wound closure area (*p* 0.1864). In my previous analysis (Figure 3.17) only result from 5 donors were analysed. This is because repeated measure ANOVA does not allow analysis with missing data points. While in another 3 donors there some missing data on day 0 due to technical problems with microscope. However, the summary measure allows this to be analysed (Agache *et al.*, 2017, Menon *et al.*, 2012). As shown in figure 3.19, no individual curve for explants 1 – 4 from donor 1 because no assessment was done on day 1.

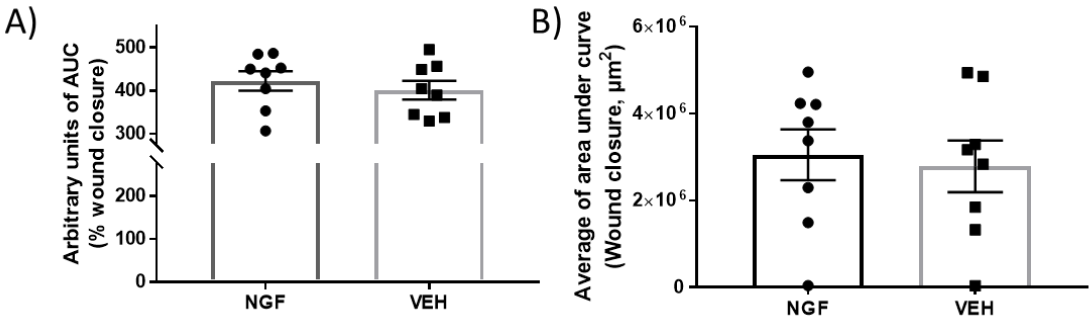

Figure 3.20: Summary measure analysis reveals no significant difference with NGF treatment*. Data from the percentage of wound closure (Arbitrary units of AUC) (A) and the area of wound closure (µm^2)(B) was transformed into area under curved and analysed by summary measures. A paired t-test shows that there is no significant difference in the wound closure between groups (n=8 donors).*

Table 3.1: Summary of area under curve analysis of wound closure

n=8	Area under curve (% Wound closure)	n=8	Area under curve (Area of wound closure, mm^2)
NGF mean (SD)	422.4 (63.91)	**NGF mean (SD)**	3.05 (1.65)
VEH mean (SD)	400.9 (61.80)	**VEH mean (SD)**	2.79 (1.67)
Ratio of geometric mean	0.9497	**Ratio of geometric mean**	0.881
95% Confident interval	0.8288 to 1.088	**95% Confident interval**	0.7181 to 1.081
t Test	t=0.8958 (df=7)	**t Test**	t=1.465 (df=7)
p value	0.4001	**p value**	0.1864

3.2.2 NGF does not influence epidermal proliferation

Next, this study examined whether topical NGF applied to the wound bed of acute wounds has an impact on cell proliferation using Ki-67 quantitative immunohistomorphometry. The rationale of this experiment is to investigate at the cellular level after the treatment. The percentage of Ki-67 positive cell at basal layer epidermal keratinocytes was first examined within untreated wounds, which showed that unwounded skin regions retained proliferation across timepoints, indicating that the tissue retained good viability *ex vivo* over the course of the experiment (Figure 3.21). A trend towards lower overall proliferation in culture compared to baseline levels was seen, though this was not significant. The percentage of Ki67 positive cells was at its peak on day 3 in the neo-epidermal region (*p* 0.0487) compare to the unwound regions, demonstrating that the model displays an upregulation of proliferation in response to the injury. When comparing to vehicle-treated wounded control explants, NGF treatment did not significantly change proliferation patterns within neo-epidermis, peri-wound and unwounded regions (Figure 3.22). The change

in pattern was therefore occurring due to the wound healing process itself. In this process the Ki-67 positive cells (<10%) can be seen scattered in the epidermis on day 1 and on day 2 the number become slightly higher and started showing line-up pattern like 'moving toward' to peri-wound. By day 3, more Ki-67 positive cells (>10%) accumulate at neo-epidermal and peri-wound (Figure 3.6). Thus, in healthy wounded human skin with normal NGF levels, the, supplementation of the tested dose of exogenous NGF did not enhance reepithelialisation.

Lastly this chapter documented for the first time the localisation of NGF, TrkA and p75-NTR protein expression changes in human skin wounds in organ culture.

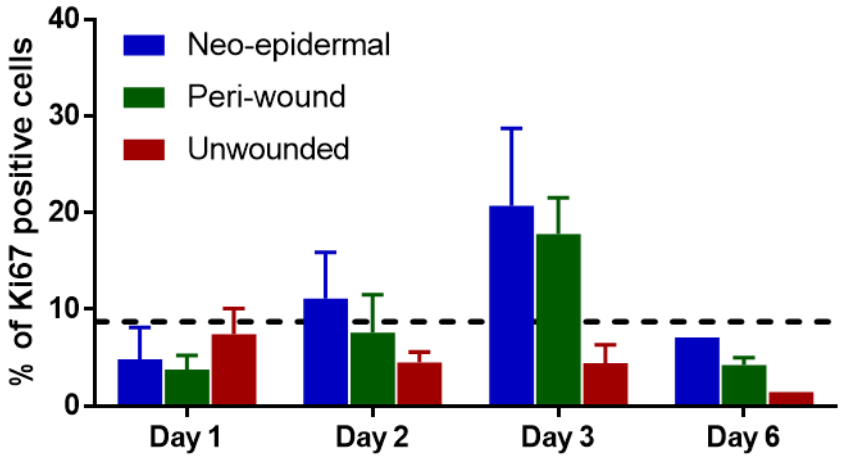

***Figure 3.21: Proliferative cell distribution in wounded human skin ex vivo**. Graph shows the percentage of Ki-67 +ve cells in neo-epidermis increased until day 3 and decrease to baseline distribution on day 6. There is no significant difference in percentage of Ki-67 +ve cells across regions and days, although on day 3, neo-epidermal and peri-wound regions showed a non-significant trend towards increased Ki-67 percentage (p 0.06). Graphs from mean of n=3 donors with 1-3 replicate explants per condition, with error displayed as SEM. One explant on day 6 from patient MSHB0941 (Refer table 2.1). Dashed line represents normal skin. p<0.05 is significant.*

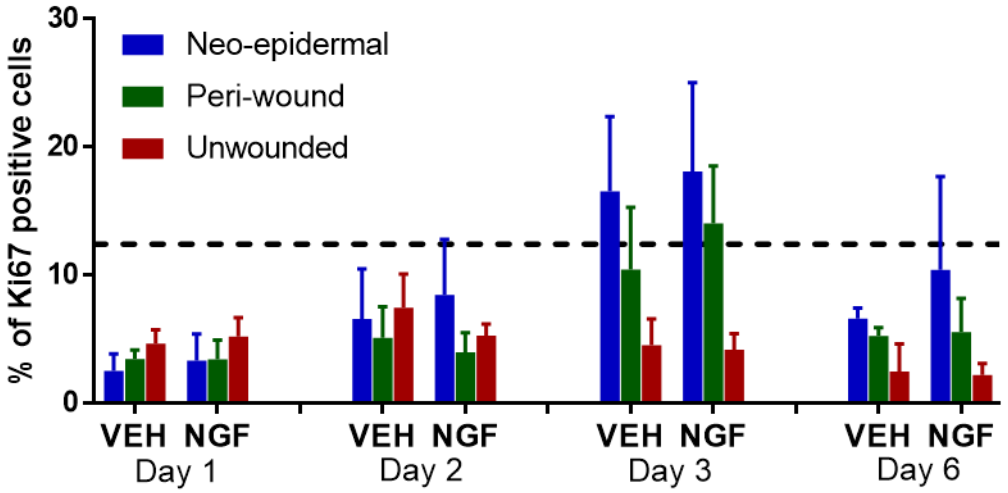

Figure 3.22: NGF does not promote epidermal proliferation in human wounded skin ex vivo*. No changes in the percentages of Ki-67 +ve cells number between treatments across timepoints. Graphs from mean of n=3 donors except for day 6 only 2 donors, with error displayed as SEM. Dash line represent normal skin. (Refer table 2.1)*

It is well known that inflammatory cells are involved in wound healing (Ng and Lau, 2015, Eming *et al.*, 2014, Yagi and Yonei, 2018), with *in vivo* studies also showing that inflammatory cells such as macrophages will influx to the wound site between days 2-7 (early inflammation phase of wound healing) (Yagi and Yonei, 2018, Yousef and Sharma, 2018).

The chemotactic role and NGF has been shown (McGrath and Uitto, 2010, Wertz, 2018, Murphrey and Zito, 2018), and so I next investigated the effect of NGF topical application on CD68 positive cell distribution. Figure 3.21 shows that there is no significant difference in number of CD68 labelled cells per mm^2 between NGF and vehicle groups in every region analysed, for every timepoints. However, the number

of CD68 positive cells within the wound bed in treatment (p <0.0001 and 0.0437) and vehicle (p 0.0042 and 0.0063) group is significantly lower on day 1 and 3 compared to normal skin respectively. While on day 6 the vehicle group showed a significant difference compared to normal skin (p 0.0063).

In peri-wound area, vehicle group showed significant difference in the number of CD68 +ve cells on day 1 (p 0.0472) and day 6 (p 0.0411). Whereby, in unwounded region it shows that NGF (p 0.0272) and vehicle (p 0.0384) group have significantly lower numbers compared to normal skin on day 1 and only vehicle group (p 0.0217) shows a significant difference on day 6 compared to normal skin. Based on these two donors the distribution of the CD68 positive cells are more likely to distribute evenly. This might also be because the whole explant itself is considered wound or this CD68 positive cells are the resident cells in the tissue (Figure 3.23). This trend is differing from *in vivo* when macrophages or CD68 positive cells infiltrate wound site highest on day 2-7 (Ludovici *et al.*, 2018, Elias, 2012).

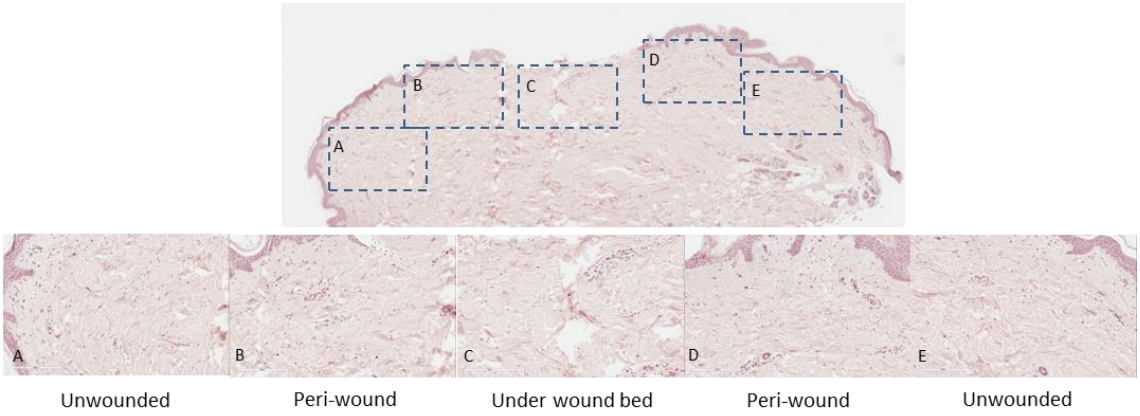

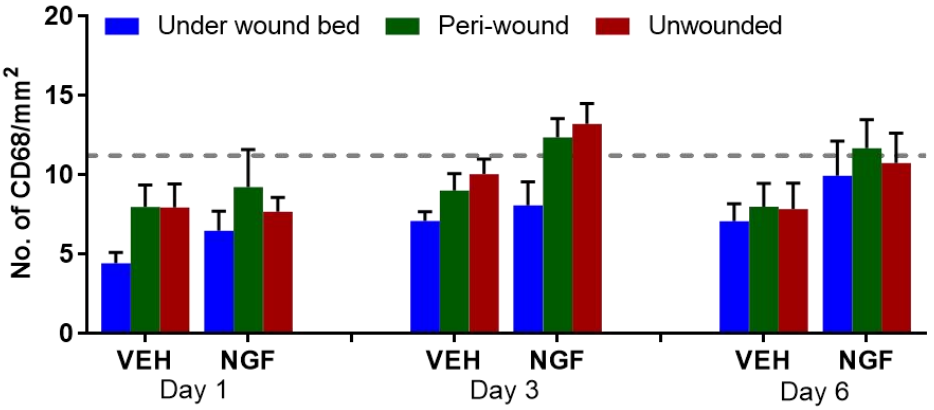

Figure 3.23: CD68 positive cell distribution in organ cultured skin wounds*. Images show the analysis regions were measurements were made (upper panel). Graph shows quantification of the infiltration and distribution of CD68 positive cells to wound area, peri-wound and unwounded regions. Data from n=6-7 explants per condition (2 donors). Error displayed as SEM. Grey dash line denotes n umber of CD68 +ve cells in normal skin. (Refer to table 2.1)*

3.2.3 Antagonising TrkA-mediated signalling inhibit wound re-epithelialisation

In the previous section 3.2, results show that exogenous NGF administered to *ex vivo* wounds does not accelerate wound re-epithelialisation compared to its vehicle. The exogenous NGF might signal through either TrkA, p75NTR, or a combination of the two, which might complicate matters. Therefore, this study wondered whether specifically antagonizing NGF-TrkA mediated signalling either in the presence of exogenous NGF or in explants with no NGF treatment might alter reepithelialisation of "healthy" wounded human skin *ex vivo*. Hence, to address this the well-established effects of K252a to block TrkA signalling was tested (Menon *et al.*, 2012, Ng and Lau, 2015).

Experiments from this PhD study showed that wounds treated with K252a significantly inhibited wound re-epithelialisation as measured by daily planimetry (Figure 3.24). This effect could not be rescued by co-treatment with exogenous NGF (Figure 3.24). Further investigation on tissue treated with K252a using histological sections shows that K252a only inhibits epidermal migration at the wound site where topical treatment was applied, while newly epithelised tissue around the edge of explant (tissue edge) was unchanged (Figure 3.25).

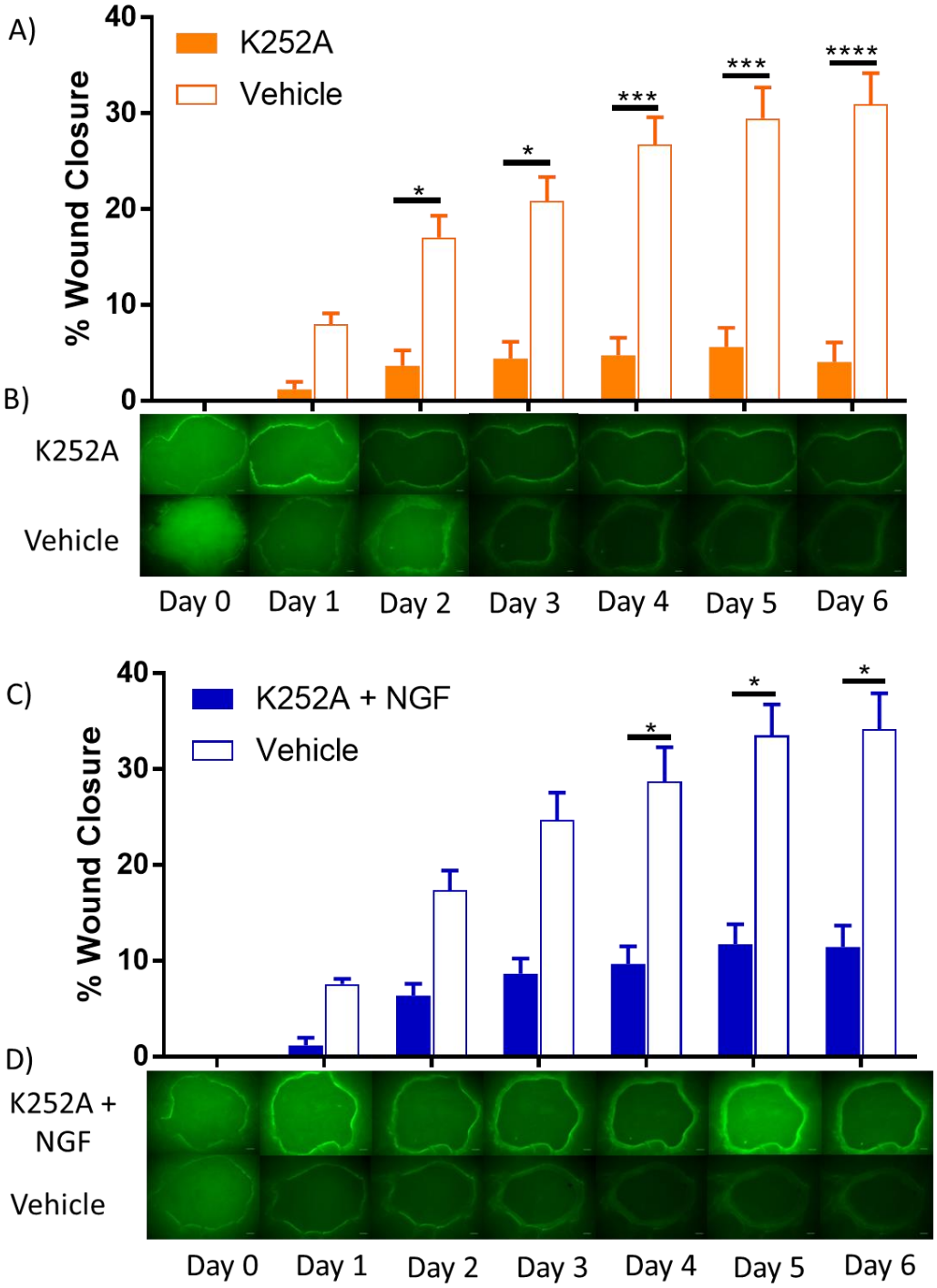

Figure 3.24: K252a inhibits epidermal repair*. Graph shows that K252a significantly inhibits epidermal repair (A).Vehicle for K252a contain 0.001% DMSO in culture media. Explants were treated with NGF after the K252a was administered for rescue experiment (C). Vehicle for rescue experiment is a mixture of 1% of BSA in PBS and 0.001% of DMSO in culture media. Representative images showing the effect of treatments on wound closure (B &D). Data was analysed on n=12 explants per condition from 4 donors. Error displayed as SEM. Bar-200µm. *p<0.05, ***p<0.001, ****p<0.0001.*

Further investigation on tissue treated with K252a using histological sections shows that K252a only inhibits epidermal migration at the wound site where topically treatment was applied, while newly epithelialised tissue around the edge of explant (tissue edge) was unchanged (Figure 4.9). The wound edge here refer to the new epilthelialised tissue at the wound bed and tissue edge refer to wounded tissue at the outer of tissue explant (refer to Figure 2.5 in method section).

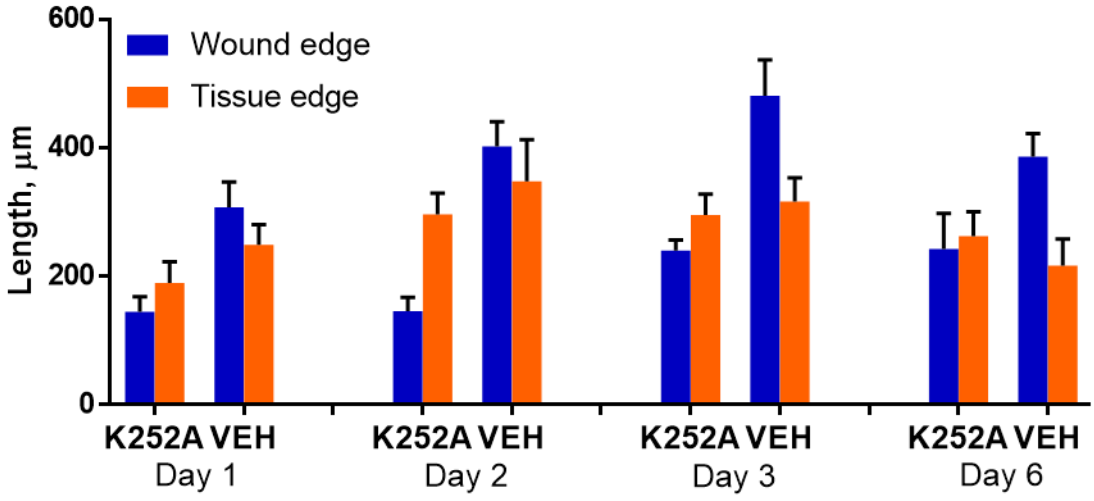

Figure 3.25: K252a shows topical effect in inhibits epidermal repair*. Graph shows the effect of K252a on length of new epithelised tissue was specific to the drug application site at wound edge (E) in two donors (n=2). Error displayed as SEM. Bar-200µm.*

Treatment with K252a does not inhibit proliferative cells in skin wounded organ culture. Figure 3.26 showed that the percentage of Ki-67 +ve cells has no significant difference between groups across timepoints and regions except in neo-epidermal region on day 3 significantly higher compared to unwound region (*p* 0.0297). However, the percentage of Ki-67 +ve cells was significantly low in neo-epidermal and peri-wound regions on day 1 and 2 in K252a group (*p* 0.0016 and 0.0095) respectively, and peri-wound on day 2 (*p* 0.0249) compared to uncultured skin.

This result might suggest that K252a does not inhibit the proliferative cells but delays the activation of proliferation.

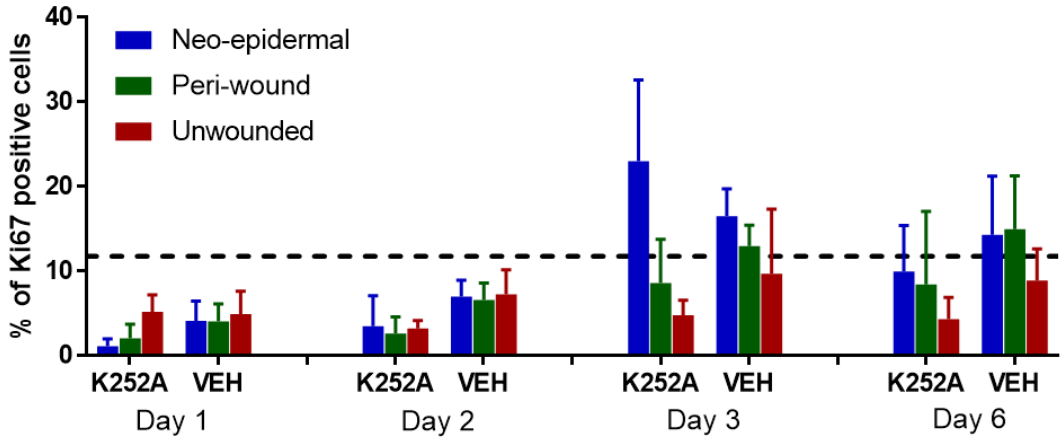

Figure 3.26: K252a does not inhibit cell proliferation. *Graph shows that there is no difference in the % of Ki-67 +ve cells between groups across timepoint. However, the % of Ki-67 +ve cells was observed higher in neo-epidermal region compared to unwounded region on day 3. Data on n=2 donors with 5-6 explants per condition was analysed using one-way ANOVA. Black dash line represents normal skin. * p<0.05, **p<0.001.*

3.2.4 Epidermal wound repair is not delayed with a NGF blocking antibody

Since immunostaining results showed that human skin cultured *ex vivo* expressed NGF protein expression as high as normal skin (See section 3.3), therefore to build upon the data in figure 3.27 this study used NGF neutralising antibody to investigate if the endogenous NGF does influence the wound healing process. This differs from the previous experiment in that K252a inhibits TrkA, while the antibody binds NGF itself and will prevent both TrkA and p75-NTR signalling.

Data from this experiment showed that the NGF neutralising antibody used in this study does not impair wound closure. NGF was co-treated alongside the neutralising antibody, which appeared slightly elevated, though significance of this result could not be determined based on the two donors used for this experiment (Figure 3.27).

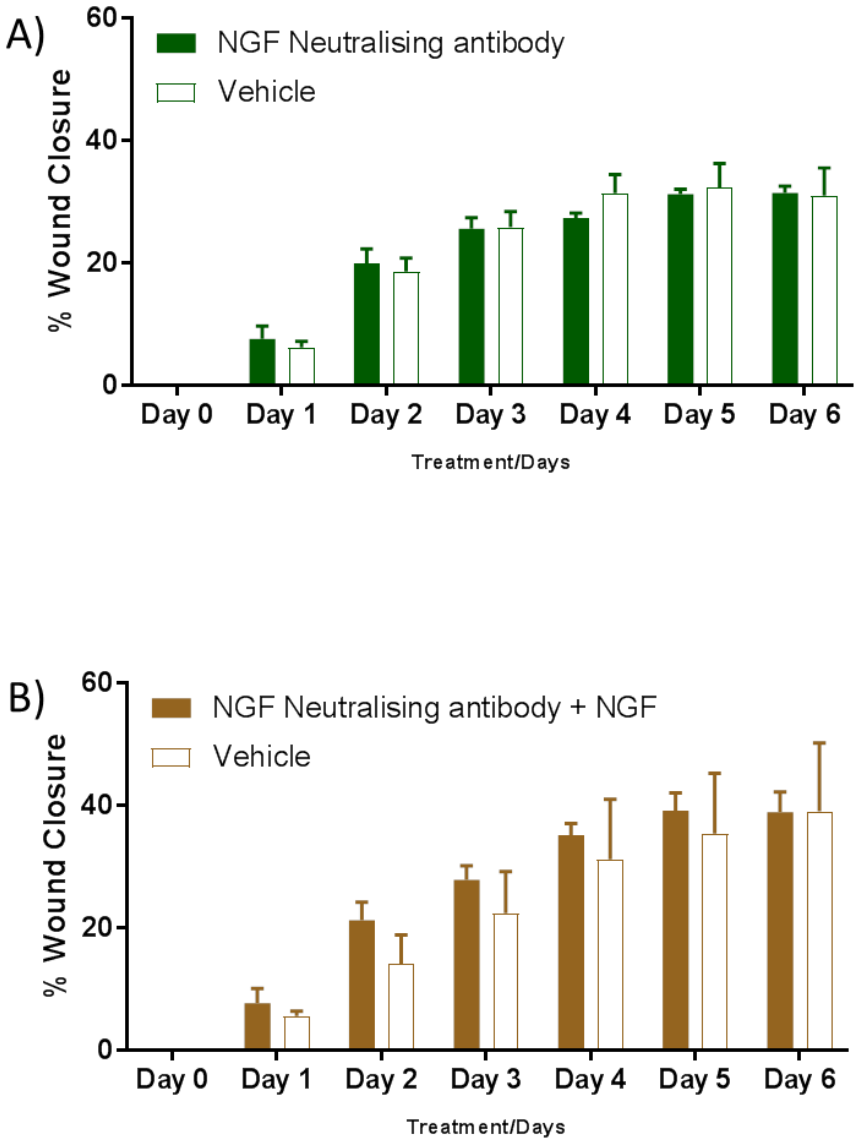

Figure 3.27: Blocking NGF signalling through a neutralising antibody does not alter epidermal repair. *Graph shows that NGF neutralising antibody did not significantly alter the rate of wound closure (A). Vehicle for neutralising antibody is PBS. When NGF was added alongside neutralising antibody, a non-significant enhancement in healing was observed compared to neutralising antibody (B).Vehicle used in (B) is 1% BSA in PBS (n=2). Experiment was run with 3-6 replicate explants (pool) per condition from 2 donors. Error displayed as SEM.*

Since results in these experiments on both the use of exogenous NGF and NGF neutralising antibody on wound closure does not produce encouraging results, this study then investigated the NGF protein level in skin organ culture by ELISA. It shows that the biopsies already contained some amount of NGF therefore adding exogenous might not enhance epidermal migration (Figure 3.28). In this experiment it shows that normal skin does contain endogenous NGF but with inconclusive results since this came from just one donor. In my knowledge, there is no previous study that has quantified endogenous NGF in human skin. The experiment would need to be repeated in the future with many more donors.

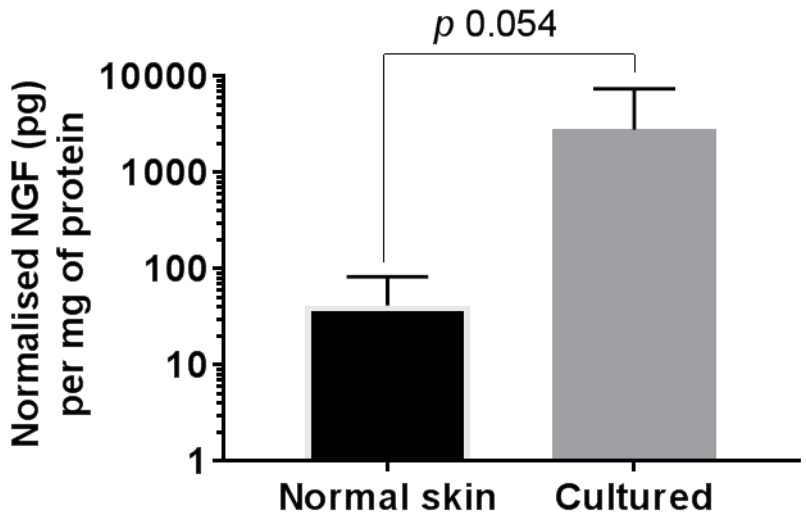

Figure 3.28: Endogenous NGF in human skin explants. *Graph shows that endogenous NGF lowers in uncultured (normal skin) and higher in cultured skin. Analysis was done on n=1 donor with 3 normal skin biopsies (uncultured) and 6 skin biopsies (cultured); one biopsies for each day. Error displayed as SD.*

3.3 TOPICAL NGF AND K252A DOES NOT ALTER NGF, TRKA AND P75-NTR PROTEIN EXPRESSION INSITU

3.3.1 Protein expression of NGF and its cognate receptors were found to be localised within epidermal human skin *ex vivo* model

It was well known that NGF (Blais *et al.*, 2013), TrkA (Shibayama and Koizumi, 1996) and p75-NTR (Di Girolamo *et al.*, 2008) is expressed in human skin (Yaar *et al.*, 1991). In this study, the protein expression of NGF, TrkA and p75-NTR in the epidermis of normal human abdominal skin (uncultured) and experimentally wounded human skin was profiled *ex vivo,* over a time-course that essentially assessed an acute wound healing response in healthy, but organ culture-stressed adult human full-thickness skin.

This study found that the expression of NGF protein was widely expressed in epidermis and dermis of human abdominal skin (Figure 5.1). However, this study focused on the epidermal layer since this *ex vivo* model is well established to look at aspect of epithelial repair. The intensity of the expression within the epidermis intensified from basal layer to stratum corneum layer (Figure 3.29). The similar expression was observed in cultured skin on day 3 (unwounded region) (Figure 3.29).

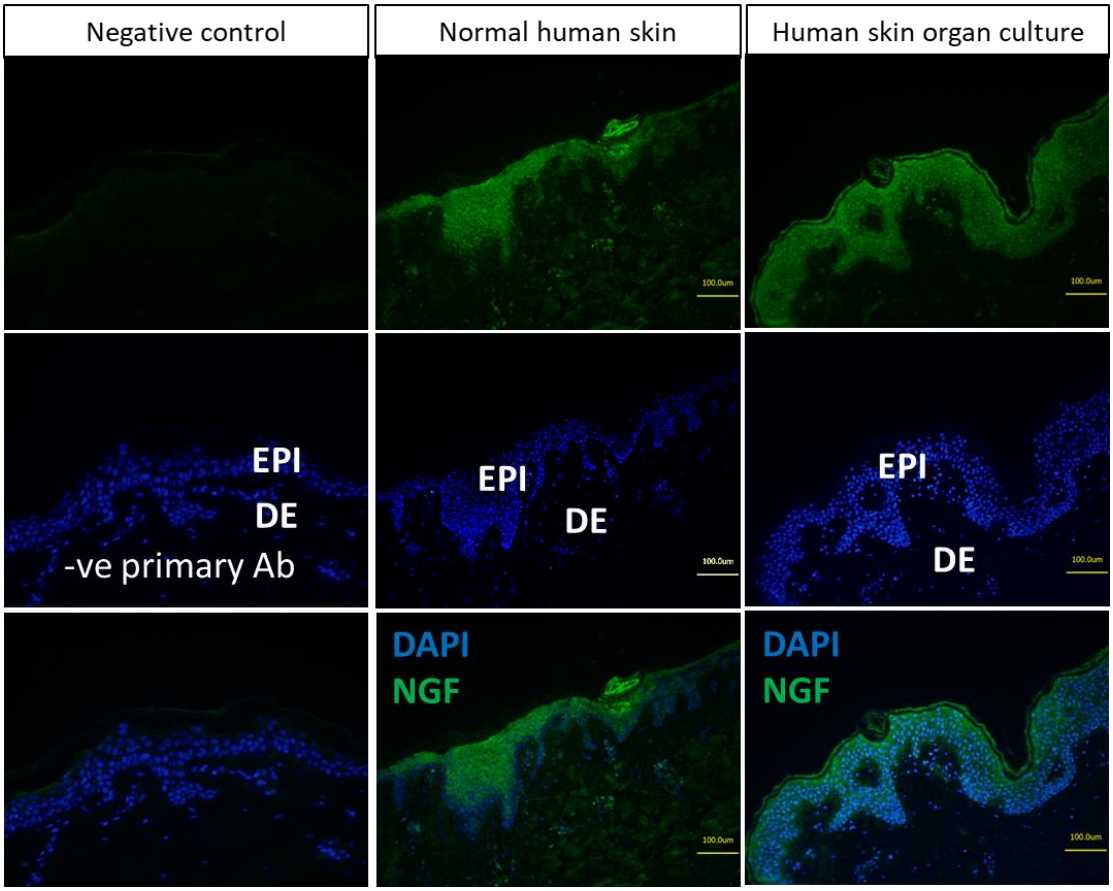

Figure 3.29: Localisation of NGF in human skin in situ and ex vivo*. NGF protein expression was detected in the epidermal layer of abdominal skin and unwound region of cultured tissue on day 3. Similar expression also was detected in normal skin (unwounded) human organ culture (day 1, 2 & 3).*

In wounded human skin organ culture, the expression of NGF protein also was found within epidermal cells of the healing wound tongue (Figure 3.30) and the similar protein expression of NGF also can be found in the suprabasal layer (Figure 3.30) in peri-wound and unwounded regions. Unlike the normal epidermis, where expression is restricted to the suprabasal layers, expression was found within all layers of the neo-epidermis (Figure 3.30). This study also showed that the cells at the front of the migrating epithelium are lacking NGF (as indicated by blue arrows in Figure 3.30).

The definition of regions can be found in the Methods chapter section 2.11 (Figure 2.5). One has to bear in mind that the entire wounded human skin organ culture is actually “wounded” but for this study; the unwounded region refers to an uninjured area in the tissue explant at least 800 - 1000 µm from the peri-wound (which this study defined immediately at the wound edge).

The quantification of the relative intensity of NGF protein expression showed a slight reduction of NGF expression at the regenerated epidermis (neo-epidermis). However, this finding was statistically unchanged compared to baseline levels (uncultured tissue from the same donor), “unwounded” areas of epidermis from cultured tissue, or peri-wound epidermis adjacent to the punch (Figure 3.30). The trend towards downregulation of NGF protein expression in new-epidermis across timepoints might be caused by tissue differentiation and stratification as within normal skin the expression was gradually more intense from basal to stratum corneum. The presence of NGF protein expression in *ex vivo* organ compared to uncultured skin was expected since NGF can be synthesised independently without nerve terminals (Rohrer et al., 1988) and it can be higher in *in vivo* denervated skin since the NGF production cannot be taken up by nerves endings (Mearow *et al.*, 1993). (Adly *et al.*, 2006, Lopez *et al.*, 1998, Micera *et al.*, 2007)

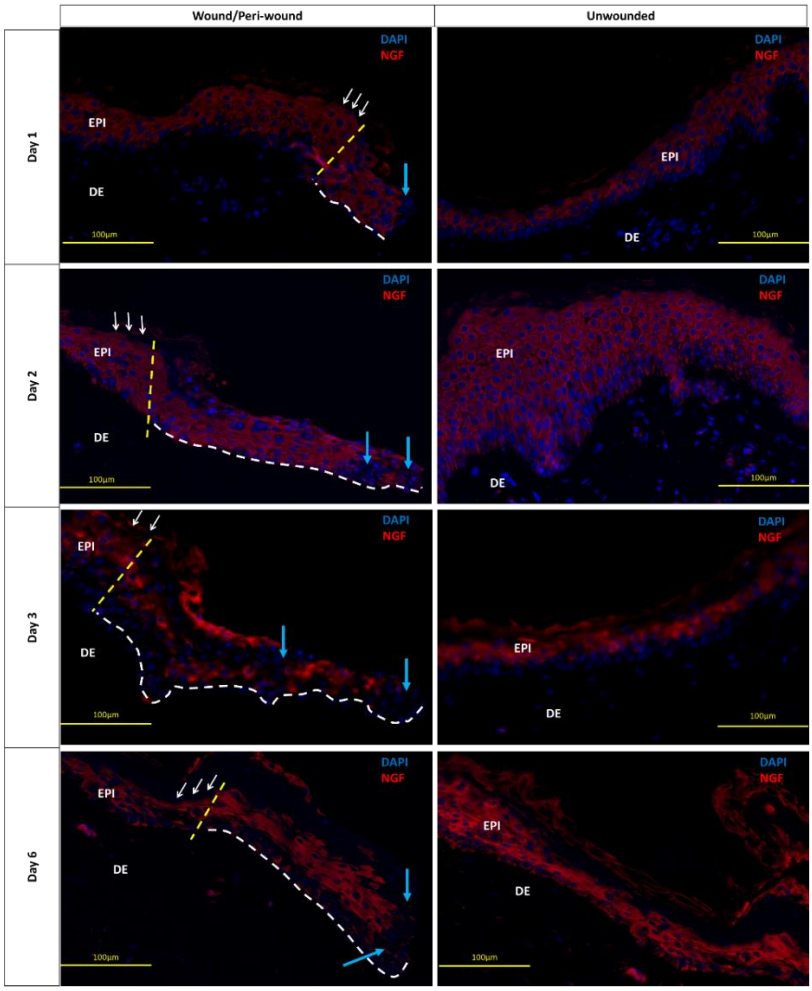

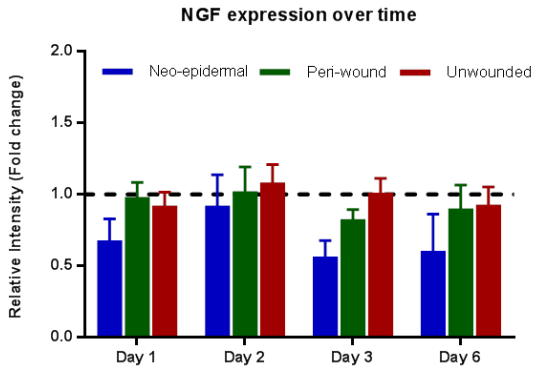

Figure 3.30: Localisation of protein expression of NGF in human skin wounded ex vivo*. Representative images showing NGF localisation in human skin wounded ex vivo over time (above; images). However, no significant difference was observed in NGF protein expression between regions over timepoints (below; graph). EPI-epidermis DE-dermis, Yellow dashed line marks wound edge border, White arrows-point to peri-wound region, blue arrows indicate the lack of NGF protein expression in neo-epidermal region and white dashed line to denote neo-epidermal region. Graph presented from n=2 donors, with 1-6 replicate explants per condition per donor donors, with error displayed as SEM. Black dashed line denotes relative intensity for uncultured skin. Bar-100 µm.*

Next, this study determined the localisation of the NGF receptors TrkA and p75-NTR during repair. In uninjured human skin TrkA protein expression is known to occur both within the epidermis and dermis, specifically on the surface of epidermal keratinocytes, dendritic cells and melanocytes (Adly *et al.*, 2006, Deinhardt and Chao, 2014, Lopez *et al.*, 1998, Shibayama and Koizumi, 1996, Zhang *et al.*, 2018). Expression of TrkA can be seen at the basal layer of epidermis but in abdominal skin the expression (staining intensity) it is thought to be lower compared to scalp skin (Lopez *et al.*, 1998). While no quantification across body site was performed, my data suggest that expression levels between scalp and abdomen are similar (Figure 3.31A). In unwounded and peri-wound regions, the staining can be seen mostly in dendritic like-cells (i.e. likely melanocytes, Langerhans cells or γδT cells). Figure 3.32 shows TrkA was sometimes co-localised with CD1a. Within the neo-epidermis (Figure 3.31A) the staining can be observed starting from day 3 onwards. This study find that the overall intensity of TrkA expression is slightly elevated with respect to uncultured skin, however, no significant differences in expression within the neo-epidermis was observed when compared to unwounded or peri-wound epidermis (Figure 3.31C).

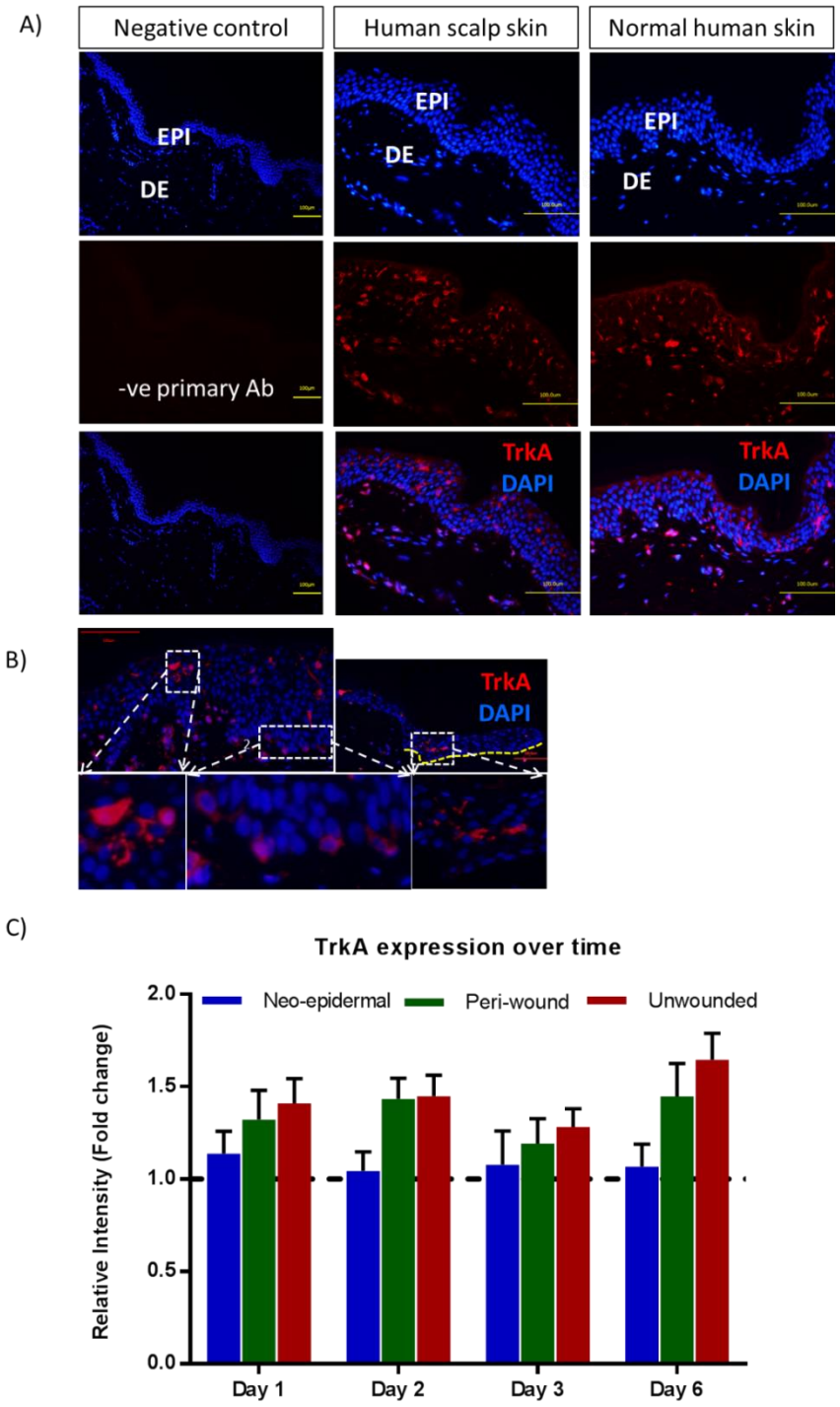

Figure 3.31: Localisation of TrkA in human scalp, human abdominal skin and wounded organ culture tissue*. TrkA protein expression was detected in epidermal layer of scalp skin (positive control) and abdominal skin (A); and untreated skin organ culture (Day 3) (B). The negative control tissue was stained without primary antibody. No significant difference was observed in TrkA protein expression between regions over timepoints (C). Graphs n=2 donors, from 1-6 replicate explants per condition per donor, with error displayed as SEM, black dash line denote relative intensity for uncultured skin. Bar-as indicated in the images and Yellow dash line indicated neo-epidermis, EPI-epidermis, DE-dermis.*

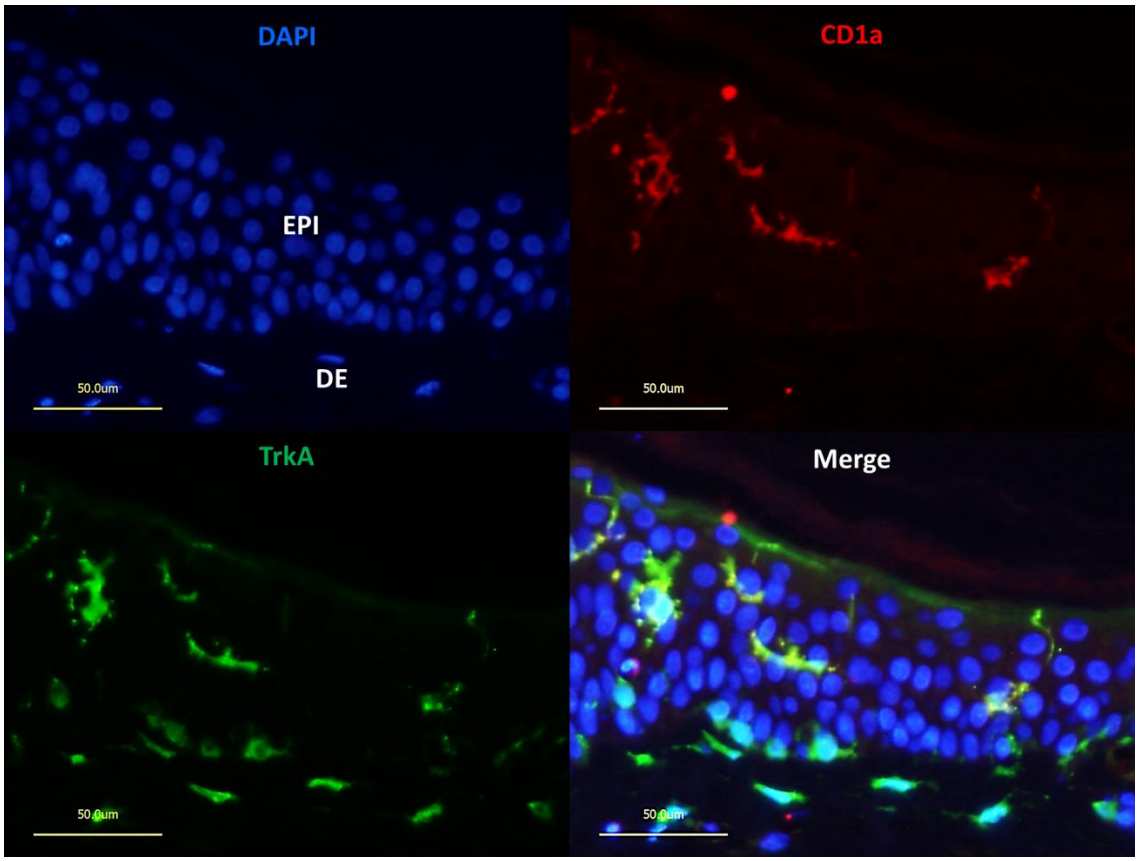

Figure 3.32: TrkA co-localised with CD1a*. Dual staining TrkA and CD1a showed that TrkA was expressed by Langerhans cells. EPI-epidermis and DE-dermis.*

Meanwhile the expression of p75NTR protein in normal skin was seen at the basal layer of epidermis (Figure 3.33 A-B). Interestingly, p75NTR protein expression in skin organ culture was generally low compared to baseline p75NTR immunoreactivity in all regions, although this difference did not reach statistical significance (Figure 3.33C). This finding was supported by (Lopez *et al.*, 1998) that p75NTR expression is dependable on nerve terminals.

A)

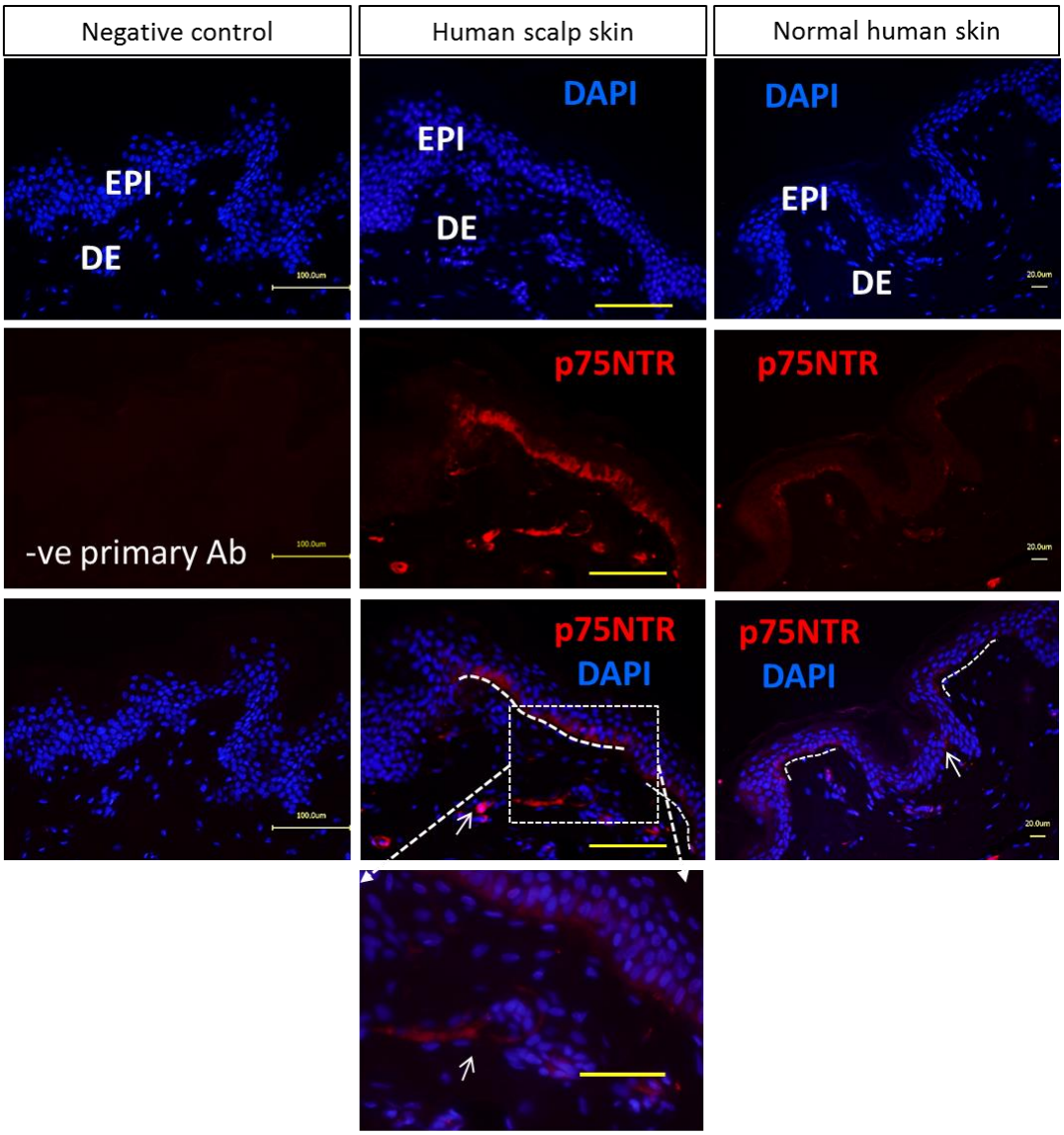
Negative control
Human scalp skin
Normal human skin
EPI
DE
DAPI
EPI
DE
DAPI
EPI
DE
-ve primary Ab
p75NTR
p75NTR
p75NTR
DAPI
p75NTR
DAPI

B)

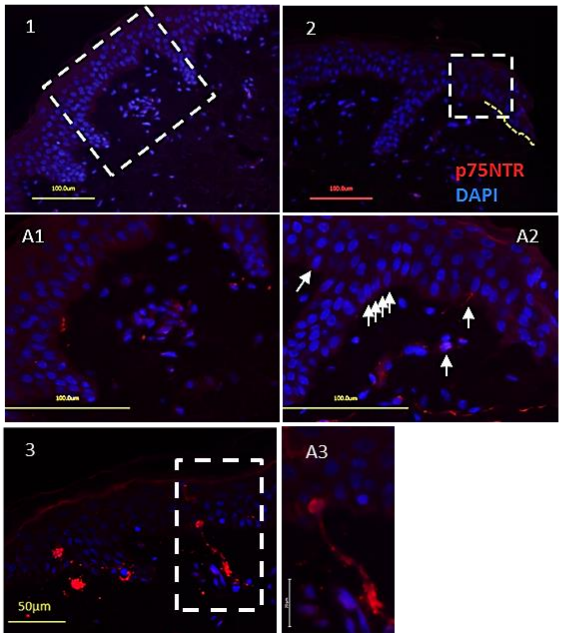
1
2
p75NTR
DAPI
A1
A2
3
A3
50µm

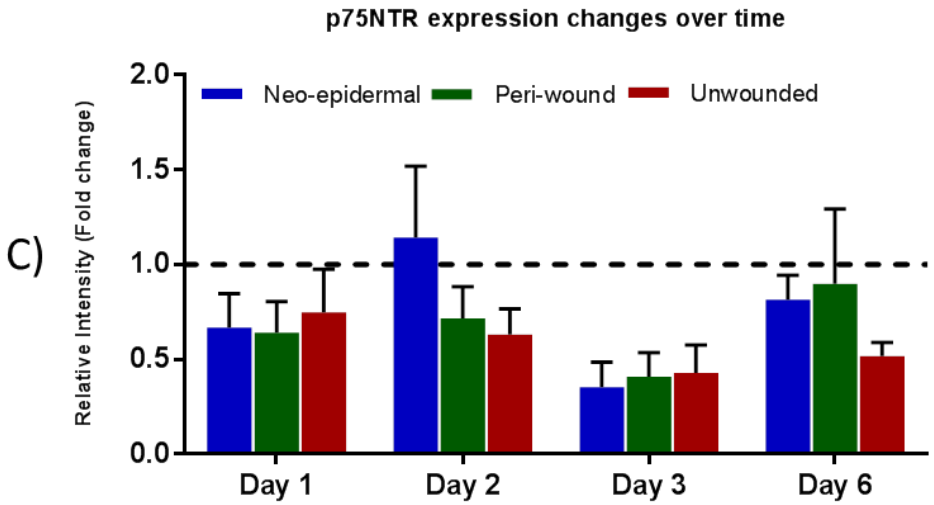

Figure 3.33: Localisation of p75NTR in human scalp, human abdominal skin and wounded organ culture tissue. *p75-NTR protein expression was detected in basal layer of epidermal in scalp (positive control) and abdominal skin (A); and untreated skin organ culture (B). No significant different was observed in p75NTR protein expression between regions over timepoints and normal skin(C). Graphs n=2 donors, from 1-6 replicate explants per condition per donor, with error displayed as SEM. Black dash line denote relative intensity for uncultured skin. Bar-100 µm and white dash line indicated neo-epidermis.*

3.3.2 Exogenous NGF treatment does not change the protein expression of endogenous NGF, or its cognate receptors

Having determined the expression profile of NGF and its receptors during *ex vivo* repair, this study wanted to understand if any were altered in manipulation of NGF signalling experiments that been presented in Chapter 4. Topical NGF application to the wound bed did not exert major changes in the protein expression of endogenous NGF compared to vehicle treated wounds (Figure 3.34 & 3.35). This was the case for neo-epidermis, peri-wound and uninjured epidermis, at all timepoints.

Immunohistology staining showed that NGF protein was expressed at the wound tongue (basal and suprabasal layers) but there was no significant difference with treatment groups or timepoints. This could be due to the new epithelial cells arrangement and in peri-wound and unwounded regions on the same explant it was expressed in suprabasal layer (Figure 3.35). However, the quantification of relative intensity on NGF protein expression showed unchanged compared to baseline (uncultured tissue from the same donor), regions or treatment groups over timepoints (Figure 3.34).

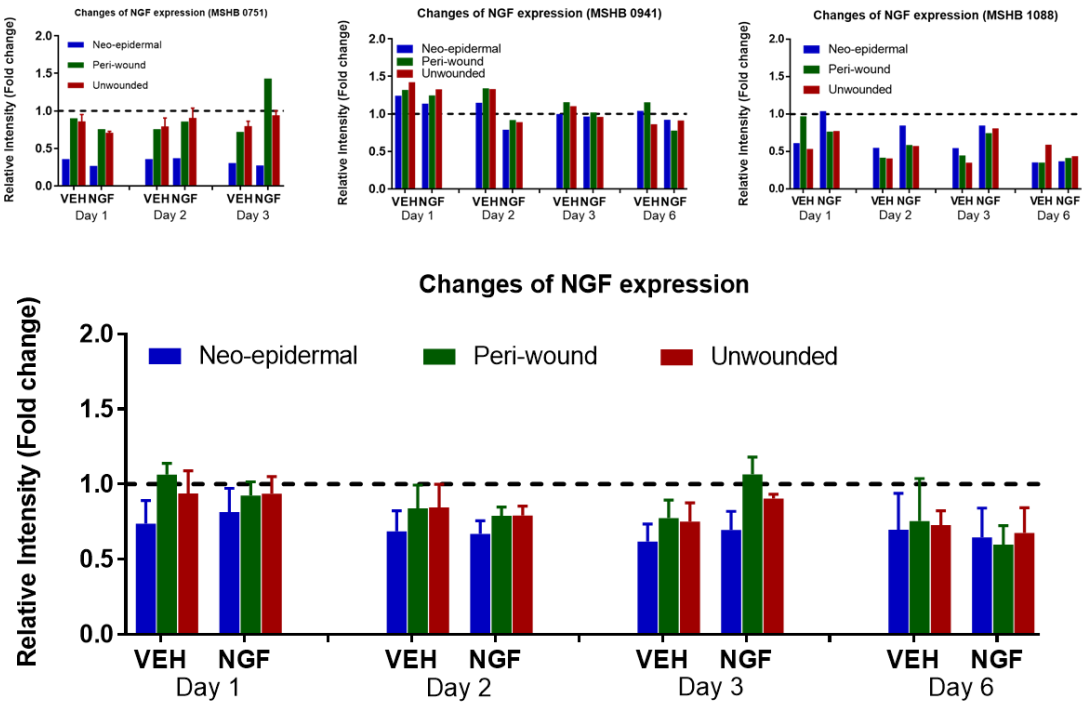

Figure 3.34: No expression changes to NGF occur in wounded human organ culture with treatment with exogenous NGF. *Graphs (above) show mean protein expression changes of endogenous NGF in NGF or vehicle organ culture from three different patients. Further, analysis of the protein expression changes following NGF or vehicle treatment in organ culture (n=3 donors) revealed no significant different in NGF protein expression between analysis regions, or across timepoints (Graph below), with error displayed as SEM. Data are normalised to expression in uncultured normal skin from the same donor (dashed line).*

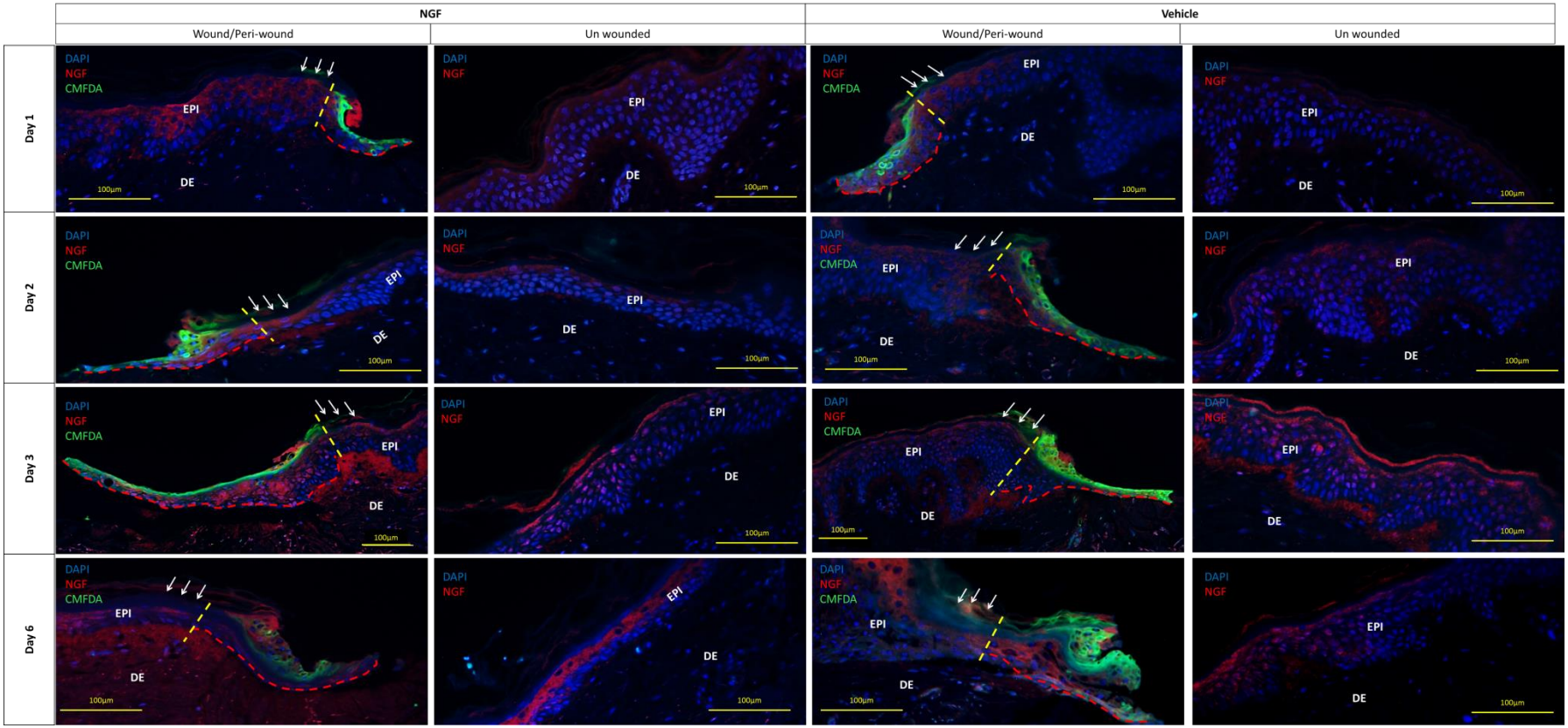

Figure 3.35: Localisation of protein expression of NGF in wounded human ex vivo skin*. Representative images showing NGF localisation in human skin wounded ex vivo and treated with NGF and its vehicle over timepoints. EPI-epidermis, DE-dermis, Yellow dashed lines mark wound edges, red dashed lines mark neo-epidermis, White arrows denote peri-wound region.*

Next this study turned its attention to the NGF receptors. TrkA protein expression is known to occur within epidermis and dermis layer, although in abdominal skin the expression is lower compare to scalp skin (Lopes et al, 1998). As previously mentioned, in this study that the protein expression of TrkA was expressed highly on the dendritic cell-like in skin epidermal layer and lower on other epidermal cells, while dual staining with CD1a showed that TrkA labelled Langerhans cells (Figure 3.32). Both NGF treated groups showed TrkA +ve labelled cells at the peri-wound peri-wound and unwounded regions on day 1 (Figure 3.36). On days 2 and 3 TrkA +ve labelled cell can also be seen within the neo-epidermal region, while the appearance of TrkA +ve labelled cell was slightly decreased on day 6. However, relative intensity analysis of TrkA protein expression showed no statistical difference between treatment groups over time and compare to normal skin (Figure 3.37).

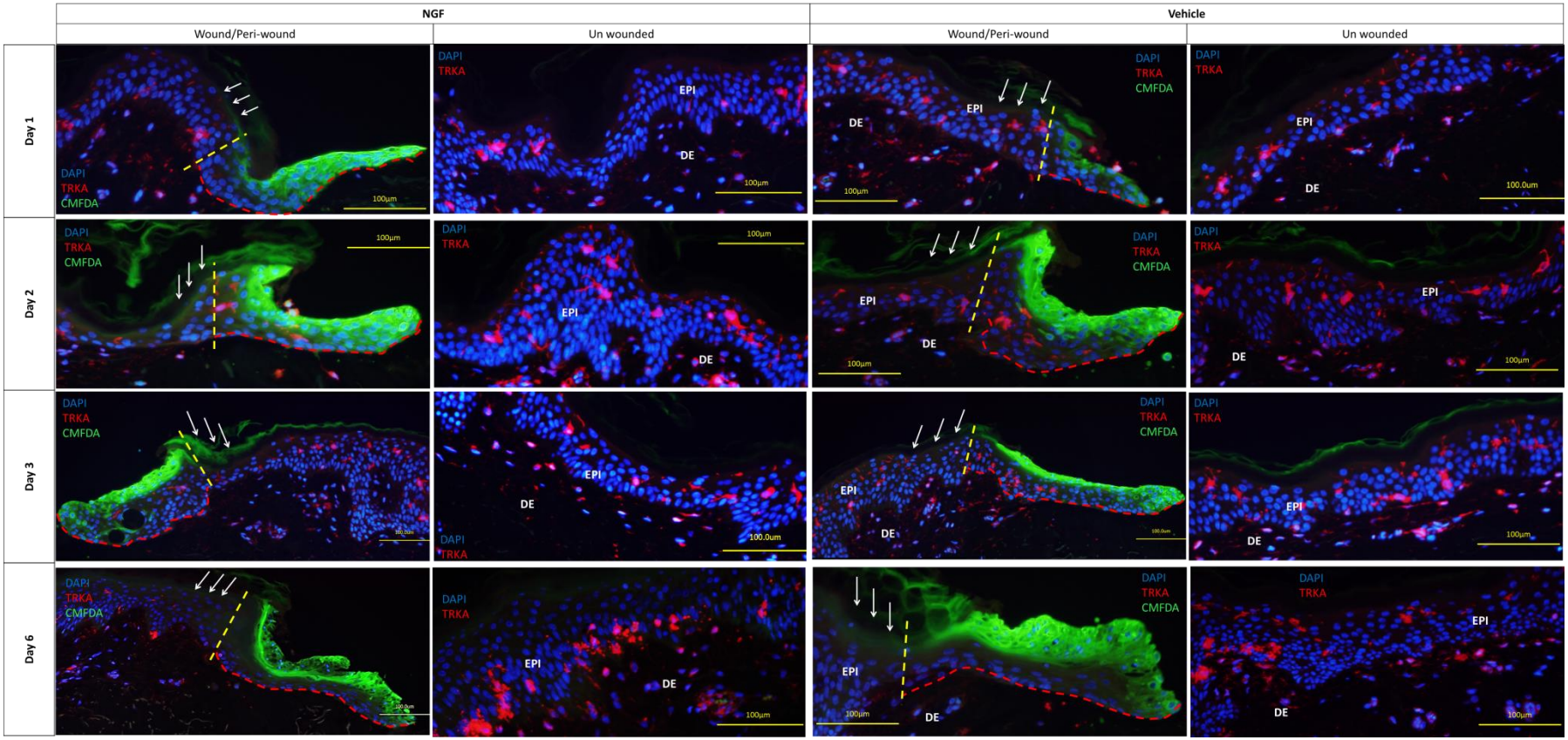

Figure 3.36: Localisation of protein expression of TrkA in wounded human skin ex vivo treated with exogenous NGF. *Representative images showing TrkA localisation in wounded human skin cultured ex vivo and treated with NGF or vehicle. EPI-epidermis, DE-dermis, Yellow dash line-to mark wound edges, White arrows-pointed to the peri-wound region and red dash line to denote neo-epidermis.*

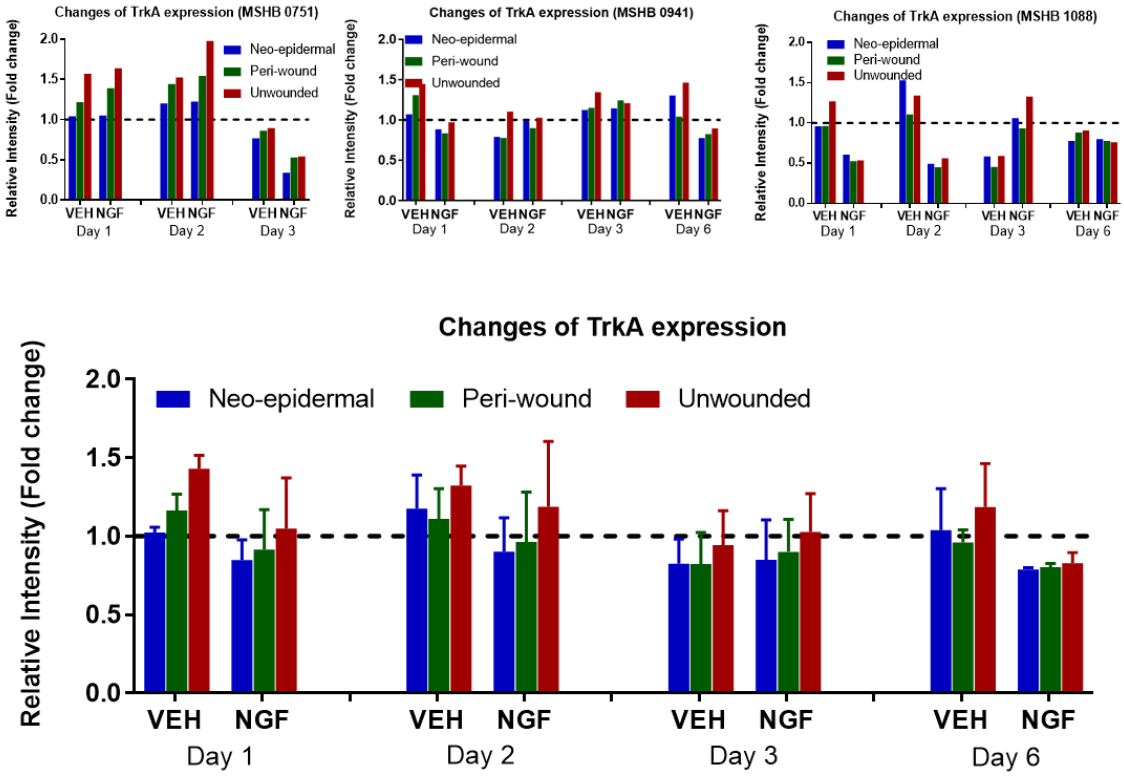

Figure 3.37: No expression changes of TrkA occurred in wounded human organ culture tissue treated with NGF. *Graphs (above) show mean expression changes of TrkA in NGF or vehicle organ cultures from three different patient. No significant difference was observed in TrkA protein expression between regions over timepoints in n=3 donors (Grah below), with error displayed as SEM. Dashed line depicts normal skin expression level.*

The data examining p75NTR protein expression during skin repair identified expression at the rete-ridges of the basal epidermal layer in unwounded skin, but the expression was negligible in *ex vivo* wounds (Figure 3.33). Treatment with NGF revealed localisation of p75NTR in the same regions as was previously noted in untreated wounds (Figure 3.38). The intensity of p75NTR expression was quantified in NGF and vehicle treated wounds (Figure 3.39). It shows that the relative intensity of p75NTR was lower compared to normal skin, in line with my data on untreated wounds. However, no significant difference between NGF and vehicle groups was found.

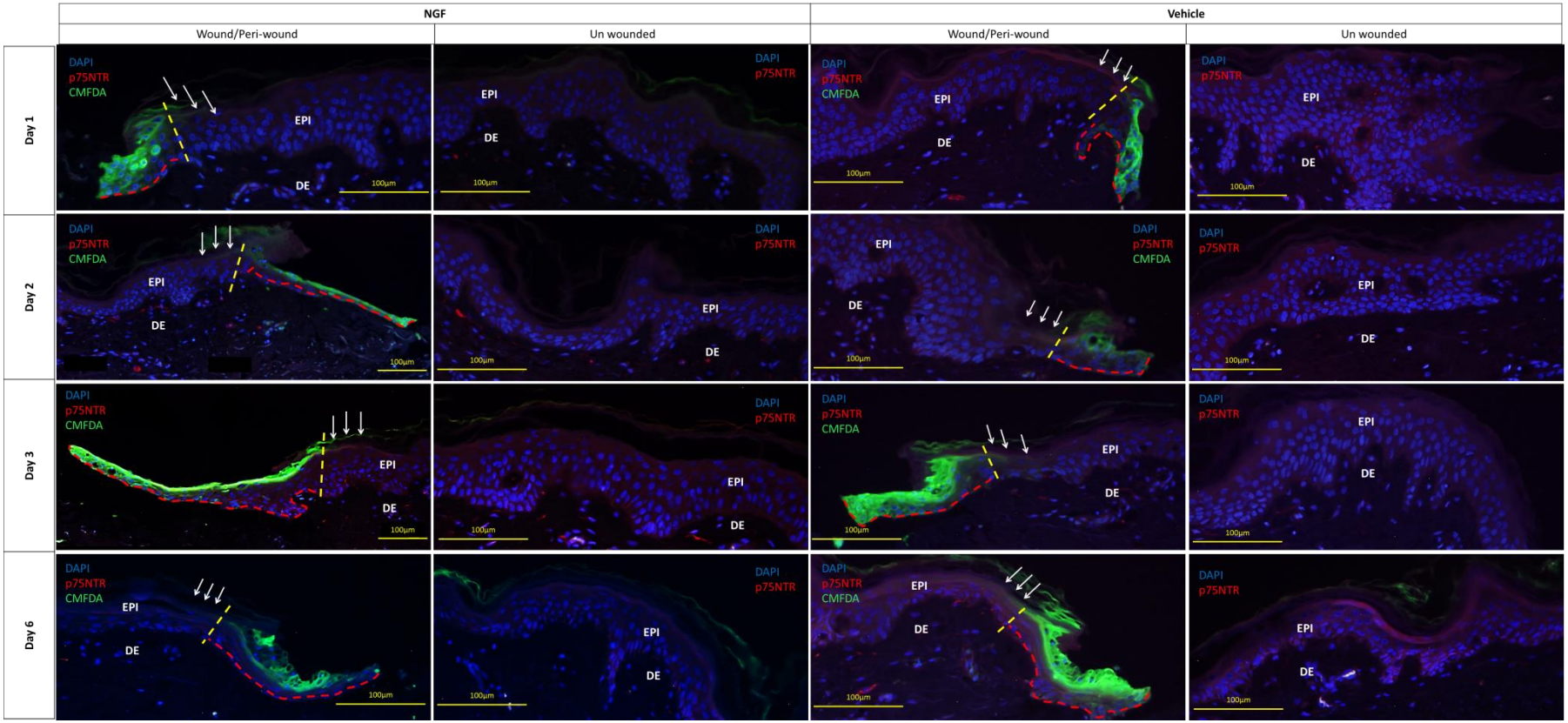

Figure 3.38: Localisation of protein expression of p75NTR in wounded human skin ex vivo in NGF treated wounds*. Representative images of p75NTR localisation in human skin wounded ex vivo treated with NGF or its vehicle group over timepoints. EPI-epidermis, DE-dermis, Yellow dash line-to mark wound edges, White arrows point to peri-wound region and red dash line to denote neo-epidermal region.*

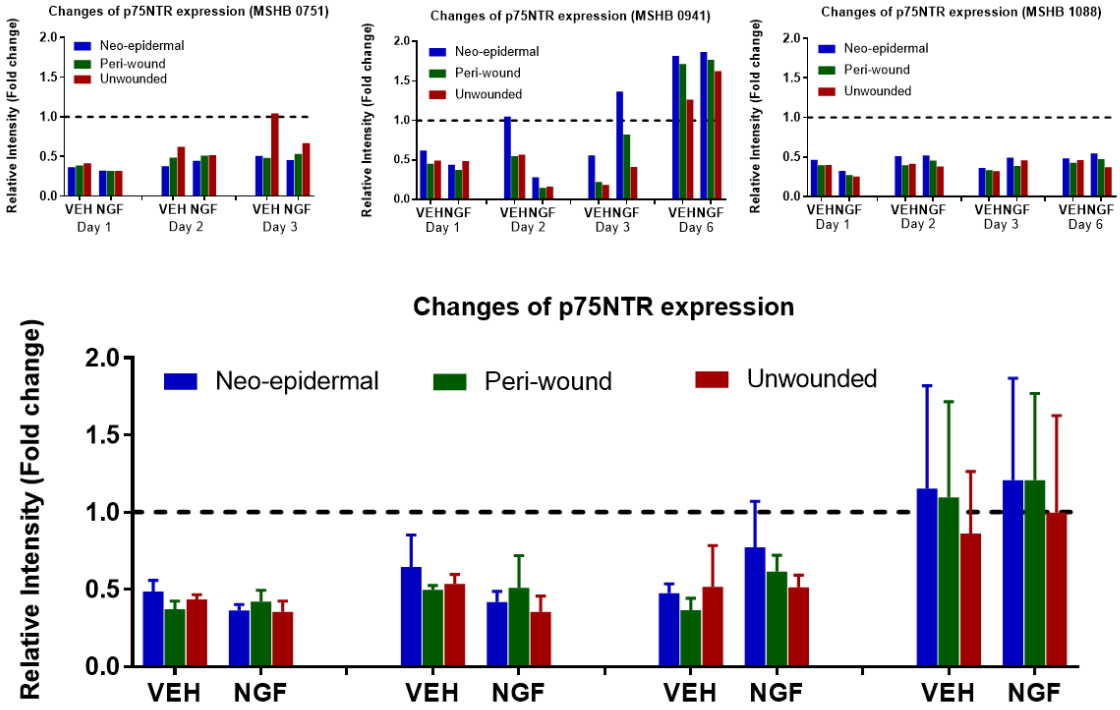

Figure 3.39: Quantification of expression changes of p75NTR in NGF treated wounded human organ culture tissue. *Graphs (above) show mean expression changes of p75NTR in NGF or vehicle organ culture from three individual patient. No significant different was observed in TrkA protein expression between regions over timepoints in n=3 donors (Graph below), with error displayed as SEM. Dashed line-normal skin.*

3.3.3 K252a does not change the protein expression of endogenous NGF, or its cognate receptors

Lastly in this chapter, changes in the percentage of NGF, TrkA and p75NTR protein expression after wound was treated with K252a and its vehicle was examined.

The relative intensity of NGF protein expression was measured after human wounded *ex vivo* was treated with the TrkA inhibitor. Figure 3.40 showed that there are no significant changes in NGF protein expression between both groups and regions across timepoints.

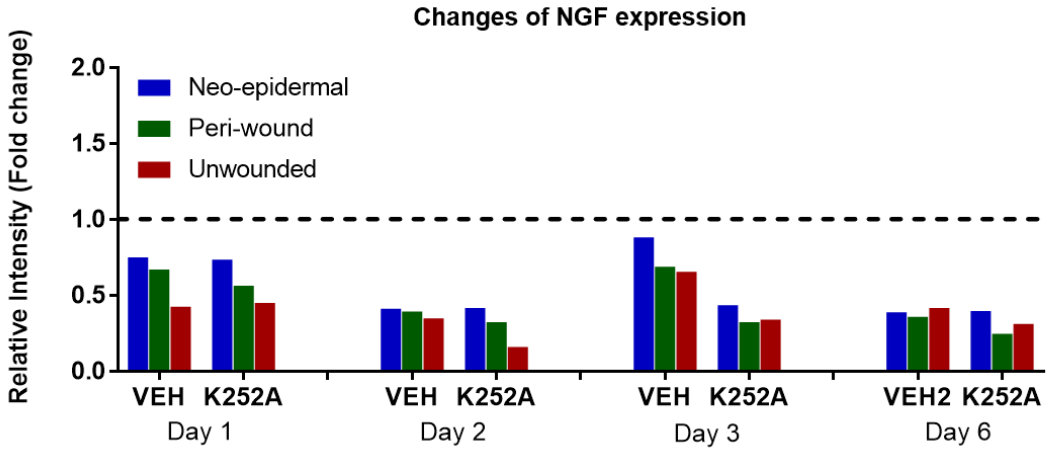

Figure 3.40: Expression changes of NGF in wounded human organ culture tissue treated with K252a. *Quantification of the expression change following NGF or vehicle treated organ culture revealed no difference in NGF protein expression between analysis regions, or across timepoints. Mean of n=1 donor (2-3 explants per condition). Data are normalised to expression in uncultured normal skin from the same donor (dashed line).*

The quantification of relative intensity of TrkA also showed no significant difference between K252a treatment and its vehicle group across timepoints and regions (Figure 3.41). This result suggests that the K252a effect is topical and not systemic as shown in Figure 3.25.

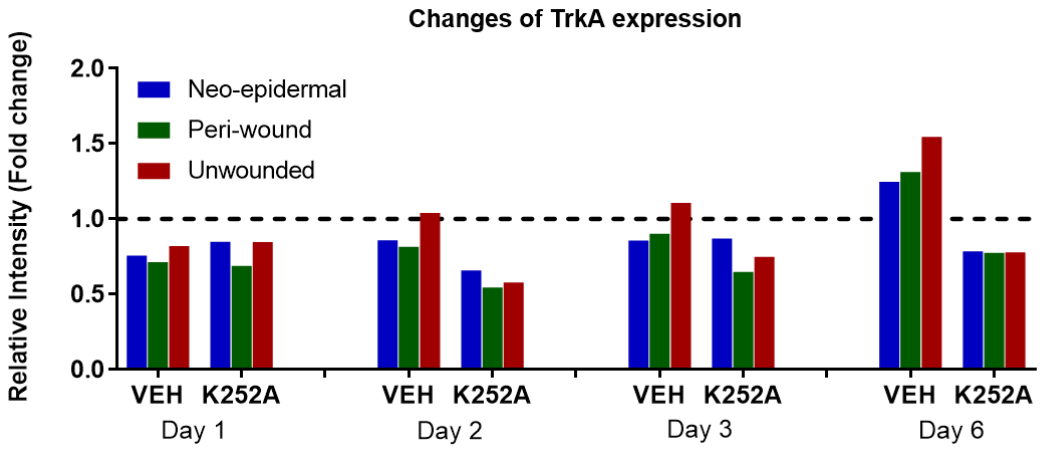

Figure 3.41: Expression changes of TrkA in wounded human organ culture tissue treated with K252a. *Quantification of the expression change following TrkA or vehicle treated organ culture revealed no significant different in NGF protein expression between analysis regions, or across timepoints. Mean of n=1 donor (2-3 explants per condition). Data are normalised to expression in uncultured normal skin from the same donor (dashed line).*

Lastly, data on p75NTR protein expression in human skin wounded *ex vivo* treated with K252a showed no significant difference between both groups and regions across timepoint (Figure 3.42). The expression was similar to normal expression pattern in normal skin (uncultured) and human wounded organ culture, both untreated and following NGF application (Figure 3.33C and 3.38).

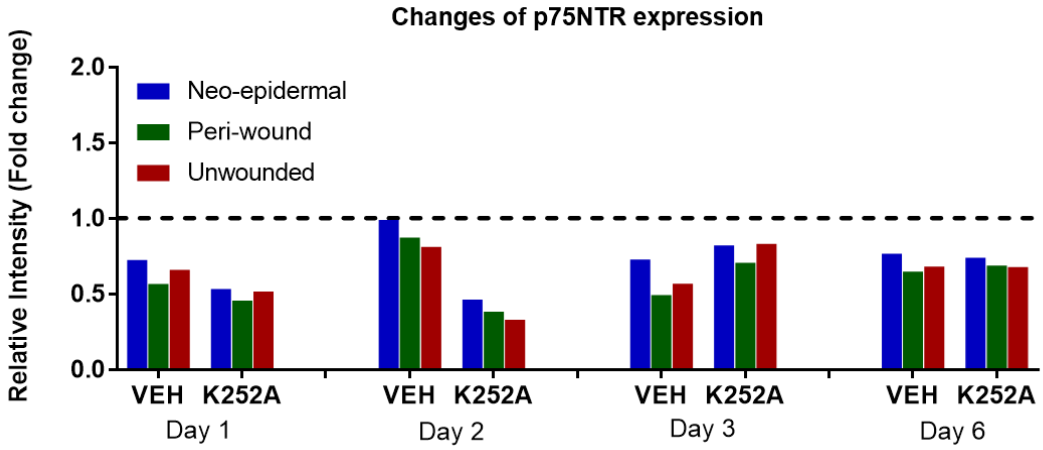

Figure 3.42: Expression changes of p75NTR in wounded human organ culture tissue treated with K252a. *Quantification of the expression change following p75NTR or vehicle treated organ culture revealed no significant different in NGF protein expression between analysis regions, or across timepoints. Mean of n=1 donor (2-3 explants per condition). Data are normalised to expression in uncultured normal skin from the same donor (dashed line).*

In conclusion, this chapter reveals for the first time that NGF and its high affinity receptor TrkA are both found within the healing epidermis of human *ex vivo* acute wounds. This is significant since it establishes the possibility for NGF signalling through its high affinity receptor TrkA, during wound re-epithelialisation of human skin wounds. In addition, my finding also suggests that production of NGF in skin *ex vivo* is indeed independent of innervation and this is in agreement with (Rohrer *et al.*, 1988) when their result showed that NGF mRNA expression in denervated embryo chick hindlimb is independent of innervation. Furthermore, this finding might enlighten their question on whether denervated adult skin contains normal or altered NGF. Previous study by (Mearow *et al.*, 1993) also showed that denervated skin in rat increased the NGF concentration because of the absence of nerve terminals to taken up and used the NGF. Even in their *in vivo* study, they showed that NGF mRNA was relative to normally innervated skin. Therefore, findings from these experiments (Rohrer *et al.*, 1988, Mearow *et al.*, 1993) were fitted to explain the similarity of NGF protein expression in my *ex vivo* organ culture that relative to the NGF protein expression in uncultured skin. Whilst, p75NTR need an adequate innervation of the skin in order to express p75NTR and TrkA need the innervation to a lesser extent (Lopez *et al.*, 1998).

DISCUSSION

CHAPTER 4

DISCUSSION

This thesis project aims to enlighten and provide new data on the role of NGF in epidermal repair by addressing specific aims in Chapter 1 which are:

1. To understand whether wounded human skin *ex vivo*, could provide a model system to examine drug effects. This present study optimised this model incorporated with a vital dye called 5-chlorometylfluorescecne diacetate (CMFDA) to enhance the wound assessment method in *ex vivo* model.
2. To characterise the normal protein expression pattern of NGF and its cognate receptors; TrkA and p75NTR during human skin repair *ex vivo*.
3. To investigate the effect of manipulation of NGF signalling on epidermal repair by adding exogenous NGF, blocking the high affinity receptor TrkA and NGF neutralising antibody into the wound.
4. The present study also the first to investigate the effect of exogenous NGF on the protein expression pattern of endogenous NGF and its cognate receptors TrkA and p75NTR in this model.

Since it is not possible to examine different doses of NGF (or any drug) within an individual patient and collect skin samples before and after treatment, this study selected the wounded human skin *ex vivo* model as the most similar to *in vivo* human wounds. Data from Chapter 3 section 3.1 demonstrates that this model can be used to track epithelial repair until sacrifice at any desired end-point, and be manipulated for drug testing (Nasir *et al.*, 2019). The skin was obtained from patients undergoing

an elective abdominoplasty surgery. The harvested skin was then kept in transport media until it reached the lab (within 12-36 hours) and further processed to create wounded human skin explants, which were then *ex vivo* cultured in WE media.

In addition, the *ex vivo* model preserves the structural anatomy of human skin. This model not only provided epidermal keratinocytes and dermal fibroblasts, but also contained various cells such as mast cells, merkel cells, macrophages (and other inflammatory cells), collagen fibers and some adipose tissues (Mendoza-Garcia *et al.*, 2015, Balaji *et al.*, 2014, Stojadinovic and Tomic-Canic, 2013, Sarkany *et al.*, 1965). For this study, some of the adipose tissue was kept intact with the tissue organ culture. The adipose tissue contains stem cells, but may also provide endocrine functions for food intake, glucose homeostasis, inflammation and angiogenesis (Driskell *et al.*, 2014) and completes the tissue structure. However, if too much adipose tissue remains this will tilt the organ culture on the absorbent pad and it will be difficult to maintain the wound surface horizontally for planimetric imaging. Furthermore, data from Figure 3.34 shows that Langerhans cells are present within the tissue. Therefore, it is conceivable that *ex vivo* wounds may respond more closely to the *in vivo* state than other cell culture approaches, even when compared to complex 3D models such as skin equivalents (Balaji *et al.*, 2014, Xu *et al.*, 2012, Steinstraesser *et al.*, 2009, Varani, 2012, Stojadinovic and Tomic-Canic, 2013, Sarkany *et al.*, 1965).

As shown in chapter 3 (Figure 3.1) this study investigated the effect of two different media on wounded human skin in organ culture. It shows that there is no significant difference between two media used in terms of epidermal re-epithelialisation or

number of proliferative cells that have been marked by Ki-67 positive staining. The differences between DMEM and WE are in terms of the composition of amino acids and organic salts. The idea of using William's E (WE) as a culture media was initially because this study has considered to include the hair follicle in analysis of wound repair, which this media was initially developed for (Philpott *et al.*, 1994). NGF is already known to play an important role in hair follicle morphogenesis and signalling (Paus *et al.*, 1994, Botchkarev *et al.*, 2000, Botchkareva *et al.*, 2000, Botchkareva *et al.*, 1999). The hair follicles may provide the additional stem cells to accelerate wound repair and in addition, NGF synthesised at wound site was known to have a chemotaxis to certain cells migration therefore enhance the wound closure. The density of hair follicles in abdominal skin is low and so the probability of finding any hair follicles in a wound by chance was very low. However, the presence of hair follicles could be determined under a dissecting microscope, which would enable wounds to be selectively created with the involvement of a hair follicle. Given the high level of interest in studying hair follicles in skin repair (Ansell *et al.*, 2011, Argyris, 1976, Brown and McDowell, 1942, Langton *et al.*, 2008, Ito *et al.*, 2005, Levy *et al.*, 2007, Jimenez *et al.*, 2012, Liu *et al.*, 2015, Martinez *et al.*, 2017), it would be interesting to use the vital dye approach that have been developed in this PhD project to examine the involvement of skin appendages to human epidermal healing, for which little research currently exists.

Utilising this method may allow one to investigate cell migration or communication between the skin appendage cells and epidermal skin migration into the wound area. It was shown by Brown and McDowell (1942) that the hair follicles repairs itself

before becoming involved in repair of the epidermis. Later, the Brown and McDowell work was supported by Argyris (1976). Several studies using reporter mouse strains have shown different cells from the hair follicle tracing into wound neo-epidermis (Taylor *et al.*, 2000, Levy *et al.*, 2005). It is also known that the lack of hair follicles impairs wound closure (Langton *et al.*, 2008), while wounds made within the growing (anagen) phase of hair cycle heal much faster (Ansell *et al.*, 2011). There is also recent interest in using hair follicles to accelerate the repair of chronic wounds (Jimenez *et al.*, 2012, Martinez *et al.*, 2016). Moreover, other appendages are also likely to influence the rate of healing (Rittie *et al.*, 2016). Therefore, using this method will provide new evidence on how the communication between skin and skin appendages may occur during repair.

Data from this study showed no significant difference between WE and DMEM. Previous studies of *ex vivo* repair have examined DMEM (Wang *et al.*, 2016, Xu *et al.*, 2012, Stojadinovic and Tomic-Canic, 2013, Mitbauerova *et al.*, 2012, Liu *et al.*, 2014), WE (Lu *et al.*, 2007, Meier *et al.*, 2013), or other different media compositions (Ueck *et al.*, 2017, Mitbauerova *et al.*, 2012, Lu and Rollman, 2004, Danso *et al.*, 2015, Wang *et al.*, 2016) for tissue culture. This study also chooses not to add serum in the culture media since it can mask drug responses one was hoping to assess. Serum in the culture media is known to provide growth factors, hormones, binding and transport proteins, assistance in attachment and spreading factors, additional amino acids, vitamins, trace elements, fatty acids and lipids (Gstraunthaler, 2003, Brunner *et al.*, 2010). Data from section 3.1.1 clearly shows that serum in the media significantly accelerates wound re-epithelialisation in organ culture (Figure 3.15). However, Figure

3.15 also showed that the percentage of re-epithelialisation had reached a plateau by day 3 or 4. This may be due to suboptimal conditions for repair in the *ex vivo* system, such as insufficient nourishment of the tissue, resulting in the rate of re-epithelialisation decreasing after several days in culture.

Since this study focus on the migration of epidermal tongue, partial thickness wound is the best option to study wound closure within the optimal time frame for *ex vivo* model. The healing tongue migration can be amongst one of the best indicators for wound closure and the easiest way to assess histologically or planimetry.

It could be argued that animal studies *in vivo* would have provided a more similar environment to examine NGF effect on repair. However, it is unclear how similar wound responses across species will be, as compared to mouse skin, human epidermis has four layers of epidermal while mouse only has two or three layer of epidermal keratinocytes (Gudjonsson *et al.*, 2007, Berking *et al.*, 2002, Gerber *et al.*, 2014). Moreover, mouse skin has the special panniculus carnosus muscle to assist in wound contraction and more skin appendages which can contribute more for wound healing (Dunn *et al.*, 2013).

Data generated during the course of this PhD project has resulted in a highly optimised model, which if taken up by others within the field would reduce the use of animals in wound healing studies (Ansell *et al.*, 2012, Stojadinovic and Tomic-Canic, 2013, Ud-Din and Bayat, 2017). Furthermore, using this model incorporated with intravital dyes one not just obtains or measures the migration of new epidermal but in the near future one might be able to assess specific cell migration or dual staining

by tagging inflammatory cells with specific antibody and assessed them longitudinally during wound healing.

However, this *ex vivo* model and other previous models have their own disadvantages. Since the skin has been cut off from the host, it lacks blood supply and nerves will degenerate (Stojadinovic and Tomic-Canic, 2013, Mendoza-Garcia *et al.*, 2015, Ueck *et al.*, 2017, Nasir *et al.*, 2019). Furthermore, when wounds are created no blood clot forms to give further protection to the wound as well as prevent blood loss (Monroe and Hoffman, 2012). However, given that this skin model has been cut off from it host the prevention of blood loss can be disregarded but this could be mean that this model can be under stress condition without the blood supply to nourish the tissue as well as fewer inflammatory cells that can only be supplied through blood vessels (Delavary *et al.*, 2011, Koh and DiPietro, 2011, Koh *et al.*, 2013). To its advantage this model does still contain its innate and inflammatory cells that reside in the skin or came from ruptured blood vessel during wound or explant creation.

Other than allowing one to manipulate the model for drug testing within the time frame requirement, this *ex vivo* organ culture also enabled monitoring during wound healing. Data in Chapter 3 section 3.1.2 showed that by employing the fluorescent cell tracer, wound healing in this model could be assessed in real time manner (longitudinally), for several healing parameters such as tissue contraction, re-epithelialisation, or epidermal stratification. This assessment method (planimetry) also mimics wound measurement in clinical setting. The planimetry and longitudinal wound assessment may be particularly important for revealing where an intervention

alters only some aspects of repair. Provided this approach produced rapid and reliable result, it may enable researchers to quickly identify which timepoints or healing processes would be most instructive for a subsequent more in depth assessment. The use of vital dyes also might make it possible to monitor the variable wound healing progress between donors. As an example, instead of assessing on a particular day, researchers can harvest tissue once the desired level of repair has occurred. Examining wounds once the control group shows 50% healing would ensure that both positive and negative drug effects to the rate of healing can be quantified. It warrants further investigation to determine whether CMFDA planimetry imaging could be applied to other translational wound healing models such as porcine *ex vivo* skin wounds, or wounded organotypic human skin constructs.

Data from this study also highlights that a major advantage of partial thickness *ex vivo* wound model allows one to study the complete re-epithelialisation process across the underlying wound bed in real time *in situ*. This has also been demonstrated by other recent studies using alternative visualisation methods (Wang *et al.*, 2016, Glinos *et al.*, 2017).

This study would suggest that it is better to use CMFDA for lineage tracing since this colourless dye contains acetates that will be cleaved by cystolic esterase and releasing a bright fluorescent product. Furthermore, this process can only happen in viable cells. This is confirmed by my data of CMFDA and propidium Iodide dual labelling (Figure 3.8). While on the other CMTPX is a fluorescent ready product it may label the damage cells as well.

While this project has utilised CMFDA and CMTPX, there are several other vital dyes that could be employed for labelling cells within the neo-epidermis (Beem and Segal, 2013, Lu and Rollman, 2004, Chao *et al.*, 2017, Johnson, 1998, Wu *et al.*, 2017, Xia *et al.*, 2018). Moreover, by combining fluorescent dyes of different wavelengths this study demonstrate that the possibility exists to follow cell migration patterns during *ex vivo* healing. Also, data generated from this study using double labelling suggest that re-epithelialisation occurs using the extending shield mechanism previously reported for organotypic wounds (Safferling *et al.*, 2013). This is important as skin equivalent models are highly simplified and it is unclear how well they replicate human *in vivo* wounds (Xu *et al.*, 2012).

Data from this study showing multiple label retaining populations towards the neo-epidermal tip was not previously reported in skin equivalents. This PhD study notes however that CMFDA did not labelled any cells within the basal layer and these labelled cells therefore appear to be cells that have yet to reach the neo-epidermal surface. Given that skin equivalents heal more rapidly and 2 mm diameter wounds are fully closed by day 3 (Safferling *et al.*, 2013), this may have been missed previously.

In this current study however, prolonged culture times up to 3 day and single/multiple labels added on later days showed some cells were labelled at basal layer of wound tongue. This might occur when the dye slipped underneath the wound tongue which is not yet tightly attached to the underlying dermal matrix (Figure 3.9).

One of the advantages of using CMFDA in this study, was that it allowed one to observe the irregularity in healing even in the single wound itself (Figure 1.4) and

appearance of centripetal migration (Figure 3.17- A inset) which is a phenomenon one is unable to detect using histology. However, at this stage this study can only suggest a few potential factors that are most critical for this phenomenon such as; 1) mechanical force, 2) localised areas with higher blood vessel branches or skin appendages, 3) increased local concentration of growth factors. Therefore, this finding is particularly important as histology of some wounds might achieve an entirely different result depending upon the plane of sectioning, further advocating planimetry imaging techniques in future studies. An irregularity in the rate of healing within experimental (i.e. circular) was also concluded by (Glinos et al., 2017) in their recent study.

Despite this, histology remains an essential tool for researchers in this field in order to understand what is happening below the wound surface, or investigating wound responses such as proliferation, or activation of target genes. However, combining a non-invasive assessment for global wound closure, followed by end-point histology will maximise data obtained. Advanced imaging techniques constitutes an exciting methodological advance in wound healing research, particularly Optical Coherence Tomography (OCT) which holds the prospect of being directly applied to investigate patient wounds (Deegan *et al.*, 2018, Greaves *et al.*, 2014). While OCT currently remains prohibitively expensive for most *ex vivo* studies, CMFDA or other approaches like UV auto-fluorescence (Wang *et al.*, 2016) may be a valid alternative as suitable equipment will be more readily available. The persistence of CMFDA within histological specimens may be especially instructive to pinpoint the wound margins, which may further aid histological assessment.

Furthermore since the planimetry wound closure using intravital dye correlated highly with the histological assessment of the same wounds (Figure 3.14), this study would suggest and encourage one to replace the laborious and more artefact-prone quantitative histomorphometry with this quickly performed and methodologically superior intravital planimetry (Nasir *et al.*, 2019).

Having optimised the assay technique with *ex vivo* wounds incorporated with vital dye monitoring, later it was utilised for drug testing experiments to explore the role of NGF. In section 3.2, topical application of NGF was chosen because this is the preferred route for skin treatment in chronic wound patients preventing serious adverse effect that have been reported when using systemically (e.g. IV, IP) (Apfel *et al.*, 1998, Apfel *et al.*, 2000, McArthur *et al.*, 2000). In culture a systemic environment could likely be initiated by placing explant directly into the culture media. My data in Figure 3.25 highlights that an inhibitor was only active at the site of administration, providing some evidence to suggest that my experimental design a topical application did not elicit systemic effects.

The NGF was chosen as a candidate drug to be tested in this model since it was known to accelerate epidermal repair in *in vitro* (Chen *et al.*, 2014, Blanco-Mezquita *et al.*, 2013, Schenck *et al.*, 2017, Paus *et al.*, 1994), and in animal studies (Chen *et al.*, 2014, Muangman *et al.*, 2004, Matsuda *et al.*, 1998, Costa *et al.*, 2002, Blanco-Mezquita *et al.*, 2013, Li *et al.*, 1980, Lawman *et al.*, 1985). However, the use of NGF in treating wounds has been discontinued since more than a decade ago when the clinical trials yielded inconclusive results (Tuveri *et al.*, 2000, Bernabei *et al.*, 1999). Tuveri et al., in their study reported that chronic vasculitis ulcers in systemic sclerosis patients did

not benefit from NGF treatment and none of leg ulcers in systemic sclerosis group healed after 8 weeks of treatment (Tuveri *et al.*, 2000). While a single case report by (Bernabei *et al.*, 1999) on bilateral pressure ulcers on elbows, one wound showed only 1/3 reduction in wound size and the other elbow also showed substantially unchanged when treated with NGF. Therefore, this study decided to investigate why NGF that has been proven effectively to enhance and accelerate epidermal migration in *in vitro* and *in vivo* study yet becomes less effective in human. By manipulating the *ex vivo* model, this study wanted to test the role of NGF during repair by monitoring wound healing in a real time manner, but also to obtain more information than has been provided before by using histology to pinpoint where the effect of exogenous NGF on the protein expression of NGF (endogenous) and its cognate receptors might be is occurring.

The NGF used in this study was NGF-2.5S from murine submaxillary gland. This 2.5S is a β-subunit (an active compound) of nerve growth factor-7S (NGF-7S). It is known that murine and human NGF shares a high degree of homology (Paoletti *et al.*, 2015, Ullrich *et al.*, 1983, Muangman *et al.*, 2004) and importantly, murine NGF-2.5S has been demonstrated to be effective in the treatment of human corneal ulcers (Lambiase *et al.*, 2007, Lambiase *et al.*, 2009, Lambiase *et al.*, 1998, Cellini *et al.*, 2006) and skin wound healing (Generini *et al.*, 2004, Tuveri *et al.*, 2000, Bernabei *et al.*, 1999, Landi *et al.*, 2003, Chiaretti *et al.*, 2002). However data on these studies is not robust as shown in Table 1.3 due to low sample number (i.e. case reports). Even in the clinical trials the sample size is relatively small and the control arm used normal saline which is an inappropriate comparator to the growth factor/drug used in the

study. In order to determine whether there is a clinically meaningful difference, larger sample sizes are required (Sakpal, 2010, Huang *et al.*, 2015).

Surprisingly, this study found that topically applied NGF did not significantly alter the reepithelialisation of experimentally wounded human skin *ex vivo*. This finding contrasts with the beneficial effects of topically applied NGF on human corneal ulcers (Lambiase *et al.*, 2007, Lambiase *et al.*, 2009, Lambiase *et al.*, 1998, Cellini *et al.*, 2006) and skin ulcer healing reported in some clinical studies (Generini *et al.*, 2004, Tuveri *et al.*, 2000, Bernabei *et al.*, 1999, Landi *et al.*, 2003, Chiaretti *et al.*, 2002).

However, this PhD research finding is also supported by some other clinical studies (Bernabei *et al.*, 1999) and (Tuveri *et al.*, 2000), which reported that NGF did not give a beneficial effect in treating skin ulcers. There are several plausible explanations for the failure of NGF in this current study to enhance epidermal repair in the *ex vivo* model.

One obvious explanation might be that the NGF dose 25 µg/mL tested here was sub-optimal. However, this is unlikely because the dose is similar to previous studies when the size of injury is accounted for (Table 1.3). In particular, in the case report by Generini *et al.*, the 0.5 mg aliquot of NGF in 10 ml of saline solution was dropped onto a large lesion of diabetic foot ulcers. This equates to 0.1 µg/mm^2, which is in line with the 0.08 µg/mm^2 in my study (Table 1.3). Also, 20 µg/mL NGF was used and proved effective in diabetic mice (Chen *et al.*, 2014). Chen et al., also reported that wounds treated with 10 and 20 µg/mL accelerated speed wound closure while at 40 µg/mL no significant different with saline group (Chen *et al.*, 2014).

Since the scarcity of human skin available for the current study made it impossible to test a wider range of NGF doses, the possibility that higher (or lower) topical NGF may yet turn out to promote epidermal repair remains to systematically explored. Ideally, such an undertaking would be complemented by wounded human skin xenotransplants on immunocompromised mice (Raychaudhuri and Raychaudhuri, 2010, Guerrero-Aspizua *et al.*, 2010), which could assess NGF effects on skin re-innervation and angiogenesis *in vivo*. Such an approach would also enable an examination of potential beneficial effects at much later wound timepoints, which is not possible in this *ex vivo* system.

As alluded to above, another conceivable explanation for the failure of NGF to promote epidermal repair in my *ex vivo* model is that the latter lacked functional nerves and blood vessels. Perhaps perfusion is essential to permit NGF to exert its complex activities appreciated under *in vivo* conditions (Chen *et al.*, 2014, Li *et al.*, 1980, Matsuda *et al.*, 1998, Kim *et al.*, 2000). However, studies from cultured human epidermal keratinocytes and fibroblasts show profound intrinsic responses to NGF in the absence of nerves or blood vessels (Botchkarev *et al.*, 2006, Albers and Davis, 2007, Pincelli *et al.*, 1994a, Micera *et al.*, 2001), and thus one would have expected at least some functional response to NGF stimulation also under organ culture conditions. It is known that human keratinocytes or fibroblasts can respond to NGF without nerves or blood vessels because NGF also work via autocrine and/or paracrine loops (Pincelli *et al.*, 1997).

Previous work on chick embryo denervated hindlimb skin reported that NGF was synthesised independent of innervation (Rohrer *et al.*, 1988) and NGF mRNA was

expressed highly in denervated rat skin. Studies done by (Mearow *et al.*, 1993) and (Rohrer *et al.*, 1988) might suggest that human skin *ex vivo* contains an abundance of NGF equivalent to uncultured skin, which is supported by my data (Figure 5.3).

As reported before, keratinocytes, fibroblasts, inflammatory cells, Schwann cells etc. can synthesize and release NGF and can use NGF for their activities (Yaar *et al.*, 1991, Pincelli *et al.*, 1994a, Di Marco *et al.*, 1991) and apoptosis was induced when endogenous NGF was blocked (Pincelli *et al.*, 1997). Here, this study would like to speculate that in organ culture with different cell types without blood vessels or nerve networking, exogenous and endogenous NGF more likely contributes to maintaining skin homeostasis by prevent apoptosis instead of accelerating neo-epidermal migration. This could be tested by extending the culture period to establish if explants remain viable for longer with NGF supplementation to the media.

Data on Ki-67+ cells in this study showed that NGF has no influence on cell proliferation that occurs in timely manner following injury as reported by (Betz *et al.*, 1993). My data shows that in this assay proliferation peaks on day 3 and slightly decreases by day 6. This results could be explained that in some donors the wound is almost healed at this point so proliferation rate is returning to normal and this result is in agreement with Leydon et al., who reported that Ki-67+ cells only start at day 1 post-injury, peak at day 3 and remain elevated at day 5 cease to normal distribution by day 14 (Leydon *et al.*, 2014). Other than proliferate in timely manner, Ki-67 distribution also depend on the size of the wound and tissue condition (Leydon *et al.*, 2014, Frade *et al.*, 2015, Betz *et al.*, 1993).

According to the data obtained from this study on CFMDA and Ki-67 positive cell distribution it suggests that migration begins before proliferation. As showed in Chapter 3, epidermal migration was evident *in situ* on day 1 as basal cells at the wound edge were CMFDA-ve. Minimal proliferation was observed through Ki-67 positive cells at this point, although a few were noted in the *peri-wound* region.

Additionally, data on CD68 positive cells in wounded human skin organ culture showed that CD68 +ve cells were evenly distributed in the tissue instead of in flux or migrating into the wound site. This could be explained that the whole organ culture itself is considered a wound or injured tissue or the CD68+ cells are skin resident cells. Another explanation is there are no blood vessels that can supply further CD68+ cells into wound site as what happen in *in vivo* condition or it is possible that these cells proliferate, differentiate, migrate or die. Therefore, this finding is different from distribution reported in *in vivo* wound models where CD68+ cells or other inflammatory cells numbers are higher at the wound site or inflamed area (Hasan *et al.*, 2006, Delavary *et al.*, 2011, Koh and DiPietro, 2011).

However, *in vivo* studies won't be able to differentiate between inflammatory cells that were in the local environment at the point of injury, and those that came from distance sites. Therefore, this study would suggest that *ex vivo* model will be useful to explore more on tissue resident inflammatory cells during wound healing.

Another possible explanation for the insignificant action of NGF to enhance epidermal repair in this study is the competition of NGF and insulin to bind into the TrkA receptor and activate the epidermal migration signalling pathway. According to (Geetha *et al.*, 2013) their study in PC12 cells suggest that TrkA is also involved in the

insulin signalling pathway. Given that TrkA has an NPXY motif and kinase regulatory loop similar to insulin receptor (INSR) hence, it was suggested that insulin can bind to the kinase regulatory loop on TrkA receptor and activate Akt and Erk5 (Negrini *et al.*, 2013) that will overlap with NGF/TrkA signalling during stimulation and forms a complex in the PC12 cells (Geetha *et al.*, 2013). Since culture media used in this study contains insulin throughout the experiment, it could be that insulin already activated downstream signalling pathways, meaning that addition of NGF did not further promote epidermal repair.

As shown in Chapter 1 (Figure 1.9) on the NGF signalling pathways, NGF will bind to the high affinity receptors and will activate different downstream signalling such as proliferation, migration, differentiation and survival. Therefore, having insulin in the culture media (which mimics systemic delivery) may have been more effective to bind to the TrkA receptors and activate other signalling pathways like Akt and ERK5, compared to the exogenous NGF that was administered topically to the wound bed. The effectiveness of the topical NGF treatment regime may have been suboptimal since the surface area of the wound is far smaller than the exposed dermal area for the whole explant.

The final possibility is that in fact NGF does not act as strong wound healing accelerator or enhancer of epidermal migration in humans. This could explain why NGF treatment in patients gave inconclusive results (Tuveri *et al.*, 2000, Bernabei *et al.*, 1999) or this could be because of the wounded human skin *ex vivo* have no nerves networking due to nerve degeneration and contribute to less p75NTR. According to (Negrini *et al.*, 2013), experiments made on PC12 cells demonstrated that

cooperation of p75NTR with TrkA is needed to intensify the effect of NGF and alter NGF/TrkA signalling pathways in neural cell differentiation. However, this effect in human non-neuronal tissue has yet to be further explored.

In order to try to address the role of NGF, for the next experiments presented in Chapter 4, this study examined the effect of TrkA inhibitor, K252a in epidermal migration with or without NGF treatment. The K252a isolated from *Nocardiopsis* sp. is a potent inhibitor for protein kinase A, C and G (Inaba *et al.*, 1993, Kase *et al.*, 1987). Nevertheless, K252a is suggested to have specific effect to inhibit TrkA (Berg *et al.*, 1992, Raychaudhuri *et al.*, 2004, Pincelli *et al.*, 1997). One cannot say that K252a is a specifically inhibiting TrkA, though it definitely inhibited wound re-epithelialisation in this experimental model but in rescue experiments by adding NGF treatment only it shows a partial rescue. This might be because of K252a effect topically not systemically Figure 3.25. Therefore adding exogenous NGF after might have reached the further cells (*peri-wound*) that has not been inhibited by K252a therefore the epithelialisation can still occur. The finding of K252a action on TrkA receptor is similar as reported by (Berg *et al.*, 1992) that no protein tyrosine phosphorylation detected after pre-treated with K252a and then treated with NGF for 60 minutes. It was also suggested that the blocked TrkA cannot be reversed in *in vitro* and *ex vivo* models where the synthesis of receptors is limited even though it can be re-cycle for a limited time (Chen *et al.*, 2005). However, no phosphorylation tests were done to determine how their findings might relate to what happened in my study.

That blocking the NGF high affinity receptor, TrkA, with K252a inhibits re-epithelialisation is perfectly in line with the work of Pincelli et al., that shows K252a

inhibits keratinocyte migration *in vitro* (Pincelli *et al.*, 1997), but epidermal migration was not impaired when treated with anti-p75NTR monoclonal blocking antibodies. This indicates that NGF effects on human keratinocyte migration, i.e. the initial key event in reepithelialisation (Wehrens *et al.*, 2016, Meier *et al.*, 2013, Eming *et al.*, 2014) may primarily be mediated via TrkA.

Besides, NGF can bind independently to TrkA (NGF/TrkA) or p75NTR (NGF/p75NTR) homodimers or bind to both receptors as heterodimers (NGF/TrkA-p75NTR) and activate different signalling pathways such as cell survival, differentiation or apoptosis (Levi-Schaffer *et al.*, 2001, Lad *et al.*, 2003, Meakin and Shooter, 1992). Even though NGF can bind to TrkA without p75NTR, the presence of p75NTR will enhance TrkA affinity binding site and enhance NGF responsiveness towards high affinity receptor (Yoon *et al.*, 1998, Hempstead, 2002, Bassili *et al.*, 2010, Negrini *et al.*, 2013). Therefore, it seems advisable to explore in suitable skin ulcer patients, besides NGF itself, also the usefulness of available small molecule TrkA agonists, such as gambogic amide (Jang *et al.*, 2007), which reportedly even up-regulates TrkA expression (Shen and Yu, 2015).

As well as blocking the high affinity receptor of NGF, blocking antibodies were also used to neutralise the endogenous NGF in the organ culture. The dose used here was the same as exogenous NGF (described in Chapter 2 section 2.4.3). However this dose was unable to neutralise the endogenous NGF since there is still some epidermal migration after the treatment but when NGF treatment was given after the neutralising antibody treatment the epidermal migration was slightly elevated (not statistically significant) compare to its vehicle group.

Micera et al., showed that NGF neutralising antibody (anti-NGF) impairs wound healing in their fibroblast monolayer wound scratch assay. While in this study, data showed that adding NGF neutralising antibody did not impair the epithelial healing process. This could be explained that this *ex vivo* model has a three dimensional structure and various cell type that may influence the effect of the anti-NGF used in this study. The immunolocalisation result in section 3.311 already showed that in normal skin NGF was expressed highly in suprabasal layer of epidermal keratinocytes and lowly expressed in basal layer therefore, this is incomparable to a monolayer of fibroblasts or keratinocytes in cultured assay. This cannot be modelled in a scratch assay or other monolayer cell assay, where all cells will behave like basal cells. The scratch assay may be conducted under conditions of NGF insufficiency, therefore the result obtained showing NGF has a big effect in scratch healing. Another explanation could be that the dose of NGF neutralising antibody used here might be low or this experiment might need a larger sample number, or maybe the topical administration is not suitable for this experiment. The topical application of anti-NGF is unlikely to get into cells and therefore can only “mop up” NGF it encounters within the ECM. NGF production will be unaffected and one hope that antibody administered is enough to quench the NGF once it is secreted, but before it finds a receptor to bind to. The NGF neutralising treatment is quite costly and skin samples also difficult to obtain and within the limited time frame I was not able to investigate multiple dosing strategies for anti-NGF. However, with enough funding and skin samples one can optimise the dose to be used in this *ex vivo* model again, or at least test it on the organotypic skin model with multiple layers of skin cells, with a monolayer of

epidermal keratinocytes used as a positive control to see if the neutralising antibody is working.

Therefore, this study would argue that topically applied exogenous NGF failed to promote epidermal repair as healthy human skin itself already contains sufficient endogenous NGF, and additional exogenous NGF provide maintenance for skin homeostasis. This explanation is supported by the abundant NGF protein expression and NGF levels seen in the epidermis throughout the wounded skin explants and at all timepoints (Figure 5.3-5.4) and is supported by the work of (Muangman *et al.*, 2004) who reported that NGF accelerates wound healing in diabetic mice but not in non-diabetic mice. This finding also supported by Chen et al., when they reported that while adding 20 μg/mL of NGF accelerate wound healing adding more NGF (40 μg/mL) did not give any beneficial effect compared to control group (Chen *et al.*, 2014). This study suggested that adding exogenous NGF into healthy skin do not have any beneficial effect.

Taken together, this study suggests that NGF and TrkA-mediated signalling are required for the repair of experimentally wounded human epidermis, and that under acute wound healing conditions *ex vivo* this occurs efficiently.

This conclusion is supported by data acquired by blocking TrkA signalling impairs re-epithelialisation, yet under normal healing conditions excess exogenous NGF does not further enhance epidermal repair, suggesting endogenous, intracutaneous NGF levels appear sufficient for optimal epidermal repair to occur in healthy human skin, even under the harsh conditions of serum-free skin organ culture. Therefore, NGF treatment may primarily benefit patients where endogenous NGF-TRKA signalling is

impaired, such as may be the case in chronic skin ulcers or diabetic skin ulcer (Anand *et al.*, 1996, Generini *et al.*, 2004, Tuveri *et al.*, 2000, Bernabei *et al.*, 1999, Landi *et al.*, 2003).

For future study one could repeat this experiment using an *ex vivo* model induced into diabetic state. Up to date, this model was only optimised in porcine skin (Ueck *et al.*, 2017) therefore one might need to further examine and optimise normal human skin *ex vivo* into diabetic condition or using diabetic human skin. However, one has to bear in mind that only certain criteria of diabetic can be inducing at one time and culturing diabetic skin also will require different approach either to maintain the skin viability, or replicate diabetic metabolic features.

This present study is the first to systematically profile NGF, TrkA, and p75NTR protein expression in experimentally wounded human skin while employing a pragmatic and clinically relevant experimental wounding assay. For this study, immunohistochemistry (IHC) staining was the best option to be used since this is the best methodology for detecting protein expression localisation in tissue (Gustashaw *et al.*, 2010, Schlederer *et al.*, 2014). IHC is also used widely by clinical pathologist to interpret tissue staining for human disease diagnosis (Schlederer *et al.*, 2014, Walker, 2006, Taylor and Levenson, 2006). Sclederer et al., found that immunohistochemistry provide important information of the localisation of protein expression in tissue whether the expression is specific in certain cell or spatial expression in certain cells type (qualitative data) and provides semi-quantitative data (Schlederer *et al.*, 2014).

As shown in 3.3 section 3.3.1 the localisation of NGF protein was detected highly in the suprabasal layer but lowly in basal epidermal cells layer in normal skin (Figure

3.29), TrkA protein expression was detected in epidermal keratinocytes mainly on dendritic-like cells and Langerhans cells (Figure 3.32), while p75NTR was expressed at the basal layer of epidermal keratinocytes (Figure 3.33). These expression patterns were translated semi-quantitatively by measuring the staining intensity of interested region. Whereby, using i.e. western blotting (Mahmood and Yang, 2012, Burnette, 1981), PCR (Southard, 2014, Stahlberg *et al.*, 2012) or ELISA (Van Weemen and Schuurs, 1971, Hnasko *et al.*, 2011) provide information on protein detection, protein identification and quantitative data of interested protein/mRNA in cells, culture media or tissue lysate.

However, analysis of protein expression by IHC has its limitation. It is a time consuming and laborious process to prepare paraffin tissue sections, staining, imaging and images analysis. For this study, two non-serial tissue sections per explant was quantified and averaged. Usually 6 image fields (as described in method chapter section 2.11; Figure 2.5) were analysed for every section and I have 70 plus explants at least for each experiment depending on the number of conditions to be tested. Even though no significant changes to the expression pattern with treatments, this study confident that these could have been detected if the changes were present.

The rationale behind examining neo-epidermal, peri-wound and unwound regions individually was because all three would allow me to evaluate the importance of NGF signalling during repair. Primarily this study wanted to assess the effect of the drug intervention on the epidermal migration, so the neo-epidermis determines the new tissue that is being laid down. The peri-wound next to the injury site is the starting point for epidermal migration (Farooqui and Fenteany, 2005) and proliferation (Yang

et al., 2017, Moll *et al.*, 1998) after skin receives a trauma (here, it refers to the wound that was created at the centre of the tissue explant), So one would assume that many physiological or physical changes happen within this area. The unwound region served as an internal control, which would indicate if any changes in protein expression occurred generally during the period in culture. Farooqui and Fenteany (2005) demonstrated that a distance 0-100 µm from the wound margin contained the highest percentage of cells protruding, while there was also a higher protrusion area (μm^2). This means there are more cells that are activated for migration and proliferation to close the wound. Their study highlighted that cells migrated to the wound bed as cell-sheet and not individually, which is supported by my cell tracing data obtained using CMFDA and CMTPX. This study would suggest that assessment of peri-wound (for 100 µm) from wound edge is sufficient to obtain appropriate information on proliferation and migration as well as other protein expression relating to wound closure assessments.

Through this *ex vivo* study it showed that NGF, TrkA and p75NTR protein expression demonstrate only minor fluctuations post-wounding whether it was untreated or treated with exogenous NGF. This study found that the expression of NGF in neo-epidermis and stratified epidermal is in line with a previous study in mice by (Matsuda *et al.*, 1998). This research showed expression of both NGF mRNA and protein in the new epithelium, while in stratified epidermis mRNA for NGF was highly expressed at the basal layer, while protein was expressed within the suprabasal layer of epidermis. However, the tested NGF dose in my study neither promoted human epidermal

keratinocyte migration (epithelial tongue length) nor increased the total area of regenerated neo-epidermis.

In this study, IHC data showed that protein expression of p75NTR was lowly expressed. It could be that the abdominal skin has fewer rete-ridges (Fernandez-Flores, 2015, Penrose and Ohara, 1973, Lawlor and Kaur, 2015) where p75NTR +ve cells normally reside. However, the most prominent explanation could be that *ex vivo* organ culture lacks free nerve endings as well as Schwann cells, which I am unable to confirm as I did not perform IHC (dual) staining to examine co-localisation. Furthermore, research performed by (Zhang *et al.*, 2018) demonstrated that overexpressing CD272 (p75NTR) without TrkA neither promoted migration and proliferation, nor promoted wound healing in mice.

Interestingly, the insignificant changes in NGF protein expression in comparison to normal skin in this model might complement the study conducted by (Rohrer *et al.*, 1988) and enlightens on their question of NGF expression in denervated adult skin. Rohrer et al., reported that denervated chick embryo hindlimb skin synthesises NGF even without innervation. They showed that NGF can be produced independently from innervation. In a different study by (Mearow *et al.*, 1993) they showed that NGF mRNA expression was also increased in denervated rat skin. The increment of NGF mRNA was correlated with the lack of nerve terminals to use the NGF (retrogradely).

Therefore, protein expression profiling results in this study raises the possibility of deficient NGF/TrkA/p75NTR signalling in skin ulcer patients. If confirmed, this underscores that activation of these signalling pathways is important for normal wound healing of human skin and that these pathways deserve systematic

exploration and therapeutic targeting, namely in patients with pathological wound healing where this signalling is defective. This study raises the prospect that ulcer treatment with topical NGF would primarily benefit those patients where endogenous NGF-TRKA signalling is impaired and that screening individual ulcer patients for intracutenous NGF/TrkA expression may help to identify those who are most likely to profit from NGF therapy. This statement is supported with my collaboration with the Tomic-Canic group from Miami University who have been profiling NGF expression in diabetic foot and leg venous ulcers using the antibody protocols that I have optimised. Their preliminary data suggests that NGF is indeed lacking in these wounds (manuscript in preparation).

In summary, this PhD project has successfully provided a model system that allows one to examine epidermal repair and lineage tracing using intravital dyes. It also confirms that epidermal repair occurs via an extending shield mechanism for the first time in human *ex vivo* organ culture. This model was then utilised to test NGF effect on epidermal repair. This study concluded that topical NGF did not provide any beneficial effect on epidermal repair in human skin *ex vivo* model, nor changed the localisation of protein expression of endogenous NGF, TrkA and p75NTR compared to vehicle treated wounds, or normal skin (uncultured). However, this project managed to document for the first time the localisation of NGF and its cognate receptor in wounded human skin in organ culture across time points. NGF and TrkA were expressed as highly as seen in normal skin, while p75NTR expression was slightly reduced compared to normal skin. Therefore, this study speculates that because normal skin contains an abundance of endogenous NGF that adding exogenous NGF

does not have beneficial effects on epidermal repair. Thus, this study would suggest that chronic wounds where NGF is downregulated such as has been indicated for diabetic ulcers are most suitable for NGF treatment.

Findings from this study highlights where future work is warranted. For example, it would be important to explore the effect of NGF treatment on epidermal repair conducted in human skin wound organ cultures under pathological conditions, which could also incorporate intravital dye assessment developed in this project. Of note, a recent study has reported using the *ex vivo* system to study wound healing in the presence of bacterial infection (Yoon et al., 2019).

It would be especially interesting to explore the effect of NGF treatment on epidermal repair in diabetic wounds *ex vivo,* given that neuropathy is a key feature of this disease. As well as the effect of NGF on altering the epidermal repair rate under diabetic conditions, it would be important to determine the level and localisation of protein expression of NGF and its cognate receptor.

In order to test this, the *ex vivo* model could be cultured under hyperglycaemic conditions, similar to those used by (Ueck *et al.*, 2017) in their study using porcine wounds *ex vivo*, by using high levels of glucose in the culture media.Another suggestion would be *ex vivo* wounding and culturing of human skin obtained from diabetic patients (i.e. from leg amputation), since there is no published study that has yet investigated this as a model. The NGF treatment could then be administered to

the wound bed to investigate the ability to accelerate wound repair under chronic diabetes condition where peripheral nerve signalling may have been impaired for many years.

Alternatively, it could be tested using an organotypic culture method such as that used by (Kabosova *et al.*, 2003). Kabosova et al., (2013) in their study showed that protein markers for pathological diabetes do not change their expression pattern whether in normal or hyperglycaemic media. Therefore, this study suggests to modify the collagen-gel approach used in Kabosova et al., (2013) such that wounded human skin organ cultures can be cultured more similarly to diabetic skin.

The outcome from these suggested experiments would provide additional evidence to indicate whether NGF might be beneficial as a treatment for impaired wound healing.

REFERENCES

ADLY, M. A., ASSAF, H. A. & HUSSEIN, M. R. 2010. Expression of Ras homologous B protein in the human scalp skin and hair follicles: hair follicle cycle stages-associated changes. *J Cutan Pathol,* 37**,** 751-7.

ADLY, M. A., ASSAF, H. A., NADA, E. A., SOLIMAN, M. & HUSSEIN, M. 2006. Expression of nerve growth factor and its high-affinity receptor, tyrosine kinase A proteins, in the human scalp skin. *J Cutan Pathol,* 33**,** 559-68.

AGACHE, P., LIHOREAU, T., MAC-MARY, S., FANIAN, F. & HUMBERT, P. 2017. The Human Skin: An Overview. *In:* HUMBERT, P. (ed.) *Agache's Measuring the Skin.* Switzerland: Springer International Publisihing.

ALBERS, K. M. & DAVIS, B. M. 2007. The skin as a neurotrophic organ. *Neuroscientist,* 13**,** 371-82.

ALBERS, K. M., PERRONE, T. N., GOODNESS, T. P., JONES, M. E., GREEN, M. A. & DAVIS, B. M. 1996. Cutaneous overexpression of NT-3 increases sensory and sympathetic neuron number and enhances touch dome and hair follicle innervation. *J Cell Biol,* 134**,** 487-97.

ALLEN, S. J., WATSON, J. J., SHOEMARK, D. K., BARUA, N. U. & PATEL, N. K. 2013. GDNF, NGF and BDNF as therapeutic options for neurodegeneration. *Pharmacol Ther,* 138**,** 155-75.

ALLEN, S. J., WILCOCK, G. K. & DAWBARN, D. 1999. Profound and selective loss of catalytic TrkB immunoreactivity in Alzheimer's disease. *Biochem Biophys Res Commun,* 264**,** 648-51.

ALOE, L., TIRASSA, P. & LAMBIASE, A. 2008. The topical application of nerve growth factor as a pharmacological tool for human corneal and skin ulcers. *Pharmacol Res,* 57**,** 253-8.

ANAND, P., TERENGHI, G., WARNER, G., KOPELMAN, P., WILLIAMS-CHESTNUT, R. E. & SINICROPI, D. V. 1996. The role of endogenous nerve growth factor in human diabetic neuropathy. *Nat Med,* 2**,** 703-7.

ANDRADE, T. A., AGUIAR, A. F., GUEDES, F. A., LEITE, M. N., CAETANO, G. F., COELHO, E. B., DAS, P. K. & FRADE, M. A. 2015. *Ex vivo* model of human skin (hOSEC) as alternative to animal use for cosmetic tests. *4th International Conference on Tissue Engineering, Icte2015, an Eccomas Thematic Conference,* 110**,** 67-73.

ANSELL, D. M., CAMPBELL, L., THOMASON, H. A., BRASS, A. & HARDMAN, M. J. 2014. A statistical analysis of murine incisional and excisional acute wound models. *Wound Repair Regen,* 22**,** 281-7.

ANSELL, D. M., HOLDEN, K. A. & HARDMAN, M. J. 2012. Animal models of wound repair: Are they cutting it? *Exp Dermatol,* 21**,** 581-5.

ANSELL, D. M., KLOEPPER, J. E., THOMASON, H. A., PAUS, R. & HARDMAN, M. J. 2011. Exploring the "hair growth-wound healing connection": anagen phase promotes wound re-epithelialization. *J Invest Dermatol.,* 131**,** 518-28. Epub 2010 Oct 7.

APFEL, S. C., KESSLER, J. A., ADORNATO, B. T., LITCHY, W. J., SANDERS, C. & RASK, C. A. 1998. Recombinant human nerve growth factor in the treatment of diabetic polyneuropathy. NGF Study Group. *Neurology,* 51**,** 695-702.

APFEL, S. C., SCHWARTZ, S., ADORNATO, B. T., FREEMAN, R., BITON, V., RENDELL, M., VINIK, A., GIULIANI, M., STEVENS, J. C., BARBANO, R. & DYCK, P. J. 2000. Efficacy and safety of recombinant human nerve growth factor in patients with diabetic polyneuropathy: A randomized controlled trial. rhNGF Clinical Investigator Group. *JAMA,* 284**,** 2215-21.

ARCHER, C. B. 2010. Functions of the Skin. *In:* BURNS, T., BREATHNACH, S., COX, N. & GRIFFITHS, C. (eds.) *Rook's Textbook of Dermatology.*

ARGYRIS, T. 1976. Kinetics of epidermal production during epidermal regeneration following abrasion in mice. *Am J Pathol.,* 83**,** 329-40.

BALAJI, S., MOLES, C. M., BHATTACHARYA, S. S., LESAINT, M., DHAMIJA, Y., LE, L. D., KING, A., KIDD, M., BOUSO, M. F., SHAABAN, A., CROMBLEHOLME, T. M., BOLLYKY, P. & KESWANI, S. G. 2014. Comparison of interleukin 10 homologs on dermal wound healing using a novel human skin ex vivo organ culture model. *J Surg Res,* 190**,** 358-66.

BALAÑÁ, M. E., CHARREAU, H. E. & LEIRÓS, G. J. 2015. Epidermal stem cells and skin tissue engineering in hair follicle regeneration. *World Journal of Stem Cells,* 7**,** 711.

BARDE, Y. A., EDGAR, D. & THOENEN, H. 1982. Purification of a new neurotrophic factor from mammalian brain. *EMBO J,* 1**,** 549-53.

BAROUCH, R., APPEL, E., KAZIMIRSKY, G., BRAUN, A., RENZ, H. & BRODIE, C. 2000. Differential regulation of neurotrophin expression by mitogens and neurotransmitters in mouse lymphocytes. *J Neuroimmunol,* 103**,** 112-21.

BASSILI, M., BIRMAN, E., SCHOR, N. F. & SARAGOVI, H. U. 2010. Differential roles of Trk and p75 neurotrophin receptors in tumorigenesis and chemoresistance ex vivo and in vivo. *Cancer Chemother Pharmacol,* 65**,** 1047-56.

BEATTIE, E. C., HOWE, C. L., WILDE, A., BRODSKY, F. M. & MOBLEY, W. C. 2000. NGF signals through TrkA to increase clathrin at the plasma membrane and enhance clathrin-mediated membrane trafficking. *Journal of Neuroscience,* 20**,** 7325-7333.

BEEM, E. & SEGAL, M. S. 2013. Evaluation of Stability and Sensitivity of Cell Fluorescent Labels When Used for Cell Migration. *Journal of Fluorescence,* 23**,** 975-987.

BERG, M. M., STERNBERG, D. W., PARADA, L. F. & CHAO, M. V. 1992. K-252a inhibits nerve growth factor-induced trk proto-oncogene tyrosine phosphorylation and kinase activity. *J Biol Chem,* 267**,** 13-6.

BERKEMEIER, L. R., WINSLOW, J. W., KAPLAN, D. R., NIKOLICS, K., GOEDDEL, D. V. & ROSENTHAL, A. 1991. Neurotrophin-5: a novel neurotrophic factor that activates trk and trkB. *Neuron,* 7**,** 857-66.

BERKING, C., TAKEMOTO, R., BINDER, R. L., HARTMAN, S. M., RUITER, D. J., GALLAGHER, P. M., LESSIN, S. R. & HERLYN, M. 2002. Photocarcinogenesis in human adult skin grafts. *Carcinogenesis,* 23**,** 181-7.

BERNABEI, R., LANDI, F., BONINI, S., ONDER, G., LAMBIASE, A., POLA, R. & ALOE, L. 1999. Effect of topical application of nerve-growth factor on pressure ulcers. *Lancet,* 354**,** 307.

BETZ, P., NERLICH, A., WILSKE, J., TUBEL, J., PENNING, R. & EISENMENGER, W. 1993. The time-dependent localization of Ki67 antigen-positive cells in human skin wounds. *Int J Legal Med,* 106**,** 35-40.

BIBEL, M., HOPPE, E. & BARDE, Y. A. 1999. Biochemical and functional interactions between the neurotrophin receptors trk and p75NTR. *EMBO J,* 18**,** 616-22.
BLAIS, M., LEVESQUE, P., BELLENFANT, S. & BERTHOD, F. 2013. Nerve growth factor, brain-derived neurotrophic factor, neurotrophin-3 and glial-derived neurotrophic factor enhance angiogenesis in a tissue-engineered in vitro model. *Tissue Eng Part A,* 19**,** 1655-64.
BLANCO-MEZQUITA, T., MARTINEZ-GARCIA, C., PROENCA, R., ZIESKE, J. D., BONINI, S., LAMBIASE, A. & MERAYO-LLOVES, J. 2013. Nerve growth factor promotes corneal epithelial migration by enhancing expression of matrix metalloprotease-9. *Invest Ophthalmol Vis Sci,* 54**,** 3880-90.
BONINI, S., LAMBIASE, A., RAMA, P., CAPRIOGLIO, G. & ALOE, L. 2000. Topical treatment with nerve growth factor for neurotrophic keratitis. *Ophthalmology,* 107**,** 1347-51; discussion 1351-2.
BOTCHKAREV, V. A., BOTCHKAREV, N. V., ALBERS, K. M., VAN DER VEEN, C., LEWIN, G. R. & PAUS, R. 1998. Neurotrophin-3 involvement in the regulation of hair follicle morphogenesis. *J Invest Dermatol,* 111**,** 279-85.
BOTCHKAREV, V. A., BOTCHKAREVA, N. V., ALBERS, K. M., CHEN, L. H., WELKER, P. & PAUS, R. 2000. A role for p75 neurotrophin receptor in the control of apoptosis-driven hair follicle regression. *FASEB J,* 14**,** 1931-42.
BOTCHKAREV, V. A., BOTCHKAREVA, N. V., PETERS, E. M. & PAUS, R. 2004. Epithelial growth control by neurotrophins: leads and lessons from the hair follicle. *Prog Brain Res,* 146**,** 493-513.
BOTCHKAREV, V. A., YAAR, M., PETERS, E. M., RAYCHAUDHURI, S. P., BOTCHKAREVA, N. V., MARCONI, A., RAYCHAUDHURI, S. K., PAUS, R. & PINCELLI, C. 2006. Neurotrophins in skin biology and pathology. *J Invest Dermatol,* 126**,** 1719-27.
BOTCHKAREVA, N. V., BOTCHKAREV, V. A., ALBERS, K. M., METZ, M. & PAUS, R. 2000. Distinct roles for nerve growth factor and brain-derived neurotrophic factor in controlling the rate of hair follicle morphogenesis. *J Invest Dermatol,* 114**,** 314-20.
BOTCHKAREVA, N. V., BOTCHKAREV, V. A., CHEN, L. H., LINDNER, G. & PAUS, R. 1999. A role for p75 neurotrophin receptor in the control of hair follicle morphogenesis. *Dev Biol,* 216**,** 135-53.
BOTHWELL, M. 1995. Functional interactions of neurotrophins and neurotrophin receptors. *Annu Rev Neurosci,* 18**,** 223-53.
BOTHWELL, M. A. & SHOOTER, E. M. 1977. Dissociation equilibrium constant of beta nerve growth factor. *J Biol Chem,* 252**,** 8532-6.
BRAUN, A., APPEL, E., BARUCH, R., HERZ, U., BOTCHKAREV, V., PAUS, R., BRODIE, C. & RENZ, H. 1998. Role of nerve growth factor in a mouse model of allergic airway inflammation and asthma. *Eur J Immunol,* 28**,** 3240-51.
BRAUN, K. M. & PROWSE, D. M. 2006. Distinct epidermal stem cell compartments are maintained by independent niche microenvironments. *Stem Cell Rev,* 2**,** 221-31.
BRONZETTI, E., CIRIACO, E., GERMANA, G. & VEGA, J. A. 1995. Immunohistochemical localization of neurotrophin receptor proteins in human skin. *Ital J Anat Embryol,* 100 Suppl 1**,** 565-71.

BROWN, J. B. & MCDOWELL, F. 1942. Epithelial healing and the transplantation of skin. *Annals of surgery,* 115**,** 1166.

BRUNNER, D., FRANK, J., APPL, H., SCHOFFL, H., PFALLER, W. & GSTRAUNTHALER, G. 2010. Serum-free cell culture: the serum-free media interactive online database. *ALTEX,* 27**,** 53-62.

BURBACH, G. J., KIM, K. H., ZIVONY, A. S., KIM, A., ARANDA, J., WRIGHT, S., NAIK, S. M., CAUGHMAN, S. W., ANSEL, J. C. & ARMSTRONG, C. A. 2001. The neurosensory tachykinins substance P and neurokinin A directly induce keratinocyte nerve growth factor. *J Invest Dermatol,* 117**,** 1075-82.

BURNETTE, W. N. 1981. "Western blotting": electrophoretic transfer of proteins from sodium dodecyl sulfate--polyacrylamide gels to unmodified nitrocellulose and radiographic detection with antibody and radioiodinated protein A. *Anal Biochem,* 112**,** 195-203.

BYRD, A. L., BELKAID, Y. & SEGRE, J. A. 2018. The human skin microbiome. *Nat Rev Microbiol,* 16**,** 143-155.

CALEY, M. P., MARTINS, V. L. & O'TOOLE, E. A. 2015. Metalloproteinases and Wound Healing. *Adv Wound Care (New Rochelle),* 4**,** 225-234.

CALZA, L., GIARDINO, L., GIULIANI, A., ALOE, L. & LEVI-MONTALCINI, R. 2001. Nerve growth factor control of neuronal expression of angiogenetic and vasoactive factors. *Proc Natl Acad Sci U S A,* 98**,** 4160-5.

CANADY, J., KARRER, S., FLECK, M. & BOSSERHOFF, A. K. 2013. Fibrosing connective tissue disorders of the skin: molecular similarities and distinctions. *J Dermatol Sci,* 70**,** 151-8.

CELLINI, M., BENDO, E., BRAVETTI, G. O. & CAMPOS, E. C. 2006. The use of nerve growth factor in surgical wound healing of the cornea. *Ophthalmic Res,* 38**,** 177-81.

CHANG, A. C., DEARMAN, B. & GREENWOOD, J. E. 2011. A Comparison of Wound Area Measurement Techniques: Visitrak Versus Photography. *Eplasty,* 11**,** e18.

CHAO, A., JIANG, N., YANG, Y., LI, H. Y. & SUN, H. Z. 2017. A Ni-NTA-based red fluorescence probe for protein labelling in live cells. *Journal of Materials Chemistry B,* 5**,** 1166-1173.

CHAO, M. V. & HEMPSTEAD, B. L. 1995. p75 and Trk: a two-receptor system. *Trends Neurosci,* 18**,** 321-6.

CHAO, M. V. 1994. The p75 neurotrophin receptor. *J Neurobiol,* 25**,** 1373-85.

CHEN, J. C., LIN, B. B., HU, H. W., LIN, C., JIN, W. Y., ZHANG, F. B., ZHU, Y. A., LU, C. J., WEI, X. J. & CHEN, R. J. 2014. NGF accelerates cutaneous wound healing by promoting the migration of dermal fibroblasts via the PI3K/Akt-Rac1-JNK and ERK pathways. *Biomed Res Int,* 2014**,** 547187.

CHEN, Z. Y., IERACI, A., TANOWITZ, M. & LEE, F. S. 2005. A novel endocytic recycling signal distinguishes biological responses of Trk neurotrophin receptors. *Mol Biol Cell,* 16**,** 5761-72.

CHETTY, R. 2019. Neurotrophic tropomyosin or tyrosine receptor kinase (NTRK) genes. *Journal of Clinical Pathology***,** jclinpath-2018-205672.

CHIARETTI, A., PIASTRA, M., CARESTA, E., NANNI, L. & ALOE, L. 2002. Improving ischaemic skin revascularisation by nerve growth factor in a child with crush syndrome. *Arch Dis Child,* 87**,** 446-8.

CHITTURI, R. T., BALASUBRAMANIAM, A. M., PARAMESWAR, R. A., KESAVAN, G., HARIS, K. M. & MOHIDEEN, K. 2015. The Role of Myofibroblasts in Wound Healing, Contraction and its Clinical Implications in Cleft Palate Repair. *Journal of international oral health: JIOH,* 7**,** 75.

COLMAN, R. W., CLOWES, A. W., GEORGE, J. N., GOLDHABER, S. Z. & MARDER, V. J. 2006. Overview of Hemostasis. *In:* COLMAN, R. W. (ed.) *Hemostasis and Thrombosis: A Basic Principle and Clinical Practice* 5th ed. USA: Lippincott Williams and Wilkins.

COSTA, N., FIORE, M. & ALOE, L. 2002. Healing action of nerve growth factor on lameness in adult goats. *Ann Ist Super Sanita,* 38**,** 187-94.

DANSO, M. O., BERKERS, T., MIEREMET, A., HAUSIL, F. & BOUWSTRA, J. A. 2015. An ex vivo human skin model for studying skin barrier repair. *Exp Dermatol,* 24**,** 48-54.

DANZBERGER, J., DONOVAN, M., RANKL, C., ZHU, R., VICIC, S., BALTENNECK, C., ENEA, R., HINTERDORFER, P. & LUENGO, G. S. 2018. Glycan distribution and density in native skin's stratum corneum. *Skin Res Technol,* 24**,** 450-458.

DEEGAN, A. J., WANG, W., MEN, S., LI, Y., SONG, S., XU, J. & WANG, R. K. 2018. Optical coherence tomography angiography monitors human cutaneous wound healing over time. *Quant Imaging Med Surg,* 8**,** 135-150.

DEINHARDT, K. & CHAO, M. V. 2014. Trk receptors. *Handb Exp Pharmacol,* 220**,** 103-19.

DELAVARY, B. M., VAN DER VEER, W. M., VAN EGMOND, M., NIESSEN, F. B. & BEELEN, R. H. J. 2011. Macrophages in skin injury and repair. *Immunobiology,* 216**,** 753-762.

DI GIROLAMO, N., SARRIS, M., CHUI, J., CHEEMA, H., CORONEO, M. T. & WAKEFIELD, D. 2008. Localization of the low-affinity nerve growth factor receptor p75 in human limbal epithelial cells. *J Cell Mol Med,* 12**,** 2799-811.

DI MARCO, E., MARCHISIO, P. C., BONDANZA, S., FRANZI, A. T., CANCEDDA, R. & DE LUCA, M. 1991. Growth-regulated synthesis and secretion of biologically active nerve growth factor by human keratinocytes. *J Biol Chem,* 266**,** 21718-22.

DI MARCO, E., MATHOR, M., BONDANZA, S., CUTULI, N., MARCHISIO, P. C., CANCEDDA, R. & DE LUCA, M. 1993. Nerve growth factor binds to normal human keratinocytes through high and low affinity receptors and stimulates their growth by a novel autocrine loop. *J Biol Chem,* 268**,** 22838-46.

DOVI, J. V., HE, L. K. & DIPIETRO, L. A. 2003. Accelerated wound closure in neutrophil-depleted mice. *J Leukoc Biol,* 73**,** 448-55.

DREIFKE, M. B., JAYASURIYA, A. A. & JAYASURIYA, A. C. 2015. Current wound healing procedures and potential care. *Mater Sci Eng C Mater Biol Appl,* 48**,** 651-62.

DRISKELL, R. R., JAHODA, C. A., CHUONG, C. M., WATT, F. M. & HORSLEY, V. 2014. Defining dermal adipose tissue. *Exp Dermatol,* 23**,** 629-31.

DUNN, L., PROSSER, H. C., TAN, J. T., VANAGS, L. Z., NG, M. K. & BURSILL, C. A. 2013. Murine model of wound healing. *J Vis Exp***,** e50265.

EGLES, C., GARLICK, J. A. & SHAMIS, Y. 2010. Three-dimensional human tissue models of wounded skin. *Methods Mol Biol,* 585**,** 345-59.

ELGHARABLY, H., ROY, S., KHANNA, S., ABAS, M., DASGHATAK, P., DAS, A., MOHAMMED, K. & SEN, C. K. 2013. A modified collagen gel enhances healing

outcome in a preclinical swine model of excisional wounds. *Wound Repair and Regeneration,* 21**,** 473-481.
ELIAS, P. M. 2012. Structure and function of the stratum corneum extracellular matrix. *J Invest Dermatol,* 132**,** 2131-3.
EMING, S. A., MARTIN, P. & TOMIC-CANIC, M. 2014. Wound repair and regeneration: mechanisms, signaling, and translation. *Sci Transl Med,* 6**,** 265sr6.
ENOCH, S., GREY, J. E. & HARDING, K. G. 2006. ABC of wound healing. Non-surgical and drug treatments. *BMJ,* 332**,** 900-3.
ETXEBARRIA, J., SANZ-LAZARO, S., HERNAEZ-MOYA, R., FREIRE, V., DURAN, J. A., MORALES, M. C. & ANDOLLO, N. 2017. Serum from plasma rich in growth factors regenerates rabbit corneas by promoting cell proliferation, migration, differentiation, adhesion and limbal stemness. *Acta Ophthalmol,* 95**,** e693-e705.
FAROOQUI, R. & FENTEANY, G. 2005. Multiple rows of cells behind an epithelial wound edge extend cryptic lamellipodia to collectively drive cell-sheet movement. *J Cell Sci,* 118**,** 51-63.
FERNANDEZ-FLORES, A. 2015. Regional Variations in the Histology of the Skin. *Am J Dermatopathol,* 37**,** 737-54.
FERRAQ, Y., BLACK, D., LAGARDE, J. M., SCHMITT, A. M., DAHAN, S., GROLLEAU, J. L. & MORDON, S. 2007. Use of a 3-D imaging technique for non-invasive monitoring of the depth of experimentally induced wounds. *Skin Res Technol,* 13**,** 399-405.
FILIPPI, M. D. 2016. Mechanism of Diapedesis: Importance of the Transcellular Route. *Adv Immunol,* 129**,** 25-53.
FRADE, M. A., ANDRADE, T. A., AGUIAR, A. F., GUEDES, F. A., LEITE, M. N., PASSOS, W. R., COELHO, E. B. & DAS, P. K. 2015. Prolonged viability of human organotypic skin explant in culture method (hOSEC). *An Bras Dermatol,* 90**,** 347-50.
FRANTZ, R. A. 2005. Identifying infection in chronic wounds. *Nursing2019,* 35**,** 73.
FRYKBERG, R. G. & BANKS, J. 2015. Challenges in the Treatment of Chronic Wounds. *Adv Wound Care (New Rochelle),* 4**,** 560-582.
GABBIANI, G., RYAN, G. B. & MAJNE, G. 1971. Presence of modified fibroblasts in granulation tissue and their possible role in wound contraction. *Experientia,* 27**,** 549-50.
GALKOWSKA, H., OLSZEWSKI, W. L., WOJEWODZKA, U., ROSINSKI, G. & KARNAFEL, W. 2006. Neurogenic factors in the impaired healing of diabetic foot ulcers. *J Surg Res,* 134**,** 252-8.
GEETHA, T., REGE, S. D., MATHEWS, S. E., MEAKIN, S. O., WHITE, M. F. & BABU, J. R. 2013. Nerve growth factor receptor TrkA, a new receptor in insulin signaling pathway in PC12 cells. *J Biol Chem,* 288**,** 23807-13.
GENERINI, S., TUVERI, M. A., MATUCCI CERINIC, M., MASTINU, F., MANNI, L. & ALOE, L. 2004. Topical application of nerve growth factor in human diabetic foot ulcers. A study of three cases. *Exp Clin Endocrinol Diabetes,* 112**,** 542-4.
GERBER, P. A., BUHREN, B. A., SCHRUMPF, H., HOMEY, B., ZLOTNIK, A. & HEVEZI, P. 2014. The top skin-associated genes: a comparative analysis of human and mouse skin transcriptomes. *Biol Chem,* 395**,** 577-91.

GETHIN, G. & COWMAN, S. 2006. Wound measurement comparing the use of acetate tracings and Visitrak(TM) digital planimetry. *Journal of Clinical Nursing,* 15**,** 422-427.

GETHIN, G. 2006. The importance of continuous wound measuring. *Wounds UK,* 2**,** 9.

GLINOS, G. D., VERNE, S. H., ALDAHAN, A. S., LIANG, L., NOURI, K., ELLIOT, S., GLASSBERG, M., CABRERA DEBUC, D., KORU-SENGUL, T., TOMIC-CANIC, M. & PASTAR, I. 2017. Optical Coherence Tomography for Assessment of Epithelialization in a Human *Ex vivo* Wound Model. *Wound Repair Regen*.

GONZALEZ, A. C. D., COSTA, T. F., ANDRADE, Z. D. & MEDRADO, A. R. A. P. 2016. Wound healing - A literature review. *Anais Brasileiros De Dermatologia,* 91**,** 614-620.

GOULD, L., ABADIR, P., BREM, H., CARTER, M., CONNER-KERR, T., DAVIDSON, J., DIPIETRO, L., FALANGA, V., FIFE, C., GARDNER, S., GRICE, E., HARMON, J., HAZZARD, W. R., HIGH, K. P., HOUGHTON, P., JACOBSON, N., KIRSNER, R. S., KOVACS, E. J., MARGOLIS, D., MCFARLAND HORNE, F., REED, M. J., SULLIVAN, D. H., THOM, S., TOMIC-CANIC, M., WALSTON, J., WHITNEY, J. A., WILLIAMS, J., ZIEMAN, S. & SCHMADER, K. 2015. Chronic wound repair and healing in older adults: current status and future research. *J Am Geriatr Soc,* 63**,** 427-38.

GRADA, A., MERVIS, J. & FALANGA, V. 2018. Research Techniques Made Simple: Animal Models of Wound Healing. *J Invest Dermatol,* 138**,** 2095-2105 e1.

GREAVES, N. S., BENATAR, B., WHITESIDE, S., ALONSO-RASGADO, T., BAGUNEID, M. & BAYAT, A. 2014. Optical coherence tomography: a reliable alternative to invasive histological assessment of acute wound healing in human skin? *Br J Dermatol,* 170**,** 840-50.

GSTRAUNTHALER, G. 2003. Alternatives to the use of fetal bovine serum: serum-free cell culture. *Altex,* 20**,** 275-81.

GUDJONSSON, J. E., JOHNSTON, A., DYSON, M., VALDIMARSSON, H. & ELDER, J. T. 2007. Mouse models of psoriasis. *J Invest Dermatol,* 127**,** 1292-308.

GUERRERO-ASPIZUA, S., GARCIA, M., MURILLAS, R., RETAMOSA, L., ILLERA, N., DUARTE, B., HOLGUIN, A., PUIG, S., HERNANDEZ, M. I., MEANA, A., JORCANO, J. L., LARCHER, F., CARRETERO, M. & DEL RIO, M. 2010. Development of a bioengineered skin-humanized mouse model for psoriasis: dissecting epidermal-lymphocyte interacting pathways. *Am J Pathol,* 177**,** 3112-24.

GUEST, J. F., AYOUB, N., MCILWRAITH, T., UCHEGBU, I., GERRISH, A., WEIDLICH, D., VOWDEN, K. & VOWDEN, P. 2015. Health economic burden that wounds impose on the National Health Service in the UK. *BMJ Open,* 5**,** e009283.

GUEST, J. F., AYOUB, N., MCILWRAITH, T., UCHEGBU, I., GERRISH, A., WEIDLICH, D., VOWDEN, K. & VOWDEN, P. 2017. Health economic burden that different wound types impose on the UK's National Health Service. *Int Wound J,* 14**,** 322-330.

GUPTA, A. & KUMAR, P. 2015. Assessment of the histological state of the healing wound. *Plastic and Aesthetic Research,* 2**,** 239-42.

GURTNER, G. C. & CHAPMAN, M. A. 2016. Regenerative Medicine: Charting a New Course in Wound Healing. *Adv Wound Care (New Rochelle),* 5**,** 314-328.

GUSTASHAW, K. M., NAJMABADI, P. & POTTS, S. J. 2010. Measuring Protein Expression in Tissue: The Complementary Roles of Brightfield and Fluorescence in Whole Slide Scanning. *Labmedicine,* 41**,** 135-142.

HALIM, A. S., NOR, F. M., MAT SAAD, A. Z., MOHD NASIR, N. A., NORSA'ADAH, B. & UJANG, Z. 2018. Efficacy of chitosan derivative films versus hydrocolloid dressing on superficial wounds. *Journal of Taibah University Medical Sciences,* 13**,** 512-520.

HALLBOOK, F., IBANEZ, C. F. & PERSSON, H. 1991. Evolutionary studies of the nerve growth factor family reveal a novel member abundantly expressed in Xenopus ovary. *Neuron,* 6**,** 845-58.

HARN, H. I., OGAWA, R., HSU, C. K., HUGHES, M. W., TANG, M. J. & CHUONG, C. M. 2017. The tension biology of wound healing. *Exp Dermatol*.

HASAN, W., JAMA, A., DONOHUE, T., WERNLI, G., ONYSZCHUK, G., AL-HAFEZ, B., BILGEN, M. & SMITH, P. G. 2006. Sympathetic hyperinnervation and inflammatory cell NGF synthesis following myocardial infarction in rats. *Brain Res,* 1124**,** 142-54.

HASHIMOTO, K., KAJITANI, N., MIYAMOTO, Y. & MATSUMOTO, K. I. 2018. Wound healing-related properties detected in an experimental model with a collagen gel contraction assay are affected in the absence of tenascin-X. *Exp Cell Res,* 363**,** 102-113.

HE, X. L. & GARCIA, K. C. 2004. Structure of nerve growth factor complexed with the shared neurotrophin receptor p75. *Science,* 304**,** 870-5.

HEIMBACH, D., ENGRAV, L., GRUBE, B. & MARVIN, J. 1992. Burn depth: a review. *World J Surg,* 16**,** 10-5.

HEMPSTEAD, B. L. 2002. The many faces of p75NTR. *Curr Opin Neurobiol,* 12**,** 260-7.

HERMAN, I. M. & LEUNG, A. 2009. Creation of human skin equivalents for the in vitro study of angiogenesis in wound healing. *Methods Mol Biol,* 467**,** 241-8.

HIROSE, M., KURODA, Y. & MURATA, E. 2016. NGF/TrkA Signaling as a Therapeutic Target for Pain. *Pain Pract,* 16**,** 175-82.

HNASKO, R., LIN, A., MCGARVEY, J. A. & STANKER, L. H. 2011. A rapid method to improve protein detection by indirect ELISA. *Biochem Biophys Res Commun,* 410**,** 726-31.

HOHN, A., LEIBROCK, J., BAILEY, K. & BARDE, Y. A. 1990. Identification and characterization of a novel member of the nerve growth factor/brain-derived neurotrophic factor family. *Nature,* 344**,** 339-41.

HUANG, E. J. & REICHARDT, L. F. 2003. Trk receptors: roles in neuronal signal transduction. *Annu Rev Biochem,* 72**,** 609-42.

HUANG, J. H., SU, Q. M., YANG, J., LV, Y. H., HE, Y. C., CHEN, J. C., XU, L., WANG, K. & ZHENG, Q. S. 2015. Sample sizes in dosage investigational clinical trials: a systematic evaluation. *Drug Des Devel Ther,* 9**,** 305-12.

INABA, H., NUMAI, T., ARAKI, M. & MIZUGUCHI, T. 1993. K252a, a potent protein kinase inhibitor, improves endotoxic lethality and glucose dyshomeostasis. *Surg Today,* 23**,** 234-40.

IP, N. Y., IBANEZ, C. F., NYE, S. H., MCCLAIN, J., JONES, P. F., GIES, D. R., BELLUSCIO, L., LE BEAU, M. M., ESPINOSA, R. & SQUINTO, S. P. 1992. Mammalian neurotrophin-4: structure, chromosomal localization, tissue distribution, and

receptor specificity. *Proceedings of the National Academy of Sciences,* 89**,** 3060-3064.

ITO, M., LIU, Y., YANG, Z., NGUYEN, J., LIANG, F., MORRIS, R. J. & COTSARELIS, G. 2005. Stem cells in the hair follicle bulge contribute to wound repair but not to homeostasis of the epidermis. *Nat Med.,* 11**,** 1351-4. Epub 2005 Nov 20.

JAMESON, J., UGARTE, K., CHEN, N., YACHI, P., FUCHS, E., BOISMENU, R. & HAVRAN, W. L. 2002. A role for skin gammadelta T cells in wound repair. *Science,* 296**,** 747-9.

JANG, S. W., OKADA, M., SAYEED, I., XIAO, G., STEIN, D., JIN, P. & YE, K. 2007. Gambogic amide, a selective agonist for TrkA receptor that possesses robust neurotrophic activity, prevents neuronal cell death. *Proc Natl Acad Sci U S A,* 104**,** 16329-34.

JANIS, J. E., KWON, R. K. & LALONDE, D. H. 2010. A practical guide to wound healing. *Plast Reconstr Surg,* 125**,** 230e-44e.

JIMENEZ, F., GARDE, C., POBLET, E., JIMENO, B., ORTIZ, J., MARTINEZ, M. L., GUTIERREZ-RIVERA, A., PEREZ-LOPEZ, V., ETXANIZ, U., NAVEDA, C., HIGUERA, J. L., EGUES, N., ESCARIO, E. & IZETA, A. 2012. A pilot clinical study of hair grafting in chronic leg ulcers. *Wound Repair Regen,* 20**,** 806-14.

JING, S. Q., TAPLEY, P. & BARBACID, M. 1992. Nerve Growth-Factor Mediates Signal Transduction through Trk Homodimer Receptors. *Neuron,* 9**,** 1067-1079.

JOHNSON, D., LANAHAN, A., BUCK, C. R., SEHGAL, A., MORGAN, C., MERCER, E., BOTHWELL, M. & CHAO, M. 1986. Expression and structure of the human NGF receptor. *Cell,* 47**,** 545-54.

JOHNSON, I. 1998. Fluorescent probes for living cells. *Histochem J,* 30**,** 123-40.

JOHNSON, R. M. & RICHARD, R. 2003. Partial-thickness burns: identification and management. *Adv Skin Wound Care,* 16**,** 178-87; quiz 188-9.

JONES, K. R. & REICHARDT, L. F. 1990. Molecular cloning of a human gene that is a member of the nerve growth factor family. *Proc Natl Acad Sci U S A,* 87**,** 8060-4.

JONES, M. L. 2018. Series 3. Wound infection 3.1: the wound infection continuum explained. *British Journal of Healthcare Assistants,* 12**,** 218-220.

JULLIEN, J., GUILI, V., REICHARDT, L. F. & RUDKIN, B. B. 2002. Molecular kinetics of nerve growth factor receptor trafficking and activation. *J Biol Chem,* 277**,** 38700-8.

KABOSOVA, A., KRAMEROV, A. A., AOKI, A. M., MURPHY, G., ZIESKE, J. D. & LJUBIMOV, A. V. 2003. Human diabetic corneas preserve wound healing, basement membrane, integrin and MMP-10 differences from normal corneas in organ culture. *Exp Eye Res,* 77**,** 211-7.

KAPLAN, D. R., HEMPSTEAD, B. L., MARTIN-ZANCA, D., CHAO, M. V. & PARADA, L. F. 1991. The trk proto-oncogene product: a signal transducing receptor for nerve growth factor. *Science,* 252**,** 554-8.

KASE, H., IWAHASHI, K., NAKANISHI, S., MATSUDA, Y., YAMADA, K., TAKAHASHI, M., MURAKATA, C., SATO, A. & KANEKO, M. 1987. K-252 compounds, novel and potent inhibitors of protein kinase C and cyclic nucleotide-dependent protein kinases. *Biochemical and Biophysical Research Communications,* 142**,** 436-440.

KAWAMOTO, K. & MATSUDA, H. 2004. Nerve growth factor and wound healing. *Prog Brain Res,* 146**,** 369-84.
KERMANI, P. & HEMPSTEAD, B. 2007. Brain-derived neurotrophic factor: a newly described mediator of angiogenesis. *Trends Cardiovasc Med,* 17**,** 140-3.
KIM, K. H., LEE, D. Y. & PARK, K. C. 2000. The Development of a Wound Healing Model Using Nerve Growth Factor(NGF) Expression in Raft Culture. *Ann Dermatol,* 12**,** 106-113.
KLEIN, R., LAMBALLE, F., BRYANT, S. & BARBACID, M. 1992. The trkB tyrosine protein kinase is a receptor for neurotrophin-4. *Neuron,* 8**,** 947-56.
KOH, T. J. & DIPIETRO, L. A. 2011. Inflammation and wound healing: the role of the macrophage. *Expert Rev Mol Med,* 13**,** e23.
KOH, T. J., NOVAK, M. L. & MIRZA, R. E. 2013. Assessing macrophage phenotype during tissue repair. *In:* GOURDIE, R. G. & MYERS, T. A. (eds.) *Methods Mol Biol.* 2013/09/14 ed. New York: Springer Science+Business Media.
KRAMER, A., DISSEMOND, J., KIM, S., WILLY, C., MAYER, D., PAPKE, R., TUCHMANN, F. & ASSADIAN, O. 2018. Consensus on Wound Antisepsis: Update 2018. *Skin Pharmacol Physiol,* 31**,** 28-58.
KRATZ, G. 1998. Modeling of wound healing processes in human skin using tissue culture. *Microscopy Research and Technique,* 42**,** 345-350.
LAD, S. P., PETERSON, D. A., BRADSHAW, R. A. & NEET, K. E. 2003. Individual and combined effects of TrkA and p75NTR nerve growth factor receptors. A role for the high affinity receptor site. *J Biol Chem,* 278**,** 24808-17.
LAMBIASE, A., COASSIN, M., SPOSATO, V., MICERA, A., SACCHETTI, M., BONINI, S. & ALOE, L. 2007. NGF topical application in patients with corneal ulcer does not generate circulating NGF antibodies. *Pharmacol Res,* 56**,** 65-9.
LAMBIASE, A., RAMA, P., BONINI, S., CAPRIOGLIO, G. & ALOE, L. 1998. Topical treatment with nerve growth factor for corneal neurotrophic ulcers. *N Engl J Med,* 338**,** 1174-80.
LANDI, F., ALOE, L., RUSSO, A., CESARI, M., ONDER, G., BONINI, S., CARBONIN, P. U. & BERNABEI, R. 2003. Topical treatment of pressure ulcers with nerve growth factor: a randomized clinical trial. *Ann Intern Med,* 139**,** 635-41.
LANGTON, A. K., HERRICK, S. E. & HEADON, D. J. 2008. An extended epidermal response heals cutaneous wounds in the absence of a hair follicle stem cell contribution. *J Invest Dermatol.,* 128**,** 1311-8. Epub 2007 Nov 22.
LAWLOR, K. T. & KAUR, P. 2015. Dermal Contributions to Human Interfollicular Epidermal Architecture and Self-Renewal. *Int J Mol Sci,* 16**,** 28098-107.
LAWMAN, M. J., BOYLE, M. D., GEE, A. P. & YOUNG, M. 1985. Nerve growth factor accelerates the early cellular events associated with wound healing. *Exp Mol Pathol,* 43**,** 274-81.
LEMASTER, A. M., KRIMM, R. F., DAVIS, B. M., NOEL, T., FORBES, M. E., JOHNSON, J. E. & ALBERS, K. M. 1999. Overexpression of brain-derived neurotrophic factor enhances sensory innervation and selectively increases neuron number. *J Neurosci,* 19**,** 5919-31.
LEON, A., BURIANI, A., DAL TOSO, R., FABRIS, M., ROMANELLO, S., ALOE, L. & LEVI-MONTALCINI, R. 1994. Mast cells synthesize, store, and release nerve growth factor. *Proc Natl Acad Sci U S A,* 91**,** 3739-43.

LEVI-MONTALCINI, R. & ANGELETTI, P. U. 1968. Nerve growth factor. *Physiol Rev,* 48**,** 534-69.
LEVI-MONTALCINI, R. 1987. The nerve growth factor 35 years later. *Science,* 237**,** 1154-62.
LEVI-MONTALCINI, R., MEYER, H. & HAMBURGER, V. 1954. *In vitro* experiments on the effects of mouse sarcomas 180 and 37 on the spinal and sympathetic ganglia of the chick embryo. *Cancer Res,* 14**,** 49-57.
LEVI-SCHAFFER, F., MICERA, A., MAQUART, F. X. & ALOE, L. 2001. Nerve growth factor is produced by human fibroblasts and modulates them: Role of nerve growth factor in tissue repair. *International Archives of Allergy and Immunology,* 124**,** 279-281.
LEVY, V., LINDON, C., HARFE, B. D. & MORGAN, B. A. 2005. Distinct stem cell populations regenerate the follicle and interfollicular epidermis. *Dev Cell,* 9**,** 855-61.
LEVY, V., LINDON, C., ZHENG, Y., HARFE, B. D. & MORGAN, B. A. 2007. Epidermal stem cells arise from the hair follicle after wounding. *The FASEB Journal,* 21**,** 1358-1366.
LEYDON, C., IMAIZUMI, M., BARTLETT, R. S., WANG, S. F. & THIBEAULT, S. L. 2014. Epithelial cells are active participants in vocal fold wound healing: an in vivo animal model of injury. *PLoS One,* 9**,** e115389.
LI, A. K., KOROLY, M. J., SCHATTENKERK, M. E., MALT, R. A. & YOUNG, M. 1980. Nerve growth factor: acceleration of the rate of wound healing in mice. *Proc Natl Acad Sci U S A,* 77**,** 4379-81.
LIANG, C.-C., PARK, A. Y. & GUAN, J.-L. 2007. *In vitro* scratch assay: a convenient and inexpensive method for analysis of cell migration *in vitro*. *Nature Protocols,* 2**,** 329.
LINDSAY, R. M. & HARMAR, A. J. 1989. Nerve Growth-Factor Regulates Expression of Neuropeptide Genes in Adult Sensory Neurons. *Nature,* 337**,** 362-364.
LIU, H. N., TUCHINDA, P., FISHELEVICH, R., HARBERTS, E. & GASPARI, A. A. 2014. Human in vitro skin organ culture as a model system for evaluating DNA repair. *Journal of Dermatological Science,* 74**,** 236-241.
LIU, J. Q., ZHAO, K. B., FENG, Z. H. & QI, F. Z. 2015. Hair follicle units promote re-epithelialization in chronic cutaneous wounds: A clinical case series study. *Exp Ther Med,* 10**,** 25-30.
LOEB, L. 1919. Wound Healing in Experimental (Ceilfibrin) Tissue. *Science,* 50**,** 502-4.
LONE, A. G., ATCI, E., RENSLOW, R., BEYENAL, H., NOH, S., FRANSSON, B., ABU-LAIL, N., PARK, J. J., GANG, D. R. & CALL, D. R. 2015. Staphylococcus aureus induces hypoxia and cellular damage in porcine dermal explants. *Infect Immun,* 83**,** 2531-41.
LOPATINA, T., KALININA, N., KARAGYAUR, M., STAMBOLSKY, D., RUBINA, K., REVISCHIN, A., PAVLOVA, G., PARFYONOVA, Y. & TKACHUK, V. 2011. Adipose-derived stem cells stimulate regeneration of peripheral nerves: BDNF secreted by these cells promotes nerve healing and axon growth de novo. *PLoS One,* 6**,** e17899.
LOPEZ, S. M., PEREZ-PEREZ, M., MARQUEZ, J. M., NAVES, F. J., REPRESA, J. & VEGA, J. A. 1998. p75 and TrkA neurotrophin receptors in human skin after spinal

cord and peripheral nerve injury, with special reference to sensory corpuscles. *Anat Rec,* 251**,** 371-83.
LU, H. & ROLLMAN, O. 2004. Fluorescence imaging of reepithelialization from skin explant cultures on acellular dermis. *Wound Repair Regen,* 12**,** 575-86.
LU, Z., HASSE, S., BODO, E., ROSE, C., FUNK, W. & PAUS, R. 2007. Towards the development of a simplified long-term organ culture method for human scalp skin and its appendages under serum-free conditions. *Exp Dermatol,* 16**,** 37-44.
LUCAS, T., WAISMAN, A., RANJAN, R., ROES, J., KRIEG, T., MULLER, W., ROERS, A. & EMING, S. A. 2010. Differential roles of macrophages in diverse phases of skin repair. *J Immunol,* 184**,** 3964-77.
LUDOVICI, M., KOZUL, N., MATERAZZI, S., RISOLUTI, R., PICARDO, M. & CAMERA, E. 2018. Influence of the sebaceous gland density on the stratum corneum lipidome. *Sci Rep,* 8**,** 11500.
MAHMOOD, T. & YANG, P. C. 2012. Western blot: technique, theory, and trouble shooting. *N Am J Med Sci,* 4**,** 429-34.
MARLIN, M. C. & LI, G. 2015. Biogenesis and function of the NGF/TrkA signaling endosome. *Int Rev Cell Mol Biol,* 314**,** 239-57.
MARTIN, P. & NUNAN, R. 2015. Cellular and molecular mechanisms of repair in acute and chronic wound healing. *Br J Dermatol,* 173**,** 370-8.
MARTIN, P. 1997. Wound healing--aiming for perfect skin regeneration. *Science,* 276**,** 75-81.
MARTINEZ, M. L., ESCARIO, E., POBLET, E., SANCHEZ, D., BUCHON, F. F., IZETA, A. & JIMENEZ, F. 2016. Hair follicle-containing punch grafts accelerate chronic ulcer healing: A randomized controlled trial. *J Am Acad Dermatol,* 75**,** 1007-1014.
MARTINEZ, M. L., ESCARIO, T. E. & JIMENEZ, A. F. 2017. Hair-follicle Transplant Into Chronic Ulcers: A New Graft Concept. *Actas Dermosifiliogr,* 108**,** 524-531.
MARTIN-ZANCA, D., HUGHES, S. H. & BARBACID, M. 1986. A human oncogene formed by the fusion of truncated tropomyosin and protein tyrosine kinase sequences. *Nature,* 319**,** 743.
MATSUDA, H., KOYAMA, H., SATO, H., SAWADA, J., ITAKURA, A., TANAKA, A., MATSUMOTO, M., KONNO, K., USHIO, H. & MATSUDA, K. 1998. Role of nerve growth factor in cutaneous wound healing: accelerating effects in normal and healing-impaired diabetic mice. *J Exp Med,* 187**,** 297-306.
MATTHEWS, J. N., ALTMAN, D. G., CAMPBELL, M. J. & ROYSTON, P. 1990. Analysis of serial measurements in medical research. *BMJ,* 300**,** 230-5.
MCARTHUR, J. C., YIANNOUTSOS, C., SIMPSON, D. M., ADORNATO, B. T., SINGER, E. J., HOLLANDER, H., MARRA, C., RUBIN, M., COHEN, B. A., TUCKER, T., NAVIA, B. A., SCHIFITTO, G., KATZENSTEIN, D., RASK, C., ZABORSKI, L., SMITH, M. E., SHRIVER, S., MILLAR, L., CLIFFORD, D. B. & KARALNIK, I. J. 2000. A phase II trial of nerve growth factor for sensory neuropathy associated with HIV infection. AIDS Clinical Trials Group Team 291. *Neurology,* 54**,** 1080-8.
MCDONALD, N. Q. & CHAO, M. V. 1995. Structural determinants of neurotrophin action. *J Biol Chem,* 270**,** 19669-72.

MCDONALD, N. Q., LAPATTO, R., MURRAY-RUST, J., GUNNING, J., WLODAWER, A. & BLUNDELL, T. L. 1991. New protein fold revealed by a 2.3-A resolution crystal structure of nerve growth factor. *Nature,* 354**,** 411-4.

MCGIBBON, D. H. 2010. Subcutaneous Fat. *In:* BURNS, T., BREATHNACH, S., COX, N. & GRIFFITHS, C. (eds.) *Rook's Texbook of Dermatology.* 8 ed. Singapore: Wiley-Blackwell.

MCGRATH, J. A. & UITTO, J. 2010. Anatomy and Organization of Human Skin. *In:* BURNS, T., BREATHNACH, S. & GRIFFITHS, C. (eds.) *Rook's Textbook of Dermatology.* 8 ed. Singapore: Wiley-Blackwell.

MEAKIN, S. O. & SHOOTER, E. M. 1992. The nerve growth factor family of receptors. *Trends Neurosci,* 15**,** 323-31.

MEAROW, K. M., KRIL, Y. & DIAMOND, J. 1993. Increased NGF mRNA expression in denervated rat skin. *Neuroreport,* 4**,** 351-4.

MEAUME, S. & HUMBERT, P. 2017. Skin Wound Healing Assessment. *In:* P., H., F., F., H., M. & P, A. (eds.) *Agache's Measuring the Skin.* Springer, Cham.

MEIER, N. T., HASLAM, I. S., PATTWELL, D. M., ZHANG, G. Y., EMELIANOV, V., PAREDES, R., DEBUS, S., AUGUSTIN, M., FUNK, W., AMAYA, E., KLOEPPER, J. E., HARDMAN, M. J. & PAUS, R. 2013. Thyrotropin-releasing hormone (TRH) promotes wound re-epithelialisation in frog and human skin. *PLoS One,* 8**,** e73596.

MENDOZA-GARCIA, J., SEBASTIAN, A., ALONSO-RASGADO, T. & BAYAT, A. 2015. Optimization of an *ex vivo* wound healing model in the adult human skin: Functional evaluation using photodynamic therapy. *Wound Repair Regen,* 23**,** 685-702.

MENON, G. K., CLEARY, G. W. & LANE, M. E. 2012. The structure and function of the stratum corneum. *Int J Pharm,* 435**,** 3-9.

MICERA, A., LAMBIASE, A., STAMPACHIACCHIERE, B., BONINI, S., BONINI, S. & LEVI-SCHAFFER, F. 2007. Nerve growth factor and tissue repair remodeling: trkA(NGFR) and p75(NTR), two receptors one fate. *Cytokine Growth Factor Rev,* 18**,** 245-56.

MICERA, A., VIGNETI, E., PICKHOLTZ, D., REICH, R., PAPPO, O., BONINI, S., MAQUART, F. X., ALOE, L. & LEVI-SCHAFFER, F. 2001. Nerve growth factor displays stimulatory effects on human skin and lung fibroblasts, demonstrating a direct role for this factor in tissue repair. *Proc Natl Acad Sci U S A,* 98**,** 6162-7.

MIRASTSCHIJSKI, U., JOKUSZIES, A. & VOGT, P. M. 2013. *Skin wound healing: Repair biology, wound and scar treatment*, Elsevier Inc.

MITBAUEROVA, A., ROLIN, G., ROBIN, S., TAUZIN, H., JACQUET, E., MURET, P. & HUMBERT, P. 2012. A human skin culture system for a wound-healing model. *Comput Methods Biomech Biomed Engin,* 15 Suppl 1**,** 102-3.

MOHAMED, R. & EL-REMESSY, A. B. 2015. Imbalance of the Nerve Growth Factor and Its Precursor: Implication in Diabetic Retinopathy. *J Clin Exp Ophthalmol,* 6.

MOLL, I., HOUDEK, P., SCHMIDT, H. & MOLL, R. 1998. Characterization of epidermal wound healing in a human skin organ culture model: acceleration by transplanted keratinocytes. *J Invest Dermatol,* 111**,** 251-8.

MONROE, D. M. & HOFFMAN, M. 2012. The clotting system - a major player in wound healing. *Haemophilia,* 18 Suppl 5**,** 11-6.

MOORE, A. L., MARSHALL, C. D., BARNES, L. A., MURPHY, M. P., RANSOM, R. C. & LONGAKER, M. T. 2018. Scarless wound healing: Transitioning from fetal research to regenerative healing. *Wiley Interdiscip Rev Dev Biol,* 7.

MOQRICH, A., EARLEY, T. J., WATSON, J., ANDAHAZY, M., BACKUS, C., MARTIN-ZANCA, D., WRIGHT, D. E., REICHARDT, L. F. & PATAPOUTIAN, A. 2004. Expressing TrkC from the TrkA locus causes a subset of dorsal root ganglia neurons to switch fate. *Nat Neurosci,* 7**,** 812-8.

MOREIRA, C. F., CASSINI-VIEIRA, P., DA SILVA, M. F. & BARCELOS, L. S. 2015. Skin Wound Healing Model - Excisional Wounding and Assessment of Lesion Area. *Bio-protocol,* 5**,** e1661.

MORTON, L. M. & PHILLIPS, T. J. 2016. Wound healing and treating wounds: Differential diagnosis and evaluation of chronic wounds. *J Am Acad Dermatol,* 74**,** 589-605; quiz 605-6.

MUANGMAN, P., MUFFLEY, L. A., ANTHONY, J. P., SPENNY, M. L., UNDERWOOD, R. A., OLERUD, J. E. & GIBRAN, N. S. 2004. Nerve growth factor accelerates wound healing in diabetic mice. *Wound Repair Regen,* 12**,** 44-52.

MURASE, K., MURAKAMI, Y., TAKAYANAGI, K., FURUKAWA, Y. & HAYASHI, K. 1992. Human fibroblast cells synthesize and secrete nerve growth factor in culture. *Biochem Biophys Res Commun,* 184**,** 373-9.

MURPHREY, M. B. & ZITO, P. M. 2018. Histology, Stratum Corneum. *StatPearls.* Treasure Island (FL).

NASIR, N. A. M., PAUS, R. & ANSELL, D. M. 2019. Fluorescent cell tracer dye permits real-time assessment of re-epithelialization in a serum-free ex vivo human skin wound assay. *Wound Repair Regen,* 27**,** 126-133.

NAWAZ, Z. & BENTLEY, G. 2011. Surgical incisions and principles of wound healing. *Surgery - Oxford International Edition,* 29**,** 59-62.

NEGRINI, S., D'ALESSANDRO, R. & MELDOLESI, J. 2013. NGF signaling in PC12 cells: the cooperation of p75(NTR) with TrkA is needed for the activation of both mTORC2 and the PI3K signalling cascade. *Biol Open,* 2**,** 855-66.

mTORC2 and the PI3K signalling cascade. *Biol Open,* 2**,** 855-66.

NG, K. W. & LAU, W. M. 2015. Skin Deep: The Basics of Human Skin Structure and Drug Penetration. *In:* DRAGICEVIC, N. & MAIBACH, H. (eds.) *Percutaneous Penetration Enhancers Chemical Methods in Penetration Enhancement.* Berlin, Heidelberg

NGO, P., RAMALINGAM, P., PHILLIPS, J. A. & FURUTA, G. T. 2006. Collagen Gel Contraction Assay. *In:* COLGAN, S. P. (ed.) *Cell-Cell Interactions: Methods and Protocols.* Totowa, NJ: Humana Press.

NICU, C., POPLE, J., BONSELL, L., BHOGAL, R., ANSELL, D. M. & PAUS, R. 2018. A guide to studying human dermal adipocytes in situ. *Exp Dermatol,* 27**,** 589-602.

NITHYA, M., SUGUNA, L. & ROSE, C. 2003. The effect of nerve growth factor on the early responses during the process of wound healing. *Biochim Biophys Acta,* 1620**,** 25-31.

NUNAN, R., HARDING, K. G. & MARTIN, P. 2014. Clinical challenges of chronic wounds: searching for an optimal animal model to recapitulate their complexity. *Dis Model Mech,* 7**,** 1205-13.

NUSSBAUM, S. R., CARTER, M. J., FIFE, C. E., DAVANZO, J., HAUGHT, R., NUSGART, M. & CARTWRIGHT, D. 2018. An Economic Evaluation of the Impact, Cost, and Medicare Policy Implications of Chronic Nonhealing Wounds. *Value in Health,* 21**,** 27-32.

ODLAND, G. & ROSS, R. 1968. Human wound repair. I. Epidermal regeneration. *J Cell Biol,* 39**,** 135-51.

OLCZYK, P., MENCNER, L. & KOMOSINSKA-VASSEV, K. 2014. The role of the extracellular matrix components in cutaneous wound healing. *Biomed Res Int,* 2014**,** 747584.

OLSSON, M., JARBRINK, K., DIVAKAR, U., BAJPAI, R., UPTON, Z., SCHMIDTCHEN, A. & CAR, J. 2019. The humanistic and economic burden of chronic wounds: A systematic review. *Wound Repair Regen,* 27**,** 114-125.

OTTEN, U., SCULLY, J. L., EHRHARD, P. B. & GADIENT, R. A. 1994. Neurotrophins: signals between the nervous and immune systems. *Prog Brain Res,* 103**,** 293-305.

PAOLETTI, F., COVACEUSZACH, S., KONAREV, P. V., GONFLONI, S., MALERBA, F., SCHWARZ, E., SVERGUN, D. I., CATTANEO, A. & LAMBA, D. 2009. Intrinsic structural disorder of mouse proNGF. *Proteins,* 75**,** 990-1009.

PAOLETTI, F., MALERBA, F., ERCOLE, B. B., LAMBA, D. & CATTANEO, A. 2015. A comparative analysis of the structural, functional and biological differences between Mouse and Human Nerve Growth Factor. *Biochim Biophys Acta,* 1854**,** 187-97.

PASTAR, I., STOJADINOVIC, O., YIN, N. C., RAMIREZ, H., NUSBAUM, A. G., SAWAYA, A., PATEL, S. B., KHALID, L., ISSEROFF, R. R. & TOMIC-CANIC, M. 2014a. Epithelialization in Wound Healing: A Comprehensive Review. *Adv Wound Care (New Rochelle).* 3**,** 445-464.

PAUS, R., LUFTL, M. & CZARNETZKI, B. M. 1994. Nerve growth factor modulates keratinocyte proliferation in murine skin organ culture. *Br J Dermatol,* 130**,** 174-80.

PENROSE, L. S. & OHARA, P. T. 1973. The development of the epidermal ridges. *J Med Genet,* 10**,** 201-8.

PETERS, E. M., HANSEN, M. G., OVERALL, R. W., NAKAMURA, M., PERTILE, P., KLAPP, B. F., ARCK, P. C. & PAUS, R. 2005. Control of human hair growth by neurotrophins: brain-derived neurotrophic factor inhibits hair shaft elongation, induces catagen, and stimulates follicular transforming growth factor beta2 expression. *J Invest Dermatol,* 124**,** 675-85.

PHILLIPS, C. J., HUMPHREYS, I., FLETCHER, J., HARDING, K., CHAMBERLAIN, G. & MACEY, S. 2016. Estimating the costs associated with the management of patients with chronic wounds using linked routine data. *Int Wound J,* 13**,** 1193-1197.

PHILPOTT, M. P., SANDERS, D., WESTGATE, G. E. & KEALEY, T. 1994. Human hair growth in vitro: a model for the study of hair follicle biology. *J Dermatol Sci,* 7 Suppl**,** S55-72.

PIELESZ, A., BINIAS, D., SARNA, E., BOBINSKI, R., KAWECKI, M., GLIK, J., KLAMA-BARYLA, A., KITALA, D., LABUS, W., PALUCH, J. & KRAUT, M. 2017. Active antioxidants in ex-vivo examination of burn wound healing by means of IR and Raman spectroscopies-Preliminary comparative research. *Spectrochim Acta A Mol Biomol Spectrosc,* 173**,** 924-930.

PINCELLI, C. & YAAR, M. 1997. Nerve growth factor: its significance in cutaneous biology. *J Investig Dermatol Symp Proc,* 2**,** 31-6.

PINCELLI, C., FANTINI, F. & GIANNETTI, A. 1994a. Nerve growth factor and the skin. *Int J Dermatol,* 33**,** 308-312.

PINCELLI, C., HAAKE, A. R., BENASSI, L., GRASSILLI, E., MAGNONI, C., OTTANI, D., POLAKOWSKA, R., FRANCESCHI, C. & GIANNETTI, A. 1997. Autocrine nerve growth factor protects human keratinocytes from apoptosis through its high affinity receptor (TRK): a role for BCL-2. *J Invest Dermatol,* 109**,** 757-64.

PINCELLI, C., SEVIGNANI, C., MANFREDINI, R., GRANDE, A., FANTINI, F., BRACCI-LAUDIERO, L., ALOE, L., FERRARI, S., COSSARIZZA, A. & GIANNETTI, A. 1994b. Expression and function of nerve growth factor and nerve growth factor receptor on cultured keratinocytes. *J Invest Dermatol,* 103**,** 13-8.

PLASSMANN, P. 1995. Measuring wounds. *J Wound Care,* 4**,** 269-72.

QING, C. 2017. The molecular biology in wound healing & non-healing wound. *Chin J Traumatol,* 20**,** 189-193.

RAFLA, K. & TREDGET, E. E. 2011. Infection control in the burn unit. *Burns,* 37**,** 5-15.

RAYCHAUDHURI, S. K. & RAYCHAUDHURI, S. P. 2010. Scid mouse model of psoriasis: a unique tool for drug development of autoreactive T-cell and th-17 cell-mediated autoimmune diseases. *Indian J Dermatol,* 55**,** 157-60.

RAYCHAUDHURI, S. P. & RAYCHAUDHURI, S. K. 2004. Role of NGF and neurogenic inflammation in the pathogenesis of psoriasis. *Prog Brain Res,* 146**,** 433-7.

RAYCHAUDHURI, S. P., SANYAL, M., WELTMAN, H. & KUNDU-RAYCHAUDHURI, S. 2004. K252a, a high-affinity nerve growth factor receptor blocker, improves psoriasis: an in vivo study using the severe combined immunodeficient mouse-human skin model. *J Invest Dermatol,* 122**,** 812-9.

REINKE, J. M. & SORG, H. 2012. Wound repair and regeneration. *Eur Surg Res,* 49**,** 35-43.

RIEGER, S., ZHAO, H., MARTIN, P., ABE, K. & LISSE, T. S. 2015. The role of nuclear hormone receptors in cutaneous wound repair. *Cell Biochem Funct,* 33**,** 1-13.

RITTIE, L., FARR, E. A., ORRINGER, J. S., VOORHEES, J. J. & FISHER, G. J. 2016. Reduced cell cohesiveness of outgrowths from eccrine sweat glands delays wound closure in elderly skin. *Aging Cell,* 15**,** 842-52.

ROBSON, M. C., STEED, D. L. & FRANZ, M. G. 2001. Wound healing: biologic features and approaches to maximize healing trajectories. *Curr Probl Surg,* 38**,** 72-140.

ROHRER, H., HEUMANN, R. & THOENEN, H. 1988. The synthesis of nerve growth factor (NGF) in developing skin is independent of innervation. *Dev Biol,* 128**,** 240-4.

RÖSSING, K., NOVAK, N., MOMMERT, S., PFAB, F., GEHRING, M., WEDI, B., KAPP, A. & RAAP, U. 2011. Brain-derived neurotrophic factor is increased in serum and skin levels of patients with chronic spontaneous urticaria. *Clinical & Experimental Allergy,* 41**,** 1392-1399.

ROTH, R. R. & JAMES, W. D. 1989. Microbiology of the skin: resident flora, ecology, infection. *J Am Acad Dermatol,* 20**,** 367-90.

ROWDEN, G., LEWIS, M. G., SHEIKH, K. M. & SUMMERLIN, W. T. 1975. Long-term organ culture of human skin: an ultrastructural and immunochemical study. *J Pathol,* 117**,** 139-49.

SAFFERLING, K., SUTTERLIN, T., WESTPHAL, K., ERNST, C., BREUHAHN, K., JAMES, M., JAGER, D., HALAMA, N. & GRABE, N. 2013. Wound healing revised: a novel reepithelialization mechanism revealed by *in vitro* and in silico models. *J Cell Biol,* 203**,** 691-709.

SAKPAL, T. V. 2010. Sample size estimation in clinical trial. *Perspect Clin Res,* 1**,** 67-9.

SALCIDO, R. S. 2017. Healing by Intention. *Advances in Skin & Wound Care,* 30**,** 246-247.

SAMAD, A., HAYES, S., FRENCH, L. & DODDS, S. 2002. Digital imaging versus conventional contact tracing for the objective measurement of venous leg ulcers. *Journal of Wound Care,* 11**,** 137-140.

SARIOLA, H. 2001. The neurotrophic factors in non-neuronal tissues. *Cell Mol Life Sci,* 58**,** 1061-6.

SARKANY, I., GRICE, K. & CARON, G. A. 1965. Organ Culture of Adult Human Skin. *Br J Dermatol,* 77**,** 65-76.

SCHENCK, K., SCHREURS, O., HAYASHI, K. & HELGELAND, K. 2017. The Role of Nerve Growth Factor (NGF) and Its Precursor Forms in Oral Wound Healing. *Int J Mol Sci,* 18.

SCHLEDERER, M., MUELLER, K. M., HAYBAECK, J., HEIDER, S., HUTTARY, N., ROSNER, M., HENGSTSCHLAGER, M., MORIGGL, R., DOLZNIG, H. & KENNER, L. 2014. Reliable quantification of protein expression and cellular localization in histological sections. *PLoS One,* 9**,** e100822.

SEATON, M., HOCKING, A. & GIBRAN, N. S. 2015. Porcine models of cutaneous wound healing. *ILAR J,* 56**,** 127-38.

SEGAL, R. A. 2003. Selectivity in neurotrophin signaling: theme and variations. *Annu Rev Neurosci,* 26**,** 299-330.

SEGAL, R. A. 2003. Selectivity in neurotrophin signaling: theme and variations. *Annu Rev Neurosci,* 26**,** 299-330.

SEN, C. K. & ROY, S. 2013. *Wound Healing*, Elsevier Inc.

SEN, C. K., GORDILLO, G. M., ROY, S., KIRSNER, R., LAMBERT, L., HUNT, T. K., GOTTRUP, F., GURTNER, G. C. & LONGAKER, M. T. 2009. Human skin wounds: a major and snowballing threat to public health and the economy. *Wound Repair Regen,* 17**,** 763-71.

SHEN, J. & YU, Q. 2015. Gambogic amide selectively upregulates TrkA expression and triggers its activation. *Pharmacol Rep,* 67**,** 217-23.

SHI, C. M., QU, J. F. & CHENG, T. M. 2003. Effects of the nerve growth factor on the survival and wound healing in mice with combined radiation and wound injury. *J Radiat Res,* 44**,** 223-8.

SHI, X., WANG, L., CLARK, J. D. & KINGERY, W. S. 2013. Keratinocytes express cytokines and nerve growth factor in response to neuropeptide activation of the ERK1/2 and JNK MAPK transcription pathways. *Regul Pept,* 186**,** 92-103.

SHIBAYAMA, E. & KOIZUMI, H. 1996. Cellular localization of the Trk neurotrophin receptor family in human non-neuronal tissues. *Am J Pathol,* 148**,** 1807-18.

SINGER, A. J. & CLARK, R. A. 1999. Cutaneous wound healing. *N Engl J Med,* 341**,** 738-46.

SINGH, S., YOUNG, A. & MCNAUGHT, C.-E. 2017. The physiology of wound healing. *Surgery (Oxford),* 35**,** 473-477.

SIVILIA, S., PARADISI, M., D'INTINO, G., FERNANDEZ, M., PIRONDI, S., LORENZINI, L. & CALZA, L. 2008. Skin homeostasis during inflammation: a role for nerve growth factor. *Histol Histopathol,* 23**,** 1-10.

SKAPER, S. D. 2017. Nerve growth factor: a neuroimmune crosstalk mediator for all seasons. *Immunology,* 151**,** 1-15.

SKOFF, A. M. & ADLER, J. E. 2006. Nerve growth factor regulates substance P in adult sensory neurons through both TrkA and p75 receptors. *Exp Neurol,* 197**,** 430-6.

SOFRONIEW, M. V., HOWE, C. L. & MOBLEY, W. C. 2001. Nerve growth factor signaling, neuroprotection, and neural repair. *Annu Rev Neurosci,* 24**,** 1217-81.

SOLOMON, A., ALOE, L., PE'ER, J., FRUCHT-PERY, J., BONINI, S., BONINI, S. & LEVI-SCHAFFER, F. 1998. Nerve growth factor is preformed in and activates human peripheral blood eosinophils. *J Allergy Clin Immunol,* 102**,** 454-60.

SOUTHARD, J. N. 2014. Protein analysis using real-time PCR instrumentation: incorporation in an integrated, inquiry-based project. *Biochem Mol Biol Educ,* 42**,** 142-51.

STAHLBERG, A., THOMSEN, C., RUFF, D. & AMAN, P. 2012. Quantitative PCR analysis of DNA, RNAs, and proteins in the same single cell. *Clin Chem,* 58**,** 1682-91.

STEINSTRAESSER, L., RITTIG, A., GEVERS, K., SORKIN, M., HIRSCH, T., KESTING, M., SAND, M., AL-BENNA, S., LANGER, S., STEINAU, H. U. & JACOBSEN, F. 2009. A human full-skin culture system for interventional studies. *Eplasty,* 9**,** e5.

STEPHENS, P., CALEY, M. & PEAKE, M. 2013. Alternative for animal wound model systems. *In:* GOURDIE, R. G. & MYERS, T. A. (eds.) *Wound Regeneration and Repair: Methods and Protocols.* Springer New York Heidelberg Dordrecht: Springer.

STOJADINOVIC, O. & TOMIC-CANIC, M. 2013. Human *ex vivo* wound healing model. *In:* GOURDIE, R. G. & MYERS, T. A. (eds.) *Wound Regeneration and Repair.* Springer New York Heidelberg Dordrecht London: Springer.

STUNOVA, A. & VISTEJNOVA, L. 2018. Dermal fibroblasts-A heterogeneous population with regulatory function in wound healing. *Cytokine Growth Factor Rev,* 39**,** 137-150.

TAYLOR, C. R. & LEVENSON, R. M. 2006. Quantification of immunohistochemistry--issues concerning methods, utility and semiquantitative assessment II. *Histopathology,* 49**,** 411-24.

TAYLOR, G., LEHRER, M. S., JENSEN, P. J., SUN, T. T. & LAVKER, R. M. 2000. Involvement of follicular stem cells in forming not only the follicle but also the epidermis. *Cell.,* 102**,** 451-61.

TENG, K. K. & HEMPSTEAD, B. L. 2004. Neurotrophins and their receptors: signaling trios in complex biological systems. *Cellular and Molecular Life Sciences,* 61**,** 35-48.

TERENGHI, G., MANN, D., KOPELMAN, P. G. & ANAND, P. 1997. trkA and trkC expression is increased in human diabetic skin. *Neurosci Lett,* 228**,** 33-6.

THEOHARIDES, T. C., ALYSANDRATOS, K. D., ANGELIDOU, A., DELIVANIS, D. A., SISMANOPOULOS, N., ZHANG, B., ASADI, S., VASIADI, M., WENG, Z., MINIATI, A. & KALOGEROMITROS, D. 2012. Mast cells and inflammation. *Biochim Biophys Acta,* 1822**,** 21-33.

THULABANDU, V., CHEN, D. & ATIT, R. P. 2018. Dermal fibroblast in cutaneous development and healing. *Wiley Interdiscip Rev Dev Biol,* 7.

TOMIC-CANIC, M., MAMBER, S. W., STOJADINOVIC, O., LEE, B., RADOJA, N. & MCMICHAEL, J. 2007. Streptolysin O enhances keratinocyte migration and proliferation and promotes skin organ culture wound healing *in vitro*. *Wound Repair Regen,* 15**,** 71-9.

TRUZZI, F., MARCONI, A. & PINCELLI, C. 2011. Neurotrophins in healthy and diseased skin. *Dermatoendocrinol,* 3**,** 32-6.

TUVERI, M., GENERINI, S., MATUCCI-CERINIC, M. & ALOE, L. 2000. NGF, a useful tool in the treatment of chronic vasculitic ulcers in rheumatoid arthritis. *Lancet,* 356**,** 1739-40.

TÜZÜN, Y., WOLF, R., ENGIN, B., KEÇICI, A. S. & KUTLUBAY, Z. 2015. Bacterial infections of the folds (intertriginous areas). *Clinics in Dermatology,* 33**,** 420-428.

UD-DIN, S. & BAYAT, A. 2017. Non-animal models of wound healing in cutaneous repair: In silico, *in vitro*, *ex vivo*, and *in vivo* models of wounds and scars in human skin. *Wound Repair Regen,* 25**,** 164-176.

UECK, C., VOLKSDORF, T., HOUDEK, P., VIDAL, Y. S. S., SEHNER, S., ELLINGER, B., LOBMANN, R., LARENA-AVELLANEDA, A., REINSHAGEN, K., RIDDERBUSCH, I., KOHRMEYER, K., MOLL, I., DANIELS, R., WERNER, P., MERFORT, I. & BRANDNER, J. M. 2017. Comparison of In-Vitro and Ex-Vivo Wound Healing Assays for the Investigation of Diabetic Wound Healing and Demonstration of a Beneficial Effect of a Triterpene Extract. *PLoS One,* 12**,** e0169028.

VAN WEEMEN, B. K. & SCHUURS, A. H. 1971. Immunoassay using antigen-enzyme conjugates. *FEBS Lett,* 15**,** 232-236.

VARANI, J. 2012. Human skin organ culture for assessment of chemically induced skin damage. *Expert Rev Dermatol,* 7**,** 295-303.

WALKER, R. A. 2006. Quantification of immunohistochemistry--issues concerning methods, utility and semiquantitative assessment I. *Histopathology,* 49**,** 406-10.

WALLACE, H. A. & BHIMJI, S. S. 2018. Wound Healing Phases. *StatPearls.* Treasure Island (FL): StatPearls Publishing and Demonstration of a Beneficial Effect of a Triterpene Extract. *PLoS One,* 12**,** e0169028.

ULLRICH, A., GRAY, A., BERMAN, C. & DULL, T. J. 1983. Human

WANG, P. H., HUANG, B. S., HORNG, H. C., YEH, C. C. & CHEN, Y. J. 2018. Wound healing. *J Chin Med Assoc,* 81**,** 94-101.

WANG, Y., GUTIERREZ-HERRERA, E., ORTEGA-MARTINEZ, A., ANDERSON, R. R. & FRANCO, W. 2016. UV fluorescence excitation imaging of healing of wounds in skin: Evaluation of wound closure in organ culture model. *Lasers Surg Med,* 48**,** 678-85.

WEHRENS, K. M., ARNOLDUSSEN, C. W., BOOI, D. I. & VAN DER HULST, R. R. 2016. Clinical Evaluation of Wound Healing in Split-Skin Graft Donor Sites Using

Microscopic Quantification of Reepithelialization. *Adv Skin Wound Care,* 29**,** 254-60.
WERTZ, P. 2018. Epidermal Lamellar Granules. *Skin Pharmacol Physiol,* 31**,** 262-268.
WIESMANN, C. & DE VOS, A. M. 2001. Nerve growth factor: structure and function. *Cell Mol Life Sci,* 58**,** 748-59.
WIESMANN, C., ULTSCH, M. H., BASS, S. H. & DE VOS, A. M. 1999. Crystal structure of nerve growth factor in complex with the ligand-binding domain of the TrkA receptor. *Nature,* 401**,** 184-8.
WONG, V. W., SORKIN, M., GLOTZBACH, J. P., LONGAKER, M. T. & GURTNER, G. C. 2011. Surgical approaches to create murine models of human wound healing. *J Biomed Biotechnol,* 2011**,** 969618.
WU, D., RYU, J. C., CHUNG, Y. W., LEE, D., RYU, J. H., YOON, J. H. & YOON, J. 2017. A Far-Red-Emitting Fluorescence Probe for Sensitive and Selective Detection of Peroxynitrite in Live Cells and Tissues. *Anal Chem,* 89**,** 10924-10931.
XIA, W., FAN, J., ZHANG, L., WANG, J., DU, J. & PENG, X. 2018. Imaging dichromate in living cells with a fluorescence probe. *Journal of Photochemistry and Photobiology A: Chemistry,* 355**,** 165-174.
XIE, Y., RIZZI, S. C., DAWSON, R., LYNAM, E., RICHARDS, S., LEAVESLEY, D. I. & UPTON, Z. 2010. Development of a Three-Dimensional Human Skin Equivalent Wound Model for Investigating Novel Wound Healing Therapies. *Tissue Engineering Part C-Methods,* 16**,** 1111-1123.
XU, W., JONG HONG, S., JIA, S., ZHAO, Y., GALIANO, R. D. & MUSTOE, T. A. 2012. Application of a partial-thickness human *ex vivo* skin culture model in cutaneous wound healing study. *Lab Invest,* 92**,** 584-99.
YAAR, M., GROSSMAN, K., ELLER, M. & GILCHREST, B. A. 1991. Evidence for nerve growth factor-mediated paracrine effects in human epidermis. *J Cell Biol,* 115**,** 821-8.
YAGI, M. & YONEI, Y. 2018. Glycative stress and anti-aging: 7. Glycative stress and skin aging. *Glycative Stress Research,* 5**,** 50-54.
YAMAGUCHI, Y. & YOSHIKAWA, K. 2001. Cutaneous wound healing: an update. *J Dermatol,* 28**,** 521-34.
YANG, B., SUWANPRADID, J., SANCHEZ-LAGUNES, R., CHOI, H. W., HOANG, P., WANG, D., ABRAHAM, S. N. & MACLEOD, A. S. 2017. IL-27 Facilitates Skin Wound Healing through Induction of Epidermal Proliferation and Host Defense. *J Invest Dermatol,* 137**,** 1166-1175.
YILDIRIMER, L., HOBSON, D., LIN, Z. Y., CUI, W. & ZHAO, X. 2017. Tissue-Engineered Human Skin Equivalents and Their Applications in Wound Healing. *In:* HASSAN, A. (ed.) *Tissue Engineering for Artificial Organs.* Germany: WILEY-VCH Verlag GmbH & Co.
YOON, S. O., CASACCIA-BONNEFIL, P., CARTER, B. & CHAO, M. V. 1998. Competitive signaling between TrkA and p75 nerve growth factor receptors determines cell survival. *Journal of Neuroscience,* 18**,** 3273-3281.
YOON, D. J., FREGOSO, D. R., NGUYEN, D., CHEN, V., STRBO, N., FUENTES, J. J., TOMIC-CANIC, M., CRAWFORD, R., PASTAR, I. & ISSEROFF, R. R. 2019. A tractable, simplified ex vivo human skin model of wound infection. *Wound Repair Regen*.

YOSHII, A. & CONSTANTINE-PATON, M. 2010. Postsynaptic BDNF-TrkB signaling in synapse maturation, plasticity, and disease. *Dev Neurobiol,* 70**,** 304-22.

YOUSEF, H. & SHARMA, S. 2018. Anatomy, Skin (Integument), Epidermis. *StatPearls.* Treasure Island (FL): StatPearls Publishing

ZACCARO, M. C., IVANISEVIC, L., PEREZ, P., MEAKIN, S. O. & SARAGOVI, H. U. 2001. p75 Co-receptors regulate ligand-dependent and ligand-independent Trk receptor activation, in part by altering Trk docking subdomains. *J Biol Chem,* 276**,** 31023-9.

ZHANG, M., ZHANG, Y., DING, J., LI, X., ZANG, C., YIN, S., MA, J., WANG, Y. & CAO, Y. 2018. The role of TrkA in the promoting wounding-healing effect of CD271 on epidermal stem cells. *Arch Dermatol Res*.

APPENDIX 1

Wound Repair and Regeneration

TECHNICAL ARTICLE

Fluorescent cell tracer dye permits real-time assessment of re-epithelialization in a serum-free ex vivo human skin wound assay

Nur Azida Mohd Nasir, MSc[1,2]; Ralf Paus, MD, FRSB[1,3,4]; David M. Ansell, PhD[1,5]

1. Centre for Dermatology Research, School of Biological Sciences, The University of Manchester, Manchester, United Kingdom,
2. School of Medical Sciences, Universiti Sains Malaysia, Kubang Kerian, Malaysia,
3. NIHR Manchester Biomedical Research Centre, The University of Manchester, Manchester, United Kingdom,
4. Manchester Academic Health Sciences Centre, The University of Manchester, Manchester, United Kingdom, and
5. Division of Cell Matrix Biology and Regenerative Medicine, The University of Manchester, Manchester, United Kingdom

Reprint requests:
Dr. D. M. Ansell, Centre for Dermatology Research, School of Biological Sciences, The University of Manchester, Manchester M13 9PT, United Kingdom.
Tel: 0044 0161 275 1684;
Email: david.ansell@manchester.ac.uk

Manuscript received: January 18, 2018
Accepted in final form: November 10, 2018

DOI:10.1111/wrr.12688

ABSTRACT

Ex vivo wounded human skin organ culture is an invaluable tool for translationally relevant preclinical wound healing research. However, studies incorporating this system are still underutilized within the field because of the low throughput of histological analysis required for downstream assessment. In this study, we use intravital fluorescent dye to lineage trace epidermal cells, demonstrating that wound re-epithelialization of human ex vivo wounds occurs consistent with an extending shield mechanism of collective migration. Moreover, we also report a relatively simple method to investigate global epithelial closure of explants in culture using daily fluorescent dye treatment and en face imaging. This study is the first to quantify healing of ex vivo wounds in a longitudinal manner, providing global assessments for re-epithelialization and tissue contraction. We show that this approach can identify alterations to healing with a known healing promoter. This methodological study highlights the utility of human ex vivo wounds in enhancing our understanding of mechanisms of human skin repair and in evaluating novel therapies to improve healing outcome.

Experimentally wounded human skin organ culture has proven to be an invaluable tool for translationally relevant preclinical research for the past 20 years.[1] Many different groups have now developed similar approaches to understand basic mechanisms of human wound healing and for identifying novel candidate wound healing promoters.[2–8] In addition, assays using porcine skin ex vivo have been established[9–11] because of its anatomical similarity and strong concordance with human healing.[12] Reconstituted skin cultures (also known as organotypic or skin equivalent cultures), which comprise keratinocytes seeded onto a fibroblast-containing collagen gel, are also available to model human wounds.[13–15] Both skin explant and skin equivalent approaches display epithelial migration across the underlying matrix to heal the wound, although ex vivo skin is thought to mimic the in vivo situation more closely.[16,17] Injury to artificial skin equivalent cultures initiates collective cell migration and wounds re-epithelialize through the formation of an extending shield,[14] although resolving whether this same mechanism is conserved in the much more complex environment found in human skin is yet to be addressed.

The accurate measurement of wound re-epithelialization in 3D experimental models has proved challenging as a result of high workload required to serially section the entire tissue, which is essential to ensure that the center of each wound is assessed. In addition, standard histology only provides a snapshot through the wound, and so, it is unclear how consistent the evaluated region might be to other areas within the wound.

Macroscopic assessment of wound closure forms the primary assessment for progression of healing in chronic wounds, given that biopsies may further jeopardize healing.[18] Thus, current ex vivo models typically examine wound healing in an entirely different plane to "real-life" observations made in the clinic.

Several recent studies have reported imaging the surface of ex vivo and organotypic wound cultures, using a range of different methods, which exploit differing spectroscopic properties of the various wound cell types. These include the use of infra-red and Raman spectroscopy,[19] measuring ultraviolet (UV) auto-fluorescence,[8] magnetic resonance imaging,[20] and revealing wound topography using fringe projection.[21] In addition, the recent article in *Wound Repair and Regeneration* by Glinos et al.[22] describes optical coherence tomography (OCT) as a method to differentiate newly formed epithelial tissue from open wound in human wounds ex vivo and provides the highest clarity of imaging reported thus far.

In our recent experiments, we have established a serum-free ex vivo human partial thickness wound model (see Methods for full details). We have been examining the green

Wound Rep Reg (2019) 27 126–133 © 2018 by the Wound Healing Society

fluorescent cell tracker dye 5-chloromethylfluorescein diacetate (CMFDA), which is taken up by viable cells in culture,[14] permitting lineage tracing experiments to understand the wound re-epithelialization process in human skin. Moreover, dye uptake can also be visualized under an upright fluorescent microscope,[23] and using this simple approach, we have optimized a method to produce a high clarity of wound imaging, approaching cellular levels of resolution. We have for the first time been able to track daily wound re-epithelialization changes of individual human wounds ex vivo over 6 days. Our study provides a simple assay that can evaluate drug responses in human wounds ex vivo, where the study of healing progression can be made longitudinally.

METHODS

Human skin was obtained with informed written consent from female donors undergoing elective abdominal surgery conducted at the University of Manchester following institutional ethical review.

Subcutaneous fat was removed, and 6-mm-diameter full-thickness skin biopsies were taken, containing a 2-mm diameter partial thickness wound, removing the epidermis and papillary dermis (Figure 1A). Any explants displaying an inconsistent size or depth of wound were excluded prior to culture. Explants were cultured at an air–liquid interface by placing each explant in a six well plate upon two absorbent pads (Millipore, Watford, UK) and a 0.45 μM nylon membrane (Millipore, Watford, UK) (Figure 1B). Two milliliter of William's E media (Life Technologies, Birchwood) supplemented with 1% penicillin/streptomycin, 2 mM L-Glutamine, 10 μg/mL insulin, and 10 ng/mL hydrocortisone (all supplements from Sigma-Aldrich, Gillingham, UK) was added to each well. Positive control explants were cultured with 10% fetal bovine serum (FBS; Life technologies, Birchwood, UK) supplemented to the media. Cultures were grown at 37 °C with 5% CO_2. Each day excess media was removed from the well and replaced with 1 mL fresh media.

Four microliters of 25 μM CMFDA (or CMTPX) (ThermoFisher Scientific, Loughborough, UK) was added to the wound surface for 30 minutes, then washed dropwise with phosphate buffered saline. For cell viability studies, 1 μg/mL of propidium iodide (PI) was cotreated alongside CMFDA. Planimetric imaging was conducted using a Leica M205 FA upright Stereomicroscope using a 5x/0.50 pLANapo LWD objective at the equivalent of 64x magnification and captured using a DFC 565FX (Leica, Wetzlar, Germany) camera through LAS AF v3.1.0.8587 software (Leica, Wetzlar, Germany). Specific band-pass filter set for green fluorescent protein was used. (Leica, Wetzlar, Germany) (Figure 1C).

For wound closure experiments fluorescent imaging with CMFDA was conducted daily. Fluorescent images were assessed using Image J (Fiji) for the area of the initial wound at day 0 (IW_0). On subsequent days (where day is denoted by n), the area of initial wound (IW_n) and the area of open wound remaining (OW_n) were measured (see Supporting Information Figure S1A). Epithelial wound closure was calculated from measurements of area of initial wound, and the open wound remaining and expressed either as the % of wound closure on each day or on the area of healing achieved on each day in square millimeter. Percentage closure = $100 - (OW_n/IW_0 \times 100)$. Area healed = $IW_0 - OW_n$. Tissue contraction was calculated by assessing changes to the initial wound defect over the wound healing period. Tissue contraction = $100 - (IW_n/IW_0 \times 100)$.

In addition, the neo-epidermis was further assessed by measuring the area of the dim band of epidermal tissue toward the migrating front and the remaining brighter area (Supporting Information Figure S1A). Tissue from five individual donors was used, with three to four explants per donor used for each treatment. The mean value of the three to four replicate explants per donor used for analysis (i.e., assessed as $n = 5$ replicate experiments from separate donors). A two-way analysis of variance (ANOVA) with repeated measures was used to analyze percentage wound closure, area healed, and contraction between FBS and control groups, over the 6 days in culture. This analysis allowed for a statistical evaluation of differences in healing as a result of timepoint or treatment group. In addition, the interaction between the two processes determined whether the evolution of healing response over time differed between treatment groups. Our analysis makes the assumption that our data are normally distributed.

Comparisons of % closure at an individual timepoint (day 2 or day 4) was assessed via a paired t test (GraphPad Prism 7.0, San Diego, CA). For all tests $p < 0.05$ was considered significant.

For histological imaging, tissue was formalin fixed for 24 hours and processed for paraffin wax embedding. Five micrometer sections were cleared with Xylene and rehydrated to water, then either stained with 4′,6-diamidino-2-phenylindole (DAPI; Fluorescence microscopy) or hemotoxylin & eosin (H&E; brightfield). Immuno-labeling with anti-keratin 1 (Abcam Cambridge, UK; Ab81623), anti-involucrin (Abcam; Ab53112), anti-occludin (Abcam; 168,986), and anti-loricrin (Abcam; Ab85679) antitobodies was performed at 1:1000 (keratin 1, loricrin, involucrin) or 1:250 (occludin) dilution overnight at 4 °C following heat-mediated retrieval with 10 mM sodium citrate, pH 6.0, and blocking with 10% goat serum for 30 minutes. Localization was visualized with Alexa-Fluor594 tagged goat anti-mouse (keratin 1) or goat anti-rabbit (occludin, involucrin, and loricrin) secondary antibody (Life Technologies), with DAPI counterstaining. Images of stained sections were captured using a BZ-9000 microscope (Keyence, Osaka, Japan).

RESULTS

Vital dyes label epithelial cells within wounds and reveal cellular migration patterns during repair

To examine cell tracker dye uptake within human ex vivo wounds in situ, we first conducted histology to validate our approach, using wounds treated topically at day 0 with the green live cell tracker dye CMFDA. In addition, given CMFDA should only mark viable cells, the membrane impermeable nuclear dye PI was cotreated to identify any cells with damaged plasma membranes. Our data showed that only epithelial cells around the edge of the wound were labeled (Figure 2A). We observed some PI positive nuclei directly at the injury site, which did not express CMFDA. A band of CMFDA labeled both basal and suprabasal epidermal cells adjacent to the wound, extending several cells away from the injury site. When these treated wounds were

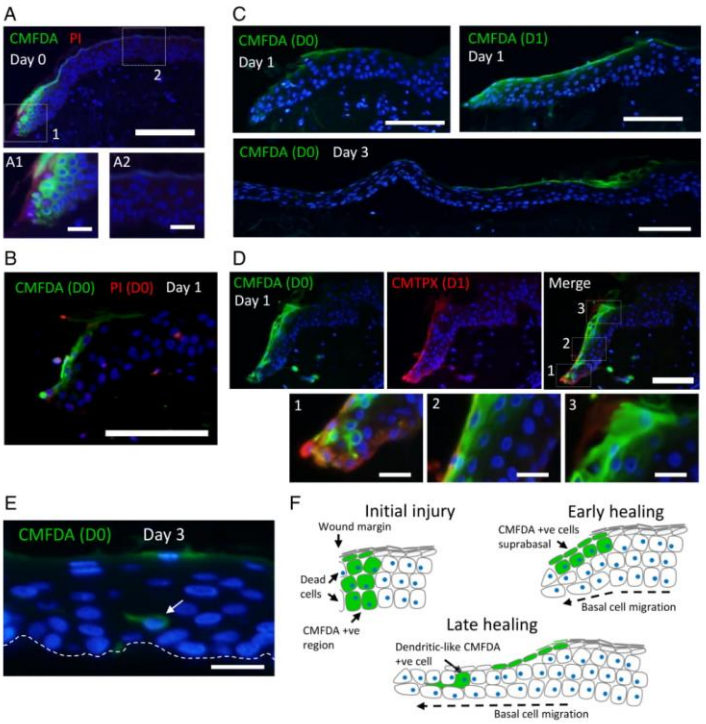

Figure 2. Epithelial repair of human ex vivo wounds progresses via an extending shield mechanism. Human ex vivo wounds were cultured in the presence of the fluorescent dyes. CMFDA and PI cotreatment at time of injury (D0) identifies live (CMFDA; green) and dead (PI; red) cells around the injury site (A), and these wounds traced to day 1 indicate PI-labeled cells are no longer present (B). CMFDA was treated at different times to examine how epithelial cells migrate, indicating that basal cells labeled on day 0 become progressively suprabasal. Treating with CMFDA on day 0 and on day 1 (inset 1) with the red cell tracker CMTPX reveals previously unlabeled cells at the epidermal tip (C). Labeled cells with a dendritic morphology were occasionally found in the neo-epidermis at later timepoints (E). Our data suggest an extending shield mechanism of repair whereby basal cells migrate from the surrounding epidermis (F). Bar =100 μm (A–D), 20 μm (E and inset images). Dotted line denotes basement membrane.

of these wounds in culture is not obvious using conventional brightfield microscope (Supporting Information Figure S1B).

Using daily CMFDA treatments, we conducted en face imaging to monitor wound closure within individual wounds over 6 days (Figure 3C). Moreover, we compared our standard serum-free explants (Control; CTL) to those cultured in the presence of 10% FBS, to determine whether significantly accelerated repair could be correctly detected in our model.[3]

Our data not only show that epithelial healing can be monitored daily intra-vitally but also revealed a clear divergence in the evolution of repair with the addition of FBS (i.e., the interaction between time and treatment factors), when we evaluated the % epithelial closure (Figure 3D) or the area of healed epidermis (Figure 3E). Measuring the explants each day also revealed that some wound contraction occurs over time (Figure 3F). However, this only accounted for around 20% of total healing observed, indicating that re-epithelialization provides the major healing mechanism. The level of contraction between control and FBS-treated wounds was unchanged (Figure 3F).

The rate of healing between individual donors was variable; although a response to FBS was reproducible and detected significant differences to healing at individual timepoints, confirming the reliability of the model (Figure 3G).

Regions of newly laid and more mature epidermis can be determined

Our daily imaging identified distinct areas of epidermal healing with a band of dim CMFDA expression toward the

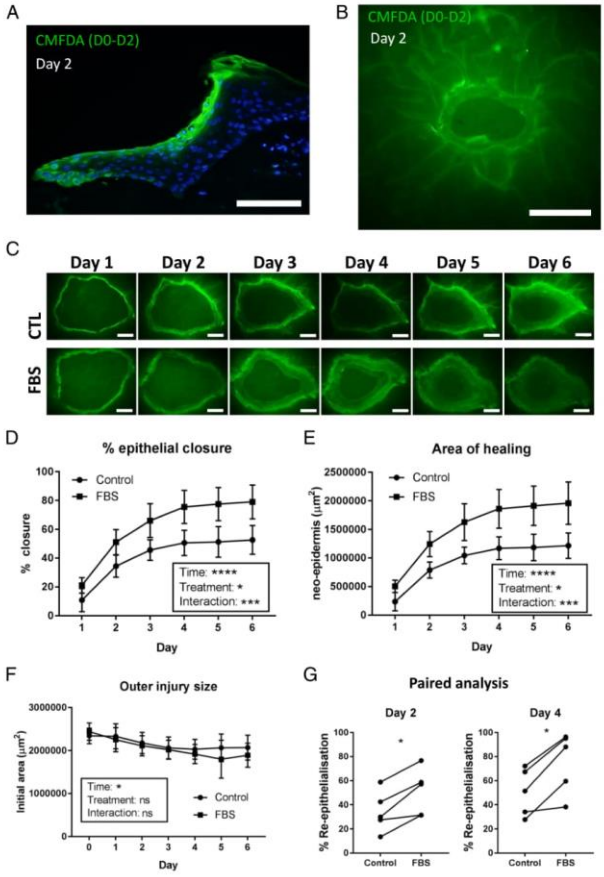

Figure 3. Daily en face fluorescent imaging longitudinally assesses epithelial healing. Daily treatments of human ex vivo wounds with CMFDA labeled the entire length of neo-epidermis (A), which could also be visualized in en face images using an upright fluorescent microscope (B). Wounds cultured with 10% FBS compared to standard media control arm were examined with daily en face imaging to track epithelial formation over time (C). Quantification revealed a significant acceleration with FBS in the % epithelial closure (D) and the area of neo-epidermis (E). Slight contraction was observed of the wounds in culture, although there was no difference between FBS or control wounds (F). Paired analysis demonstrates the variability in healing between donors, but that the FBS response is reproducible (G). Data in D–F were analyzed using two-way ANOVA with repeated measures, while G used a paired *t* test. Graphs show mean ± SEM in D–F and in G the mean of each individual donor (n = 5 donors). *$p < 0.05$, ***$p < 0.001$, ****$p < 0.0001$. Bar = 1 mm (A), 100 µm (B), and 500 µm (C). [Color figure can be viewed at wileyonlinelibrary.com]

epidermal front, with brighter areas nearer to the margin (Figure 4A). As the CMFDA dye accumulates over time with our daily dosing regimen, and based on our observations with CMFDA and CMPTX dual labeling (Figure 2), we hypothesized that bright regions indicated cells that had been labeled early (and probably several times), while dim areas likely reflected newly laid tissue that was not labeled until a late timepoint. We therefore wondered if these areas could define cornified and noncornified regions of the healing epidermis, as recently described to occur in human

continuous expression of keratin 1 within the suprabasal layer, indicating that early differentiation had already completed by this point. We also stained wounds for later stages of epithelial differentiation. Involucrin or occludin was absent from the tip of healing, but again present in both dim and bright regions, although often looked less well-organized in the dim region (Figure 4D). The cornified envelope marker loricrin was never found in dim regions but was sometimes detected toward the boundary of the bright region (Figure 4D). Collectively these data indicate that the brighter region reflected a more organized epidermis.

We quantified these dim and bright regions in our serum-free and 10% FBS-treated explants, where we find that the dim and bright regions are both significantly altered by time, although we find no statistically significant change between the treatments (Figure 4E).

DISCUSSION

Our data and other recent studies[8,22] highlight the major advantage of ex vivo models incorporating partial thickness wounds, where complete re-epithelialization across the underlying dermal matrix can now be studied in real-time in situ. Our data show that noninvasive fluorescent imaging can be employed to longitudinally examine ex vivo wounds for several healing parameters (tissue contraction, re-epithelialization, and epidermal maturation). This may be particularly important for revealing where an intervention alters only some aspects of repair. Our approach may enable researchers to quickly identify which timepoints or healing processes would be most instructive for a subsequent more in depth assessment. Furthermore, given the variable level of healing between donors, it may be possible to use vital dyes to monitor healing progression of cultures. For example, instead of assessing on a particular day, researchers can harvest tissue once the desired level of repair has occurred. Examining wounds once the control group shows 50% healing would ensure that both positive or negative drug effects to the rate of healing can be quantified. It warrants further investigation to determine whether CMFDA en face imaging could be applied to other translational wound healing models such as porcine ex vivo skin wounds or wound organotypic human skin constructs.

While our study has utilized CMFDA and CMTPX, there are several other vital dyes that could be employed for labeling cells within the neo-epidermis.[23–28] Moreover, by combining fluorescent dyes of different wavelengths, we demonstrate that the possibility exists to follow cell migration patterns during ex vivo healing. Our data using cell tracing suggest that re-epithelialization occurs using the extending shield mechanism previously reported for organotypic wounds.[14] This is important as skin equivalent models are highly simplified and it is unclear how well they replicate human in vivo wounds.[16] Our data do reveal that a few rare cells labeled on day 0 can persist within the neo-epidermis at late stages of repair. The exact origin of these cells is unclear given that our CMFDA treatment on day 0 will also label cells within the dermis. However, the dendritic morphology suggests that they are unlikely to be keratinocytes, which alongside fibroblasts are the only two cell types typically found in artificial skin constructs.

One important conclusion of the recent Glinos *et al*. study is that experimental (i.e., circular) wounds often show different rates of healing within different areas of the same wound, a phenomenon that is unappreciated because of the use of histology in examining ex vivo repair. We also frequently observe irregular healing in different regions of a single wound (Figure 4A), with areas displaying especially pronounced centripetal migration (Figure 4A inset). However, at this stage, we are not able to pinpoint the factors that are most critical for this. This finding is particularly important as histology of some wounds might achieve an entirely different result depending upon the plane of sectioning, further advocating en face imaging techniques in future studies.

Despite this, histology remains an essential tool for researchers in this field to understand what is happening below the wound surface or investigating wound responses such as proliferation or activation of target genes. However, combining a noninvasive assessment for global wound closure followed by end-point histology will maximize data obtained. Advanced imaging techniques constitute an exciting methodological advance in wound healing research, particularly OCT which holds the prospect of being directly applied to investigate patient wounds.[29,30] While OCT currently remains prohibitively expensive for most ex vivo studies, CMFDA or other approaches like UV auto-fluorescence[8] may be a valid alternative as suitable equipment will be more readily available. The persistence of CMFDA within histological specimens may be especially instructive to pinpoint the wound margins, which may further aid histological assessment. In conclusion, by using a simple dye based approach we have been able to lineage trace epidermal cells and conduct an accurate intravital examination during wound re-epithelialization of human skin. This current study highlights the utility of ex vivo human skin assays, which have been frequently neglected in favor of less physiological skin equivalent cultures.

ACKNOWLEDGMENTS

Authors thank Dr Steven Marsden and staff at the Bioimaging facility for technical support, Mr Peter Walker and staff at the Histology facility for providing access to equipment, and Dr Jack Wilkinson, Centre for Biostatistics, for assistance with statistical analysis. Authors gratefully acknowledge the donors, surgeons, and Manchester Skin Health Biobank, without whom this study would not have been possible.

Source of Funding: Funding for the study was provided via a studentship to NAMN from Universiti Sains Malaysia and The Ministry of Higher Education, Malaysia. The microscopes used in this study were purchased via grants from BBSRC, Wellcome Trust, and the University of Manchester Strategic Fund.

Conflicts of Interest: Authors declare no conflict of interest.

REFERENCES

1. Kratz G. Modeling of wound healing processes in human skin using tissue culture. *Microsc Res Tech* 1998; 42: 345–50.
2. Meier NT, Haslam IS, Pattwell DM, Zhang GY, Emelianov V, Paredes R, et al. Thyrotropin-releasing hormone (TRH) promotes wound re-epithelialisation in frog and human skin. *PLoS*

One 2013; 8: e73596. https://doi.org/10.1371/journal.pone.0073596.
3. Pastar I, Stojadinovic O, Yin NC, Ramirez H, Nusbaum AG, Sawaya A, et al. Epithelialization in wound healing: a comprehensive review. *Adv Wound Care (New Rochelle)* 2014; 3: 445–64.
4. Mendoza-Garcia J, Sebastian A, Alonso-Rasgado T, Bayat A. Optimization of an *ex vivo* wound healing model in the adult human skin: functional evaluation using photodynamic therapy. *Wound Repair Regen* 2015; 23: 685–702. https://doi.org/10.1111/wrr.12325.
5. Jozic I, Vukelic S, Stojadinovic O, Liang L, Ramirez HA, Pastar I, et al. Stress signals, mediated by membranous glucocorticoid receptor, activate PLC/PKC/GSK-3β/β-catenin pathway to inhibit wound closure. *J Invest Dermatol* 2017; 137: 1144–54.
6. Sivamani RK, Pullar CE, Manabat-Hidalgo CG, Rocke DM, Carlsen RC, Greenhalgh DG, et al. Stress-mediated increases in systemic and local epinephrine impair skin wound healing: potential new indication for Beta blockers. *PLoS Med* 2009; 6: e1000012.
7. Tomic-Canic M, Mamber SW, Stojadinovic O, Lee B, Radoja N, McMichael J. Streptolysin O enhances keratinocyte migration and proliferation and promotes skin organ culture wound healing in vitro. *Wound Repair Regen* 2007; 15: 71–9.
8. Wang Y, Gutierrez-Herrera E, Ortega-Martinez A, Anderson RR, Franco W. UV fluorescence excitation imaging of healing of wounds in skin: evaluation of wound closure in organ culture model. *Lasers Surg Med* 2016; 48: 678–85.
9. Ueck C, Volksdorf T, Houdek P, Vidal YSS, Sehner S, Ellinger B, et al. Comparison of in-vitro and ex-vivo wound healing assays for the investigation of diabetic wound healing and demonstration of a beneficial effect of a Triterpene extract. *PLoS One* 2017; 12: e0169028.
10. Yeung CC, Holmes DF, Thomason HA, Stephenson C, Derby B, Hardman MJ. An *ex vivo* porcine skin model to evaluate pressure-reducing devices of different mechanical properties used for pressure ulcer prevention. *Wound Repair Regen* 2016; 24: 1089–96.
11. Yang QP, Larose C, Della Porta AC, Schultz GS, Gibson DJ. A surfactant-based wound dressing can reduce bacterial biofilms in a porcine skin explant model. *Int Wound J* 2017; 14: 408–13.
12. Sullivan TP, Eaglstein WH, Davis SC, Mertz P. The pig as a model for human wound healing. *Wound Repair Regen* 2001; 9: 66–76.
13. Garlick JA, Taichman LB. Fate of human keratinocytes during reepithelialization in an organotypic culture model. *Lab Invest* 1994; 70: 916–24.
14. Safferling K, Sutterlin T, Westphal K, Ernst C, Breuhahn K, James M, et al. Wound healing revised: a novel reepithelialization mechanism revealed by in vitro and in silico models. *J Cell Biol* 2013; 203: 691–709.
15. Egles C, Garlick JA, Shamis Y. Three-dimensional human tissue models of wounded skin. *Methods Mol Biol* 2010; 585: 345–59.
16. Xu W, Jong Hong S, Jia S, Zhao Y, Galiano RD, Mustoe TA. Application of a partial-thickness human *ex vivo* skin culture model in cutaneous wound healing study. *Lab Invest* 2012; 92: 584–99.
17. Andrade TA, Aguiar AF, Guedes FA, Leite MN, Caetano GF, Coelho EB, et al. *Ex vivo* model of human skin (hOSEC) as alternative to animal use for cosmetic tests. *Proc Eng* 2015; 110: 67–73.
18. Eming SA, Martin P, Tomic-Canic M. Wound repair and regeneration: mechanisms, signaling, and translation. *Sci Transl Med* 2014; 6: 265sr6.
19. Pielesz A, Binias D, Sarna E, Bobinski R, Kawecki M, Glik J, et al. Active antioxidants in ex-vivo examination of burn wound healing by means of IR and Raman spectroscopies-preliminary comparative research. *Spectrochim Acta A Mol Biomol Spectrosc* 2017; 173: 924–30.
20. Lone AG, Atci E, Renslow R, Beyenal H, Noh S, Fransson B, et al. *Staphylococcus aureus* induces hypoxia and cellular damage in porcine dermal explants. *Infect Immun* 2015; 83: 2531–41.
21. Ferraq Y, Black D, Lagarde JM, Schmitt AM, Dahan S, Grolleau JL, et al. Use of a 3-D imaging technique for non-invasive monitoring of the depth of experimentally induced wounds. *Skin Res Technol* 2007; 13: 399–405.
22. Glinos GD, Verne SH, Aldahan AS, Liang L, Nouri K, Elliot S, et al. Optical coherence tomography for assessment of epithelialization in a human *Ex vivo* wound model. *Wound Repair Regen* 2017; 13: 12600.
23. Lu H, Rollman O. Fluorescence imaging of reepithelialization from skin explant cultures on acellular dermis. *Wound Repair Regen* 2004; 12: 575–86.
24. Beem E, Segal MS. Evaluation of stability and sensitivity of cell fluorescent labels when used for cell migration. *J Fluoresc* 2013; 23: 975–87.
25. Chao A, Jiang N, Yang Y, Li HY, Sun HZ. A Ni-NTA-based red fluorescence probe for protein labelling in live cells. *J Mater Chem B* 2017; 5: 1166–73.
26. Johnson I. Fluorescent probes for living cells. *Histochem J* 1998; 30: 123–40.
27. Wu D, Ryu JC, Chung YW, Lee D, Ryu JH, Yoon JH, et al. A far-red-emitting fluorescence probe for sensitive and selective detection of peroxynitrite in live cells and tissues. *Anal Chem* 2017; 89: 10924–31.
28. Xia W, Fan J, Zhang L, Wang J, Du J, Peng X. Imaging dichromate in living cells with a fluorescence probe. *J Photochem Photobiol A Chem* 2018; 355: 165–74.
29. Deegan AJ, Wang W, Men S, Li Y, Song S, Xu J, et al. Optical coherence tomography angiography monitors human cutaneous wound healing over time. *Quant Imaging Med Surg* 2018; 8: 135–50.
30. Greaves NS, Benatar B, Whiteside S, Alonso-Rasgado T, Baguneid M, Bayat A. Optical coherence tomography: a reliable alternative to invasive histological assessment of acute wound healing in human skin? *Br J Dermatol* 2014; 170: 840–50.

SUPPORTING INFORMATION

Additional supporting information may be found online in the Supporting Information section at the end of the article.

Figure S1. CMFDA imaging en face highlights different regions of wounds. CMFDA images show distinctive features which were assessed (A). The area of the initial wound (uninterupted white line), the area of the open wound (white dotted line) and regions of dimly fluorescent (i.e. newly laid unstratified epidermis) and bright areas of epidermis can be delineated (white dashed line). Using brightfield microscopy the outer wound edge is visible, though other features of wounds are not obvious, while moisture within the wound adds glare that interferes with imaging (B). Bar = 500 μm.

APPENDIX 2

Real time planimetry assessment of reepithelialisation in wounded human skin organ culture

Nur Azida Mohd Nasir[1,2], Ralf Paus[1,3] , David M Ansell[1,4]
[1]Centre for Dermatology Research, The University of Manchester, M13 9PT Manchester, United Kingdom. [2]School of Medical Sciences, Universiti Sains Malaysia, 16500 Kelantan, Malaysia. [3]NIHR Manchester Biomedical Research Centre, Manchester, UK. [4]Division of Cell Matrix Biology and Regenerative Medicine, The University of Manchester.

Wound healing has long been studied in organ-cultured, experimentally wounded human skin. While this translationally relevant preclinical wound healing assay neatly complements live animal models, one major drawback of the assay is that tissue needs to be assessed via serial histology, which is time-consuming and laborious, precludes the *ex vivo i*nvestigation of a single wounded skin fragment over a time course, and may generate misleading data, depending on where and how exactly the tissue was sectioned and stained. To overcome these limitations, we describe here a methodology for assessing total epithelial wound closure (i.e. reepithelialisation/epidermal repair) *ex vivo* in a serum-free organ culture assay using full-thickness human skin fragments and intravital cell tracker dyes (5-chloromethylfluorescein diacetate). This method enables the healing epithelium to be examined intravitally and in real time, and to morphometrically measure the total area of epidermal repair *ex vivo*. We show that this simple, rapid and instructive method correlates with morphometrically assessed reepithelialisation as measured by standard histology and quantitative histomorphometry of fixed and sectioned human skin fragments at a given time point. Moreover, we demonstrate the ability of this approach to detect significantly accelerated healing in the presence of a positive control (10% serum). Given that wounds often reepithelialise often in an irregular fashion, which is not detected by histology, the global intravital assessment method reported here generated more accurate data on overall epidermal repair *ex vivo*. This methodology also establishes a readout for assessing experimental wounds (i.e. global wound closure), which is more akin to that used in standard clinical setting. **Keywords**: Planimetry assessment, wound healing, epidermal repair, organ culture, *ex vivo*

APPENDIX 3

A novel approach to assessing wound healing in human skin organ cultures

D. Ansell, N.A. Nasir and R. Paus

The University of Manchester, Manchester, U.K.

Human skin explants provide a sophisticated (three-dimensional) and translationally relevant model to examine several aspects of wound healing, most notably the re-epithelialization process. Several groups have established models that incorporate injury of one form or another to either skin explants or artificial skin constructs, which have been used to evaluate drug activity. However, the widely accepted method of assessment of re-epithelialization is via histology through the centre of the wound, which is labour intensive and time consuming, yet provides only a snapshot through a single plane of the wound. We have developed a whole-tissue immunohistochemistry methodology that can rapidly evaluate global wound closure of an explant wounded with a partial-thickness excision. This method correctly detects significant changes in the rate of repair with positive control agents, outperforming standard histology conducted on the same wounds. Moreover, using this approach we can appreciate new features of the wound such as the uniformity of healing in different regions of the wound, the extent of epidermal stratification, and the presence of filopodia. Our methodology may provide a mechanism to increase the throughput of wounded explant studies, to permit screening of potential wound healing therapies in a human three-dimensional model.